Therapeutic cannabinoids: Using *Dictyostelium discoideum* to investigate the mechanism of action of cannabigerol

Joseph Oddy

Research thesis submitted for the degree of Doctor of Philosophy at the Royal Holloway University of London in May 2020

Declaration of Authorship

I, Joseph Laurence Damstra-Oddy, hereby declare that the work presented in this thesis is my own unless otherwise stated, and that all published work has been acknowledged. Furthermore, I affirm that I have neither fabricated nor falsified the results reported herein.

Signed: 

Date: 22/05/2020

Abstract

Cannabis has been used to treat many diseases for centuries. Recent medical interest has focused on the potential of cannabinoids to treat diseases such as multiple sclerosis, epilepsy, and cancer where research has focused on investigating cannabidiol (CBD). However, other cannabinoids, such as cannabigerol (CBG), remain poorly characterised and are being explored as potential treatments. The molecular mechanisms by which cannabinoids treat diseases remain unclear, despite suggested targets including adenosine, mTOR, transient receptor potential transporters and cannabinoid receptors. This study aimed to identify molecular mechanisms of CBG, using *Dictyostelium discoideum* as a model system and translating results to a clinical setting. Initially, a targeted approach was undertaken where the effects of CBG on adenosine transport (and DNA methylation) was investigated. From this approach, CBG elevated DNA methylation in *D. discoideum* dependent upon adenosine transport via the equilibrative nucleoside transporter 1 (ENT1). In addition, an unbiased approach was taken in which screening of a mutant library for CBG resistance identified inositol polyphosphate multikinase (IPMK), a known regulator of mTOR activity, as a potential target. Both CBG and CBD increased mTORC1 activity in wild type cells. Elevated expression of IPMK increased mTORC1 activity, but surprisingly, subsequent treatment with both CBG and CBD reduced mTORC1 activity, suggesting that cannabinoids functioned as pro-homeostatic regulators of mTORC1 activity through IPMK. Translating these results into mouse embryonic fibroblasts, CBG and CBD also increased mTORC1 activity in an IPMK-dependent manner. Finally, in primary human peripheral blood mononuclear cells (PBMCs) derived from healthy volunteers CBG and CBD also increased mTORC1 activity, but decreased mTORC1 activity in primary human PBMCs derived from patients with multiple sclerosis. Thus, this study identifies a pro-homeostatic role for CBG and CBD in mTORC1 regulation via IPMK, conserved between *D. discoideum* and humans, providing new insights into the potential therapeutic mechanism of these cannabinoids.

Contents

List of Tables and Figures

Abbreviations

4EBP1	Eukaryotic translation initiation factor 4E (eIF4E)-binding protein 1
A_{2A}	Adenosine receptor
Ado	Adenosine
ADP	Adenosine diphosphate
AMP	Adenosine monophosphate
AMPK	5' adenosine monophosphate-activated protein kinase
ANOVA	Analysis of variance
ATP	Adenosine triphosphate
BLAST	Basic Local Alignment Search Tool
cAMP	Cyclic adenosine monophosphate
Cannabinoids	In this thesis, refers to phytocannabinoids
$CB_{1/2}$	Cannabinoid receptor 1 or 2
CBD	Cannabidiol
CBDA	Cannabidiolic acid
CBDV	Cannabidivarin
CBG	Cannabigerol
CBP	CREB Binding Protein
cDNA	complementary DNA
CREB	cAMP response element-binding protein
dIPMK	*Dictyostelium discoideum* IPMK
DMSO	Dimethyl sulfoxide
DNA	Deoxyribonucleic acid
DNMA	DNA-Methyltransferase
DNMT	DNA-Methyltransferase
EAE	Experimental autoimmune encephalomyelitis
EKO	ENT1 knockout

Endocannabinoids	Cannabinoids found endogenously in humans
ENT1	Equilibrative nucleoside transporter 1
FOXO	Forkhead box transcription factors
GC-MS	Gas chromatography-mass spectrometry
GCVH1	Glycine cleavage system H protein 1
GPR55	G protein-coupled receptor 55
HECT	Homologous to the E6-AP Carboxyl Terminus domain
HERC2	HECT and RLD domain containing E3 ubiquitin protein ligase 2
hIPMK	*Homo sapiens* IPMK
Hv	Healthy volunteers
IP_3	Inositol trisphosphate
IP_4	Inositol 1, 3, 4, 5-tetrakisphopsphate
IP_5	Inositol pentakisphosphate
IP_6	Inositol hexaphosphate
IP_7	5-diphosphoinositol pentakisphosphate or inositol pyrophosphate
iPCR	Inverse Polymerase Chain Reaction
IPMK	Inositol polyphosphate multikinase
kDa	Kilodalton
LBK1	Liver kinase B1, also known as Serine/threonine kinase 11 (STK11)
LC-MS	Liquid chromatography–mass spectrometry
LST8	(Mammalian) lethal with SEC13 protein 8
LY294002	PI3K inhibitor
MEF	Mouse embryonic fibroblast
mRNA	Messenger RNA
MS	Multiple Sclerosis
mTOR	Mechanistic (or mammalian) target of rapamycin

mTORC1/2	mTOR complex 1 or 2
NBTI	Nitrobenzylthioinosine (ENT inhibitor)
NCBI	National Center for Biotechnology Information
NHI	Non-homologous integrant
p4EBP1	Phosphorylated 4EBP1
PBMC	Peripheral blood mononuclear cell
PCR	Polymerase chain reaction
pDM324	Extrachromosomal expression vector with C-terminal RFP tag
Phytocannabinoids	Cannabinoids derived from the *Cannabis sativa* plant
PI3K	Phosphoinositide 3-kinase
Pictilisib	PI3K inhibitor
PIP_2	Phosphatidylinositol (4,5)-bisphosphate
PIP_3	Phosphatidylinositol (3,4,5)-trisphosphate
PKB	Protein kinase B (also known as Akt)
PKBA	Protein kinase B (A) (also known as Akt)
PKGB	Protein kinase B (G)
pLPBLP	Plasmid for generating gene disruptions
PTEN	Phosphatase and tensin homolog
PwMS	Patients with multiple sclerosis
qPCR	Quantitative polymerase chain reaction
RCC1	Regulator of chromosome condensation 1
REMI	Restriction enzyme-mediated integration
RFP	Red fluorescent protein
RLD	RCC1-like domains
RNA	Ribonucleic acid
RT-PCR	Reverse transcription polymerase chain reaction

S6	Ribosomal protein S6 kinase (also known as S6K or S6K1)
TAE	Tris base, acetic acid and EDTA
TBS	Tris-buffered saline
THC	Tetrahydrocannabinol
THC:CBD	A mixture of tetrahydrocannabinol and cannabidiol
TNF-α	Tumour necrosis factor alpha
TRP	transient receptor potential channels
TSC	Tuberous sclerosis complex
WT	Wild type

Acknowledgements

Firstly, I would like to thank my supervisor, Professor Robin Williams. He has provided me with support and guidance for the last four years. He has given me advice, mentoring, training and maybe most importantly, he has been very patient. I would also like to thank my advisors Professor Peter Bramley and Doctor James McEvoy for all the advice and help they have provided.

Without funding from GW pharmaceuticals this project would not have been possible, so thank you to everybody at GW, especially Dr Will Hind. I would also like to extend a big thank you to all my collaborators who have helped me. Thank you for help with MEFs and inositol phosphates, Dr Yann Desfougères, Dr Miranda Wilson and Professor Adolfo Saiardi at UCL. Thank you for help with PBMC-based experiments, Lisa Costelloe, Dr Eric Downer and John-Mark Fitzpatrick at Trinity College Dublin. Thank you for adenosine experiments, Dr Nicola Gray, Martina Cherubin and Dr Mark Dallas at the University of Reading. Thank you for allowing me to come to the lab and learn techniques, Dr Fu-Sheng Chang and Professor Catherine Pears at the University of Oxford.

Every member of the Williams Lab has helped me. Eleanor Warren has been on the same journey with me during this degree, she has taught me many things, given me wonderful friendship and provided me with lots of support. Her and Judith Schaf have ensured I keep going throughout my degree and I am very grateful to both. Devdutt Sharma, Christopher Perry, Marco Cocorocchio, Kate Augustin and Lizzy Kelly welcomed me into the lab and gave me the start I needed to pursue this project. Fraser Morgan provided me with a year of motivation and enjoyment. Rob Prouse was an essential friend and colleague. Thank you, Erwann Pain, for help with adenosine-related experiments in *D. discoideum*. George Heslop-Harrison, Anthony Goddard, Sonia Shinhmar and Maryam Nagib have all been great additions to the lab and helped me with the final push to the end of my degree. Other colleagues have also helped me during my time at Royal Holloway, Alaa Hussien-Ali, Ellie Crompton, Sahar Akbarivala, Dr Jamuna Selvakumaran, Dr Versha Prakesh, and Yee King also gave me a lot of help when needed.

In addition, Elise Damstra-Oddy, who was my girlfriend at the start of my PhD and is now my wife has kept me going through easy and difficult parts of my degree. Without my parents I would have come nowhere near to getting an undergraduate degree, nevermind a PhD, so I am grateful to their encouragement and the sacrifices they have made for me to be where I am. I am also grateful to my grandma, my siblings and all my family.

Thank you, everyone.

1 Introduction

1.1 Cannabinoids

1.1.1 History of *C. sativa*

Cannabis sativa is an annual herbaceous plant native to east, south and central Asia. *C. sativa* was originally cultivated as fibre for clothing and oil for cooking, lamps and paints (Li, 1973). The flowers of the plant also contain the psychoactive chemical compound, tetrahydrocannabinol (THC), which can have a euphoric effect if the flower is either smoked or cooked (Mansouri et al., 2009; Perrotin-Brunel et al., 2011). In addition to these effects, *C. sativa* has been used as a natural remedy for many ailments for thousands of years (Vinet and Zhedanov, 2011). *C. sativa* from 1700 BC to the modern day has been suggested as a remedy for a variety of ailments, including senility (Russo, 2007), glaucoma (Colasanti, 1990), inflammation (Osbaldeston, 2000), pain relief (Lozano, 2001), infection (Russo, 2007), anxiety (Devinsky et al., 2014), diarrhoea (Russo, 2007), anorexia (McCoy et al., 2018), consumption (Butrica, 2002), and convulsion (for rabies or epilepsy) (Perucca, 2017). However, research now focuses on the molecular mechanisms of specific chemical compounds derived from *C. sativa*, called phytocannabinoids, and how these mechanisms can have therapeutic effects.

1.1.2 Economic Value of Cannabinoid-Based Therapeutics

Therapeutic cannabinoids are currently prescribed as legal and controlled treatments for anorexia in patients with AIDs or undergoing cancer treatment (Calhoun et al., 1998), multiple sclerosis (Etges et al., 2016), and epilepsy (Gray et al., 2019). Over €500 million has been invested in the *C. sativa* industry, much of which has gone into medical research and production (Consultancy.eu, 2019). The medical *C. sativa*-based market could be worth €58 billion annually by 2028 (Consultancy.eu, 2019). In the US, it is estimated that the legal *C. sativa* market could be worth $73.6 Billion By 2027, 71% of which is in the medical sector (GVR, 2020).

1.1.3 Chemistry of cannabinoids

Phytocannabinoids are a diverse class of chemical compounds that are defined by the ability to act on cannabinoid receptors. Phytocannabinoids are derived from *C. sativa* (Taura et al., 2007) and endocannabinoids are similar compounds found in the body (Bermudez-Silva et al., 2016). From here on out “cannabinoids” refers to phytocannabinoids, and endocannabinoids will be termed as such. There are 113 different cannabinoids that have been isolated from *C. sativa* plants (Vinet and Zhedanov, 2011). There are two main forms of cannabinoid, all are produced from geranyl pyrophosphate along with either olivetolic acid (OLA) or divarinolic acid (DVA) (Figure 1.1) (Mechoulam et al., 2014). From OLA and geranyl pyrophosphate, cannabigerolic acid

synthase produces cannabigerolic acid (CBGA) (Degenhardt et al., 2017). CBGA can readily de-carboyxylate into CBG. From CBGA, synthases can produce tetrahydrocannabinolic acid (THCA), cannabidiolic acid (CBDA) or cannabichromenic acid (CBCA), all of which can readily de-carboyxlate into the non-acidic forms of THC, cannabidiol (CBD), and cannabichromene (CBC) (Degenhardt et al., 2017). CBG, CBD and THC all contain an aromatic ring and a five carbon side chain, however, CBD and THC both also contain a cyclohexene ring.

Cannabinoids are not equally abundant in *C. sativa* extracts and different plants contain varying levels of each cannabinoid, usually the most abundant cannabinoid is either THC, CBD or cannabigerol (CBG) (De Meijer and Hammond, 2005). The relative cannabinoid level in extracts varies widely depending upon the breeding purpose of *C. sativa* and conditions grown (Table 1.1) (Potter et al., 2008; Swift et al., 2013; Vandrey et al., 2015; Valdeolivas et al., 2015). For instance, if a *C. sativa* strain has been selectively bred to produce a more potent psychoactive effect then an extract will contain relatively more THC (Swift et al., 2013), while some plants are bred to contain more CBD to make them more saleable (Valdeolivas et al., 2012). However, CBG is present at higher levels in some forms of *C. sativa* (Swift et al., 2013) and CBG is relatively under-researched compared to CBD and THC. This search was performed on Pubmed using "cannabigerol", "cannabidiol" and "tetrahydrocannabinol" on [07/05/2020] indicated 144 research articles have been published relating to CBG, while 2985 and 9492 research articles have been published relating to CBD and THC respectively (PubMed, 2020). Given that CBG is often present in *C. sativa* extracts used therapeutically (Vandrey et al., 2015; Valdeolivas et al., 2015) and is understudied amongst cannabinoids, this project aimed to investigate molecular mechanisms of CBG.

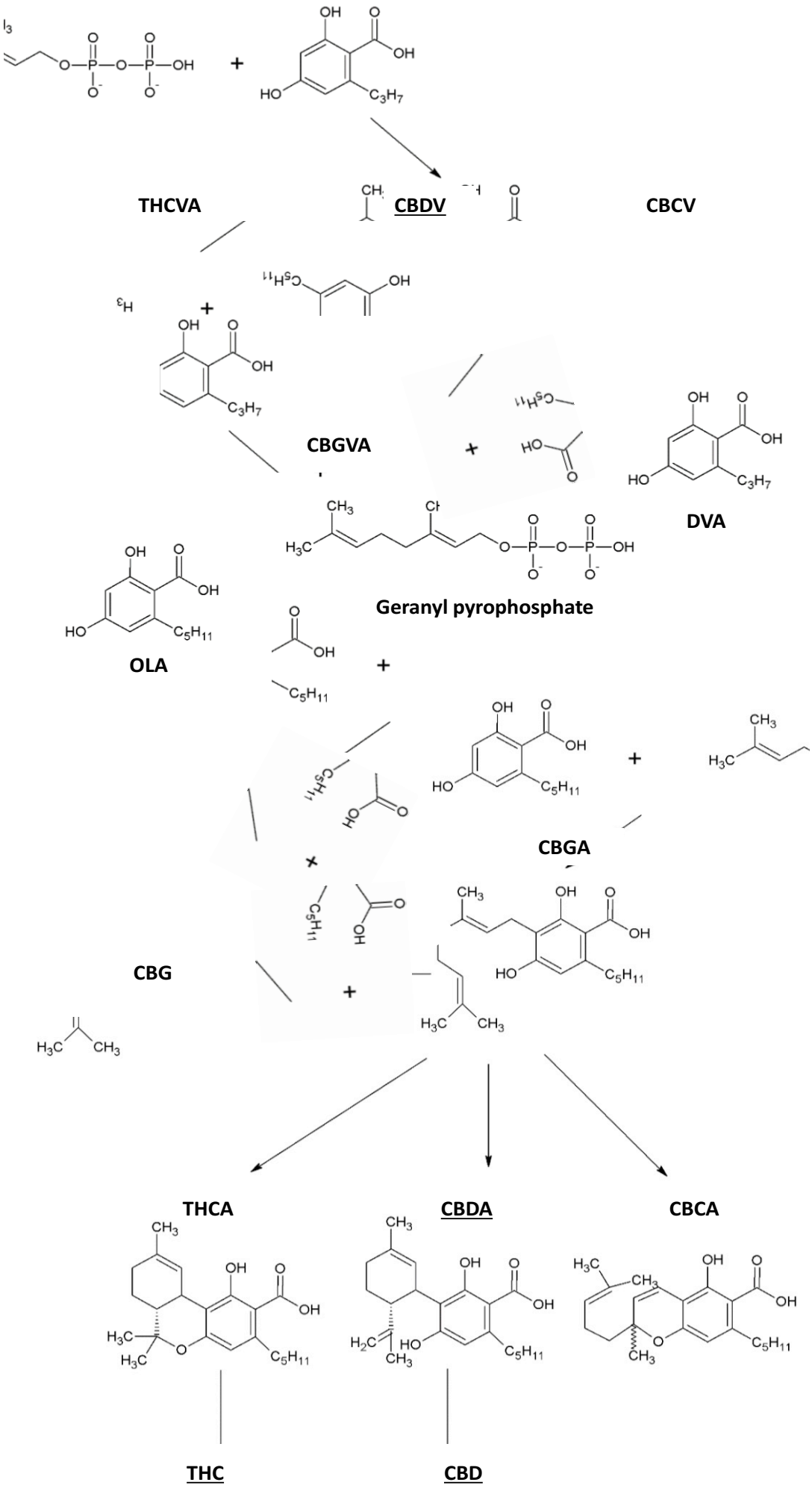
THCVA
CBDV
CBCV
CBGVA
DVA
Geranyl pyrophosphate
OLA
CBGA
CBG
THCA
CBDA
CBCA
THC
CBD

Figure 1.1: Cannabinoid biosynthesis. Cannabinoids are produced by the addition of either olivetolic acid (OLA) or divarinolic acid (DVA) to geranyl pyrophosphate. Cannabigerol (CBG), cannabidiolic acid (CBDA) and tetrahydrocannbinol (THC) are produced with olivetolic acid, while cannabidivarin (CBDV) is produced with diverinolic acid. CBGA – cannabigerolic acid, THCA – tetrahydrocannabinloc acid, CBCA – cannabichromenic acid, CBGVA – cannabigerovarinic acid, THCVA – tetrahydrocannabivarinic acid, CBCV – cannabichromevarinic acid. Underlined are cannabinoids that are examined in this thesis. Data derived from Mechoulam et al., 2014.

Study	Form of *C. sativa*	THC %	CBD %	CBG %
Potter et al., 2008	Powder	95.83	0.42	3.75
Potter et al., 2008	Resin	44.25	52.13	3.63
Potter et al., 2008	Herbal	87.35	4.08	8.57
Potter et al., 2008	Sinsemilla	96.48	0.69	2.83
Vandrey et al., 2015	Medical	91.53	3.39	5.08
Swift et al., 2013	Marijuana police seizures, USA	89.28	6.13	4.59
Swift et al., 2013	Sinsemilla police seizures, USA	95.04	1.65	3.31
Swift et al., 2013	Marijuana police seizures, UK	87.50	4.17	8.33
Swift et al., 2013	Sinsemilla police seizures, UK	96.55	0.69	2.76
Swift et al., 2013	Indoor grown police seizures, Australia (NSW)	95.75	0.70	3.55
Swift et al., 2013	Outdoor grown police seizures, Australia (NSW)	86.81	0.17	13.02
Valdeolivas et al., 2012	Huntington's disease model treatment (THC-based)	98.31	0.42	1.27
Valdeolivas et al., 2012	Huntington's disease model treatment (CBD-based)	3.40	94.98	1.62

Table 1.1: Cannabinoid content in *C. sativa* extracts. Cannabinoid content in *C. sativa* extracts in previous studies is shown here to indicate the variation in cannabinoid content between extracts, and the relatively high level of CBG in extracts not specifically bred for enhanced CBD or THC. This data is represented as a ratio between the three cannabinoids THC, CBD and CBG, due to the many different ways the original data is demonstrated in Potter et al., 2008, Vandrey et al., 2015, Swift et al., 2013 and Valdeolivas et al., 2012.

1.1.4 Efficacy of THC and CBD in disease treatment

1.1.4.1 Pathology of epilepsy

One pathology that cannabinoids are effective in treating is epilepsy. This is a disorder of the central nervous system resulting in seizures and is defined as at least two unprovoked seizures occurring more than 24 hours apart (Fisher et al., 2014). Epilepsy affects 65 million people worldwide and results in increased mortality, comorbidities and disability (World Health Organization, 2016). A seizure is defined as an abnormal, synchronous excitation of a neuronal population, typically lasting seconds or minutes but can be prolonged and continuous (Helen E. Scharfman, 2007).

Seizures can occur anywhere in the brain, however, in children seizures often occur in the temporal and frontal lobes (Rzezak et al., 2007). In adults, the mesial part of the temporal lobe is a common region of seizure origin (Cendes, 2005). The mesial temporal lobe is made up of the hippocampus and amygdala which control emotion and the uncus controlling smell. Therefore, seizures originating in this region can result in strong emotions like fear or the sensation of a unpleasant smells (Hamasaki et al., 2014). Wherever seizures originate, they can rapidly propagate through the brain into different regions, for example from the temporal to frontal lobes, and each spread increases the further risk of spread of seizure. If a seizure spreads wide enough throughout the brain, it can be classified as a general seizure involving the entire brain and altering consciousness. During epilepsy, neuronal loss often occurs in the hippocampus (Kälviäinen et al., 1998). Neuronal loss is often accompanied by gliosis (proliferation or hypertrophy of multiple glial cell types), granule cell dispersion and an atrophy of the hippocampus (Spencer and Spencer, 1994; Blümcke et al., 2002).

A seizure is essentially caused due to an imbalance or inability to balance the ionic levels either side of a neuronal membrane (Scharfman, 2007). This is important because healthy brain signals are spread through a controlled change in ionic levels. Normally potassium levels are at a high concentration within neurons and sodium at a high concentration extracellularly. This leads to a net negative transmembrane potential (Hill et al., 2014). If this balance is altered, then depolarisation of the membrane can occur and transmitted through the neuron (Kaplan et al., 2017). This leads to neurotransmitter release and further action potentials (Fišar, 2009). One key component in maintaining and renewing the membrane balance is sodium-potassium ATPase pumps, which transport sodium ions out of the cell and potassium ions into the cell (Hill et al., 2014). Blocking these pumps is sufficient to cause a seizure in experimental conditions (Vaillend et al., 2002). In addition, glia may be key regulators of ion concentration outside of neurons (Duffy and MacVicar, 1999).

Seizures themselves can also change transmembrane gradients, as a seizure is often followed by a rise in extracellular potassium ion which can lead to a further depolarisation of neurons (Sypert and Ward, 1974). Therefore seizures can result in a vicious cycle where a transmembrane potential perturbation can create more and more perturbations (Scharfman, 2007). Furthermore, abnormalities in the sodium channels could result in a decreased threshold for an action potential, this is the case in generalised epilepsy with febrile seizures (Meisler et al., 2001).

Another factor that impacts the spread and severity of seizures is synaptic transmission. In the synapse, an action potential is carried forward to another neuron through the release of neurotransmitters, such as γ-aminobutyric acid (GABA) and glutamate (Kullmann and Semyanov, 2002). GABA is an inhibitory transmitter and glutamate is an excitatory transmitter. GABA receptors becoming desensitised to GABA can result in a reduced inhibitory effect (Butler et al., 2018). Chloride ions are usually transported through GABA receptors into cells, however, if other chloride ion transporters are defective then this is not possible and can lead to seizures (Dzhala et al., 2005). Glutamate innervates many neuron types and exposure to glutamate may have little effect overall, and may even increase inhibition of principal cells because they require less glutamate to reach threshold for depolarisation (Sun et al., 2002).

Synchronisation of a network of neurons is key to causing a seizure (Li et al., 2012). The pyramidal cells of the cortex are interconnected by glutaminergic synapses, therefore a large amount of glutmate released in postsynaptic spaces can result in numerous cells activated at one time (Johnston and Brown, 1984). Gap junctions, which connect neighbouring cells through direct intercellular channels, may also aid in synchronisation of neuronal action potentials (Traub et al., 2004).

One major contributor to the development of epilepsy is calcium ion accumulation in hippocampal neurons (Nazıroğlu et al., 2012). Transient receptor potential vanilloid 1 (TRPV1) is a calcium-permeable channel and epilepsy mediator in the hippocampus. This protein is activated by high temperature (Muller et al., 2019), anandamide (Umathe et al., 2012), oxidative stress (Aviello et al., 2012), capsaicin (Maiese, 2017) and inflammatory products (Muller et al., 2019). Activation of TRPV1 can result in glutamate release (Fawley et al., 2014), therefore, the duration of postsynaptic stimulation is increased by activation of TRPV1 channels (Shoudai et al., 2010). This finding led to the exploration of TRPV1 as a potential treatment target for epilepsy. In temporal lobe epilepsy there is an increased expression of TRPV1 in the hippocampus (Sun et al., 2013).

Cannabinoids receptors, such as CB_1, CB_2 and GPR55 are also key regulators of neuronal transmission and implicated in disease control of epilepsy (Galiazzo et al., 2018). The two most

commonly studied endocannabinoids in humans are anandamide and 2-arachidonoylglycerol (2-AG) (McPartland et al., 2006). CB_1 receptors are abundant in the CNS, particularly the cortex, basal ganglia, hippocampus and cerebellum, mostly on axon terminals and pre-axonal segments (Holm et al., 1980; Liu et al., 2009; Jones et al., 2010; Pandolfo et al., 2011; Busquets-Garcia et al., 2018). CB_2 receptors are expressed at a lower level in the CNS and is more present in microglia, vasculature, immune cells and some neurons, such as dopaminergic neurons in the ventral tegmental area and hippocampal CA3 neuronal cells (Arévalo-Martín et al., 2003; O'Sullivan et al., 2009; Chen et al., 2017). GPR55 are located primarily in the brain and peripheral nervous system (PNS), GPR55 activation in the PNS an result in increased intracellular calcium release in neurons leading to neuronal excitability (Lauckner et al., 2008). Expression of CB_1 receptors is reduced in epileptic hippocampal regions (Ludányi et al., 2008). Low and high dose anandamide-induced effects on correlate with CB_1 receptors and TRPV1 activation (Umathe et al., 2012). Endocannabinoid signalling can be used as negative feedback by neurons to halt an action potential and reduce release of glutamate across the synapse (Figure 1.2) (Busquets-Garcia et al., 2018). Therefore, CB_1 receptor activation by endocannabinoids produces neuroprotection in the hippocampus and inhibits epileptic seizures in models (Romigi et al., 2010; Citraro et al., 2013). However, endocannabinoid signalling may reduce seizure threshold, which would allow progression of epilepsy (Wallace et al., 2002). Mice with just the CB_1 receptor knocked out show heightened seizure sensitivity, mice with just the CB_2 receptor knocked out do not, but mice with both receptors knocked out resulted in 80% of them becoming epileptic (Rowley et al., 2017).

Adenosine is another key signalling molecular involved in epilepsy. Adenosine is an endogenous anticonvulsant, released after a seizure as a terminator and works through the adenosine receptor 1 protein (During and Spencer, 1992; Lado and Moshé, 2008). The anti-convulsant effect of adenosine occurs through the upregulation of presynaptic neuron inhibition, preventing runaway excitement in feed-forward synaptic circuits (Huber et al., 2001; Boison, 2012), thus adenosine stabilises the post-synaptic membrane potential. Adenosine therefore acts to stop the spread of a seizure and elevated extracellular adenosine levels can reduce seizure frequency (Li et al., 2008; Fukuda et al., 2010). A reduction of extracellular adenosine can be caused by over-expression of adenosine kinase, which phosphorylates adenosine to produce adenosine monophosphate (AMP) (Lovatt et al., 2012). An increased expression of adenosine kinase (ADK), can result in a much quicker progression of the disease, as it reduces the inhibitory tone of adenosine in the brain, reducing the threshold for seizure generation. Inhibition of adenosine receptors, for example through long term used of the asthma treatment theophylline, can result in seizures and epilepsy development (Korematsu et al., 2008; Fukuda

et al., 2010). Experimental data in mice found that kainic acid-induced epilepsy in animals lacking the adenosine receptor led to massive neuronal cell loss and death within 5 days compared to a non-convulsive status epilepticus in wild type mice (Fedele et al., 2006).

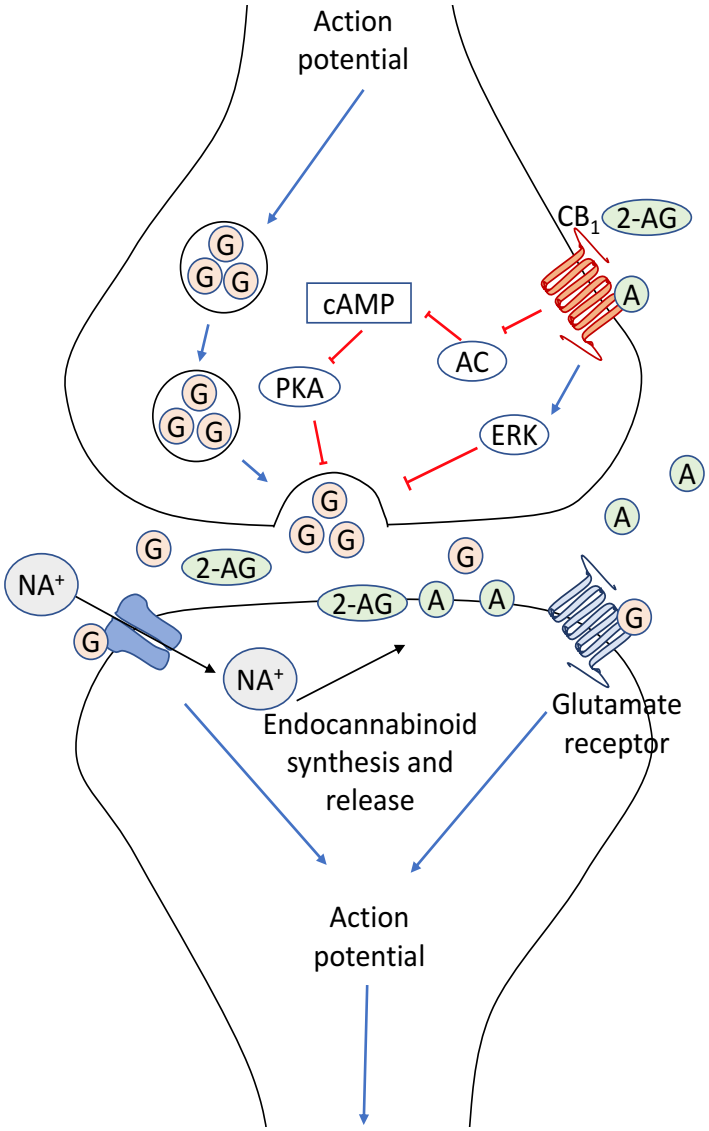

Figure 1.2: Cannabinoid receptors. Endocannabinoids control neuronal transmission and action potentials. An action potential causes the release of glutamate across the synapse from the presynaptic neuron. Glutamate stimulates an action potential in the postsynaptic neuron through glutamate receptors and sodium ion channels. However, this also creates a feedback in which endocannabinoids are produced from fatty acids in the postsynaptic neuron. These then release into the synapse and inhibit the further release of glutamate from the presynaptic neuron, thus inhibiting neuronal signalling. Adapted from (Busquets-Garcia et al., 2018). AC = adenylyl cyclase, A = anandamide, G = glutamate, ERK = extracellular signal-regulated kinase, PKA = protein kinase A, cAMP = cyclic adenosine monophosphate.

Furthermore, ADK overexpression is linked to epileptogenesis. ADK is primarily expressed in astrocytes and is a major metabolic clearance protein for adenosine (Studer et al., 2006). Neurological injuries or inflammation can result in astrogliosis, in which astroglia proliferation and increase is size (Pekny and Nilsson, 2005). Many in vivo studies have found that astrogliosis

results in ADK overexpression (Steinhäuser and Boison, 2012; Boison and Aronica, 2015; Boison and Steinhäuser, 2018), and in humans with temporal lobe epilepsy there is an overexpression of ADK. In the immediate aftermath of a brain injury, stroke or seizure, adenosine is released from cells to attempt to halt neuronal transmission (Weltha et al., 2019). After this inflammation occurs which triggers astrogliosis and ADK overexpression and therefore adenosine deficiency (Li et al., 2012). In addition, this increases the abundance of methyl groups in the transmethylation pathway, resulting in increased DNA methylation (Williams-Karnesky et al., 2013). DNA methylation has an inhibitory effect on gene expression, reducing expression of nearby genes and increasing the likelihood of further inhibitory epigenetic changes such as histone deacetylation (Rountree et al., 2000). In general, DNA methylation is a key regulator of gene control and is often cell-type specific (Moore et al., 2013). DNA methylation is also a key regulator of development (Pucci et al., 2013), cell fate (Kredich and Martin, 1977), cell cycle (Müller et al., 2013) and is dysregulated in many diseases, such as cancer (Jaenisch and Bird, 2003).

DNA methylation has been studied as a possible marker or controller of epilepsy since it was discovered that DNA methylation inhibitor treatment reduced spontaneous neurotransmission and network activity in hippocampal slices (Levenson et al., 2006). A global increase in DNA-methyltransferase activity and DNA methylation was correlated with spontaneous recurrent seizures in mice and reversed by adenosine augmentation (Williams-Karnesky et al., 2013). However, increased DNA methylation may not be sufficient to cause epilepsy alone, as pharmacological inhibition of DNA methylation did not alter epilepsy in a rat model (Parrish et al., 2013).

Another key cellular signalling mechanisms associated with epilepsy is a modified mechanistic target of rapamycin (mTOR) pathway. Mutations in the tuberous sclerosis complex (TSC) proteins or phosphatase and tensin homolog (PTEN) protein lead to abnormal neuronal proliferation and growth in animal models (LaSarge and Danzer, 2014). Humans with mutations in either of the two TSC proteins develop cortical tubers found in the cortex or subcortical white matter and lead to the development of refractory seizures, surgical removal of which often reduces seizure occurrence (Weiner et al., 2006). These tubers promote hyperexcitability of neurons and seizures (Mühlebner et al., 2016). Dysregulation of mTOR signalling can also lead to changes in gene and protein expression that increase the likelihood of neuronal excitability and seizures (Boer et al., 2010). In Hemimegaloencephaly there is an overreaction of mTOR signalling in some neural tissue, potentially caused by somatic mutations in genes involved in the pathway (Crino, 2015; Ikeda and Mirsattari, 2017). Focal dypslasias are another type of

epilepsy with cortical development malformations and are associated with mutations in either the mTOR gene itself or other components of the pathway (Lim et al., 2015).

The many disparate pathways and cellular components involved in epilepsy has led to multiple treatments being found. In 30-40% of cases, the disorder is not adequately controlled, leaving potentially 20 million epilepsy patients without a means of properly controlling their disorder (Cook et al., 2013). One target for AEDs is voltage-gated sodium channels. These channels control the rising phase of neuronal action potentials. AEDs that target these channels are oxcarbazepine, zonisamide, phenytoin, carbamazepine, lamotrigine and possibly valproate (Yaari et al., 1986; Schmutz et al., 1994; Ambrósio et al., 2002; Leppik, 2004). The other main mechanism of action of AEDs is to act on γ-aminobutyric acid (GABA) transmission (Davies, 1995). The spread of seizure activity across the nervous system is due to high-frequency repetitive spike firing, which these drugs block. Impairment of GABAergic transmission by GABA antagonists or by genetics induces epileptic seizures (Sperk et al., 2004). This is the mechanism of action of both benzodiazepines and barbiturates (Davies, 1995).

A potential treatment for epilepsy, that may reduce the number of patients with the AED-resistant disease is cannabinoids. Cannabis has been suggested as a treatment for epilepsy since at least 900 CE, but was probably in use long before (Meier and Rosenthal, 1976). In modern times Cannabis was listed in the US 1854 dispensatory as a possible remedy for muscle spasms (Szaflarski and Martina Bebin, 2014). In recent years research into Cannabis and cannabinoids as potential therapeutics for epilepsy has increased, in addition, self-medicating epilepsy patients have begun to use Cannabis to alleviate symptoms (Szaflarski and Bebin, 2014). Some studies have found that Cannabis use can make epilepsy symptoms worse (Gordon and Devinsky, 2001). This may be because of the THC present in the self-medicated Cannabis (Szaflarski and Martina Bebin, 2014). Another reason in which Cannabis may have a negative effect on those self-medicating is that these are often people who are suffering from the worst kinds of epilepsy that no drug has treated and are desperately trying alternative medications. CBD, a non-psychoactive constituent of Cannabis decreases frequency of seizures in patients suffering from epilepsy that AEDs could not control (Devinsky, Patel, et al., 2018). Potential mechanisms of action for treatment of epilepsy with CBD are through the equilibrative nucleoside transporter, orphan G-protein-coupled receptor GPR55, transient receptor potential of vanilloid type-1 channel, 5-HT1a receptor and α3 and α1 glycine receptors (Bisogno et al., 2001; Russo, 2005; Hejazi et al., 2006; Carrier et al., 2006; Ryberg et al., 2007) .

An initial study into the efficacy of cannabinoids on epilepsy found that CBD reduced convulsant activity and abolished jaw and limb cramping in a cobalt-induced epilepsy rat model (Chiu et al., 1979). However, THC treatment of the cobalt-induced epilepsy rat model resulted in increased

neuronal firing and excitation, indicating that CBD may be an effective treatment for epilepsy, but that THC may exacerbate the disease (Chiu et al., 1979). In mice induced into an epilepsy-like state by electroshocks or with convulsant drugs, CBD pre-treatment prevented convulsions, seizure spread and lethality of seizures (Consroe et al., 1982). CBD was also found to have anti-seizure properties in acute seizure models (electroshock mice and rats) and a chronic neuroprotective effect in a corneal kindled-epilepsy model mouse (Klein et al., 2017). In a mouse model of Dravet syndrome, CBD was found to reduce seizure frequency, duration and severity and autistic-like social deficits (Kaplan et al., 2017). Similarly, in a mouse model of Angelman syndrome, a genetic disorder with epilepsy-like symptoms, CBD was found to attenuate seizures and neuronal signalling (Gu et al., 2019). Finally, CBD has recently been found to reduce seizures in a zebrafish model of epilepsy-related tuberous sclerosis complex disease (Serra et al., 2019). CBD has therefore been found to have anti-seizure effects in animal models of epilepsy, providing a potential treatment for the disease.

As certain cannabinoids (in particular CBD) were found to be safe and efficacious in treating epilepsy in animal models, clinical trials examined how effective the treatment was in humans. In an early study on the efficacy of cannabinoids on epilepsy, CBD was found to reduce convulsive episodes in most patients, and 50 % of patients treated with CBD remained free of convulsive episodes (Cunha et al., 1980). In a clinical trial using a highly purified CBD-enhanced *C. sativa* extract, called Epidiolex®, cannabinoid treatment reduced seizures by around 50 % at 12 and 48 weeks of treatment (Devinsky et al., 2018(b)). The efficacy of CBD treatment was also assessed by clinical trial on a rare and severe form of childhood-onset epilepsy, Lennox-Gastaut syndrome (Halford et al., 2018). Here, CBD treatment over 60 weeks was found to reduce total seizures by 48-62 % and drop seizures, where the child collapses during the seizure, by 48-70 % (Halford et al., 2018). In addition, 88 % of caregivers reported an improvement in overall condition of the Lennox-Gastaut syndrome patients (Halford et al., 2018). To examine the potential of CBD to treat another rare form of epilepsy, a clinical trial examined the effects of CBD on patients with Dravet syndrome, which is a severe infant epilepsy in which seizures are triggered by hot temperature or fevers (Devinsky et al., 2019). Here, CBD was found to reduce total seizures by 39-51 % after 48 weeks of treatment, and 85 % of caregivers reported that the overall condition of the patient improved (Devinsky et al., 2019). In another study, the efficacy and safety of cannabidiol preparations containing THC (at a proportion of 50:1 for CBD:THC), were found to be effective at reducing seizures by 70 % and the treatment was well tolerated (McCoy et al., 2018). This efficacy has led to Epidiolex® prescription legalisation in many countries, most commonly for the treatment of drug-resistant epilepsy (Abu-Sawwa and Stehling, 2020).

1.1.4.2 Pathology of multiple sclerosis

Another pathology that cannabinoids are effective in providing symptomatic relief is multiple sclerosis. This is a chronic, inflammatory and neurodegenerative disease which begins with demyelination of neurons and leads to variable axonal and neuronal injury (Wingerchuk and Carter, 2014). Multiple sclerosis (MS) causes disability in young adults and reduces life expectancy by 5 to 10 years (Riccio and Rossano, 2015; NHS, 2018). The disease causes an interruption of myelin tracts in the CNS, initially causing weakness, diminished dexterity, visual loss, instability and ataxia (Hauser and Oksenberg, 2006). This can then develop into bladder dysfunction, chronic fatigue, pain, vertigo, spasms, memory loss and reduced ability to carry out cognitive tasks (Hauser and Oksenberg, 2006). The damage generally occurs in the white matter of the brain, which has a higher proportional of myelinated neurons to grey matter (Kornek et al., 2000).

Although neuronal demyelination can occur throughout the central nervous system in multiple sclerosis, some regions are more commonly damaged than others. Where veins become inflamed in the brain, due to increased inflammatory cytokine release and immune response, white matter lesions form (Tallantyre et al., 2008). Cortical lesions are also associated with peripheral vein inflammation and demyelination within the brain was associated with proximity to inflammation in the blood-brain barrier (Kutzelnigg et al., 2005; Howell et al., 2011; Choi et al., 2012). Legions in the brain are also associated with areas of low perfusion, this is thought to increase the likelihood of oxidative damage and therefore demyelination through this method (Holland et al., 2012). While demyelination can occur anywhere in the brain, the areas of low perfusion are less likely to remyelinate and therefore have longer, sustained damage.

MS is characterised by inflammation at the blood-brain barrier due to the auto-reaction of multiple immune cells (T cells, B lymphocytes, macrophages and microglial cells) against brain and spinal cord white matter (Rajesh et al., 2007). This causes one or two relapses annually into neurological dysfunction in 85 % of MS patients in the early phases of the disease, usually followed by remission (Riccio and Rossano, 2015). However, these cause neurological injuries that eventually build up and increase the risk of disability over time (Rudick et al., 2006).

Immune cells, which are constituent in peripheral blood mononuclear cells (PBMCs) produce pro-inflammatory cytokines which increase the progression of MS (Simpson et al., 2015). These cells include T lymphocytes, B cells and monocytes (Yu et al., 2007) and in individuals with MS, the immune cells become activated and breakdown the blood-brain barrier, eventually crossing it and leading to axonal degradation and myelin damage in the central nervous system (CNS) (Bar-Or et al., 2003). In immune cells, mTORC1 activity is often at a much higher rate than in

healthy individuals, which contributes to the overproduction of pro-inflammatory cytokines (Carbone et al., 2014). Therefore, many MS therapies are immunomodulatory and target peripheral immune cells.

The causes of MS are still unknown, there is a correlation of familial, geographical and ethnic inheritance. One gene locus strongly associated with MS is the HLA-DRB1 locus, as does the copy number of HLA-DR2 (GAMES and Transatlantic Multiple Sclerosis Genetics Cooperative, 2003; Modin et al., 2004). Both protein products of these genes are components of the human leukocyte antigen (HLA) complex, which helps the immune system distinguish between self and pathogens. They attach to proteins outside the cell and display them to the immune system, which then will either recognise them as foreign or self and trigger an appropriate response. However, there is a possibility that mutations in these proteins could result in a presentation of the encephalitogenic peptide (present in myelin) as a foreign protein, resulting in an immune response and attack to that protein (Oksenberg and Barcellos, 2005). However, exact causal mutations are not yet understood.

There are multiple disease-modifying therapies (DMTs) currently available that slow disease progression and relieve some symptoms. One of the main DMTs available as a therapeutic for MS is interferon beta and glatiramer acetate. The exact mechanism of action for these treatments are unknown but they reduce blood brain barrier disruption, modulate T- and B-cells and cytokine functions and the glatiramer acetate stimulates regulatory T cells (Dhib-Jalbut, 2002). These drugs reduce clinical relapse rate by a third, but have little effect on progressive MS (Wingerchuk and Carter, 2014). A general immunosuppression drug can be used for rapidly worsening MS: mitoxantrone. However, its use is limited to two years due to the cumulative dose-related cardiomyopathy (Hartung et al., 2002). The use of mitoxantrone is associated with leukaemia, which has prevented doctors prescribing it in all but necessary cases (Marriott et al., 2010). Natalizumab is a monoclonal antibody that targets the α4 subunit of an antigen expressed on lymphocyte and monocyte surfaces (Haarmann et al., 2015). Natalizumab prevents interaction with this antigen and a cell adhesion molecule on the brain vascular endothelium. This prevents lymphocytes entering the central nervous system and therefore prevents them from triggering acute MS lesions. However, use of natalizumab increases the risk of a central nervous system infection by the John Cunningham virus (Kleinschmidt-DeMasters and Tyler, 2005). This can lead to multifocal leukoencephalopathy and death or irreversible neurological disability. Therefore, patients on natalizumab are monitored closely to prevent this from occurring. Mitoxantrone, natalizumab and interferon beta are all intravenous DMTs, however, other forms of DMTs can be used by MS patients.

Oral DMTs are used for relapsing MS. Fingolimod reduces relapse by around 50% compared to interferon treatment (Cohen et al., 2010). Fingolimod traps lymphocytes in lymph nodes, this prevents them from entering the CNS and therefore prevents MS lesions. However, it can result in mild lymphopenia and an increased risk of viral infections (Ratchford et al., 2012). Fingolimod also has significant effects of cardiac smooth muscle and for this reason is not recommended to patients with heart disease (Cohen et al., 2010). Another orally taken DMT is terifunomide. Terifunomide is also taken as a treatment for rheumatoid arthritis (Greene et al., 1995). It inhibits dihydroorotate dehydrogenase which is required for proliferating cells, thereby reducing immune system response. Terifunomide can cause diarrhoea, nausea, alopecia and increased risk of infection (O'Connor et al., 2011). An additional orally ingested DMT is dimethyl fumarate. Dimethyl fumarate has little impact on the liver, since once ingested it is hydrolysed to monomethyl fumarate which is eliminated through respiration. It reduces oxidative cell stress and modulates nuclear factor κB, both could provide anti-inflammatory effects (Linker et al., 2011; Albrecht et al., 2012). The main side effects of terifunomide are gastrointestinal, but it is well tolerated in general (Fox et al., 2016). A reduction by around one third in mean lymphocyte cell count is usually observed with terifunomide treatment, and lymphopenia can develop in patients on this drug, therefore blood cell count is monitored for patients who take this (Berkovich and Weiner, 2015). In addition, infection risk could by increased by taking this treatment. There are also MS DMTs that are emerging in recent years.

Alemtuzumab is a new drug that has a lower relapse rate than interferon treatment. Alemtuzumab is a humanised anti-CD52 monoclonal antibody (Coles et al., 2012). It depletes and repopulates circulating T lymphocytes and B lymphocytes. This changes the number, proportions and function of the lymphocyte subsets. This does produce a risk of infection, but the risk appears to decrease with time (Wray et al., 2018). There is also a cumulative risk for autoimmune diseases in patients with alemtuzumab treatment for MS (Cossburn et al., 2011). Ocrelizumab is a humanised monoclonal antibody for CD20 (Montalban et al., 2017). Ocrelizumab is effective at reducing the rate of disability in MS patients, through depletion of CD20-expressing B cells. However, infection rate increased on taking the drug (Montalban et al., 2017). There are multiple drugs in use to treat MS. Many produce side effects that would not be tolerated for other drugs, however, given the severity of MS it is still beneficial for patients to take the drugs. There is still research going on to try to find drugs with fewer side effects and possibly that can stop MS.

There has also been a suggestion that the endocannabinoid system may be involved in MS disease development and a potential target for treatment. In many experimental models of MS and in patients, there was a large amount of change in CB_1 and CB_2 expression compared to

healthy controls (Chiurchiù et al., 2018). In fact, THC treatment of a mouse model of MS reduced neurodegeneration and chronic disability (Pryce et al., 2003). Activation of CB_2 receptors in autoreactive T cells was also essential for the control of inflammation in a mouse model of MS by reducing T cell differentiation and immune cell accumulation in the CNS (Maresz et al., 2007; Kong et al., 2014). In addition, CB_2 receptor inhibition of *ex vivo* T lymphocytes from MS patients inhibited cell proliferation and immune response without causing cell death (Malfitano et al., 2013). Mice lacking CB_1 receptors poorly tolerated inflammatory insults and were more likely to develop neurodegeneration (Pryce et al., 2003; Chiurchiù et al., 2018), while CB_2 receptor deletion in T cells from MS model mice led to increased T cell proliferation, reduced apoptosis, elevated inflammatory cytokine release and worsened symptoms (Maresz et al., 2007). THC was found to limit inflammation, disease development, CNS infiltration and microglial activation while promoting myelin repair, potentially through THC activation of CB_1 receptors (Pryce et al., 2015; Moreno-Martet et al., 2015). It is unclear as yet, how much involvement the endocannabinoid system has in modulating the response of MS to phytocannabinoid treatment.

A potential target for MS treatment is the mTOR pathway. mTOR promotes the myelination of the CNS (Wahl et al., 2014). In MS oligodendrocytes can fail to differentiate and therefore do not produce new myelin, thus resulting in a demyelinated lesion and reduced myelin repair over time (Kornek, 2000). A study in 2017 on mouse experimental autoimmune echepalomyelitis (EAE) cells found that the disease model had a lower activation of the PI3K/Akt/mTOR pathway (Giacoppo et al., 2017). The phosphorylation of these proteins found lower levels in the disease model, but when treated with CBD there was an increase in phosphorylation. Non-phosphorylated PI3K/Akt/mTOR proteins did not significantly change with treatment, meaning there was an increase in activation of the pathway, but not protein levels. CBD treatment of these cells found a reduction in inflammatory cell infiltration of CNS tissues. It is thought that this could be through CBD activation of CB_1 and CB_2 receptors (Keating, 2017). In addition, the side effects of CBD and other cannabinoids (such as THC) could be much more tolerated than other drugs. For example, one study found that common side effects of Sativex® treatment (CBD and THC) were confusion, dizziness, fatigue, increased appetite (Ferrè et al., 2016). In the trial Sativex® reduce spasticity and pain. The full effect of cannabinoids on the treatment of MS has yet to be explored, but they provide a potential treatment of symptoms and potentially the causes of the disease with few side effects.

One common and effective animal model for MS is the experimental allergic autoimmune encephalomyelitis (EAE) mouse model (Robinson et al., 2014). In this model, mice undergo active immunisation with myelin-derived proteins such that mice T-lymphocytes recognise the endogenous myelin sheaths of neurons as foreign bodies and begin to attack them (Robinson et

al., 2014). The effect created in an EAE model mouse is very similar to that which occurs in patients with MS (Robinson et al., 2014). In EAE model mice, treatment with Sativex® (which is a complex botanical, the therapeutic effects of which are derived from the totality of the product, and not THC/CBD alone.)was found to reduce spasticity by 40 % and was as effective as baclofen (a known MS treatment) (Hilliard et al., 2012). Another study found that CBD effectively diminished inflammation, demyelination, axonal damage and inflammatory cytokine expressive in an EAE model of MS (Rahimi et al., 2015). Purified CBD was found to have anti-apoptotic, neuroprotective effects in the EAE model of MS (Grassi et al., 2016) while reducing inflammatory cytokine production (Giacoppo et al., 2017). Interestingly, application of a topical CBD cream also exerted neuroprotective effects and reduced paralysis of hind limbs in an EAE model of MS, as well as reducing cytokine release and tissue damage in the spleen (Giacoppo et al., 2015). CBD treatment of EAE mouse models of MS was found to potentially work through decreased T cell infiltration into the central nervous system and an increase in myeloid-derived suppressor cells, which would remyelinate neurons (Elliott et al., 2018). Although the efficacy of cannabinoid treatment of MS has been illustrated in animal models, clinical trials are necessary to determine if these effects remain in a clinical setting.

As cannabinoids were found to be safe and efficacious in treating MS in animal models, clinical trials examined whether this effect occurred in humans. One clinical study revealed that Sativex® was effective in reducing pain and sleep disturbance in MS for up to five weeks (Rog et al., 2005). In a follow-up study two years later, patients who continued with treatment were found to have positive benefits on pain reduction and sleep (Rog et al., 2007). In a clinical trial in Germany, a similar mixture of THC and CBD was found to decrease spasticity in MS patients as add-on therapy or monotherapy (Koehler et al., 2014). Sativex® is provided as an oromucosal spray which is an add-on therapy for patients with moderate to severe multiple sclerosis spasticity resistant to other medications (Flachenecker et al., 2014). Furthermore, a clinical trial of Sativex® for MS patients found that the therapeutic was both well-tolerated and effective against MS-related spasticity, from one to three months of treatment (Flachenecker et al., 2014). Overall, THC and CBD mixture mucosal spray has been effective for around half of patients in all clinical trials at reducing MS-related spasticity (Zettl et al., 2016). This efficacy has led to Sativex® prescription legalisation in many countries, for the treatment of MS-related symptoms (Etges et al., 2016).

1.2 Mechanisms of action of cannabinoids

1.2.1 Cannabinoid interaction with cannabinoid receptors

The first known targets of cannabinoids in animals were cannabinoid receptors. These are G-protein-coupled receptors that mediate the effect of endocannabinoids in the body (Howlett et al., 2002). Cannabinoid receptor 1 (CB_1) is prominent in the central nervous system (Herkenham et al., 1991) while cannabinoid receptor 2 (CB_2) is expressed in the brain, testes and spleen (Liu et al., 2009). In the absence of exogenous cannabinoids, these proteins regulate synaptic transmission (Paradisi et al., 2008). However, THC activates these receptors, while CBD acts as an indirect antagonist (Laprairie et al., 2015). One study found that pharmacological cannabinoid receptor antagonism ameliorated tremor and spasticity in MS model mice (Baker et al., 2000). Another study found that expression of CB_1 in neurons was required for cannabinoid-mediated suppression of MS-like symptoms in an EAE model mouse, while CB_2 expression on T cells was required for a cannabinoid-mediated reduction in immune cell-mediated inflammation (Maresz et al., 2007). Loss of CB_1 expression was found to decrease motor performance in a mouse model of Huntington's disease (Mievis et al., 2011). However, as only THC has been found to activate CB_1, the mechanism of action of non-THC cannabinoids for the treatment of diseases is unlikely to occur through CB_1 or CB_2. CBD treatment elevated the production of endogenous anandamide in schizophrenic patients, which if a similar effect was found in epilepsy patients, could potentially reduce seizures, as anandamide is typically low in the CNS of epilepsy patients (Romigi et al., 2010; Leweke et al., 2012).

Another cannabinoid receptor has been discovered in the form of G-protein coupled receptor 55 (GPR55), which again is activated by THC, but not CBD (Lauckner et al., 2008). However, one study found that CBD may inhibit neurotransmission through GPR55, as pharmacological inhibition of the protein blocked the effects (Kaplan et al., 2017). The potential of CBD to block intracellular calcium release through GRP55 indicates a potential use of CBD as a treatment of epilepsy, as this would reduce depolarisation of neurons and the reduction of action potential transmission or an increased threshold (Devinsky et al., 2014). Research on the effects of cannabinoids on GPR55, therefore, remains unclear, but both CBD and THC may have antagonistic effects on this protein.

1.2.2 Cannabinoid interaction with transient receptor potential channels

Another protein family that are known to be biochemical targets of cannabinoids are the transient receptor potential (TRP) channels. These are a family of membrane proteins involved in the transport of ion entry into cells, mediating the sensing of temperature, pressure, pH,

smell, taste, vision and pain (Ishimaru and Matsunami, 2009; Muller et al., 2019). TRP channels are ionotropic cannabinoid receptors, as endocannabinoids modulate TRP vanilloid 1 (TRPV1) (Zygmunt et al., 1999) and TRP melastatin 8 (TRPM8) (De Petrocellis et al., 2007). In contrast, THC acts potently at TRPV2, moderately at TRPV3 and TRPV4, but does not modulate TRPV1 (De Petrocellis et al., 2011), and both CBD and CBG stimulate TRPV1 and TRPV2 and antagonise TRPM8 (De Petrocellis et al., 2011). CBD was found to reduce seizure sensitization from repeated pentylenetetrazol (PTZ) treatment in a TRPV1-dependent manner (Vilela et al., 2017). Furthermore, in another mouse model of epilepsy, CBD increased the seizure threshold in wild type mice, while this effect was not observed in TRPV1-ablated mice, except at high concentrations of CBD (Gray et al., 2019). This would reduce extracellular calcium release and downregulate neuronal hyperexcitability, which would also reduce epileptogenesis (De Petrocellis et al., 2011). Therefore, the anti-seizure properties of CBD may be regulated through TRPV1.

1.2.3 Cannabinoid interaction with adenosine transport and signalling

Many previous studies have indicated that cannabinoids may exert therapeutic action through adenosine transport and signalling. Adenosine is a nucleoside, a regulator of inflammation and an endogenous anticonvulsant (Weltha et al., 2019). This molecule is released during seizures and terminates seizures through activation of adenosine receptors (Boison, 2013). Adenosine kinase over-expression in epilepsy can result in an elevation of adenosine storage in astroglial cells (Williams-Karnesky et al., 2013). This reduces free extracellular adenosine available to inhibit seizures and therefore can result in increased frequency and severity of seizures (Weltha et al., 2019). Furthermore, intracellular adenosine levels are linked to DNA methylation (Kredich and Martin, 1977; Hermes et al., 2007). DNA methylation occurs when a DNA methyltransferase transfers a methyl group from S-adenosyl methionine to DNA, resulting in the production of S-adenosylhomocysteine which is converted into adenosine and homocysteine (Figure 1.3). Therefore, elevated intracellular adenosine results in decreased DNA methylation, and likewise, decreased intracellular adenosine results in increased DNA methylation. The links between adenosine and DNA methylation are important to the progression of epilepsy, known as epileptogenesis. This is because elevated DNA methylation results in epileptogenesis, and adenosine treatment inhibits epileptogenesis through reducing DNA methylation (Williams-Karnesky et al., 2013).

Previous studies have indicated that cannabinoids may block adenosine uptake. CBD has been found to increase extracellular adenosine in rat nucleus accumbens (Mijangos-Moreno et al., 2014) and inhibit the uptake of adenosine into macrophages and microglia by inhibition of

equilibrative nucleoside transporter 1 (ENT1) (Carrier et al., 2006; Liou et al., 2008). CBD-dependent inhibition of adenosine uptake through ENT1 was found to have an anti-inflammatory effect in rat retinal microglial cells and reduced diabetes-related retinal damage in this model (Liou et al., 2008). The neuroprotective effect of CBD treatment on hypoxia in newborn mice was also found to be dependent upon adenosine signalling, as pharmacological inhibition of an adenosine receptor (A_{2A}) reversed the neuroprotective effects (Castillo et al., 2010). CBD may, therefore, act to reduce seizures by modulating adenosine transport or signalling. The extent to which cannabinoid modulation of adenosine transport could affect DNA methylation is not well characterised, however, one study found that THC exposure of rats resulted in dysregulation of DNA methylation in the nucleus accumbens (Watson et al., 2015).

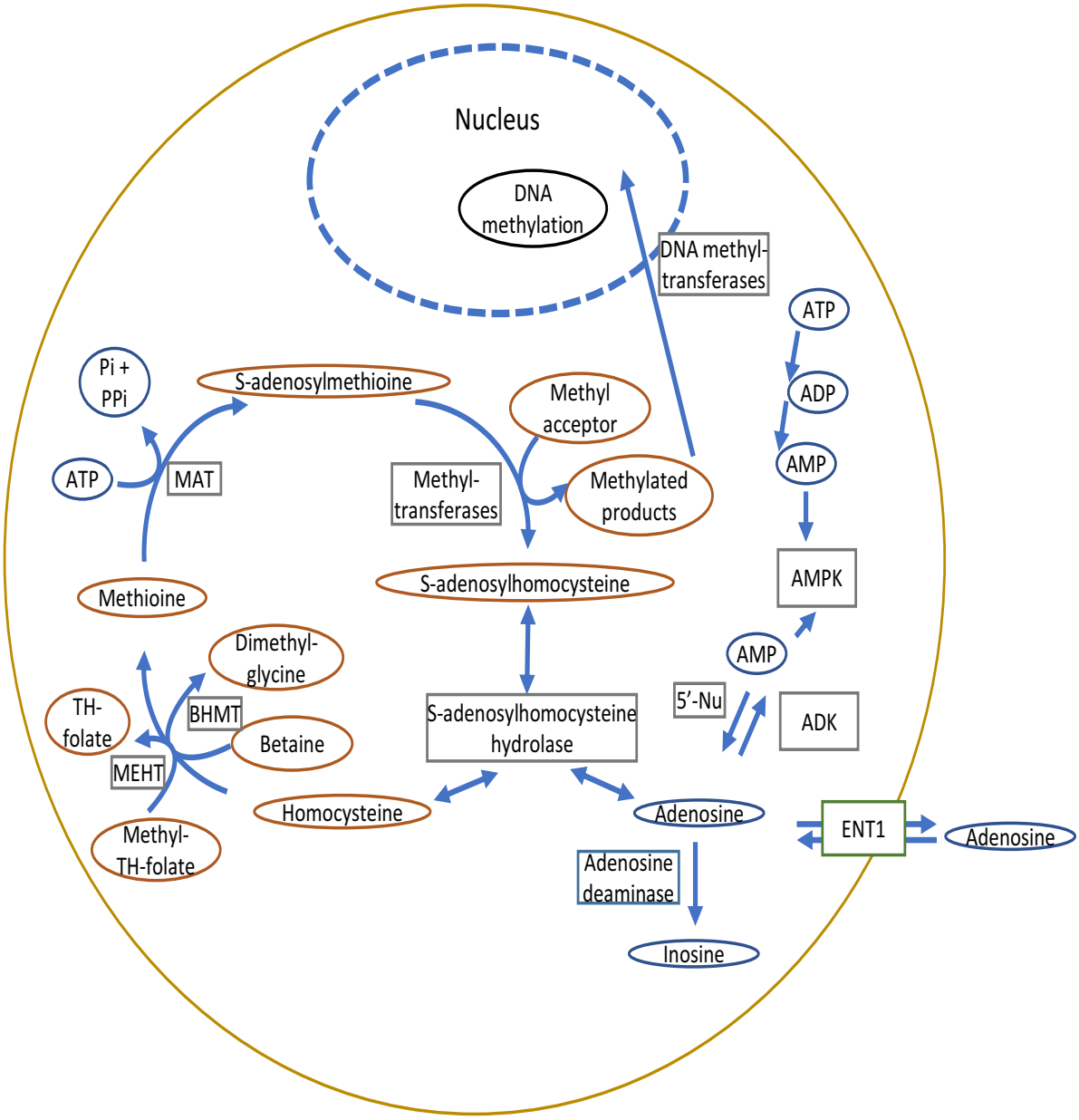

Figure 1.3: Adenosine transporter and DNA methylation. ENT1 (and other adenosine transporters) can transport adenosine into or out of the cell down concentration gradients. Inside the cell, adenosine is rapidly phosphorylated by ADK into AMP, which can activate AMPK. Adenosine is a substrate and inhibitor of S-adenosylhomocysteine hydrolase. S-adenosylhomocysteine is an inhibitor of methyltransferases. Therefore, an elevated level of intracellular adenosine rapidly results in inhibition of the methyltransferase pathway and as a result, decreased DNA methylation (Hermes et al., 2007). TH-Folate: tetrahydrofolate; MEHT: 5-methyltetrahydrofolate–homocysteine S-methyltransferase; MAT: methionine adenosyl transferase; BHMT: betaine–homocysteineS-methyltransferase,5'-Nu: -5'-nucleotidase.

1.2.4 Cannabinoid interaction with mTOR signalling

In previous studies, cannabinoids have been found to regulate mechanistic target of rapamycin (mTOR)-related signalling. The signalling cascade through mTOR integrates intra- and extracellular signals and regulates metabolism, growth, proliferation and survival (Figure 1.4 and

Figure 1.5) (Laplante and Sabatini, 2009). mTOR signalling usually occurs through one of two complexes, mTORC1 or mTORC2, which regulates apoptosis and cell survival (Shaw and Cantley, 2006; Saiki et al., 2011; Kim et al., 2011; Saxton and Sabatini, 2017). Growth factors stimulate mTORC1 through insulin and Ras signalling pathways, while energy depletion results in AMPK activation which inhibits mTORC1 (Shaw and Cantley, 2006; Chakraborty et al., 2010; Pal et al., 2019). Amino acids regulate mTORC1, when leucine is imported into cells this activates mTORC1 through inositol polyphosphate multikinase (IPMK) (Kim et al., 2011). mTORC1 can then regulate protein synthesis, lipid biosynthesis and organelle creation (Laplante and Sabatini, 2009) and limits catabolic processes such as autophagy (Bort et al., 2019). Protein synthesis activation by mTORC1 is promoted by phosphorylation of the eukaryotic initiation factor 4E (eIF4E)-binding protein 1 (4EBP1) and the p70 ribosomal S6 kinase 1 (S6) (Kim et al., 2011). mTORC2 regulates cell survival, metabolism and proliferation through protein kinase B (PKB, also known as Akt) (Kazyken et al., 2019). PKB inhibition results in activation of forkhead box protein (FOXO) transcription factors which control the expression of genes involved in these processes (Wu et al., 2016). PKB can also regulate mTORC1 activity through inhibition of downstream effectors or inhibition of upstream inhibitors (tuberous sclerosis complex (TSC)) (Huang and Manning, 2009). PKB itself is activated by growth factor signalling, which results in the production of phosphatidylinositol (3,4,5)-trisphosphate (PIP_3) by phosphoinositide 3-kinases (PI3K), including IPMK (Chang et al., 2014; Herrero-Sánchez et al., 2016). While insulin signalling can result in inhibition of PKB by diphosphoinositol pentakisphosphate (IP_7), which is produced by a combination of inositol kinase proteins including IPMK, inositol hexakisphosphate (IP6) kinase 1 (IP6K1) and inositol hexakisphosphate and diphosphoinositol-pentakisphosphate kinase 2 (PPIP5K2) (Mackenzie and Elliott, 2014; Kim et al., 2017; Yousaf et al., 2018). mTOR complexes are therefore seen as key regulators of many cellular activities and are often examined as potential therapeutic targets.

Preclinical studies have suggested that CBD upregulates mTORC1 activity, through PI3K- and PKB-dependent manner in neurons of a mouse model of MS, while treating the disease (Giacoppo et al., 2017). In addition, CBD was found to reduce symptoms of psychosis in a rat model while elevating mTORC1 activity (Renard et al., 2016). On the other hand, THC exposure led to an increase in schizophrenia- and psychosis-like symptoms in rats while reducing mTORC1 activity in neurons (Renard et al., 2017(a); Renard et al., 2017(b)). In addition, some studies have found that cannabinoids reduce mTORC1 activity in certain models. In a zebrafish model of tuberous sclerosis complex-associated epilepsy, mTORC1 activity was found to be constitutively elevated, while CBD treatment both reduced seizures and mTORC1 activity in the brain (Serra et al., 2019). Furthermore, in a mouse model of breast cancer, CBD induced apoptosis through downregulation of mTORC1 activity (Sultan et al., 2018). Together, these studies indicate that CBD may have therapeutic effects through regulation of mTORC1 activity. However, these previous studies also suggest contradictory effects of CBD treatment on mTORC1 activity and provide no mechanism for this action.

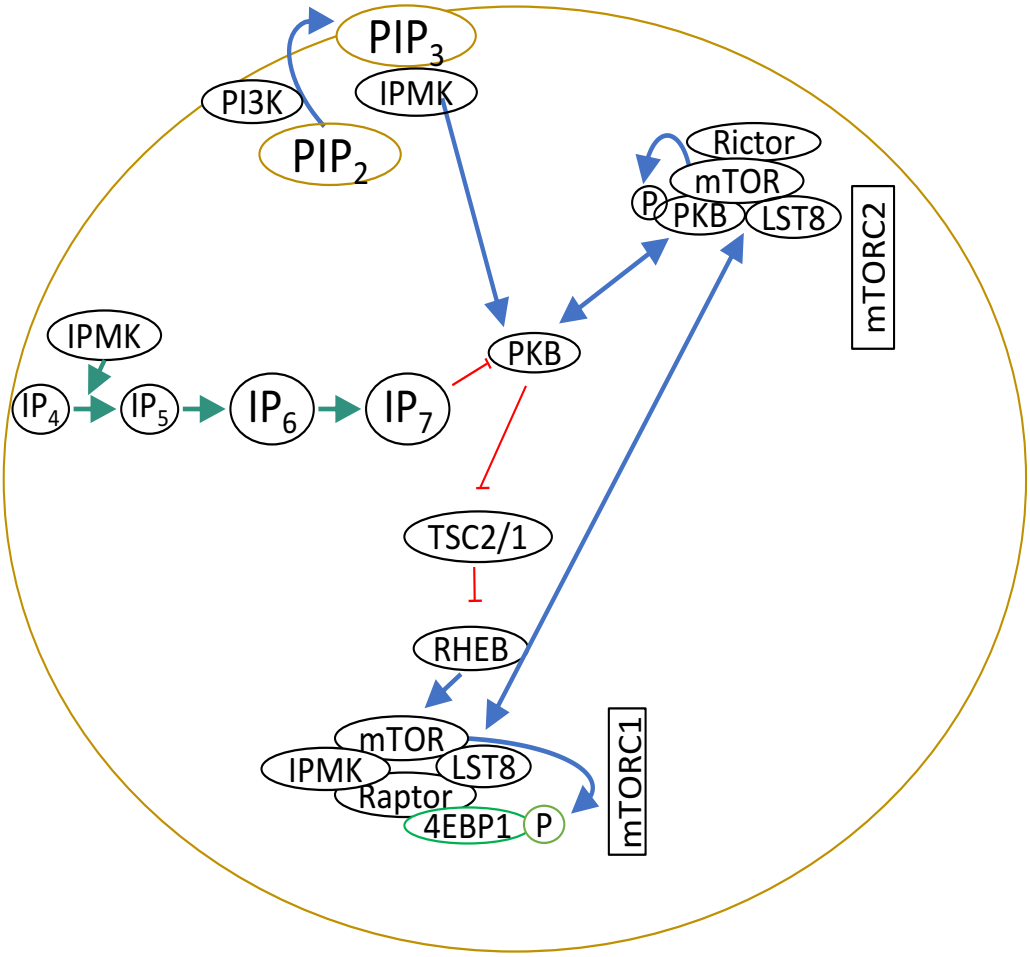

Figure 1.4: mTORC1 signalling components. The protein components of the mTOR signalling pathways are diverse. Often components such as PKB and IPMK can have multiple and opposite roles. Here is a simplified diagram of key components of both mTORC1 and mTORC2.

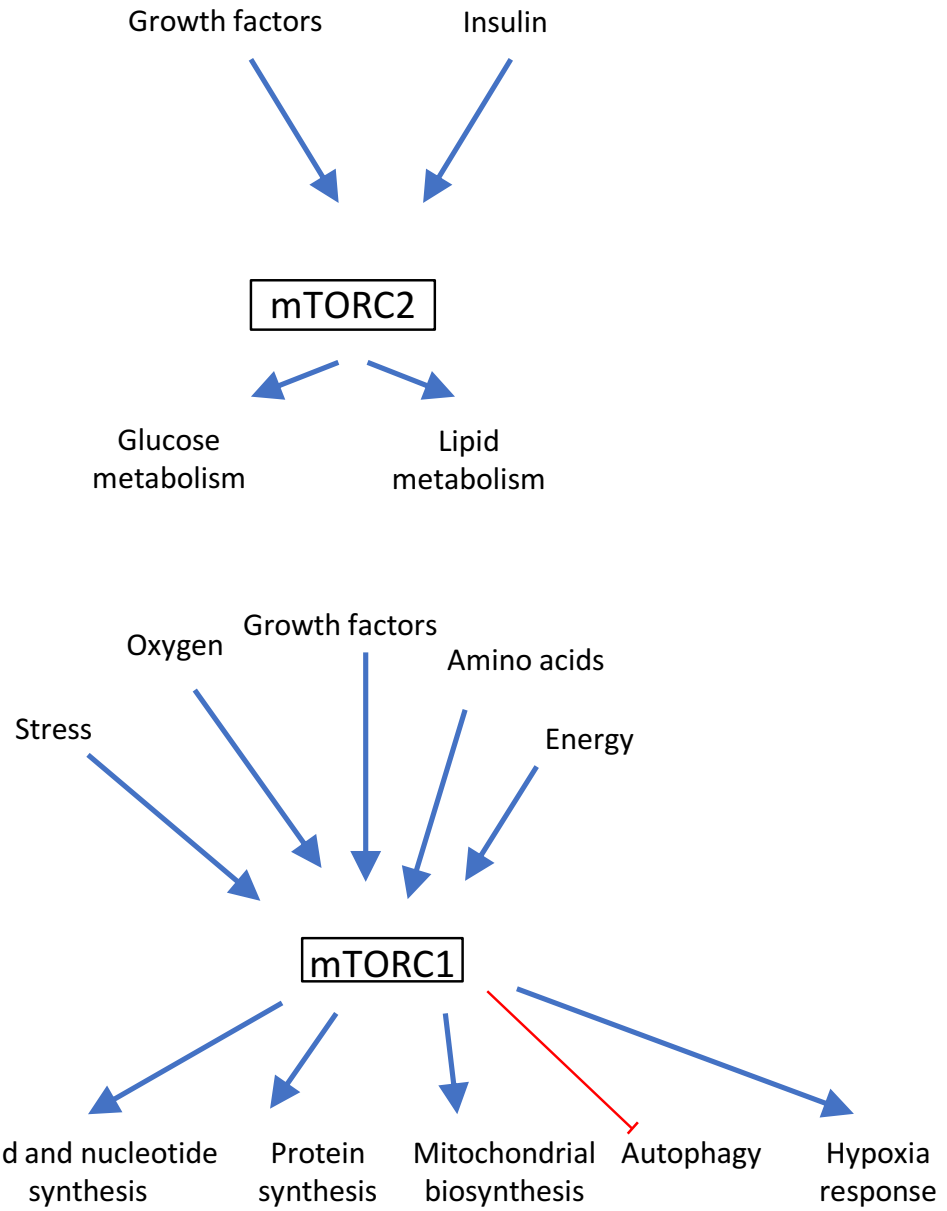

Figure 1.5: mTORC1 and mTORC2 signalling. mTORC1 and mTORC2 are keystones in cell signalling. Regulation of proliferation, survival, metabolism, biosynthesis occurs through mTOR signalling. This brings together energy, insulin, amino acid, glucose and growth factor signalling.

1.1.3 CBG and therapeutic potential

Recent research has focused on the potential therapeutic effects of CBG, given the level of CBG present in therapeutically effective *C. sativa* extracts. In one study, CBG was found to be effective as a neuroprotectant in a mouse Huntington's disease model (Valdeolivas et al., 2015). In addition, CBG reduced reactive oxygen species production in colonic epithelial cells and nitrite production in peritoneal macrophages, suggesting it could have a beneficial effect on inflammatory bowel disease (Borrelli et al., 2013). Similarly, CBG has been shown to have

neuroprotective effects in an *in vitro* model of neuroinflammation (Gugliandolo et al., 2018) where it reduced oxidative stress and increased cell viability (Gugliandolo et al., 2018). Furthermore, CBG reduced tumour growth in colorectal cancer cells and the number of tumours formed in a murine model of colon cancer (Borrelli et al., 2014). Another potential therapeutic role for CBG has been the appetite-stimulant effects of CBG treatment found in a healthy mouse model (Brierley et al., 2016). This appetite-stimulant effect held in a chemotherapy mouse model, where CBG also partially normalised glucose, amino acid and lipid metabolism (Brierley et al., 2019). CBG, therefore, has numerous potential therapeutic functions.

1.3 *Dictyostelium discoideum* as a pharmacogenetic model

Dictyostelium discoideum is a eukaryotic social amoeba commonly used as a pharmacogenetic model organism. *D. discoideum* was first found living in forest detritus in North America (Raper, 1941) and further characterisation revealed that this species was part of the Amoebozoa phylum (Schilde and Schaap, 2013). This organism is often used as a model for chemotaxis (Chisholm and Firtel, 2004), cell differentiation (Uchinomiya and Iwasa, 2013), motility (Robery et al., 2011) and signal transduction (Chang et al., 2020). Phylogenetic analysis revealed that *D. discoideum* was more evolutionarily close to animals than plants, but that fungi split from the animal line more recently than *D. discoideum* (Bapteste et al., 2002; Eichinger et al., 2005). However, a common fungal model organism, yeast, has undergone a higher rate of evolutionary change than *D. discoideum*, meaning that the amoeba is in many ways genetically more similar to animals than yeast (Insall, 2005). The genome of *D. discoideum* contains around 12500 genes and the genome is 34 megabases long (Eichinger et al., 2005). The *D. discoideum* genome is haploid and fully sequenced, allowing the use of this organism as a pharmacogenetic model to examine the molecular mechanisms of many natural compounds. This approach allows rapid identification of proteins responsible for sensitivity to a compound and examination of related signalling pathways.

D. discoideum has a lifecycle with both single- and multicellular aspects, allowing the organism to be used as a model of development, social behaviour and cell differentiation. In a nutrient-rich environment, *D. discoideum* grows as a single-celled organism, phagocytosing bacteria and dividing by binary fission (Raper, 1941). However, during starvation *D. discoideum* can aggregate into a multicellular structure (Figure 1.6), whereby cyclic cAMP release acts as a chemoattractant such that cells migrate towards each other (Brenner and Thoms, 1984). Following aggregation, cells form a multicellular motile slug (pseudoplasmodium) which moves towards attractants that indicate potentially nutrient-rich areas (Kourtis and Tavernarakis, 2009). Development of *D. discoideum* then occurs through the formation of fruiting bodies, which consist of viable spores and a stalk made up of dead cells (Marée and Hogeweg, 2002). During development, due to the

change in nutrient availability and morphology of cells, protein content and gene expression changes, potentially indicating a distinct range of drug targets in pharmacogenetic studies (Sekine et al., 2018). Furthermore, pharmacogenetic studies can also be used to assess the toxicity of a compound, alongside any inhibitory effects it may have on growth (Perry et al., 2020). The development of *D. discoideum* has been used as a simple model for the development of higher eukaryotes to test the safety of epilepsy treatment (Tillner et al., 1998). More recently, characterisation of the γ-secretase complex, which is involved in Alzheimer's disease, also employed development in *D. discoideum* as a phenotypical readout for protein function (Sharma et al., 2019). The multiple aspects of the *D. discoideum* lifecycle, therefore, allow this amoeba to be a useful simple biomedical model.

D. discoideum has also been a useful organism for studying cell-cell signalling. Cyclic AMP is released by starving *D. discoideum* (Chang et al., 2020). Starving cells aggregate through chemotaxis, guided by waves of cAMP (Singer et al., 2019). During early aggregation, cells at the centre of an aggregate periodically release cAMP. This is then detected by cells further away and relayed by surrounding cells in waves (Wessels et al., 1996). Cells chemotax towards the cAMP signal centre, up the gradient during the rising phase of the waves, resulting in a periodic movement to the centre. Initial variations in cell density cause a further increase in cell density in the densest areas, and this results in a centre of aggregation (Levine and Reynolds, 1991). *D. discoideum* have evolved to begin the process of aggregation by cAMP signalling upon starvation, therefore, gene expression begins to change at the point of starvation and components involved in cAMP detection, amplification and breakdown are expressed (Dinauer et al., 1980). cAMP is detected by G protein coupled cAMP receptors and when cAMP is present a transmembrane adenylyl cyclase (AcA). AcA produces cAMP which is then secreted amplifying the cAMP signal and receptor activation, which causes a negative feedback and reduces cyclase activity in this wave (Dinauer et al., 1980). As cAMP concentration rises and falls this process is repeated. cAMP is degraded outside the cell by continuously excreted cAMP phosphodiesterase, reducing the extracellular concentration of cAMP further, allowing the cycle to begin again (Parent and Devreotes, 1996). These findings have helped in the understanding of cell-cell communication and coordination of cell movements within a multicellular organism (Singer et al., 2019).

Due to the sequencing of the *D. discoideum* genome and that the genome is haploid, this organism has been useful for carrying out pharmacogenetic studies. To this end, a mutagenic library was created in *D. discoideum* by random genomic disruption through restriction enzyme-mediated integration of plasmid DNA (Kuspa and Loomis, 1992). The mutant library can be examined for resistance to a pharmacological compound, to identify its molecular mechanism.

Such a method has been used to establish molecular mechanisms of a range of compounds, including naringenin (Misty et al., 2006; Waheed et al., 2014), curcumin (Cocorocchio et al., 2018), CBD (Perry et al., 2020).

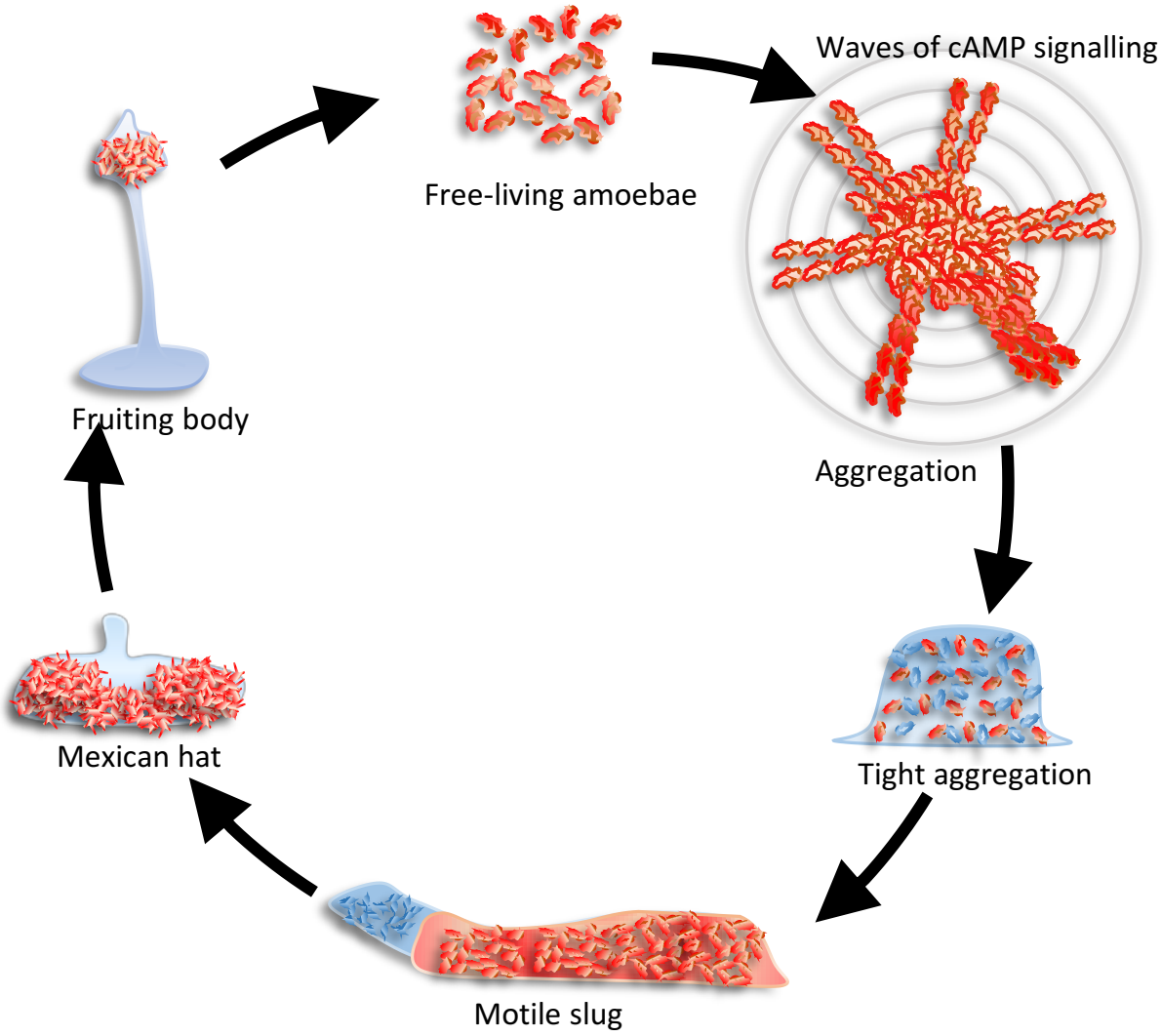

Figure 1.6: The *D. discoideum* life cycle. During the growth phase, *D. discoideum* exists as a free living single celled organism. Red represents *D. discoideum* which have the capability of a free living lifecycle. In blue are cells that have differentiated into becoming future stalk cells. During times of nutrient depletion *D. discoideum* aggregate through cAMP signalling, producing waves and a concentration gradient, highest at the centre of the aggregate. In the tight aggregation, differentiation cells are mixed, however, eventually the cells form a motile slug and the pre-stalk cells are at the leading edge. Once favourable conditions are sensed cells undergo differentiation into spore and stalk cells, initially forming a Mexican hat shape and eventually a fully formed fruiting body.

In fact, *D. discoideum* is a well-established model for use in epilepsy research and discoveries made using *D. discoideum* have been confirmed in mammalian models and impacted the clinical process. Using *D. discoideum* the anti-epileptic drug valproic acid (VPA) was found to inhibit phosphoinositide signalling, which indicated that VPA may treat epilepsy through phosphoinositide regulation (Chang et al., 2012). A structure-activity relationship in *D.*

discoideum found that decanoic acid reduced phosphoinositide production more potently than VPA and this led to the discovery that decanoic acid was more effective in seizure models than VPA (Chang et al., 2013; Augustin et al., 2018).

Lithium is a common treatment for bipolar disorder, however the mechanism of action was relatively unknown (Shaltiel et al., 2004). Using *D. discoideum* both lithium and VPA were found to block development (Williams et al., 2002). Screening the mutant library in *D. discoideum* identified a lithium-resistant mutant and an inactive prolyl oligopeptidase protein responsible for this resistance. An orthologue of this protein has been linked to patients with bipolar disorder previously (Breen et al., 2004). Loss of prolyl oligopeptidase was found to elevate inositol triphosphate levels (IP_3), which appeared to overcome the reduction of IP_3 levels caused by lithium treatment (King et al., 2009). This mechanism was found to also exist in mammalian neurons where lithium caused an enlargement of neuronal growth cones and IP_3 treatment or inhibition of prolyl oligopeptidase reversed this (Williams et al., 2002).

In addition, this technique has previously been used to examine the molecular mechanism of the cannabinoid CBD (Perry et al., 2020). Using the mutant library screen, proteins responsible for the action of CBD were identified as part of the glycine cleavage system. Using gas chromatography-mass spectrometry (GC-MS) analysis CBD was found to reduce cellular methionine levels, while CBD did not affect methionine levels in cells lacking the glycine cleavage system H protein 1 (GCVH1). CBD modulation of methionine levels was found to be conserved in rat cells (Perry et al., 2020).

Furthermore, an examination of the molecular mechanisms of caffeine found that caffeine inhibits PI3K and mTORC2 activity in *D. discoideum*, which in turn inhibits the synthesis of cyclic adenosine monophosphate (cAMP) (Tariqul Islam et al., 2019), confirming a mechanism found previously in mouse embryonic fibroblasts (Saiki et al., 2011). In another study, mTORC1 inhibition of two-pore channel protein opening was examined using *D. discoideum* (Chang et al., 2020) and confirmed a mechanism previously suggested in mammalian cells (Cang et al., 2013; Ogunbayo et al., 2018). DNA methylation has also been examined in *D. discoideum* and a DNA methyltransferase (DNMA) found to be responsible for the silencing of retrotransposons (Kuhlmann et al., 2005). *D. discoideum* has therefore previously been used to identify a molecular target for a cannabinoid and other compounds and these effects were found to be conserved in mammalian systems.

1.5 Aims and Objectives

This research project aims to investigate and characterise potential molecular mechanisms of the cannabinoid, CBG. Initially, the effect of CBG on *D. discoideum* growth and development will be investigated, to indicate the potency in this model and potential developmental effects. This information will then be employed in a targeted approach to investigating CBG function relating to the *D. discoideum* ENT1 protein in adenosine transport and downstream effects on DNA methylation. The CBG growth sensitivity will also be employed to carry out an unbiased approach to identify components of signalling pathways (mTOR) that are involved in the CBG molecular mechanism. Finally, mammalian and clinical models will be used to examine whether the findings in *D. discoideum* are conserved.

2 Methods

(See Appendix 9.1 for Materials)

2.1 Assessment of relative research output for cannabinoids

To assess the relative research output for each cannabinoid, a literature search was performed using “cannabigerol”, “cannabidiol” and “tetrahydrocannabinol” on PubMed (PubMed, 2020).

2.2 Storage of cell lines

D. discoideum cell lines were stored at -80 °C in freezing media (Horse serum, 7% DMSO).

2.3 Maintenance of cell lines

Cells were taken from storage monthly and grown on SM agar plates in the presence of *Raoultella planticola* before being grown axenically in HL5 media with 1 % glucose. HL5 media was supplemented with 100 µg/ml penicillin and 100 µg/ml streptomycin, and cells were maintained at 22 °C in shaking suspension at 220 rpm in flasks, or without shaking in tissue culture dishes. Cells in shaking culture were maintained in 100 ml flasks in 10 ml media to ensure aeration, bunged with cotton wool and covered with foil.

2.4 Growth assays of *D. discoideum* cells

Wild type (AX3 and AX2), dIPMK^{+}, hIPMK^{+}, PKBA^{-}, PKBA^{-}IPMK^{+}, ENT1^{-} and DNMA^{-} *D. discoideum* cells were harvested and diluted in axenic to 2 x 10^{4} cells/ml. Aliquots of cells (10 ml) were grown (at 22 °C) in shaking culture in the presence of increasing concentrations of CBG dissolved in DMSO (0.5 % v/v for all concentrations and control). Cells were maintained in 100 ml flasks in 10 ml media to ensure aeration, bunged with cotton wool and covered with foil. Cell number was recorded between 72 and 168 hours, cell numbers were normalised to the solvent (DMSO)-only control at 168 hours (control). A secondary plot was calculated using the rate of exponential growth, from 96-144 hours, at each concentration and normalised to the no compound vehicle control (DMSO only). Each replicate (n) is a separate biological replicate. Experiments were carried out with mutant cells at the same time as wild type cells, and one biological replication (n) was carried out per week, in which a cell line was grown in the presence of all concentrations of CBG (and DMSO only). Therefore, if n=7 is stated, seven separate biological replicates were carried out, at different times.

To count cells, 10 µl was taken from each flask and placed in a haemocytometer (depth 0.1 mm, Neubauer). Using a Nikon TMS, 25 squares in the haemocytometer were counted, which represented cells in 1/10000 mls. Therefore, the number was multiplied by 10^4 to find cells per ml. If a sample was contaminated it was not counted, and initially there were some replicates missed as it was unclear which concentrations would be key to finding the IC_{50}.

2.5 Development assays of *D. discoideum* cells

Wild type (AX3) *D. discoideum* cells were washed in phosphate buffer twice (2.2 g KH_2PO_4 (monobasic), 0.7 g K_2HPO_4 (dibasic) per litre) then resuspended in phosphate buffer at 1 x 10^7 cells/ml. Cells (1 x 10^7) were then loaded onto nitrocellulose filters and placed on absorbent filter pads with 500 µl of phosphate buffer containing specific concentrations of DMSO and CBG. Filters were left at 22 °C for 24 hours and then imaged to record developmental phenotypes. Development assays were recorded with a Dissection microscope (Leica) with a QICAM FAST 1394 camera (QImaging). Successful development was measured as an array of fully developed fruiting bodies at 24 hours, regardless of specific shape or size.

2.6 Bioinformatics protein analysis

To identify homologous proteins across species the Protein function of the Basic Local Alignment Search Tool (BLAST) was used from the National Centre for Biotechnology Information (NCBI) (https://blast.ncbi.nlm.nih.gov). Primary protein sequences were obtained from uniprot.org and cross referenced against the non-redundant protein sequences (nr) database of BLAST using blastp (protein-protein BLAST).

Sequences were aligned using ClustalW (http://www.ebi.ac.uk/Tools/msa/clustalo/) which was used to align amino acid sequences.

Molecular Evolutionary Genetic Analysis version 7 (MEGA 7) was used to carry out phylogenetic analysis of each protein studied. To produce phylogenetic trees the neighbour-joining statistical method was performed with the bootstrap method test of phylogeny with 500 replications.

Protein domains were identified based on annotations from InterPro (https://www.ebi.ac.uk/interpro/).

2.7 Transfection of *D. discoideum* by electroporation

D. discoideum cells were washed twice times in ice-cold electroporation buffer H50 (20 mM HEPES, 50 mM KCl, 10 mM NaCl, 1 mM MgSO4, 5 mM NaHCO3, 1 mM NaH2PO4, pH 7.0) and resuspended to a concentration of 5 x 10^7 cells/ml. 100 µl of cells and 10 µg of vector were added to a chilled 1 mm gap electroporation cuvette and incubated on ice for 5 minutes. Then, a pulse of 850 V (capacitance 25 µF) was carried out. Cells were incubated on ice for 5 minutes before being transferred into HL5 media. Transfected knockout cells were selected for after 24 hours with 10 µg/ml blasticidin, and over-expressor cells were selected for with 10 µg/ml G418.

2.8 Polymerase chain reaction (PCR) amplification

Amplification of DNA was carried out using GoTaq® G2 Flexi DNA polymerase or Q5 high fidelity DNA polymerase. A standard 20 µl reaction was carried out using 0.1-5 µg of DNA template, 4 µl of GoTaq® Flexi buffer, 2 mM $MgCl_2$, 0.5 mM dNTP mix, 0.5 µM primers and 0.1 µl GoTaq® Flexi DNA polymerase (5 units/µl), made up to 20 µl with nuclease-free water. For creation of over-expressor plasmids, Q5 high fidelity DNA polymerase was used for PCR reactions. Here, a 20 µl reaction contained 0.5 µg of DNA template, 0.5 µM primers, 4 µl 5x Q5 buffer, 0.5 mM dNTP mix, 0.2 µl Q5® DNA polymerase (2 units/µl), made up to 20 µl with nuclease-free water. DNA amplifications were carried out using a PCR machine with an initial denaturing step for 1 minute at 95 °C, followed by 32 cycles of 95 °C for 30 s (denaturation), 50-65 °C for 30 s (annealing) and 6 8°C for 1 minute per 1000 bps (extension) before a final extension step at 68 °C for 10 minutes.

2.9 Restriction digests

Restriction digests were carried out according to manufacturer's instructions (all restriction enzymes were obtained from Thermo Scientific). In cases where multiple enzymes were required, appropriate buffer conditions were found using the DoubleDigest Calculator (Thermo Scientific).

2.10 Agarose gel electrophoresis

To visualise and separate DNA, gel electrophoresis was carried out. Gels contained 1 % agarose in TAE buffer supplemented with ethidium bromide. Loading buffer was added to DNA samples before running and 1 kb hyperladder was used as a marker for DNA size. Gels were run at 110 V for 30 minutes in 1X TAE (Tris base, acetic acid and EDTA) buffer and DNA was visualised using UV illumination.

2.11 Bacterial transformation

Chemically competent *Escherichia coli* cells (from TOP10 chemically competent *E. coli*, Thermofisher, C4040-10) were thawed on ice and 1-10 µg of plasmid was placed directly into the cells. Contents were mixed gently and incubated on ice for 5 minutes, heat-shocked for 1 minute at 42 °C. Samples were transferred to ice again and incubated for a further 5 minutes and 250 µl of LB media was added to each vial and incubated at 37 °C for 1 hour. Cells were plated onto LB agar plates containing 100 µg/ml ampicillin.

2.12 Plasmid extraction from bacterial cells

Bacterial cells were grown overnight (in 5 ml of LB media containing 100 µg/ml ampicillin) at 37 °C on a shaker at 220 rpm. Bacteria were collected by centrifugation at 17000 g for 2 minutes at room temperature and the supernatant discarded. Plasmid was extracted from the cell pellet by GeneJet® plasmid mini-prep kit (according to manufacturer's protocol), HiSpeed Plasmid Maxi Kit or by a non-commercial method. The non-commercial method began with adding 200 µl of resuspension solution to cells collected by centrifugation (10 ml 0.5 M EDTA, 90 g glucose, 6.25 ml 2 M Tris. pH 8.0, made up to 500 ml), which was mixed by vortex. Then 200 µl of lysis solution (50 ml 10% SDS, 20 ml 0.5 M NaOH, made up to 500 ml) was added and mixed by inversion followed by incubation for 5 minutes. 300 µl of neutralisation solution (147 g potassium acetate, 57.5 ml glacial acetate acid, made up to 500 ml) was added and mixed by inversion. Samples were then centrifuged at 17000 *g* for 15 minutes at room temperature and supernatant was collected into new tubes containing 420 µl of isopropanol and mixed. This was centrifuged at 17000 *g* for a further 15 minutes at room temperature and supernatant discarded. Next, 500 µl of 70 % ethanol was added and samples mixed before centrifugation at 17000 *g* for 5 minutes at room temperature and the supernatant discarded. Samples were then placed on a heat block at 50 °C for 10 minutes to dry the DNA. DNA was resuspended in 30 µl nuclease-free water.

2.13 Extraction of genomic DNA

D. discoideum cells were collected from flasks and centrifuged at 500 *g* for 3 minutes. Cells were then washed twice in a phosphate buffer (16.2 mM KH_2PO_4, 4 mM K_2HPO_4. pH 6.8) and then DNA was extracted using DNeasy® Blood and tissue kit or Wizard Genomic DNA Purification Kit (according to manufacturers' protocols).

2.2.14 Creation of knockout cell lines in *D. discoideum*

To knock out ENT1 (and attempt to knockout IPMK), a knockout cassette was generated by PCR amplification of the 5' and 3' arms of the ENT1 gene. This created homologous regions that could be used to recombine with each target gene (Figure 2.1). *NcoI* and *KpnI* cut sites were inserted into the 5' arm of the ENT1 gene (5' and 3' of the arm respectively) and *SpeI* and *PstI* cut sites were inserted into the 3' arm of the ENT1 gene (5' and 3' of the arm respectively). These cut sites were inserted by adding them to primers used to create the knockout cassette. This ensured that during PCR amplification of the regions of ENT1 in interest, each cut site was added. The arms were sequentially cloned into the pLPBLP vector at sites flanking the blasticidin-resistance gene. Transfection of this knockout construct into wild type (AX3) *D. discoideum* resulted in a disruption to the ENT1 gene via homologous recombination, which was checked by PCR amplification of genomic control, vector control and knockout bands (Figure 2.2).

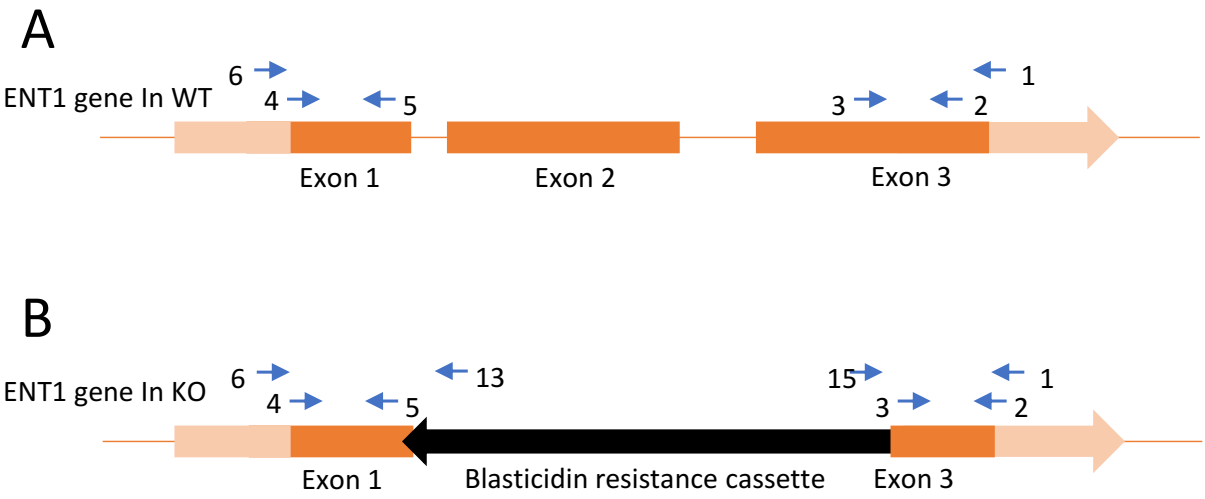

Figure 2.1: ENT1 gene before and after ablation. A: In wild type (WT) cells, the ENT1 gene has three exams. PCR amplification was carried out with primer pair 4 and 5 and primer pair 3 and 2 (see primer table, Appendix 9.1) to create homologous arms to the ENT1 gene to allow the insertion of a blasticidin resistance gene into the centre of ENT1, thus ablating the gene. **B:** In ENT1 KO cells the blasticidin resistance gene has removed exon 2 and some of exons 1 and 3. Correct insertion of the knockout cassette can be analysed by PCR using primer pair 6 and 13 and primer pair 15 and 1.
Dark orange boxes represent exons that are either part of, or altered by, the knockout cassette. Light orange boxes and arrows are parts of exons that remain intact in the genome. In black is the blasticidin resistance cassette.

Cells transfected with knockout constructs were then grown in 10 µg/ml blasticidin in 96 well plates. Cells resistant to blasticidin were collected and centrifuged in PCR tubes before lysis with 24 µl lyse B solution (10 mM TRIS-HCL pH 8.3, 50 mM KCL, 2.5 mM MgCl2, 0.45% TWEEN, 0.45% NP40 substitute**)** and 1 µl proteinase K. Cells were incubated at room temperature for 5 minutes

before heat inactivation for 5 minutes at 95 °C. 2 µl of the cell lysate was analysed by PCR amplification to confirm successful homologous integration.

To confirm that homologous recombination resulted in ablation of ENT1 expression, RT-PCR was carried out. RNA was extracted from wild type and knockout cells using RNeasy mini kit (according to manufacturer's protocol). To avoid DNA contamination in RNA extracts the DNA-free kit (according to manufacturer's protocol). cDNA was synthesised using the RevertAid First Strand cDNA synthesis kit using oligo(dT)$_{18}$ primers (according to manufacturer's protocol). PCR amplification was carried out of the knockout gene and Ig7 (positive control housekeeping gene, which produces the mitochondrial large subunit rRNA (*DDB_G0294034*) (Fukuzawa et al., 2006)).

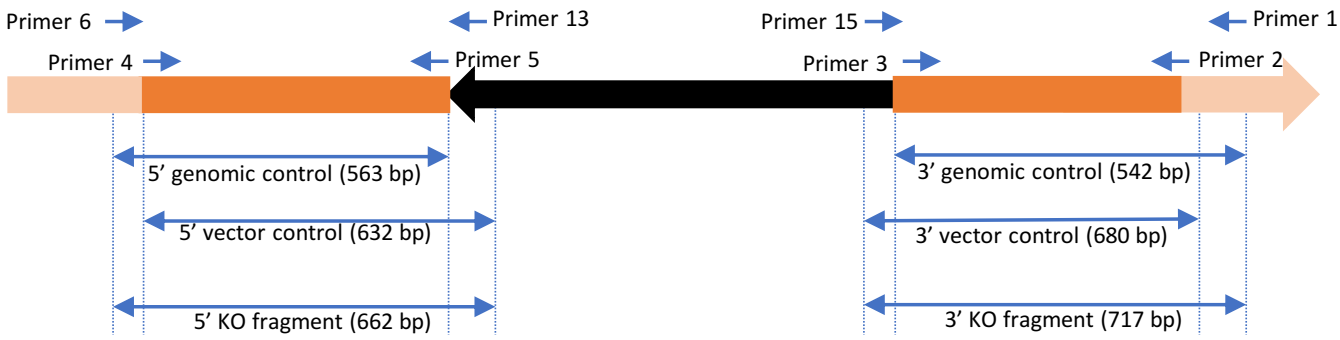

Figure 2.2: ENT1 gene after ablation with primer pairs used for checking. Using the labelled PCR pairs (Appendix 9.1), in PCR amplification, genomic control bands on an electrophoresis gel are visible in wild type, knockout and non-homologous integrant cell lines. Vector control bands are visible in non-homologous integrant and knockout cell lines. KO bands are only visible in knockout cell lines. This is because the pale orange is not present in the knockout cassette, so any plasmid in cells or incorrect insertion sites would not give a KO band.
Dark orange boxes represent exons that are either part of the knockout cassette. Light orange boxes and arrows are parts of exons that remain intact in the genome and are not part of the knockout casstte. In black is the blasticidin resistance cassette.

2.2.15 Analysis of intra- and extracellular adenosine in microglia (carried out at Reading University)

This was carried out by Dr Nicola Gray, Martina Cherubin and Dr Mark Dallas at the University of Reading. To determine whether CBG blocked adenosine transport, a mammalian cell line was employed (Jimmerson et al., 2017). Cell suspension was collected (approx. 500,000 cells) in 500 µL methanol and centrifuged at 13 400 rpm for 10 minutes. For targeted LC-MS profiling, 100 µl sample was then combined with 300 µl water in a 96-well plate and mixed before analysis. Cell medium was also collected and centrifuged for 10 minutes and diluted 1 in 10 with water. Where quantification was performed, 25 µl internal standard solution was added to 20 µl sample and 155 µL water and vortexed mixed before LC-MS analysis.

Liquid chromatography-tandem mass spectrometry analysis was performed using a Shimadzu Nexera UHPLC system and LCMS-8050 triple quadrupole mass spectrometer (Shimadzu Corp., Japan). Chromatography was performed using a Discovery HS F5 150 x 2.1 mm, 3.0 µm column (Supelco, UK). Gradient elution was performed using 0.1 % formic acid in water (mobile phase A) and 0.1 % formic acid in acetonitrile (mobile phase B) at a flow rate of 0.25 mL/minutes, starting at 0% B for 2 minutes, increasing to 25% B at 5.0 minutes, 35% B at 11.0 minutes, 95% B at 15.0 minutes and holding for 5.0 minutes before returning to 0% B for a 5.0 minutes re-equilibration. Column temperature was maintained at 40 °C and an injection volume of 0.5 µl was used.

The mass spectrometer was operated in electrospray ionisation (ESI) mode using positive and negative polarity switching. Data was acquired using multiple reaction monitoring (MRM). The electrospray voltages applied were 4.5 kV (positive mode) and -3.5 kV (negative mode). The interface temperature, heat block temperature and desolvation line temperature were 300 °C, 400 °C and 250 °C respectively. The nebulising gas and drying gas were nitrogen at 3.0 l/minute and 10 l/minute respectively, and the heating gas (air) was delivered at 10 l/minute. Data were acquired and processed using LabSolutions software (Shimadzu Corp.).

Cell medium samples were analysed using the same LC-MS system as described above using a Discovery HS F5 150 x 2.1 mm, 3.0 µm column (Supelco, UK). Gradient elution was performed using 0.1 % formic acid in water (mobile phase A) and 0.1 % formic acid in acetonitrile (mobile phase B) at a flow rate of 0.35 mL/minute, starting at 0% B for 1.4 minutes, increasing to 25% B at 3.5 minutes, 35% B at 7.5 minutes, 95% B at 10.3 minutes and holding for 3.4 minutes before returning to 0% B for a 3.2 minutes re-equilibration. Column temperature was maintained at 40 °C and an injection volume of 1 µL was used.

The mass spectrometer was operated in electrospray ionisation (ESI) mode using positive and negative polarity switching. Data was acquired using multiple reaction monitoring (MRM) and analyte transitions are shown in Supplementary Information (Table S1). The electrospray voltages applied were 4.5 kV (positive mode) and -3.5 kV (negative mode). The interface temperature, heat block temperature and desolvation line temperature were 300 °C, 400 °C and 250 °C respectively. The nebulising gas and drying gas were nitrogen at 3.0 L/minute and 10 L/minute respectively, and the heating gas (air) was delivered at 10 L/minute. Data was acquired using LabSolutions software and processed using LabSolutions Insight (Shimadzu Corp.).

2.2.16 Analysis of DNA methylation in *D. discoideum*

To identify whether CBG modulated DNA methylation in *D. discoideum*, the effect of CBG treatment was examined in this model. To carry this out, wild type cells (AX3) were maintained in control conditions (in the presence of solvent only) or in the presence of 0.25 µM CBG for 24 hours. Genomic DNA was then extracted (using the Wizard Genomic DNA Purification Kit), 200 ng DNA was used per sample (measured by Nanodrop) and total DNA methylation was quantified by colorimetry-based immunochemical binding of methylated DNA (Antonini et al., 2019). A commercial plate reader kit specific for DNA methylation was used (according to manufacturer's protocol) with colorimetric reading at 450 nm.

2.2.17 *D. discoideum* mutant screen

To identify *D. discoideum* mutants resistant to CBG a restriction enzyme-mediated insertional (REMI) library containing 11,000 mutants was employed (provided by Cardiff and Manchester Universities). This library was created at Cardiff University by transfection of wild type *D. discoideum* (AX4) with the restriction enzymes DpnII and NlaIII and linearized DNA (the REMI plasmid digested with BamH1) containing a blasticidin-resistance gene. This resulted in the incorporation of the blasticidin-resistance gene into the *D. discoideum* genome at compatible sites, disrupting the genes at the site of integration. Successfully created mutants were selected for in the presence of blasticidin.

To find mutants resistant to CBG during growth, the pool of mutant cells (11,000) was incubated for 10 days with 8, 10 and 12 µM CBG. These concentrations were chosen as they are in excess of CBG needed to inhibit growth by >90% in wild type cells after 7 days. Cells were seeded at 2.5 x 10^4 cells/ml. Resulting CBG-resistant cells were isolated and made isogenic by growth at 10 cells/plate on *R. planticola* on SM plates. Once isogenic, the location of the REMI insert determined using an inverse PCR technique to isolate the flanking DNA (Keim et al., 2004).

Genomic DNA was extracted from CBG-resistant mutants using Qiagen DNeasy kit, according to manufacturer's protocol. Genomic DNA (10 µl or approximately 20 µg) was then digested with 5 units of *RsaI* at 37 ºC for 1 hour in Tango buffer. The digest was purified by ethanol precipitation, where DNA was incubated for 16 hours in 0.3 M sodium acetate and 20 µl 100 % ethanol at -20 °C, which was collected by centrifugation at 5 °C, 16000 *g* for 15 minutes. The DNA was then resuspended in nuclease-free water and circularised by ligation with 0.5 µl T4 DNA ligase in 10 µ reactions at room temperature for 1 hour. PCR was used to amplifying the *D.*

discoideum genomic sequence flanking the blasticidin-resistance gene with primers P9 and P10, with an annealing temperature of 50 °C.

PCR products were then analysed through one of two methods. Either purified by QIAquick® PCR purification kit (according to manufacturer's protocol and sent directly for sequencing with the p9 and p10 primers (13 and 14 in Appendix Figure 9.1). Alternatively, PCR products were ligated into the TOPO pCR® 2.1 vector and cloned into bacteria using the TOPO TA cloning® kit (according to manufacturer's protocol). The plasmid was then sent for sequencing with the T7 and M13 primers (16 and 17 in Appendix Figure 9.1).

2.2.18 qPCR analysis of CBG-resistant mutants

RNA was extracted from wild type and mutant cells maintained in control conditions using the RNeasy kit, and cDNA was produced First-strand cDNA synthesis kit. cDNA was then analysed by qPCR using primers 100 bp apart from the gene of interest (IPMK). Total expression levels were quantified by qPCR using SYBR® Green Jump Start™ Taq Ready Mix, as per manufacturer's instructions. Fold changes were calculated using the ΔΔ-Ct method. Expression levels were normalized to the constitutively expressed Ig7 housekeeping gene, which produces the mitochondrial large subunit rRNA (DDB_G0294034) (Fukuzawa et al., 2006).

2.2.19 Creation of dIPMK-RFP and hIPMK-RFP cell lines and imaging (and attempt at ENT1-RFP)

RNA was extracted from wild type *D. discoideum* using RNeasy mini kit (according to manufacturer's protocol). DNA was removed from the RNA using the DNA-free kit. cDNA was synthesised using the RevertAid First Strand cDNA Synthesis Kit using oligo(dT)18 primers (according to the manufacturer's protocol). The *D. discoideum* IPMK (DDB_G0281737) was amplified by PCR of the dIPMK gene cDNA and the human IPMK (hIPMK: Uniprot Q8NFU5, NCBI GeneID 55847) was synthesised with *D. discoideum* codon bias (GenScript) and both genes were cloned into the pDM324 plasmid containing a C-terminal red fluorescent protein (RFP) tag (Veltman et al., 2009) to create an over-expressor construct. The vector was electroporated into wild type (AX3) *D. discoideum* cells and selected by growth in the presence of geneticin (G418) at 10 μg/mL. Cells expressing the plasmids were imaged using fluorescent microscopy under 1% agar.

2.2.20 RFP expression confirmation by Western Blot

To confirm the expression of RFP constructs, Western blot analysis was carried out. The cells were then harvested and resuspended in western blot loading buffer (total volume 30 ml of 2X Laemmli Sample Buffer containing: bromophenol blue approx. 0.001 g, 2-mercaptoethanol (2-ME) 3 ml, 100 % glycerol 6 ml, 10% SDS solution 12 ml, 0.5 M Tris-HCl 7.5 ml, H_2O 1.5 ml) at a concentration of $2.5x10^7$ cells/ml. The samples were boiled at 98 °C for 6.5 minutes and then frozen at -20 °C. Samples were then loaded onto a 15% polyacrylamide gel and run at 70 volts for 30 minutes and 100 volts for 1 hour. The gel was transferred for 17 hours onto a PVDF 0.2 µm membrane at 15 volts at 5 °C. The membrane was blocked twice for 1 hour each with 5% milk Tris-buffer saline with 1% Tween (TBST). The blots were incubated with primary antibody (anti-RFP), at 1 in 1000 concentration in 5% milk TBST for 18 hours, washed with TBST, then incubated with fluorescently labelled (800) secondary antibody (anti-rat) at 1 in 10000 concentration in 5% milk TBST for 1 hour, washed with TBST and imaged. Streptavidin (1:5000 Streptavidin) was used as a loading control (Davidson et al., 2013).

2.2.21 Western blot analysis of mTORC1 activity in *D. discoideum*

Wild type (AX3), $IPMK^+$, $PKBA^-$ and $PKB^-/PKGB^-$ *D. discoideum* cells were treated with purified CBG, CBD, cannabidiolic acid (CBDA) and cannabidivarin (CBDV) (phytocannabinoids at a concentration of 0.25 µM) or a PI3K inhibitor (60 µM) (LY294002) for 1 hour or with solvent only (DMSO). The cells were then harvested and resuspended in western blot loading buffer (total volume 30 ml of 2X Laemmli Sample Buffer containing: bromophenol blue approx. 0.001 g, 2-mercaptoethanol (2-ME) 3 ml, 100 % glycerol 6 ml, 10% SDS solution 12 ml, 0.5 M Tris-HCl 7.5 ml, H_2O 1.5 ml) at a concentration of $2.5x10^7$ cells/ml. The samples were boiled at 98 °C for 6.5 minutes and then frozen at -20 °C. Samples were then loaded onto a 15% polyacrylamide gel and run at 70 volts for 30 minutes and 100 volts for 1 hour. The gel was transferred for 17 hours onto a PVDF 0.2 µm membrane at 15 volts at 5 °C. The membrane was blocked twice for 1 hour each with 5% milk Tris-buffer saline with 1% Tween (TBST). The blots were incubated with primary antibody (p4EBP1), at 1 in 1000 concentration in 5% milk TBST for 18 hours, washed with TBST, then incubated with secondary antibody (anti-rabbit (horseradish peroxidase conjugated)) at 1 in 5000 concentration in 5% milk TBST for 1 hour, washed with TBST and imaged using chemifluorescent substrate. Streptavidin (1:5000 Streptavidin) was used as a loading control (Davidson et al., 2013).

2.2.22 Higher order inositol phosphate analysis in *D. discoideum*

Wild type (AX3) and *IPMK*$^{+}$ cells (1 x 10^7) were treated with vehicle solvent only control (DMSO) or 0.25 µM CBG or CBD for 1 or 24 hours. Inositol polyphosphates were analysed as previously described (Pisani et al., 2014). Cell pellets were dissolved in 1 M perchloric acid (40 µl) containing 3 mM EDTA, incubated on ice for 10 minutes, centrifuged (10 minutes, 20000 *g* at 4 ˚C) and the supernatant was neutralised with 1 M potassium carbonate (18 µl). Samples were incubated on ice for 2 hours, centrifuged at 20000 *g* and the supernatants collected. Samples were mixed with OrangeG and run on a 35 % polyacrylamide gel for 17 hours at 4 °C at 600 V and 6 mA. Gels were stained with toluidine blue, then scanned with a desktop computer for image analysis with ImageStudio Lite (Li-Cor, version 5.0).

2.2.23 Mouse embryonic fibroblast cell culture

Mouse embryonic fibroblasts were grown in tissue culture flasks (in Dulbecco's Modified Eagle Medium (DMEM) containing 10% fetal bovine serum (FBS)) at 37 ˚C, 5% CO2, and regularly passaged. Fresh cells were used monthly. Cells were collected using Trypsin (0.25 % Trypsin, 0.1 % EDTA).

2.2.24 Western blot analysis of mTORC1 activity in mouse embryonic fibroblasts

Wild type and IPMK$^{-/-}$ mouse embryonic fibroblasts (Maag et al., 2011) were treated with solvent control only (DMSO) or 4 µM CBG or CBD or PI3K inhibitor (10 µM) (Pictilisib) for 24 hours in Dulbecco's Modified Eagle Medium (DMEM) containing 10% fetal bovine serum (FBS). Cells were seeded at 1.5 x 10^5 per sample, and following a 24-hour treatment, cells were collected (Trypsin) and lysed using RIPA buffer containing 2% phosphatase inhibitor and 1% protease inhibitor. Cell lysates were boiled in western blot loading buffer at 96°C for 6.5 minutes and then proteins were separated by 15% polyacrylamide gel run at 70 volts for 30 minutes and 100 volts for 1 hour and transferred to a 0.2µm PVDF membrane for 17 hours. The membrane was blocked with 5% milk Tris-buffered saline and incubated overnight at 4°C with 1:1000 diluted primary antibody p4EBP1, total 4EBP1, actin (loading control) in TBS with Tween 20 (TBST) for 2 hours at room temperature with 1:5000 diluted horseradish peroxidase-conjugated secondary antibody anti-rabbit and anti-mouse. The signals were detected with chemifluorescent substrate and recorded on an Odyssey CLx.

2.2.25 Primary peripheral blood mononuclear cell collection from human volunteers (carried out at Trinity College Dublin)

Healthy volunteers (Hv) and people with multiple sclerosis (pwMS) attending clinics at Beaumont Hospital, Dublin, Ireland, were recruited for this study. This experiment was carried out by Lisa Costelloe, Dr Eric Downer and John-Mark Fitzpatrick. Written informed consent was obtained from each participant and the study received ethical approval from the Beaumont Hospital Ethics (Medical Research) and the Faculty of Health Sciences Research Ethics Committee, Trinity College Dublin, Ireland. The recruitment of pwMS into the study was via a Consultant Neurologist and all pwMS had a relapsing-remitting (RR) form of MS as defined by the revised McDonald criteria (Kurtzke 1983, Polman et al., 2011) including patient history, clinical signs and symptoms, physical examination and adjunctive diagnostic tools including MRI. Some pwMS were on immunomodulatory treatment including gilenya, dimethyl fumarate and plegridy. Healthy volunteers with no history of autoimmune, cardiovascular, respiratory or degenerative disease were included. Healthy volunteers were matched based on age and gender. Details of participant demographics are presented in Table 1. Primary peripheral blood mononuclear cells PBMCs were prepared from venous whole blood samples by way of venipuncture (max 50 ml per donor collected in EDTA tubes) from healthy control participants (mean age 42.0 ± 2.6 years; n = 6) and pwMS (mean age 35.3 ± 5.0 years; n = 6). PBMCs were isolated by density separation over Lymphoprep™. In summary, whole blood samples were diluted 1:1 with sterile PBS and gently overlaid onto Lymphoprep. Each sample was subjected to centrifugation while in contact with Lymphoprep, the PBMC layer was separated, washed with PBS and resuspended in RPMI [supplemented with 10% FBS, penicillin and streptomycin (100 µg/ml for both)]. PBMCs were ($1x10^6$ cells/ml; 3 ml per well) maintained in culture for at least 2 hours prior to treatment with highly-purified CBD or CBG (100 nM), or THC:CBD combinations (20 nM:17 nM) for 24 hours.

2.2.26 Western blot analysis of mTORC1 activity in primary peripheral blood mononuclear cells

PBMCs were lysed using RIPA buffer containing 2% phosphatase inhibitor and 1% protease inhibitor. Cell lysates were boiled in western blot loading buffer at 96°C for 6.5 minutes and then proteins were separated by SDS-PAGE gel electrophoresis (15%) and transferred to a 0.2 µm PVDF membrane for 17 hours. The membrane was blocked with 5% milk Tris-buffered saline and incubated overnight at 4°C with 1:1000 diluted primary antibody (p4EBP1), total 4EBP1, IPMK, actin in Tris-buffer saline (TBS) with Tween 20 (TBST) and 2 hours at room temperature with

1:5000 diluted horseradish peroxidase-conjugated secondary antibody anti-rabbit, anti-mouse. The signals were detected with chemifluorescent substrate and recorded on an Odyssey CLx (Li-Cor).

2.2.27 Statistical analysis

Normality tests for data were carried out using Shapiro-Wilks. If data were found to be normally distributed, then a One-Way ANOVA with a Post-Hoc Test of either Dunnett's or Bonferroni's multiple comparisons. Bonferroni's was used when each data set was compared to all others, for example wild type (control), mutant (control), mutant (treatment A), mutant (treatment B). While a Two-Way ANOVA would be used if the sample included wild type (control), wild type (treatment A), wild type (treatment B), mutant (control), mutant (treatment A), mutant (treatment B). As this full data set was not present in the first example, a Two-Way ANOVA could not be carried out and the author found the best alternative to be a Bonferroni Post-Hoc Test on a One-Way ANOVA. Dunnett's was used to compare multiple treatments to a control, for example wild type (control), wild type (treatment A), wild type (treatment B).

If data were found to not be normally distributed then a Kruskal-Wallis Test with a Dunn's Multiple Comparison Post-Hoc Test, or Mann Whitney test was carried out to test for significance. Mann Whitney Test was used to compare two data sets at a time. Dunn's was used to compare multiple data sets to a control, for example wild type (control), wild type (treatment A), wild type (treatment B).

Significance was found if $P \leq 0.05$. In all graphical representations of data * denotes $p<0.05$, ** denotes $p<0.01$. Data are represented as mean ± SEM. Statistical analysis was carried out using GraphPad Prism Software. In this thesis, n number represents biological replicates for all experiments.

From visual inspection of the data, homogeneity of variances was assumed to be met. In addition, where ANOVA tests were carried out, this takes into account whether the variance within a data set was larger than variance between data sets when providing significance.

Chapter 3: Examining adenosine transport regulation as a molecular mechanism of CBG

3.1 Introduction

Cannabigerol (CBG) is an abundant, non-psychotropic cannabinoid without fully characterised molecular targets. CBG is present in *Cannabis sativa* plants often at a similar concentration to cannabidiol (CBD), but usually lower than tetrahydrocannabinol (THC) (Swift et al., 2013). However, both CBG and CBD are non-psychoactive, so present a large advantage as potential therapeutics with fewer side effects. The molecular mechanisms of CBG are relatively understudied compared to CBD and THC (Abrams, 2018), however, the three cannabinoids share a similar molecular structure (Figure 1.1) (Hill et al., 2014). Given that *C. sativa* extracts containing CBG are effective epilepsy treatments (Devinsky, Verducci, et al., 2018) and multiple sclerosis treatments (Serpell et al., 2013), it remains important to understand if CBG has therapeutic potential (Freeman et al., 2019). Therefore, this chapter aimed to search for molecular mechanisms of CBG.

One molecular mechanism of cannabinoids that has previously been examined is the inhibition of adenosine signalling and transport. This mechanism provides a therapeutic potential for cannabinoids in the treatment of a range of diseases where adenosine signalling pathway is impacted by disease pathophysiology. As a result, adenosine signalling is a therapeutic drug target for schizophrenia (Rosse, 2017), epilepsy (Zhang et al., 2018), Alzheimer's disease (Lee et al., 2018), and acute kidney injury (Grenz et al., 2012). CBD, a similar cannabinoid to CBG, is known to inhibit adenosine transport through ENT1 (Carrier et al., 2006; Liou et al., 2008). Furthermore, adenosine transport is linked through biochemical pathways to DNA methylation, whereby intracellular adenosine levels and DNA methylation have an inverse relationship (Figure 1.3) (Hermes et al., 2007; Williams-Karnesky et al., 2013). Since the study of biochemical pathways in mammalian systems can be time-consuming and expensive (Cosson et al., 2002; Steinert and Heuner, 2005), *D. discoideum* can be employed as a simple model system to examine molecular mechanisms of compounds (Williams, 2005; R.S.B. Williams et al., 2006; Schaf et al., 2019). Thus, to investigate whether the molecular mechanism of CBG involved adenosine signalling and to examine this mechanism, a simple biomedical model was employed.

3.2 Results

3.2.1 Effects of CBG on *Dictyostelium discoideum* growth and development

As a first step to characterise the effects of CBG on cells, *D. discoideum* growth was measured in the presence of CBG. In these experiments, wild type cells were grown in the presence of increasing concentrations of CBG over 168 hours. Cells were then counted daily. Under control conditions (in the presence of solvent only), wild type (AX3) *D. discoideum* cell growth showed a lag phase until 96 hours, an exponential phase to 144 hours and a stationary phase starting at 168 hours (Figure 3.1 A). At low concentrations, CBG (0.02 µM) did not significantly inhibit growth. In contrast, CBG at 0.1 µM and higher concentrations significantly inhibited growth at 168 hours ($P<0.01$, Mann Whitney test). Data arising from this analysis (rate of growth and Log of concentration) was used to calculate an IC_{50} of 0.22 µM (Figure 3.1 B). These data show a dose-dependent reduction in growth of *D. discoideum* caused by CBG.

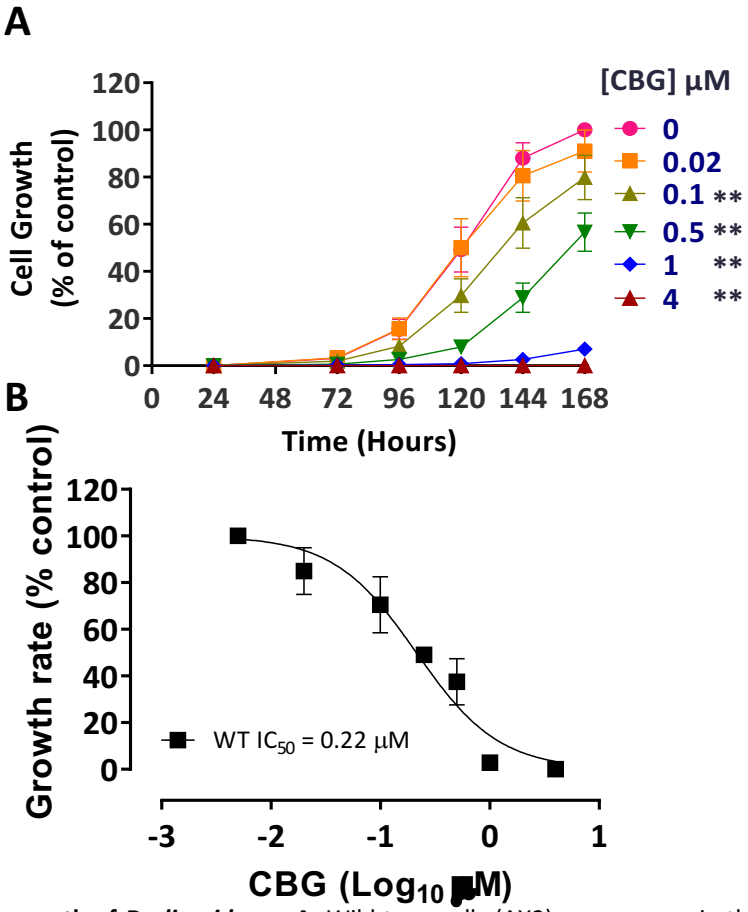

Figure 3.1: CBG inhibits growth of *D. discoideum*. A: Wild type cells (AX3) were grown in the presence of increasing concentrations of CBG (and solvent only control, 0) for 168 hours. CBG inhibited cell growth in a concentration-dependent manner (n=10). Data were not normally distributed (Shapiro Wilks), therefore a Mann Whitney test was carried out to test for significance of inhibition by each concentration of CBG compared to control at 168 hours, ** - $p<0.01$. Graphs show mean ± SEM. Growth rate at each concentration of CBG was used to produce a secondary plot. **B:** Secondary plot analysis was used to determine the IC_{50} = 0.22 µM (n=10). The 95 % confidence intervals (CI) for these data were 0.14 to 0.31 µM.

To further analyse the effects of CBG treatment on *D. discoideum*, response of this model to CBG during development was measured. During development, a distinct set of signalling pathways, and thus proteins, are involved compared to growth, potentially providing different cellular targets in the model system (Kuspa and Loomis, 1992). To determine the effect of CBG on development, wild type *D. discoideum* cells (AX3) were starved for 24 hours in a saline solution containing CBG at a range of concentrations up to five times the concentration shown to block growth (20 µM). The phenotype expected if development was occurring correctly, was a tall thin stalk and round spore head, but natural variation was expected, including slightly different shaped spore heads, a straight, curved or wavy stalk, and a variation of sizes. When development is blocked or delayed in *D. discoideum*, this is verified by the development at 24 hours not being at the correct stage, i.e. perhaps at the slug or mound stage (Cocorocchio et al., 2018; Kelly et al., 2018; Sharma et al., 2019). Under control conditions (in the presence of solvent only), development occurred, leading to the formation of fruiting bodies, comprised of a stalk and a spore head (Figure 3.2 A). In the presence of CBG up to 20 µM, no difference in developmental phenotype was observed, thus fruiting bodies formed, comprised of a stalk and a spore head (Figure 3.2 B, C, D). These experiments indicated that CBG did not affect multicellular development of *D. discoideum* up to 20 µM and implied CBG had a non-toxic inhibitory effect on growth. Development of a stalk and spore head was not changed, the variation in size and shape was expected, but future work could determine the relevance of these changes if any. This also implied that CBG was not lethal to *D. discoideum* and instead inhibited a specific action involved in growth.

3.2.2 Examining adenosine transport modulation as a potential molecular mechanism of CBG

One potential molecular mechanism of CBG is adenosine signalling. A cannabinoid with similar structure to CBG, CBD, has previously been shown to affect adenosine signalling and adenosine transport via the equilibrative nucleoside transporter, ENT1 (Carrier et al., 2006; Liou et al., 2008). In these previous studies, CBD was found to inhibit adenosine uptake by ENT1 into rat macrophages and microglia (Liou et al., 2008), with the effect conserved in a whole organism experiment in mice (Carrier et al., 2006). The primary function of the mammalian ENT1 protein is to transport adenosine, however, this protein also has a low affinity for general nucleosides across the plasma membrane (Baldwin et al., 2004). The *D. discoideum* proteome was searched using BLAST to identify potential ENT1 orthologues. One potential ENT1 orthologue (Dictybase ID: DDB_G0283439) was found in *D. discoideum* using this method and alignment of the *D. discoideum* and *H. sapiens* ENT1 proteins (using Clustal W) indicated that the two proteins shared 30.4 % amino acid identity (Figure 3.3 A), key transmembrane domains and a membrane

localisation motif (Figure 3.3 B). Phylogenetic analysis (using MEGA 7 to produce a neighbour-joining tree with 500 Bootstrap replications) showed the *H. sapiens* and *D. discoideum* ENT1 to be within the same clade, suggesting a common evolutionary origin (Figure 3.3 C). The ENT1 protein in *D. discoideum* was therefore identified as an adenosine signalling-related protein

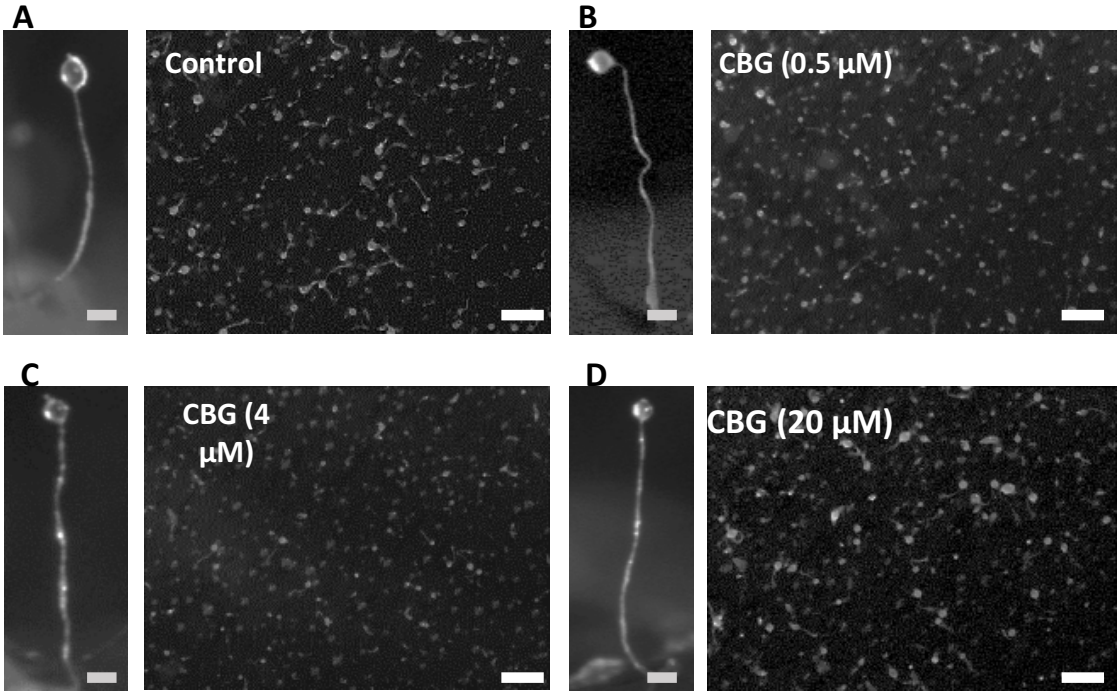

Figure 3.2: CBG does not affect development of *D. discoideum*. Wild type *D. discoideum* cells, developed for 24 hours under starvation conditions. **A:** In the absence of CBG (solvent only), fruiting bodies formed, viewed from the side comprised of a stalk and a rounded spore head at the top of stalks (scale bar: 250 μm for side view) and viewed from top the field of view contains numerous examples of fruiting bodies (scale bar: 1 mm for top view). **B, C, D:** In the presence of CBG (0.5, 4 or 20 μM), development of the fruiting was unaffected. *D. discoideum* cells, developed for 24 hours under starvation conditions formed fruiting bodies, viewed from the side comprised of a stalk and a rounded spore head at the top of stalks and viewed from the top a field of mature fruiting bodies viewed.

which could be explored to examine modulation of activity by CBG.

In order to examine potential effects of CBG on ENT1 in *D. discoideum*, a cell line lacking ENT1 was made. This cell line was created using a homologous recombination plasmid containing sections of ENT1 genomic DNA. The ENT1 genomic DNA sections were synthesised by PCR amplification of 5' and 3' regions of the ENT1 gene, and then each fragment was inserted into opposite sides of a blasticidin-resistance gene in the pLPBLP plasmid (Figure 3.4 A). To ensure the plasmid was correctly constructed, a restriction digest was carried out with restriction enzymes cleaving at the 5' and 3' ends of each insert and across the whole knockout cassette (Figure 3.4 B). The plasmid was then transfected into wild type (AX3) *D. discoideum* cells and PCR screening was carried out to ensure homologous recombination had occurred at the ENT1 genomic location (Figure 3.5 A and B). Cells found to have undergone homologous recombination were isolated and then reverse transcriptase (RT)-PCR was carried out to confirm

that ENT1 gene expression was ablated and expression was lost (Figure 3.5 C). Therefore, a *D. discoideum* cell line lacking ENT1 expression (ENT1^{-}) had been successfully created and could be examined to determine the effect of CBG treatment on ENT1 activity.

A

```
Dictyostelium discoideum      MTNRDEYSPLVDITETSKAPLDKNGLAWICFLILGVGLLFPFNCYVAASDYFSDLYGDSY   60
Homo sapiens                  -------------MTTSHQPQDRYKAVWLIFFMLGLGTLLPWNFFMTATQYFTNRLDMSQ   47
                                           **: * *:   .*: *:::*:* *:*:* :::*::**::  . *

Dictyostelium discoideum      SFLMSLA-------------------------YNYIQ--------WLLLFVSIFVMPRFS   87
Homo sapiens                  NVSLVTAELSKDAQASAAPAAPLPERNSLSAIFNNVMTLCAMLPLLLFTYLNSFLHQRIP  107
                              .. :  *                          :* :          *: ::. *:  *:

Dictyostelium discoideum      FKSRTILFLLAGSLILFYMPFN-NMIFGR---NEKVSMGISLLCTFASGCLASLLFGTVL  143
Homo sapiens                  QSVR-----ILGSLVAILLVFLITAILVKVQLDALPFFVITMIKIVLINSFGAILQGSLF  162
                               . *     : ***: : : *  . *: :   :    : *:::  .  ..:.::* *:::

Dictyostelium discoideum      GLVALFPGEYTGAVMSGNGVAGMIAMALQIITKVSVPATAHGNQESGLIFFFLAGGVLII  203
Homo sapiens                  GLAGLLPASYTAPIMSGQGLAGFFASVAMICA----IASGSELSESAFGYFITACAVIIL  218
                              **..*:*..**. :***:*:**::* .  * :     *:.   .**.: :*: * .*:*:

Dictyostelium discoideum      CLLCFLVLLQLPITKYYLANFEASKLKENGSVNGIESGDGDAKPKK------SAR---QW  254
Homo sapiens                  TIICYLGLPRLEFYRYYQQLKLEGPGEQETKLDLISKGEEPRAGKEESGVSVSNSQPTNE  278
                               ::*:* * :* : :**       .  ::: .:: *..*:     *:      *     :

Dictyostelium discoideum      MGELLNILKKVWREALVVFTVFFTTLSIFPGLTQLIQTSNEHQLSSDW----FIIVFFSI  310
Homo sapiens                  SHSIKAILKNISVLAFSVCFIFTITIGMFPAVTVEVKSSIAG--SSTWERYFIPVSCFLT  336
                                .:  ***::   *: *  :*  *:.:**.:*  :::*     ** *    : :  *

Dictyostelium discoideum      FMVGDFIGRTVPKWFIIFTPSNLWIPTFL--RLAFFPLFALCI------KPLVFNNNAWY  362
Homo sapiens                  FNIFDWLGRSLTAVFMWPGKDSRWLPSLVLARLVFVPLLLLCNIKPRRYLTVVFEHDAWF  396
                              * : *::**::   *:    .. *:*:::  **.*.**: **         :**:::**:

Dictyostelium discoideum      FVFMFIFSISNGYCGTLAMIFGPTKAEEHEKEYAGIIMSFFLNFGIWVSTHFAFLLSYLV  422
Homo sapiens                  IFFMAAFAFSNGYLASLCMCFGPKKVKPAEAETAGAIMAFFLCLGLALGAVFSFLFRAIV  456
                              :.**  *::**** .:*.* ***.*.:  * * ** **:*** :*: :.: *:**:  :*

Dictyostelium discoideum      TGSTGINF* 430
Homo sapiens                  --------- 456
```

B

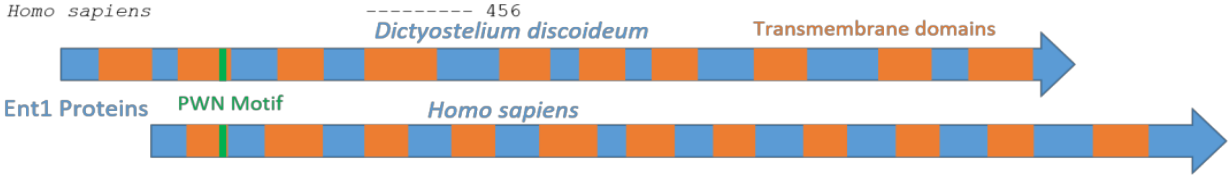

C

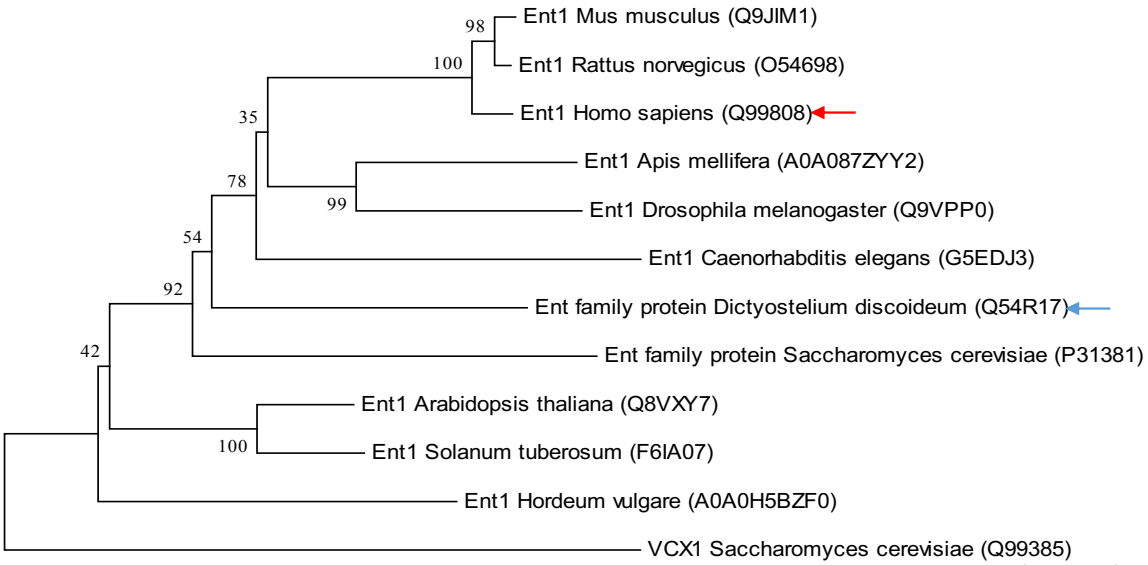

Figure 3.3: Similarity between *D. discoideum* and *H. sapiens* ENT1 proteins. **A:** *D. discoideum* (Q54R17) and *H. sapiens* (Q99808) ENT1 protein sequence alignment was carried out on Clustal Omega. The two proteins share a sequence identity of 30.4 %. Asterisks identical, colons highly similar and full stops are similar. **B:** Both the human and *D. discoideum* ENT1 proteins share the plasma membrane localisation PWN motif (green) and transmembrane domains (orange). **C:** Phylogenetic analysis of ENT1 proteins suggests that the *D. discoideum* protein (blue arrow) is located within the same clade as the Human protein (red arrow), suggesting a common evolutionary origin. The *D. discoideum* ENT1 protein appears to be more closely related to *H. sapiens* protein than either protein is to plant or yeast orthologues.

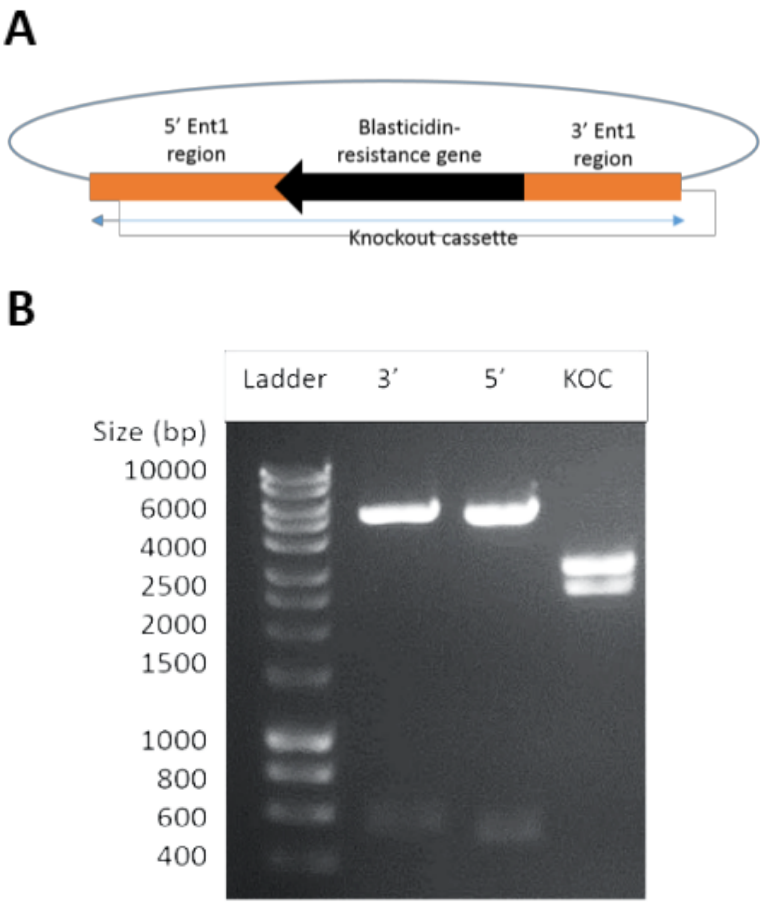

Figure 3.4: Preparing an ENT1 knockout plasmid. A: The ENT1 knockout plasmid containing the 5' and 3' ENT1 regions flanking the blasticidin-resistance gene. **B:** Restriction digest analysis was used to confirm the presence of ENT1 regions within the pLPBLP ENT1 knockout plasmid. Restriction digest with *NcoI* and *KpnI* resulted in a 542 bp fragment for the 3' end and restriction digest with *SpeI* and *PstI* resulted in a 564 bp fragment for the 5' end. A digest with *SpeI* and *KpnI* across the inserted region confirmed the presence of the knockout construct (2665 bp).

In order to investigate the role of ENT1 as a molecular mechanism of CBG, an attempt was made to over-express ENT1. In these experiments, the coding region of the *D. discoideum* ENT1 gene was reverse transcribed and inserted into a C-terminal RFP over-expression plasmid (pDM324 (Veltman et al., 2009)). To ensure the plasmid was correctly constructed, digestion with restriction enzymes that cleaved at the 5' and 3' ends of the ENT1 insert was carried out, revealing that an insert of the correct size (1293 bp) for ENT1 was present in this plasmid in the correct location (Figure 3.6). The whole gene was then sequenced on both strands to ensure no mutations were introduced during cloning. Thereafter, the plasmid was transfected into *D. discoideum*, however, no RFP fluorescence was visible. An ENT1 over-expression construct was therefore not successfully created.

To investigate a role in regulating the response of *D. discoideum* to CBG, ENT1-ablated cells were examined for a change in sensitivity to CBG during growth. In these experiments, ENT1$^-$

cells were grown in the presence of increasing concentrations of CBG over 168 hours. Under control conditions (in the presence of solvent only), ENT1$^-$ *D. discoideum* cell growth showed a lag phase until 96 hours, an exponential phase to 144 hours and a stationary phase starting at 168 hours (Figure 3.7 A). Similarly to wild type cells, CBG concentrations from 1 µM and higher significantly inhibited ENT1$^-$ cell growth at 168 hours ($P<0.05$, Mann Whitney test). Data arising from this analysis (rate of growth and Log of concentration) was used to calculate an IC_{50} of 0.50 µM, which was significantly higher than the wild type IC_{50} of 0.22 µM ($P<0.01$, one-way ANOVA with Bonferroni's Multiple Comparison Test) (Figure 3.7 B). These data showed ENT1 ablation reduced sensitivity to CBG in *D. discoideum*, implicating regulation of ENT1 as a potential molecular mechanism of CBG in *D. discoideum*.

To determine whether CBG blocked adenosine transport through ENT1, a mammalian cell line was employed. Here, mouse BV2 microglial cells were maintained in control conditions (in the presence of solvent only) or treated with CBG (at 0.5, 2.5, 4 and 6 µM) for 24 hours. Then, cell and media content was analysed by liquid chromatography-mass spectrometry (LC-MS) (Jimmerson et al., 2017). This analysis revealed that CBG treatment of microglia did not alter intracellular adenosine levels significantly (Figure 3.8 A). However, extracellular adenosine levels significantly increased with CBG treatment at all concentrations (Figure 3.8 B) ($P<0.01$, one-way ANOVA with Dunnett's Multiple Comparison Test). These data indicated that CBG may block adenosine transport into microglia.

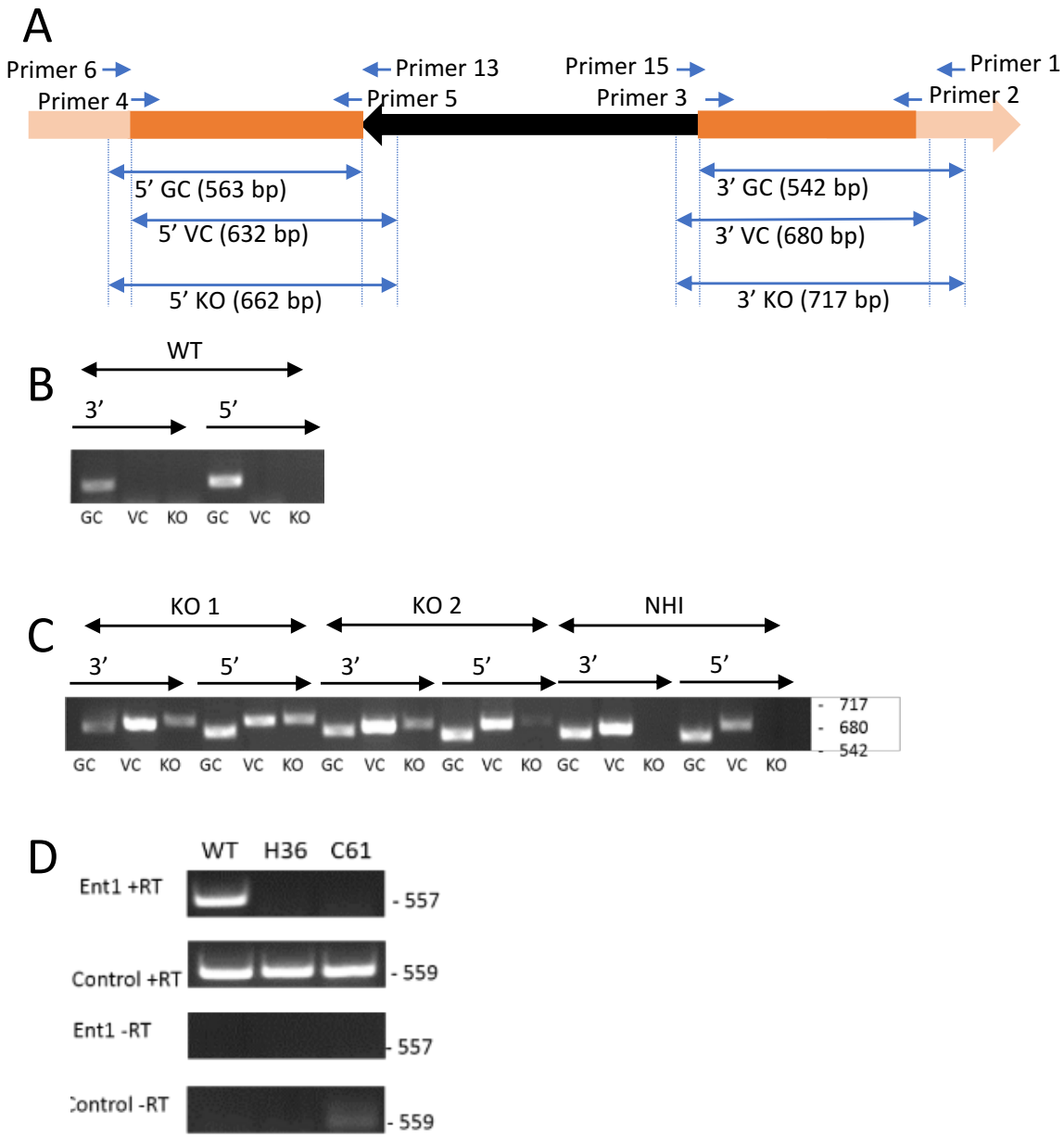

Figure 3.5: Production of ENT1 knockout cell line in *D. discoideum*. A: A blasticidin-resistance gene was inserted into the ENT1 gene using homologous recombination. PCR was used to confirm this, using the primers labelled on the gene (primers in Appendix 9.1). **B and C:** DNA from wild type (**B**) and potential ENT1 knockout cells (**C**) was isolated and PCR amplification was used to detect the presence of the blasticidin-resistance gene inserted into the correct region of ENT1 to knockout the gene. The wild type cell line (WT) had only genomic control (GC) bands. The two cell lines with successful insertions of the blasticidin-resistance gene into the ENT1 gene (KO) have genomic control bands, vector control (VC) bands and knockout bands (KO). The unsuccessful insertion of blasticidin-resistance gene into the ENT1 gene (NHI) had only genomic control and vector control bands. **C:** Reverse transcriptase PCR of WT and ENT1 KO strains. A PCR band of expected size (557 bp) is only shown in cDNA derived from WT cells (ENT1 + RT), although cDNA from both WT and the two mutants contained control (Ig7) cDNA. No DNA contamination was present, since samples without reverse transcriptase (-RT) did not show amplified products.

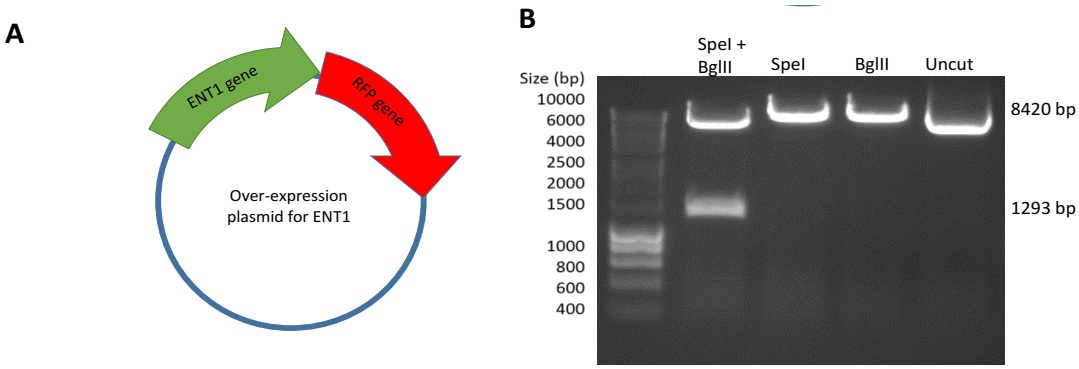

Figure 3.6: Production of an ENT1-RFP over-expressor plasmid. A: Map of planned ENT1 over-expressor plasmid. **B:** An ENT1-RFP plasmid was created in pDM324 (7564 bp) with an RFP tag at the C-terminal of the protein. There were *SpeI* and *BglII* restriction enzyme digestion sites at the 5' and 3' ends of the ENT1 over-expressor insert (1293 bp), respectively. These were used to digest the ENT1 over-expressor plasmid and confirm the presence of the ENT1 insert. In addition, the enzymes were used singularly to ensure that the insert was between the two and correctly located. The plasmid was then transfected into wild type *D. discoideum*, however this did not result in expression of ENT1-RFP.

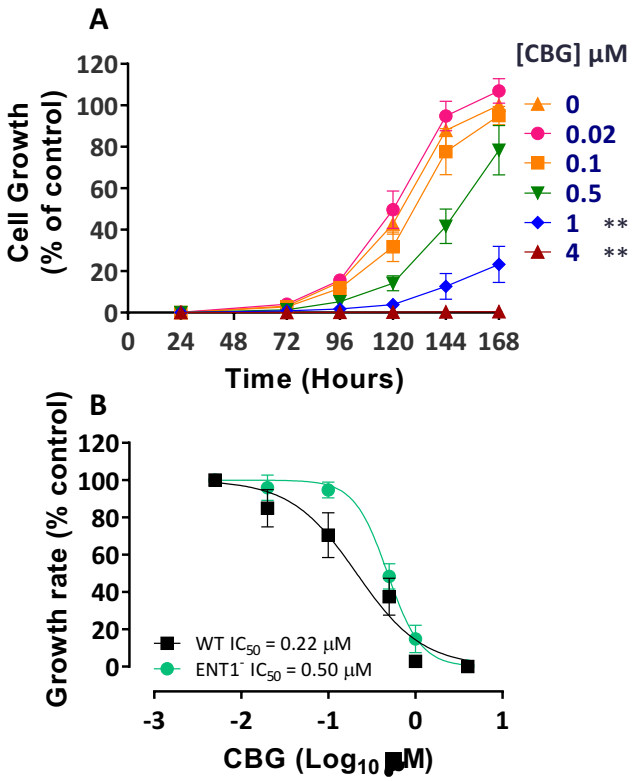

Figure 3.7: Ablation of ENT1 in *D. discoideum* leads to resistance to CBG in growth. A: ENT1$^-$ cells were grown in the presence of increasing concentrations of CBG in shaking culture for one week. Growth was calculated as a % of each cell line in control conditions (in the absence of CBG), n=7. CBG inhibited growth in a concentration-dependent manner. Data arising from comparing the growth rate at differing concentrations of CBG was used to create a secondary plot. Data were not normally distributed (Shapiro-Wilks), therefore a Mann Whitney test was carried out to test for significance of inhibition by each concentration of CBG compared to control at 168 hours, ** - $p<0.01$. Graphs show mean ± SEM. **B:** Secondary plot analysis was used to determine the IC_{50}, ENT1$^-$ IC_{50} = 0.50 µM (n=7) (95% CI: 0.43 - 0.57 µM). The wild type (WT) IC_{50} (0.22 µM) was significantly lower than ENT1$^-$ IC_{50} ($p<0.01$). Data were normally distributed according to Shapiro-Wilks. A one-way ANOVA with Bonferroni's Multiple Comparison Test was carried out to test significance.

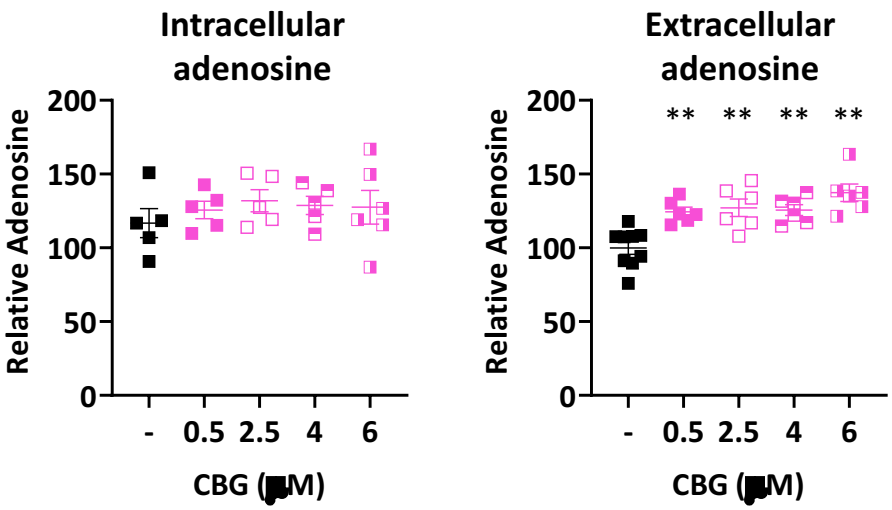

Figure 3.8: CBG treatment increases extracellular adenosine in microglia. Wild type microglia were maintained in control conditions or treated with CBG at 0.5, 2.5, 4 or 6 µM for 24 hours. Then cell and media content were analysed for adenosine levels by LC-MS. Data normally distributed by Shapiro-Wilks, statistical significance analysed by Dunnett's multiple comparison ANOVA, ** is $p<0.01$. **A:** CBG did not significantly alter intracellular adenosine in microglia, n=5. **B:** CBG significantly elevated extracellular adenosine levels of microglia, n=6.

3.2.3 Examining DNA methylation modulation as a potential molecular mechanism of CBG

As loss of ENT1, an adenosine transporter, reduced the potency of CBG in *D. discoideum*, and CBG was found to elevate extracellular adenosine in microglia, the effects of CBG on a downstream process of adenosine transport were examined. Adenosine has previously been found to regulate DNA methylation (Williams-Karnesky et al., 2013), providing a readout for adenosine transport-related effects of CBG. In *D. discoideum*, there is one DNA methyltransferase protein, DNMA, which methylates cytosine residues in DNA (Uniprot ID: Q54JH6, DictyBase ID: DDB_G0288047, based in AX2 wild type cells) (Kuhlmann et al., 2005; Katoh et al., 2006). This enzyme is an orthologue of the *H. sapiens* DNMT 2 protein, which is less active than other DNA methyltransferases. Other, more active DNA methyltransferases exist in *H. sapiens* in the form of DNMT 1 and DNMT 3 (Müller et al., 2013). The *H. sapiens* DNMT 2 and *D. discoideum* DNMA share 43.6 % identity (Clustal W) (Figure 3.9 A), the key S-adenosyl-L-methionine-dependent methyltransferase domains (Figure 3.9 B) and phylogenetic analysis (using MEGA 7 to produce a neighbour-joining tree with 500 Bootstrap replications) showed the two proteins to be within the same clade, suggesting a common evolutionary origin (Figure 3.9 C). *D. discoideum* and other species such as *Drosophila melanogaster* and *Schizosaccharomyces pombe* only contain DNA methyltransferases of the DNMT 2 family (Müller et al., 2013).

To determine whether CBG affected DNMA activity in *D. discoideum*, a cell line lacking DNMA activity was examined for a change in sensitivity to CBG during growth. In these experiments,

wild type cells (AX2) and cells lacking DNMA ($DNMA^-$) were grown in the presence of increasing concentrations of CBG over 168 hours. Under control conditions (in the absence of CBG), wild type (AX2) and $DNMA^-$ *D. discoideum* cell growth showed a lag phase until 96 hours, an exponential phase to 144 hours and a stationary phase starting at 168 hours (Figure 3.10 A and B). In wild type cells (AX2), CBG concentrations from 0.5 µM and higher significantly inhibited cell growth at 168 hours ($P<0.01$, Mann Whitney test). In $DNMA^-$ cells, CBG concentrations from 2 µM and higher significantly inhibited cell growth at 168 hours ($P<0.05$, $P<0.01$ for 3 and 4 µM CBG, Mann Whitney test). Data arising from this analysis (rate of growth and Log of concentration) was used to calculate a wild type (AX2) IC_{50} of 0.30 µM and an IC_{50} for $DNMA^-$ of 1.16 µM. The IC_{50} for $DNMA^-$ was significantly higher than the wild type IC_{50} ($P<0.01$, one-way ANOVA with Bonferroni's Multiple Comparison Test) (Figure 3.10 C). These data showed DNMA ablation created a reduction in sensitivity to CBG in *D. discoideum*, implicating the signalling pathway involved in DNA methylation and adenosine transport as a potential molecular mechanism for CBG in *D. discoideum*.

In order to identify whether CBG modulated DNA methylation in *D. discoideum*, the effect of CBG treatment was examined in this model. To carry this out, wild type cells (AX3) were maintained in control conditions (in the presence of solvent only) or in the presence of 0.25 µM CBG for 24 hours. Genomic DNA was extracted and total DNA methylation was quantified by colorimetry-based immunochemical binding of methylated DNA (Antonini et al., 2019). Treatment with CBG led to a 1.6-fold increase in DNA methylation in *D. discoideum* (Figure 3.11 A) ($P<0.05$, One-Way ANOVA with Dunnett's Post-Hoc). To determine if this effect was related to adenosine signalling, wild type cells were treated with an ENT family protein inhibitor, nitrobenzylthioinosine (NBTI). The NBTI inhibitor has shown nanomolar activity against mammalian ENTs, with a higher specificity for ENT1 than other ENTs (Boswell-Casteel and Hays, 2017). Therefore, wild type cells were treated with 5 nM NBTI for 24 hours and examined for total DNA methylation. Treatment with NBTI in this experiment led to a 1.8-fold increase in DNA methylation in *D. discoideum* (Figure 3.11 A) ($P<0.01$, One-Way ANOVA with Dunnett's Post-Hoc). To determine if these effects were dependent on ENT1 transport of adenosine, the experiment was repeated in cells lacking the ENT1 protein. To carry this out, $ENT1^-$ cells were maintained in control conditions (in the presence of solvent only) or treated with 0.25 µM CBG or 5 nM NBTI for 24 hours. Cells lacking ENT1 had an elevated basal level (1.5-fold) of DNA methylation compared to wild type cells ($P<0.05$, one-way ANOVA with Bonferroni's Multiple Comparison Test) (Figure 3.11 B). However, treatment with CBG or NBTI did not significantly alter DNA methylation in cells lacking ENT1 (Figure 3.11 B). These data suggested that CBG

regulated DNA methylation in *D. discoideum* and that this occurred through an adenosine-ENT1 related mechanism.

A

```
Dictyostelium discoideum      MEQLRVLEFYSGIGGMHYGLQESGVDFQVIQSFDINTNANLNYKYTFNEDS-SQKSIESY   59
Homo sapiens                  MEPLRVLELYSGVGGMHHALRESCIPAQVVAAIDVNTVANEVYKYNFPHTQLLAKTIEGI   60
                              ** *****:***:****:.*:** :  **: ::*:** **  ***.* . .   *:**.

Dictyostelium discoideum      SVEELEGFKANAWLMSPPCQPFTRLGLQKDDQDNRTNSFFHLLDVLTKIKDPPTYILIEN   119
Homo sapiens                  TLEEFDRLSFDMILMSPPCQPFTRIGRQGDMTDSRTNSFLHILDILPRLQKLPKYILLEN   120
                              ::**:: :. :  ***********:* * *  *.*****:*:**:* :::. *.***:**

Dictyostelium discoideum      VFGFAKKGSSNTRDHLLDTLIKMNYSFQEFHLSPQQFGLANQRLRYFCIAKRNGKL-NFK   178
Homo sapiens                  VKGFEV---SSTRDLLIQTIENCGFQYQEFLLSPTSLGIPNSRLRYFLIAKLQSEPLPFQ   177
                              * **     *.*** *::*: : .:.:*** *** .:*: *.***** *** :.:   *:

Dictyostelium discoideum      ----------KEQDKHNEKVDENKLNNNSNNNNEQ-NKYDNL--------KILDHIPGYD   219
Homo sapiens                  APGQVLMEFPKIESVHPQKYAMDVENKIQEKNVEPNISFDGSIQCSGKDAILFKLETAEE   237
                                        * :. * :*   :  *: .::* *   .:*.          ::.   . :

Dictyostelium discoideum      FHTTLE-ECDEISNYFDKDLTDDELYEKYKVPHNLLLSKGMLFDIKQKDSKTSNCVTKSY   278
Homo sapiens                  IHRKNQQDSDLSVKMLKDFLEDDTDVNQYLLPPKSLLRYALLLDIVQPTCRRSVCFTKGY   297
                              :* . : :.*   : :.. * **   ::* :* : **  .:*:** *  .: * *.**.*

Dictyost                      GKFIEGTGSIIQMDNNFKAD-----------INDNKSLIPLKLRYFSPKEITRLHGFPEE   327
Homo sap                      GSYIEGTGSVLQTAEDVQVENIYKSLTNLSQEEQITKLLILKLRYFTPKEIANLLGFPPE   357
                              *.:******::*  ::.:.:            :: ..*: ******:****:.* *** *

Dictyostelium discoideum      FKFSPKLTTIQCYRLIGNSLNVKIVSELLKVLVSPNEEEEQQEQQKEKEGKK* 379
Homo sapiens                  FGFPEKITVKQRYRLLGNSLNVHVVAKLIKILYE------------------- 391
                              * *  *:*. * ***:******::*::*:*:* .

43.6% identity
```

B

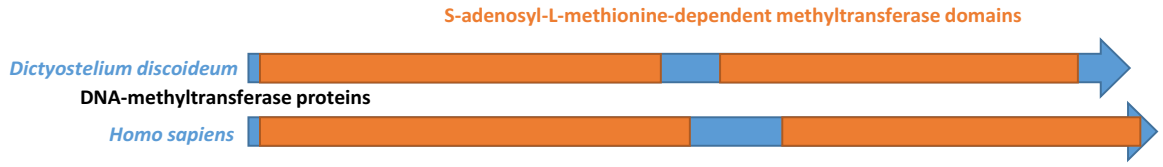

C

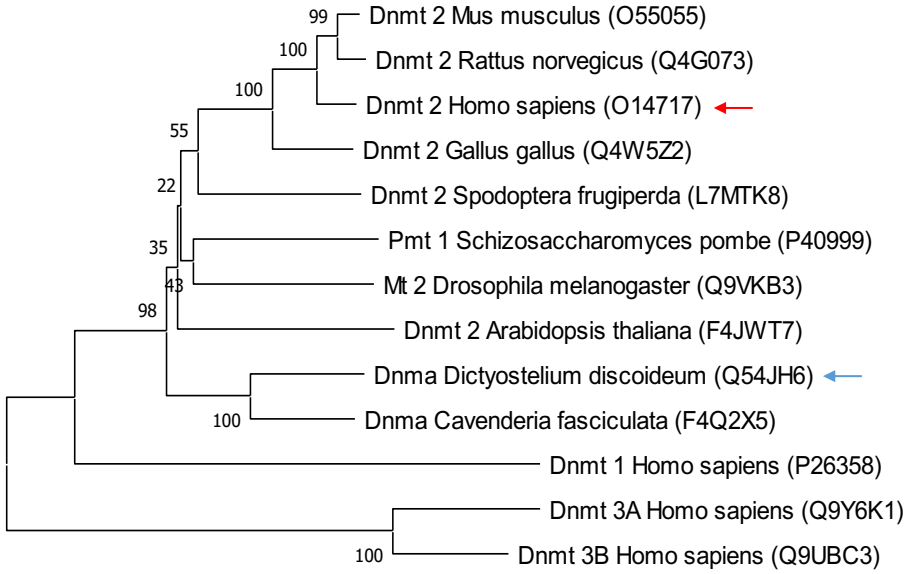

Figure 3.9: Similarity between *D. discoideum* and *H. sapiens* DNA methyltransferase proteins. **A:** *D. discoideum* (Q54JH6) and *H. sapiens* (Q14717) DNMT 2 family protein sequence alignment was carried out on Clustal Omega. The two proteins were found to share a sequence identity of 43.6 %. Asterisks identical, colons are highly similar and full stops are similar. **B:** Both the human and *Dictyostelium* proteins were found to share the S-adenosyl-L-methionine-dependent methyltransferase domains (orange). **C:** Phylogenetic analysis of DNA methyltransferase proteins suggested that the *D. discoideum* DNMA protein (blue arrow) was located within the same clade as the Human DNMT2 protein (red arrow), suggesting a common evolutionary origin. The *D. discoideum* DNMA protein appeared to be more closely related to *H. sapiens* DNMT 2 protein than either protein was to other DNA transferase (DNMT 1 and 3) family proteins.

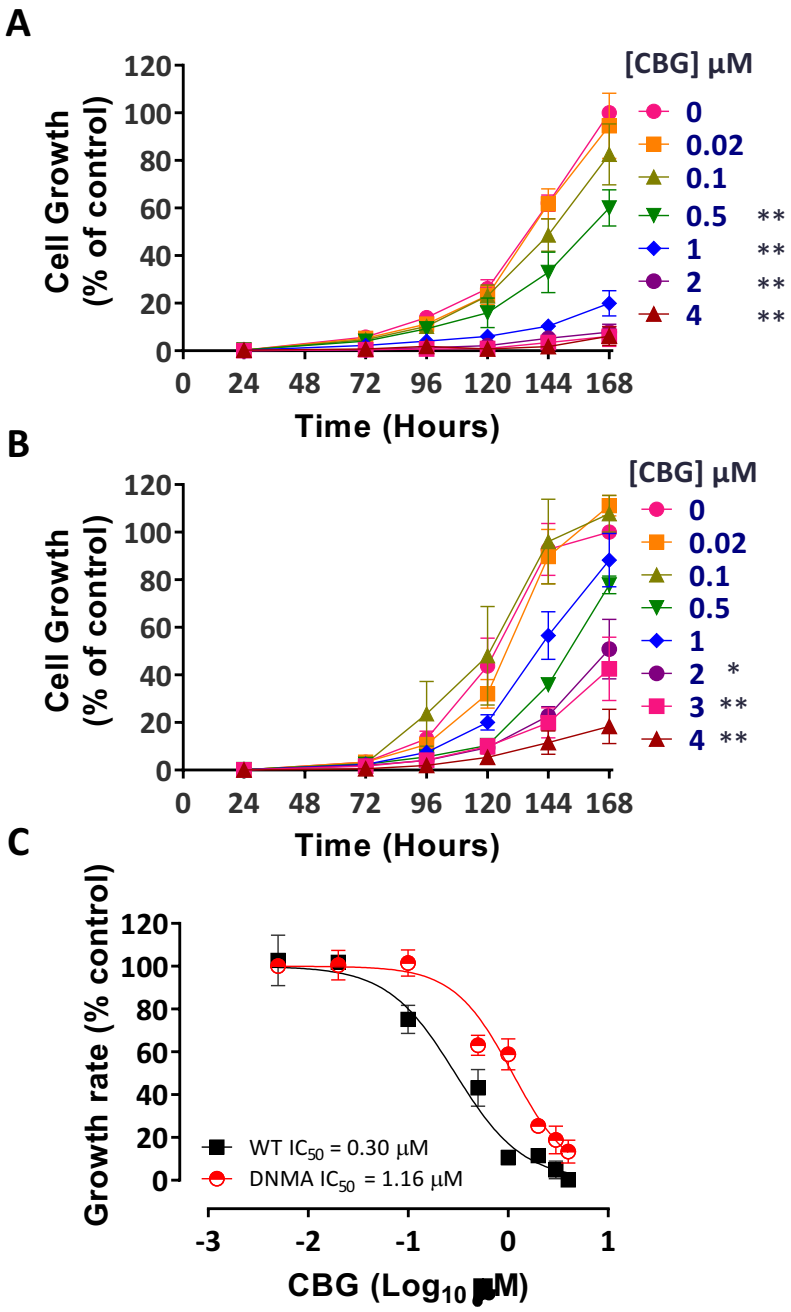

Figure 3.10: Ablation of DNMA in *D. discoideum* leads to resistance to CBG in growth. A and B: Wild type (AX2) (**A**) and DNMA$^-$ cells (**B**) were grown in the presence of increasing concentrations of CBG in shaking culture for one week. Growth was calculated as a % of each cell line in control conditions (in the absence of CBG), n=7 and n=9. CBG inhibited growth in a concentration-dependent manner. Data arising from comparing the growth rate at differing concentrations of CBG was used to create a secondary plot. Data were not normally distributed (Shapiro-sWilks), therefore a Mann Whitney test was carried out to test for significance of inhibition by each concentration of CBG compared to control at 168 hours, * - p<0.05, ** - p<0.01. Graphs show mean ± SEM. **C:** Secondary plot analysis was used to determine the IC_{50}, wild type (AX2) IC_{50} = 0.30 µM (95% CI: 0.21 - 0.41 µM) and DNMA$^-$ IC_{50} = 1.16 µM (95% CI: 0.93 - 1.44 µM). The wild type (WT) is significantly lower than DNMA$^-$ IC_{50}. Data were normally distributed according to Shapiro-Wilks. A one-way ANOVA with Bonferroni's Multiple Comparison Test was carried out to test significance.

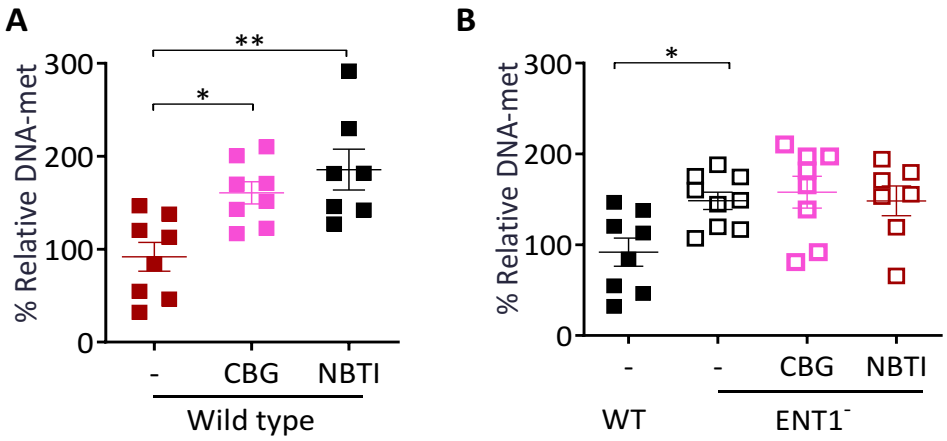

Figure 3.11: CBG treatment and ENT1 ablation increase DNA methylation in *D. discoideum*. A and B: Wild type and ENT1- cells were maintained in control conditions (in the absence of CBG or NBTI (-)) or treated with 0.25 µM CBG or 5 nM NBTI. Data were normally distributed (Shapiro-Wilks), therefore a One-Way ANOVA with Tukey's Multiple comparison test was carried out to test for significance, * - $p<0.05$, ** - $p<0.01$. Graphs show mean ± SEM. **A:** CBG and NBTI (ENT inhibitor) both elevated DNA methylation in wild type cells (n=8). **B:** ENT1$^-$ had an elevated basal level of DNA methylation compared to wild type cells. In addition, treatment with CBG or NBTI did not alter DNA methylation in ENT1$^-$ cells (n=8).

3.3 Discussion

In this chapter, the effects of CBG on adenosine transport and related downstream signalling pathways were examined. Using this approach, CBG was found to inhibit the growth of *D. discoideum* in a concentration-dependent manner, while not affecting development. These effects suggested that CBG had specific molecular mechanisms in *D. discoideum* and not a general toxic effect. Then, based on previous literature identifying adenosine transport regulation as a molecular mechanism of cannabinoids (Carrier et al., 2006; Liou et al., 2008), the relationship between CBG and ENT1 (an adenosine transporter) was analysed. A cell line lacking ENT1 was significantly resistant to CBG during growth. Further experiments in microglia cells revealed that CBG appeared to block the uptake of adenosine. Together these data strongly implied that CBG may inhibit adenosine uptake through ENT1. To investigate whether CBG blocked adenosine uptake in *D. discoideum* the relationship between CBG and a downstream signalling pathway of adenosine transport, DNA methylation, was analysed. Here, a cell line lacking DNA methyltransferase was also found to be resistant to CBG during growth. To confirm the relation between the DNA methylation and CBG, DNA methylation quantification was

carried out and DNA methylation was found to increase following CBG treatment in wild type cells. This implied that CBG was blocking adenosine uptake in these cells. However, CBG did not affect DNA methylation in cells lacking the ENT1. This suggested that in *D. discoideum* CBG upregulated DNA methylation through inhibition of adenosine uptake.

In this study, CBG inhibited growth of *D. discoideum* cells with an IC_{50} of 0.22 µM. In the same model system, a previous study found that CBD inhibited growth with an IC_{50} of 1.9 µM (Perry et al., 2020). Other cannabinoids, cannabidiolic acid (CBDA) and cannabidivarin (CBDV), showed similar potency in this model with IC_{50} values of 0.89 and 2.16 µM respectively (Perry, 2019). Therefore, data provided here suggest that CBG is between 4 and 10 times more potent at *D. discoideum* growth inhibition than CBD, CBDV and CBDA. Comparing these potencies to other systems, such as human keratinocyte cells, where CBG inhibited cell growth with an IC_{50} of 2.3 µM, while CBD, THC, and cannabinol (CBN) inhibited growth of these cells with IC_{50}s of 2.0, 2.9 and 2.1 µM respectively (Wilkinson and Williamson, 2007). Previous studies imply a similar potency of CBG and other cannabinoids in mammalian cells. However, data in *D. discoideum* indicates that CBG inhibits growth at a slightly higher potency than other cannabinoids.

In this chapter, CBG was found to inhibit the growth of *D. discoideum* cells at a similar concentration to those used previously *in vivo* animal model studies. In this chapter, CBG concentrations ranging from 0.1 to 4 µM were found to inhibit the growth of *D. discoideum* cells. In rats, 100 mg/kg and 120 mg/kg CBD administered in an intraperitoneal injection 1 hour before experimentation resulted in a brain concentration of CBD of 9.8 µM after 1 hour and 21.6 µM after 2 hours, which attenuated epileptiform activity (Hill et al., 2014). In another study, 120 mg/kg oral treatment with CBG also resulted in therapeutically relevant effects, as CBG here doubled food intake (Brierley et al., 2016). In a human study, 800 mg (an average of around 120 mg/kg) of CBD administered orally, resulted in peak plasma concentrations of CBD (at one to two hours post-treatment) ranging between 0.006 and 0.866 µM (with an average of 0.245 µM) (Haney et al., 2016). Lower concentrations of cannabinoids have also been shown to be therapeutically effective. For example, in mice 10 mg/kg CBD administered daily in an intraperitoneal injection for 14 days treated MS symptoms (Giacoppo et al., 2017). Likewise, in human trials, daily 10-20 mg/kg treatment with CBD administered orally for 14 weeks reduced drop-seizure frequency (Devinsky et al., 2018(a)). Therefore, while CBG use in *D. discoideum* is not therapeutically relevant, concentrations of CBG used in this study appear to be consistent with previous *in vitro* and *in vivo* cannabinoid studies.

To examine whether a molecular mechanism of CBG involved the adenosine transporter, ENT1, in *D. discoideum*, a cell line lacking this protein was tested for resistance to CBG during growth. Ablation of ENT1 resulted in increased resistance to CBG during growth in *D. discoideum*,

indicating that a molecular mechanism of CBG may involve ENT1 or proteins within an ENT1-related signalling pathway. The ablation of ENT1 may be partially compensated for by the only other known adenosine transporters in *D. discoideum* (Dictybase ID: DDB_G0281515 (ENT2) and DDB_G0281513 (ENT3)). The two additional adenosine transport proteins are not normally expressed during the unicellular growth phase of the *D. discoideum* lifecycle, while ENT1 is (Rot et al., 2009). As previous studies have indicated ENT1 is a target of CBD in rat microglial cells (Liou et al., 2008) and in this chapter, CBG was found to inhibit growth of *D. discoideum*, only ENT1 was explored as a part of potential molecular mechanism of CBG. However, *D. discoideum* cells lacking ENT1 may compensate by altering the time of expression of ENT2 or ENT3. Future qPCR analyses of this would provide data on this proposal and LC-MS could be used to analyse a change in adenosine levels after ENT1-ablation and during CBG treatment (Jimmerson et al., 2017). Here, CBG is found to regulate growth of *D. discoideum* partially through the adenosine transporter, ENT1, future experiments may determine whether this is as a result of blocking adenosine transport or through another mechanism.

In addition to ENT1 ablation, to further understand the relationship between CBG and adenosine transport an unsuccessful attempt at creating a cell line over-expressing ENT1 and recapitulating the ablated protein was made. The inability to over-express ENT1 could be due to problems with protein dysfunction when GFP-tagged (Wiedenmann et al., 2009), in which case a smaller fluorescent tag may increase the likelihood of successful over-expression (Plamont et al., 2016). Alternatively, a small protein tag such as a FLAG tag could be utilised in the over-expression of ENT1 in *D. discoideum* (Veltman et al., 2009; Zhao et al., 2013). Future research should address this problem and recapitulate the wild type sensitivity to CBG in *D. discoideum*, by using an ENT1 over-expressor in ENT1 ablated cells.

In this chapter, ablation of the adenosine transporter, ENT1, is found to reduce sensitivity to CBG during growth. Furthermore, treatment of microglia cells with CBG resulted in an elevated extracellular level of adenosine. In addition, DNA methylation which is inversely related to adenosine levels (Kredich and Martin, 1977; Boison et al., 2002), is increased by CBG treatment, and ENT1 ablation or inhibition in *D. discoideum*. Together, these data indicate that CBG treatment may inhibit adenosine uptake in both *D. discoideum* and microglia cells. This would be consistent with previous studies finding that a cannabinoid like CBG, CBD, inhibits adenosine uptake via ENT1 (Carrier et al., 2006). ENT proteins are adenosine transporters that allow passive flow of adenosine across the cell membrane along its gradient (Pastor-Anglada and Pérez-Torras, 2018). In nucleus accumbens of mice lacking ENT1, there is a decrease in extracellular adenosine levels, implying a higher basal intracellular concentration of adenosine in this brain region of mice (Nam et al., 2011). Conversely, in the striatum of a mouse model of Huntington's disease,

ENT1 was found to be over-expressed, and treatment with ENT1 inhibitors increased extracellular adenosine, implying that in this disease model intracellular adenosine is lower than extracellular (Kao et al., 2017). Previous studies, along with data found in this chapter, indicate that ENT1 is an adenosine transporter which is more likely to increase adenosine uptake. Furthermore, this chapter indicates that CBG may be an inhibitor of ENT1-related adenosine uptake, although future experiments analysing adenosine in *D. discoideum* lacking ENT1 and treated with CBG are needed to confirm this.

Adenosine regulation of DNA methylation is implicated as a part of a molecular mechanism of CBG by the data found in this chapter. Here, CBG was found to increase DNA methylation in *D. discoideum* mimicking the effect of the adenosine transporter inhibitor NBTI. In addition, cells lacking the adenosine transporter protein ENT1 are resistant to the effects of CBG on DNA methylation and have a constitutively elevated level of DNA methylation. The dysregulation of DNA methylation has been implicated in epileptogenesis, which is the progression of epilepsy, and therefore could be an important molecular mechanism for the treatment of epilepsy (Williams-Karnesky et al., 2013). Adenosine acts as an inhibitor of DNA methylation, and through elevated adenosine and reduced DNA methylation, epileptogenesis in rats is inhibited (Williams-Karnesky et al., 2013). A pathological over-expression of ADK results in DNA hypermethylation, due to a lower level of adenosine (Williams-Karnesky et al., 2013). The relationship between adenosine and DNA methylation is a result of both being components of the transmethylation pathway (Kredich and Martin, 1977). DNA methylation relies on methyl group donation from S-adenosylmethionine facilitated by DNA methyltransferases, this results in the production of S-adenosylhomocysteine which is converted into adenosine and homocysteine. The reaction occurs at equilibrium and therefore will only continue if adenosine and homocysteine are continually removed. Therefore, an increase in adenosine blocks the pathway and results in decreased DNA methylation and conversely a decrease in adenosine allows the pathway to continue and increases DNA methylation (Kredich and Martin, 1977; Boison et al., 2002). In this study we find CBG treatment and inhibition or removal of adenosine transporters results in an increase in DNA methylation in *D. discoideum*. This could be due to a decrease in adenosine uptake caused by CBG or adenosine transporter inhibition, thus resulting in the continuation of the transmethylation pathway and hypermethylation of DNA. As CBG appears to modulate adenosine signalling and DNA methylation in this model potential therapeutic role for the compound in epilepsy treatment could be further explored in *in vivo* models.

Chapter 4: Discovery and exploration of potential regulators of the molecular mechanism of CBG in *D. discoideum*

4.1 Introduction

In addition to adenosine signalling explored in the previous chapter, there are many other molecular mechanisms suggested for cannabinoids. These proposed molecular mechanisms include TRPV1 (Borrelli et al., 2014), GPR55 (Devinsky et al., 2014), and the one-carbon cycle and methionine signalling (Perry et al., 2020). However, little research has been carried out into CBG molecular mechanism discovery. Therefore, here an unbiased approach is undertaken to discover novel molecular mechanisms of CBG.

The model organism *D. discoideum* was employed to identify molecular pathways affected by CBG treatment. This model organism has a fully sequenced genome with a range of orthologous proteins present in the proteome, and mutant libraries which have previously been employed to identify potential molecular mechanisms of compounds (Kuspa and Loomis, 1992; Williams, 2010). Screening of mutant libraries in *D. discoideum* has been used to discover molecular mechanisms for CBD (Perry et al., 2020), curcumin and its derivatives (Cocorocchio et al., 2018), valproic acid (Chang et al., 2015), naringenin (Waheed et al., 2014), and bitter tastants (Robery et al., 2013). In some cases, molecular mechanisms of compounds identified in *D. discoideum* using these methods have been validated in mammalian models (Perry et al., 2020) and provided an underlying molecular mechanism for epilepsy treatment (Chang et al., 2015; Augustin et al., 2018). The depth and breadth of research using *D. discoideum* pharmacogenetics suggest that it could be a suitable model for discovering novel molecular mechanisms of CBG.

4.2 Results

4.2.1 Screening of *D. discoideum* mutant library for CBG-resistant mutants

To identify novel molecular mechanisms of CBG in *D. discoideum*, a mutant library screening approach was carried out. This method relied on the growth inhibitory effect of CBG described in the previous chapter and aimed to identify mutant cells that were resistant to the effects of CBG during growth. In these experiments, wild type and *D. discoideum* mutant library cells from a library containing 11,000 mutants were treated with CBG at a range of concentrations in excess of that necessary to block growth (8 µM, 10 µM, 12 µM) for 10 days and screened for resistance (Figure 4.1 A). Under control conditions (in the presence of solvent only), wild type cells grew to confluency (Figure 4.1 B). Wild type cells in the presence of CBG did not grow. In contrast, *D. discoideum* mutant library cells resistant to CBG grew to confluency in the presence or absence of CBG (Figure 4.1 B). In three screens of mutant libraries treated with 8 µM CBG, 12 mutants were isolated in each of the first two screens and one mutant in the last screen. In three screens of mutants treated with 10 µM CBG, nine mutants were isolated in each of the first two screens and seven mutants in the last screen. In the screen of mutants treated with 12 µM, CBG nine mutants were isolated. From this approach, 59 isogenic CBG-resistant mutants were isolated.

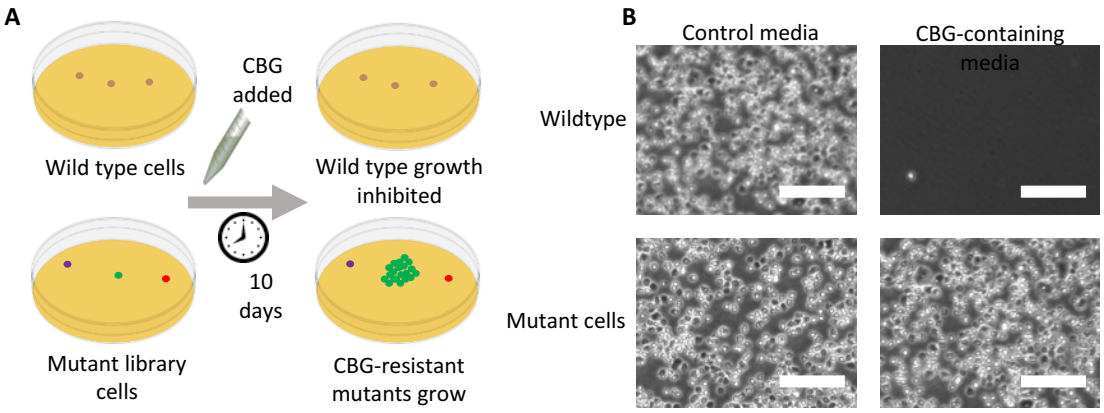

Figure 4.1: An unbiased *D. discoideum* screen was employed to find CBG-resistant mutants. A: Schematic of a mutant library screen to identify mutants resistant to the growth inhibition effect of CBG, where wild type cell growth is inhibited by CBG. However, mutants from an insertional library continue to grow in the presence of CBG, and these can be isolated and the protein controlling CBG sensitivity identified. **B:** Wild type and mutant library cells were either maintained in control conditions or treated with CBG (10 µM), and mutants resistant to CBG were able to grow. Scale bar = 0.25 mm.

Following the isolation of CBG-resistant mutants, each mutant was analysed to identify the molecular mechanisms controlling CBG sensitivity. In each mutant, a restriction enzyme-

mediated mutational insert (REMI) disrupted expression of a gene, leading to a disruption of protein expression controlling CBG sensitivity. In order to identify this protein, the location of the mutational insert in the *D. discoideum* genome for each CBG-resistant mutant was determined. Here, iPCR was carried out and insert location sequences were obtained for 35 of the CBG-resistant *D. discoideum* mutants (Figure 4.2). Of these 35 sequences, 23 were too short to match to a specific region of the genome, giving multiple potential locations for the insert and were therefore discarded. However, 12 sequences of sufficient length were found to match to an area of the *D. discoideum* genome, and BLAST (Basic Local Alignment Search Tool) was used to determine the location of each mutagenic insert. From the 12 sequences that matched locations in the *D. discoideum* genome, six unique loci were found (Figure 4.3 and Table 4.1). One cell line contained an insert in the 5' region of the open reading frame (ORF) of the gene *DDB_G0269494* encoding a protein of no known function (http://dictybase.org/). Another cell line contained an insert in the 5' region of the ORF in the *DDB_G0292968* gene encoding a putative licheninase protein. Two cell lines contained inserts 80 base pairs (bp) downstream of the ORF of the *DDB_G0295181* gene encoding a tRNA-Tyr-GUA-6. One cell contained an insert in the 5' region of the ORF of the *DDB_G0272242* gene, encoding the calcium upregulated I (CupI) protein. Three cell lines contained inserts in the 3' region of the ORF of the *DDB_G0279435* gene encoding a Regulator of chromosome condensation 1 (RCC1) domain-containing protein. Finally, four cell lines contained inserts 880 bp downstream of the ORF of the *DDB_G0281737* gene encoding the inositol polyphosphate multikinase (IPMK) protein. From this approach, six proteins that were potentially involved in the molecular mechanisms of CBG in *D. discoideum* had been discovered.

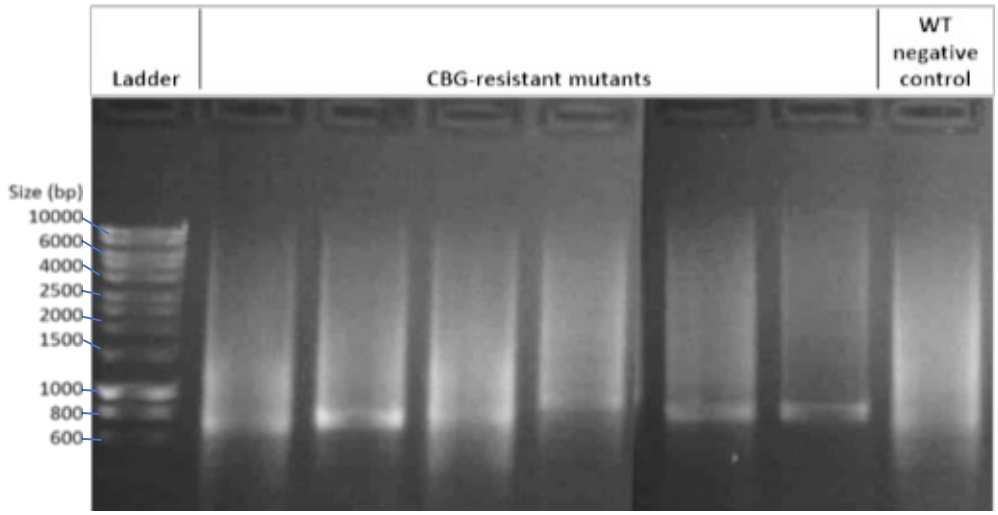

Figure 4.2: Identification of insertion sites in CBG-resistant mutants. The iPCR of 6 isogenic CBG-resistant mutants and a wild type negative control, separated on an electrophoresis gel. The PCR fragment is sequenced as above to determine the location of the insert, which is 1.5 kb (Faix et al., 2004), in each mutant.

The proteins that were potentially involved in the molecular mechanisms of CBG identified in the *D. discoideum* mutant screen were examined to identify possible *H. sapiens* orthologues and determine the cellular roles of each protein. In order to carry this out, each *D. discoideum* protein was analysed using BLAST for *H. sapiens* orthologues. The protein product of DDB_G0269494 was uncharacterised in *D. discoideum* with no known function and had no *H. sapiens* orthologue, therefore was unlikely to provide a therapeutically relevant molecular mechanism of CBG in *H. sapiens*. The putative licheninase, which may hydrolyse the β-(1,4)-D-glucosidic linkages in mixed-linkage glucans containing both (1,3)- and (1,4)-bonds (Borriss et al., 1980), did not have a *H. sapiens* orthologue, therefore was unlikely to provide a therapeutically relevant molecular mechanism of CBG in *H. sapiens*. The tRNA (tRNA-Tyr-GUA-6), which transfers a tyrosine residue to a growing polypeptide chain during protein synthesis (Izuchi et al., 1990), had no *H. sapiens* orthologues, therefore was also unlikely to provide a therapeutically relevant molecular mechanism of CBG in *H. sapiens*. The protein CupI, may have a role in calcium signalling in *D. discoideum* (Farinholt et al., 2019), but also had no *H. sapiens* orthologues, therefore was unlikely to provide a therapeutically relevant molecular mechanism of CBG in *H. sapiens*. From this approach, no *H. sapiens* orthologue had been found for four of the proteins potentially involved in the molecular mechanism of CBG in *D. discoideum* and therefore they were unlikely to represent a possible therapeutic molecular mechanism and were not further explored.

Protein name	Gene code	Independently identified (times)	Location of insert
N/A	DDB_G0269494	1	C-terminus ORF
Putative licheninase	DDB_G0292968	1	N-terminus ORF
tRNA-Tyr-GUA-6	DDB_G0295181	2	80 bp downstream of ORF
CupI	DDB_G0272242	1	N-terminus ORF
RCC1-domain containing protein	DDB_G0279435	3	C-terminus ORF
IPMK	DDB_G0281737	4	886 bp downstream of ORF

Table 4.1: Insertion sites discovered in CBG-resistant *D. discoideum* REMI mutants. The gene identity was found on Dictybase.org, as was the gene code. The number of times independently isolated is a total of how many times a different CBG-resistant REMI mutant was found to have its insert at the listed position. Where a human homologue has been found the human gene name has been given.

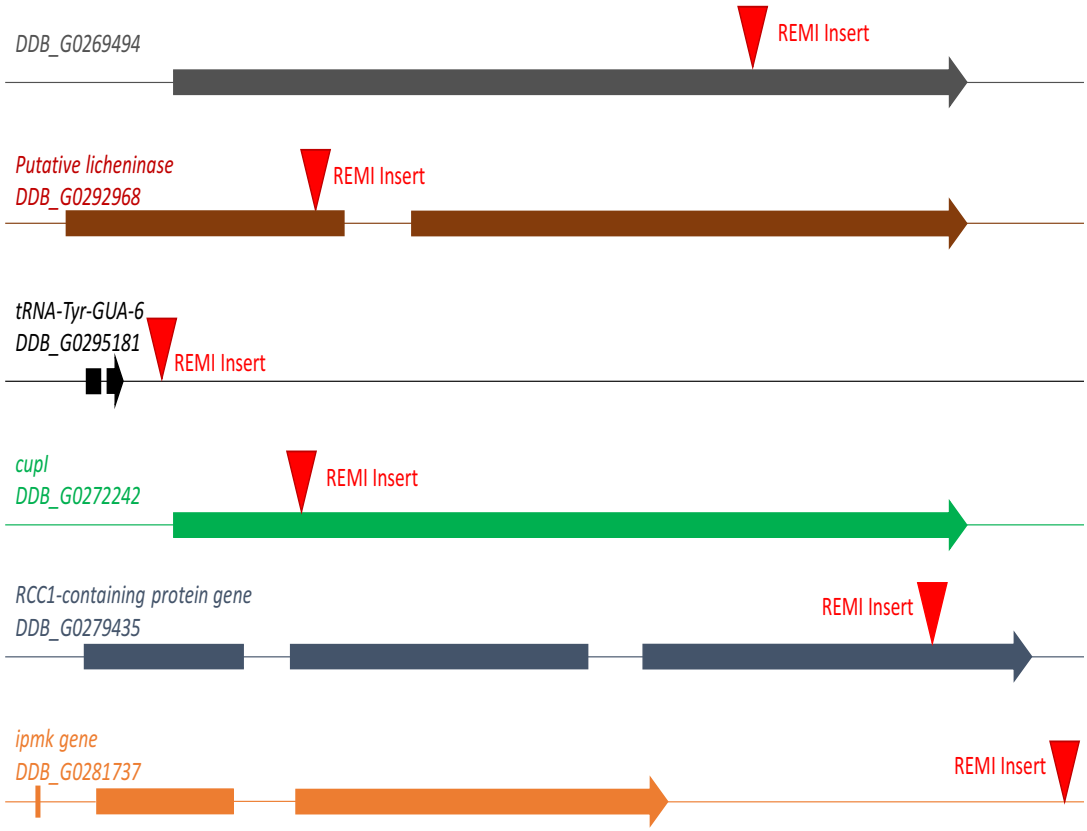

Figure 4.3: A: Diagram of discovered insertion sites of mutational inserts in CBG-resistant mutants. Arrows and boxes represent the exons of the above genes, the straight lines through them represent genomic DNA and where a straight line is between an arrow and a box, or two boxes, it represents an intron. The red triangle on each gene is the location of the REMI mutational insert in that mutant, which is 1.5 kb (Faix et al., 2004). Size of boxes and arrows is in scale with the size of the gene.

One protein identified in the CBG-resistance screen, the RCC1-containing (RC) protein, provided a likely orthologue of an interesting *H. sapiens* protein domain. This RC protein is likely to function as a GTPase regulator (Cubillos-Rojas et al., 2014). In order to determine the similarity between the *D. discoideum* RC protein (Uniprot ID: Q54WU2; DDB_G0279435) and the *H. sapiens* HERC2 protein (Uniprot ID: O95714) containing RCC1 domains (Figure 4.4 A), an amino acid alignment (using Clustal W) was carried out. The *H. sapiens* HERC2 protein contained three RCC1 domains and these domains shared amino acid identity compared to the RCC1 domain of the RC protein in *D. discoideum* of 24.6% with RCC1 1, 25.3% with RCC1 2 and 23.6% with RCC1 3 (Figure 4.4 B). Phylogenetic analysis (using MEGA 7 to produce a neighbour-joining tree with 500 Bootstrap replications) showed the *H. sapiens* and *D. discoideum* RCC1 domains to be within the same clade, suggesting a common evolutionary origin (Figure 4.4 C). Each of the *H. sapiens* RCC1 domains in the HERC2 protein and the RCC1 domain in the *D. discoideum* protein also shared a proline residue, which if mutated in the first RCC1 domain of the *H. sapiens* HERC2

protein can cause Angelman syndrome (HERC2^{P594L}) (Cubillos-Rojas et al., 2016). In the CBG-resistant mutant, the mutational insert was located in the open reading frame of the gene, which suggested that the protein would not be correctly expressed. Thus, the RCC1 domain-containing protein provided a potential molecular mechanism with possible therapeutic relevance if the effects were conserved in the RCC1 domains of the *H. sapiens* HERC2 protein.

Another protein identified in the CBG-resistance screen, IPMK, provided a likely orthologue of an interesting *H. sapiens* protein. This IPMK protein functions as a phospholipid and phosphatidylinositol kinase (Kim et al., 2016). In order to determine the similarity between the IPMK in *D. discoideum* (Uniprot ID: Q54TI0) and the single orthologue in the *H. sapiens* IPMK protein (Uniprot ID: Q8NFU5), an amino acid alignment was carried out (using Clustal W) which indicated that the two IPMK proteins share 33.2 % amino acid identity (Figure 4.5 A) and both contain inositol phosphate-binding domains and ATP-binding domains (Figure 4.5 B). Phylogenetic analysis (using MEGA 7 to produce a neighbour-joining tree with 500 Bootstrap replications) showed the *H. sapiens* and *D. discoideum* IPMK proteins to be within the same clade, suggesting a common evolutionary origin (Figure 4.5 C). This may be of potential therapeutic interest as the IPMK protein in *H. sapiens* has many functions varying from mTORC1 regulation (Kim et al., 2002; Kim et al., 2011) to histone de-acetylase regulation (Watson et al., 2012), and 5' AMP-activated protein kinase (AMPK) and Liver Kinase B1 (LBK1) regulation (Bang et al., 2012; Dailey and Kim, 2012; Bang et al., 2014). The IPMK protein was, therefore, a potential molecular mechanism with possible therapeutic relevance if the effects were conserved in the *H. sapiens* IPMK protein.

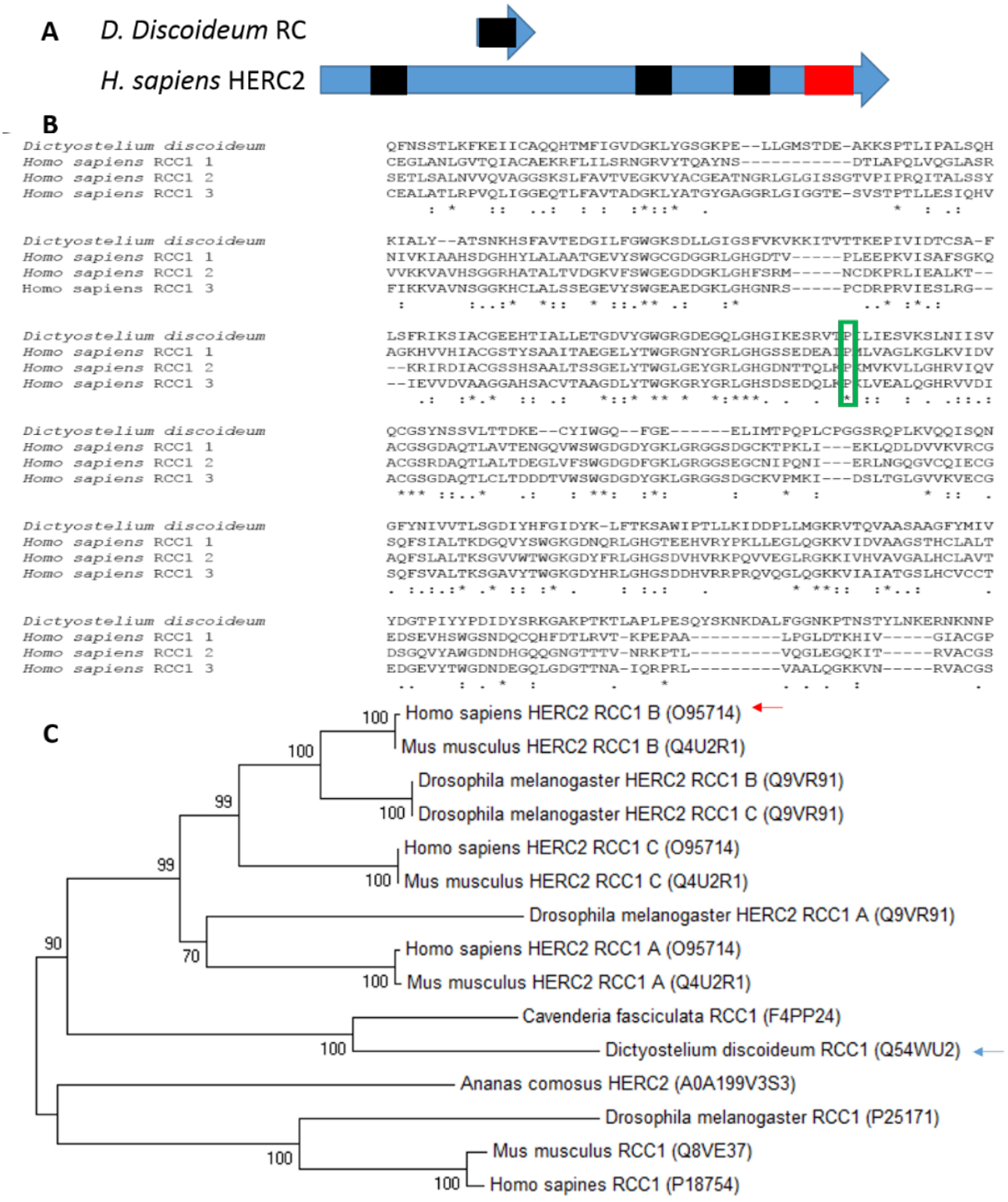

Figure 4.4: Protein sequence alignment of the *H. sapiens* HERC2 protein RCC1 domains and the *D. discoideum* RC protein. A: The *D. discoideum* RC protein the *H. sapiens* HERC2 protein. In black are RCC1 domains, in red are HECT domains. **B:** Clustal Omega analysis was carried out on the RCC1 domains in the *D. discoideum* RC protein (Q54WU2) and the *Homo sapiens* HERC2 protein (O95714) and were found to be similar in sequence. Asterisks identical, colons are highly similar and full stops are similar. Highlighted in green is the proline (RCC1 1 of HERC2) that when mutated is responsible for the cause of Angelman syndrome in HERC2. **C:** Phylogenetic analysis of RCC1 domains suggests that the *D. discoideum* protein (blue arrow) is located within the same clade as the Human protein (red arrow), suggesting a common evolutionary origin. The *D. discoideum* RCC1 appears to be more closely related to *H. sapiens* RCC1 domains in HERC2 than the *H. sapiens* RCC1 protein is to any of them.

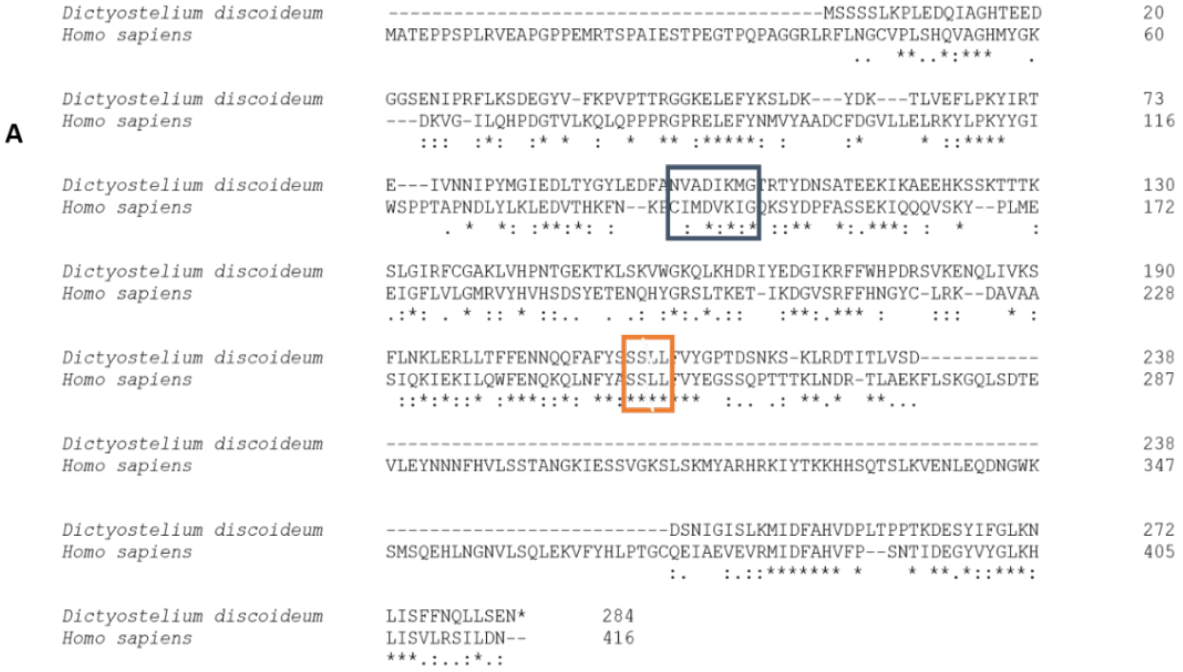

Figure 4.5: Similarity between *D. discoideum* and *H. sapiens* IPMK proteins. **A:** *D. discoideum* (Q54TI0) and *H. sapiens* (Q8NFU5) IPMK sequence alignment was carried out on Clustal Omega. They share an amino acid identity of 33.2%. Asterisks identical, colons are highly similar and full stops are similar. **B:** Comparison of *Homo sapiens* and *Dictyostelium discoideum* IPMK proteins. Both the human and *Dictyostelium* proteins share inositol binding domains (blue) and ATP binding domains (orange). **C:** Phylogenetic analysis of IPMK proteins suggests that the *D. discoideum* protein (blue arrow) is located within the same clade as the Human protein (red arrow), suggesting a common evolutionary origin. The *D. discoideum* IPMK protein appears to be more closely related to *H. sapiens* protein than either protein is to plant or yeast orthologues.

4.2.2 The effects of IPMK over-expression on sensitivity to CBG during growth

To determine how the mutagenic insert 880 bp downstream of the IPMK led to resistance to CBG, the effect of the insert on IPMK expression had to be measured. To carry this out, quantitative polymerase chain reaction (qPCR) analysis was used to measure IPMK mRNA levels in wild type and mutant cells. To this end, wild type and mutant cells were grown under the same conditions and RNA was extracted from both cell types. Analysis by qPCR revealed that the expression levels of IPMK in the mutant cells were significantly higher than wild type cells (Figure 4.6) ($P<0.05$, Mann-Whitney Test). This suggested that disruption of the *D. discoideum* genome at this position resulted in three-fold increased IPMK expression and that this increase in expression resulted in resistance to CBG.

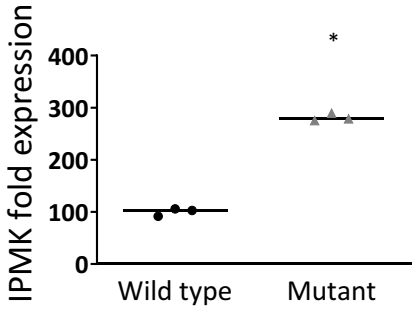

Figure 4.6: IPMK levels in the CBG-resistant mutant. The CBG-resistant mutant found to contain a mutagenic insert 880 bp downstream of IPMK was examined by qPCR analysis for a change in IPMK expression compared to wild type cells. Total mRNA was collected from each cell line and RT-PCR was used to create cDNA. Then qPCR was carried out and the CBG-resistant mutant was found to have elevated IPMK mRNA levels compared to the wild type ($P<0.05$, unpaired t-test), n=3. Expression levels were normalized to the constitutively expressed Ig7 housekeeping gene, which produces the mitochondrial large subunit rRNA (Fukuzawa et al., 2006).

To validate that CBG-resistance in the mutant was due to elevation of IPMK expression, a *D. discoideum* cell line over-expressing IPMK was created. This cell line was created using an RFP over-expression plasmid which contained a *D. discoideum* IPMK (dIPMK) insert (Figure 4.7 A). The dIPMK insert was created by reverse transcription (RT-PCR) of IPMK mRNA and then cloned into the RFP-containing plasmid (pDM324 (Veltman et al., 2009)). To ensure the plasmid was correctly constructed, digestion with restriction enzymes that cleaved at the 5' and 3' ends of the dIPMK insert was carried out. This restriction enzyme digestion revealed that an insert of the correct size (856 bp) for dIPMK was present in this plasmid in the correct location (Figure 4.7 B). The whole gene was then sequenced to ensure no mutations had occurred. Thereafter, the plasmid was transfected into *D. discoideum* and presence of the dIPMK-RFP protein was examined by western blot using an anti-RFP antibody. This analysis found that dIPMK^{+} cells showed a specific 50 kDa RFP-containing protein which was absent in wild type cells and consistent with the expression of full-length dIPMK-RFP (Figure 4.7 C). Furthermore, protein extracts from wild type and dIPMK over-expressing cells (dIPMK^{+}) cells contained a similar level

of protein, as evidenced by the control protein (streptavidin). This experiment confirmed that the *D. discoideum* IPMK-RFP protein was present in *D. discoideum* cells.

To determine where in *D. discoideum* cells dIPMK localised, fluorescent microscopy was carried out. Cells expressing dIPMK-RFP were imaged using a wide-field fluorescence microscope. This analysis indicated that dIPMK-RFP was localised in the cytoplasm and nucleus (Figure 4.7 D). Therefore, a *D. discoideum* cell line over-expressing dIPMK had been successfully created and a cell line was available to examine the role of human IPMK in the molecular mechanism of CBG.

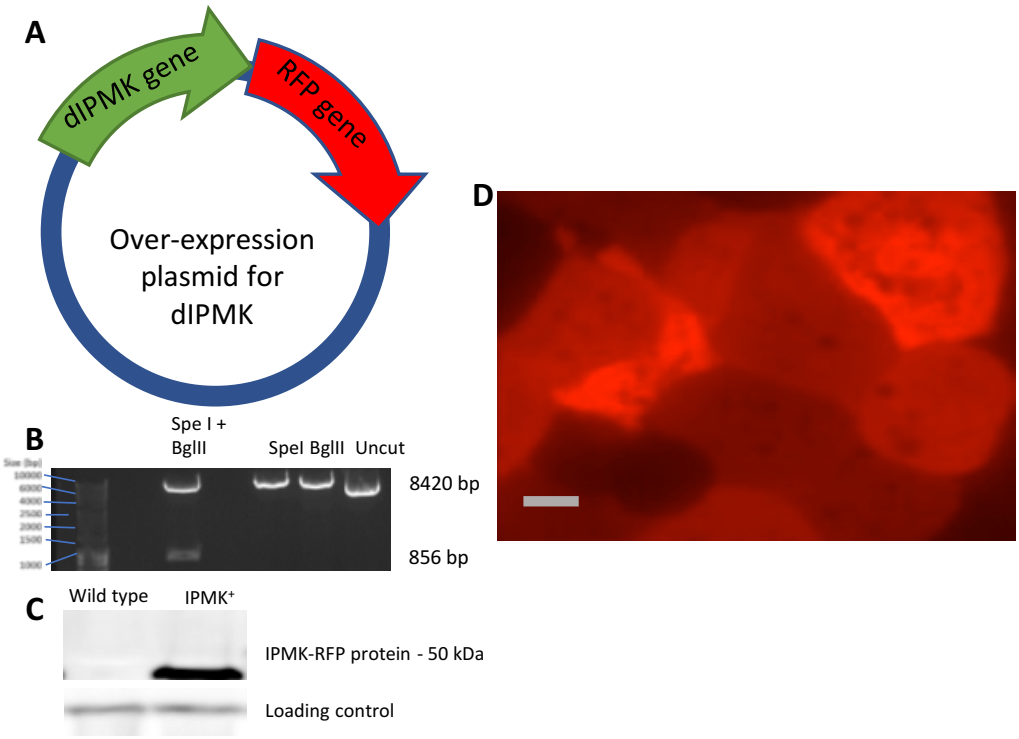

Figure 4.7: Production of an IPMK-RFP over-expressor cell line. A: An IPMK-RFP plasmid was created in pDM324 (7564 bp) with an RFP tag at the C-terminal of the protein. **B:** There were *SpeI* and *BglII* restriction enzyme digestion sites at the 5' and 3' ends of the IPMK over-expressor insert (856 bp), respectively. These were used to digest the IPMK over-expressor plasmid and confirm the presence of the IPMK insert. In addition, the enzymes were used singularly to ensure that the insert was between the two and correctly located. The plasmid was then transfected into wild type *D. discoideum.* **C:** The presence of IPMK-RFP was confirmed by western blot analysis, using an antibody against RFP. No protein was detected by the anti-RFP antibody in wild type cells. A protein the expected size of IPMK and RFP was detected in the IPMK-RFP expressing cells. Loading control protein was streptavidin. **C:** Cellular localisation of IPMK in IPMK-RFP expressing cells was confirmed by fluorescent microscopy. The IPMK protein localised to the cytoplasm. Scale bar 10 µm**.**

To confirm that the CBG-resistance observed in the *D. discoideum* mutant was due to elevated IPMK expression, dIPMK$^+$ cells were examined for resistance to CBG during growth. In these experiments, dIPMK$^+$ cells were grown in the presence of increasing concentrations of CBG over 168 hours. Under control conditions (in the presence of solvent only), dIPMK$^+$ growth showed a lag phase until 96 hours, an exponential phase to 144 hours and a stationary phase starting at 168 hours (Figure 4.8 A). Similarly to wild type cells, CBG concentrations above 1 µM significantly

inhibited dIPMK^{+} cell growth at 168 hours (P<0.01, Mann Whitney test). Data arising from comparing the growth rate at differing concentrations of CBG was used to calculate a dIPMK^{+} IC_{50} for CBG of 0.64 µM (Figure 4.8 B), which was significantly higher than the wild type IC_{50} of 0.22 µM (P<0.01, one-way ANOVA with Bonferroni's Multiple Comparison Test (Figure 3.1). These data showed dIPMK over-expression created a reduction in sensitivity to CBG in *D. discoideum*, recapitulating the effect seen in the mutant screen and confirming IPMK as a regulator of *D. discoideum* response to CBG.

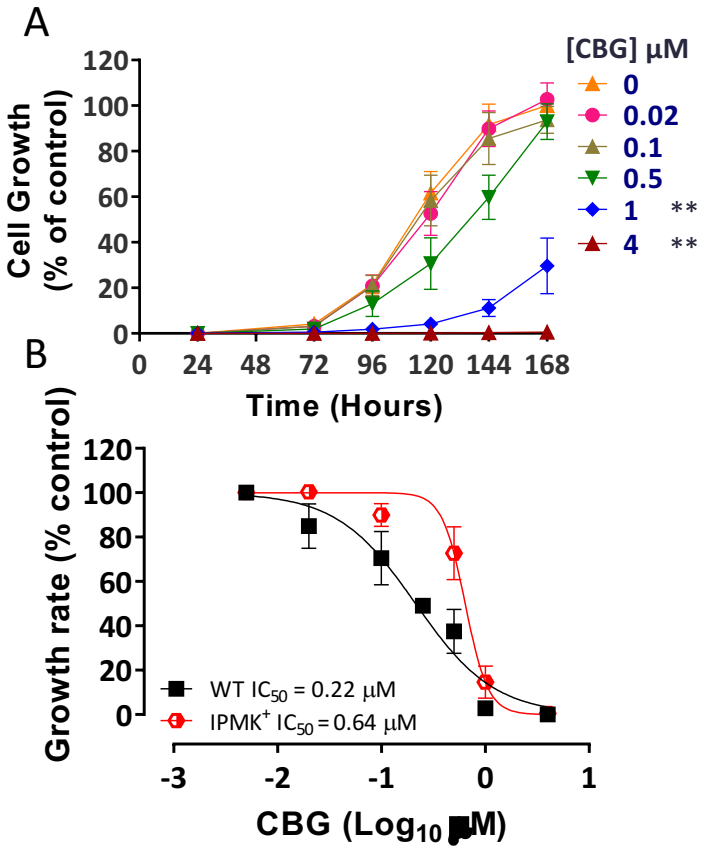

Figure 4.8: Elevated IPMK leads to resistance to CBG during growth in *D. discoideum*. A: Cells over-expressing dIPMK (dIPMK^{+}) were grown in the presence of increasing concentrations of CBG (and solvent only control; 0) for one week. CBG inhibited cell growth in a concentration-dependent manner (n=6). This data was used to produce a secondary plot. **B:** Secondary plot analysis was used to determine the IC_{50} = 0.64 µM (95 % confidence intervals 0.14 to 0.31 µM) (n=6), while in wild type cells this was IC_{50} = 0.22 µM (n=10). Cells over-expressing IPMK were found to have a significantly higher IC_{50} compared to wild type cells (p<0.01). Data were normally distributed according to Shapiro-Wilks. A one-way ANOVA with Bonferroni's Multiple Comparison Test was carried out to test significance.

In addition to a dIPMK over-expressor cell line, attempts were made to create a cell line lacking IPMK to further examine the role of IPMK in regulating *D. discoideum* cellular response to CBG. To this end, a plasmid designed to ablate IPMK expression in *D. discoideum* was designed (Figure 4.9 A) and transfected into *D. discoideum* cells (Figure 4.9 B). However, after 960 potential knock

out cell lines had been examined and only non-homologous integrants found (Figure 4.9 C) this experiment was halted. A cell line lacking IPMK expression was therefore not created in *D. discoideum*, potentially due to the IPMK protein being essential for *D. discoideum* survival.

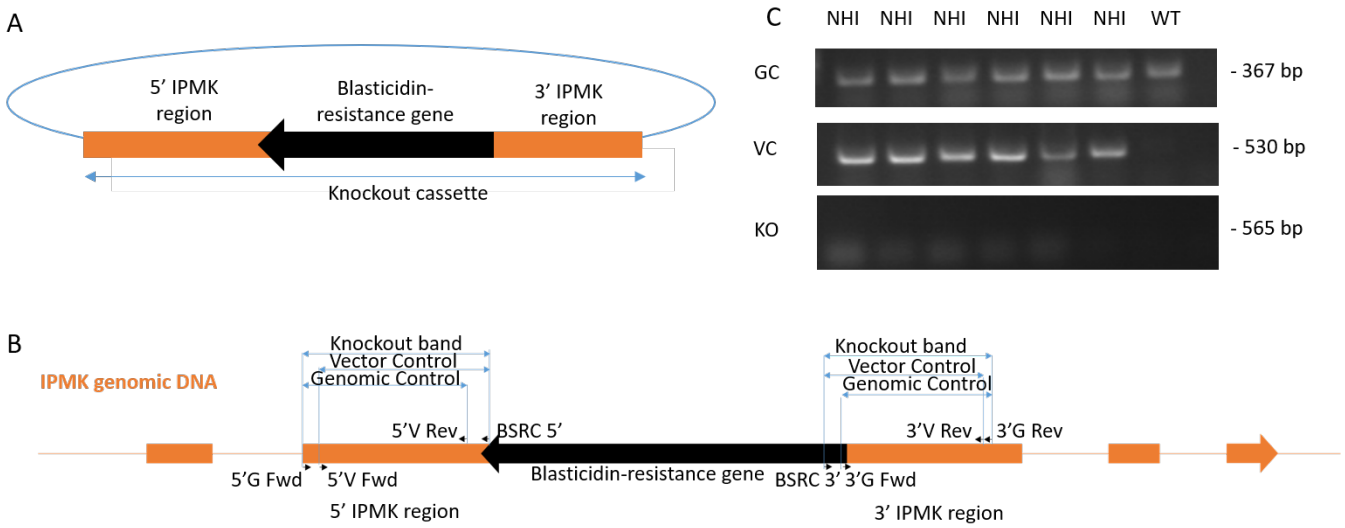

Figure 4.9: Production of plasmid for the ablation of IPMK. A: An IPMK ablation plasmid was created using the pLPBLP plasmid, the 5' and 3' IPMK regions are PCR amplified from genomic DNA and ligated into the pLPBLP plasmid either side of the blasticidin-resistance cassette. **B:** This plasmid was then transfected into *D. discoideum* so that through homologous recombination the blasticidin-resistance gene could replace a section of the IPMK gene in the genome. **C:** The knockout cassette was transfected into wild type *D. discoideum*. DNA from IPMK knockout screen cells was isolated and PCR amplification was used to detect the presence of the blasticidin-resistance gene inserted into the correct region of IPMK to knockout the gene. Genomic control (GC) and vector control (VC) bands were present in non-homologous integrants (NHI), while a knockout band (KO) was not present. 960 cell lines were tested, with only non-homologous integrants found.

4.3 Discussion

In this chapter, a *D. discoideum* mutant library was employed to discover potential novel molecular mechanisms of CBG. In the previous chapter, CBG was found to inhibit the growth of *D. discoideum* but not development. These effects suggested that CBG had specific molecular mechanisms in *D. discoideum* and not a general toxic effect. To identify which proteins were involved in this effect, a *D. discoideum* mutant library was screened for CBG-resistant mutants and two proteins possibly involved in the molecular mechanisms of CBG were identified with the potential for translational activity. Following the identification of IPMK as a protein potentially involved in the molecular mechanism of CBG in *D. discoideum*, elevated IPMK was found to be a possible cause of CBG-resistance. This effect was recapitulated with the expression of dIPMK-RFP in *D. discoideum* cells, leading to an increase in resistance to CBG. Therefore, IPMK was confirmed as a regulator of the effects of CBG on *D. discoideum* growth and potentially a target for the molecular mechanism of CBG.

Although the mutant screen carried out in this study identified six potential proteins that may be involved in the molecular mechanism of CBG in *D. discoideum*, it is likely that this is not a full representation of proteins that regulate the molecular mechanism of CBG in this model. The limitations of the screen used in this study result from the creation of the mutant library using restriction enzyme-mediated insertion (REMI) (Kuspa and Loomis, 1992). Within this mutant library, some insertion sites are duplicated and only 57 % of the sites are estimated to be unique. Within the pool of mutants containing unique insertion sites, 71 % of inserts (40 % of the total inserts) were found within coding regions of genes and 15 % (9 % of total) were found within promoter regions of genes. In total, insertion sites in the mutant library are estimated to be present in 43 % of the genes in the *D. discoideum* and some genes contain multiple unique insertion sites (Gruenheit et al., 2019). That there is only a 43 % coverage of *D. discoideum* genes in the mutant library limits the potential to discover proteins that regulate the molecular mechanism of CBG that are likely to be lethal if expression is ablated or altered. As the underlying principle of a mutant screen is that loss of a protein necessary for the molecular mechanism of a compound results in cells becoming resistant to the effects of the compound, then, by definition, a vital protein would not be found using this method (Kelly et al., 2018). Therefore, an essential protein for *D. discoideum* survival that interacts with CBG is unlikely to be identified using this method. Consequently, use of the *D. discoideum* mutant library had limitations and was unlikely to find every potential protein involved in the molecular mechanism of CBG in this model organism, however, this method can be used to discover some proteins involved in the molecular mechanism of CBG with potential therapeutic relevance.

One protein potentially involved in regulating the molecular mechanism of CBG found in the mutant screen was the RC protein, which contains an RCC1 domain orthologous to domains found in the *H. sapiens* HERC2 protein. Importantly, the human protein has clinical relevance since the mutation of one proline residue in the first RCC1 domain causes Angelman syndrome and that proline residue is shared with the *D. discoideum* RCC1 domain. Angelman syndrome is a complex genetic disorder associated with epilepsy that mainly affects the nervous system with symptoms including delayed intellectual development and cranial deformities (C.A. Williams et al., 2006). In *H. sapiens*, HERC2 has ubiquitin ligase activity, regulates the activity of tumour proteins p53, and is involved in DNA repair, cell cycle, regulation and iron metabolism (Cubillos-Rojas et al., 2016). Recent experiments have found that CBD has the potential to treat Angelman syndrome by attenuating seizures in mice models of Angelman syndrome, but suggested no potential mechanism (Gu et al., 2019). This effect could be through the HERC2 protein, as the proline mutation is likely to cause a conformational change in the protein structure, leading to lack of function or decrease in function of HERC2 (Harlalka et al., 2013). If CBG binds to the RCC1 domain it may alter the protein structure, further biochemical binding affinity assays could be used to examine this (Carrier et al., 2006). Although it is unclear how cannabinoid treatment could alter the HERC2 protein structure, due to the similarities between the *D. discoideum* and *H. sapiens* RCC1 domains in the two proteins, CBG could potentially target the RCC1 domains of both proteins. Therefore, the RC and HERC2 proteins represent exciting prospects to explore as regulators of a molecular mechanism of CBG.

Another protein potentially involved in the regulation of the molecular mechanism of CBG found in the mutant screen was the IPMK protein. The *H. sapiens* orthologue of the *D. discoideum* IPMK protein has many functions such as mTORC1 regulation (Kim et al., 2002; Kim et al., 2011), inositol phosphate production (Saiardi et al., 1999; Resnick et al., 2005), histone de-acetylase regulation (Watson et al., 2012), and AMPK and LBK1 regulation (Bang et al., 2012; Dailey and Kim, 2012; Bang et al., 2014). The involvement of IPMK in all these biological processes, suggests a role for CBG in the treatment of tuberous sclerosis (Bang et al., 2012; Samueli et al., 2016), epilepsy (Russo et al., 2013), cancer (Shaw and Cantley, 2006), multiple sclerosis (Giacoppo et al., 2017), schizophrenia (Renard et al., 2016), Alzheimer's disease (Xu et al., 2011), obesity and diabetes (Bang et al., 2012). Due to these numerous cellular roles and potential involvement in so many diseases, IPMK represented an exciting prospect to explore as a protein involved in the regulation of the molecular mechanism of CBG.

The CBG-resistant mutant containing a mutational insert 880 bp downstream of the IPMK open reading frame was examined by qPCR to determine if the insert affected IPMK expression, with

the aim to recapitulate the phenotype in wild type cells. The CBG-resistant mutant discovered in the mutant screen was found to have an elevated level of IPMK expression compared to wild type cells. An insertion in this location may have interfered with the suppression of IPMK expression, however, the scope of this study meant that no further research could be carried out to determine why an insert in this location resulted in elevated IPMK expression. Therefore, dIPMK over-expression was experimentally recapitulated using the RFP over-expression vector, pDM324 (Veltman et al., 2009). This over-expression plasmid has previously been used to over-express vacuole membrane protein 1 in *D. discoideum* (Calvo-Garrido et al., 2014). Once over-expressed, the dIPMK-RFP protein was found to localise to the cytoplasm and nucleus of *D. discoideum* cells, an expected result as it lacked the specific nuclear localisation signal found in the *H. sapiens* form of the IPMK protein (Nalaskowski et al., 2002). Therefore, the *D. discoideum* CBG-resistant mutant was confirmed to have elevated IPMK expression and an experimentally created cell line recapitulated this IPMK over-expression.

In addition, an attempt was made to create a cell line lacking IPMK to further examine the role of this protein in regulating response to CBG treatment. However, this attempt was ended after 960 cell lines were examined for loss of IPMK and no cell lines were found with ablated IPMK. Loss of IPMK could be lethal to *D. discoideum* as IPMK loss is lethal in *Drosophila melanogaster* (Malabanan and Blind, 2016), *Trypanosoma brucei* (Cestari et al., 2018), and the early embryonic stages of *Mus musculus* development (Maag et al., 2011). Therefore, IPMK is likely to be crucial for the survival of *D. discoideum* (Maag et al., 2011). The vital role for IPMK could be in the production of inositol pentakisphosphate (IP_5) or inositol hexaphosphate (IP_6) in specific morphogenetic processes and cellular survival (Frederick et al., 2005). This is likely to be the case as IPMK from *Arabidopsis thaliana* expressed in *D. melanogaster* can rescue the lethal phenotype of IPMK loss, and the only activity of *A. thaliana* IPMK in *D. melanogaster* was IP_4 production (Malabanan and Blind, 2016). Therefore, efforts at creating a *D. discoideum* cell line lacking IPMK were halted at 960 attempts. However, future methods could be used such as reduced expression through siRNA (Saiki et al., 2011), expression of non-endogenous IPMK (Malabanan and Blind, 2016) or artificial replacement of inositol phosphates in *D. discoideum* when ablating the native protein to maintain essential functions (Miyamoto et al., 2002; Jackson et al., 2007).

To determine if IPMK over-expression in the CBG-resistant mutant was responsible for resistance to CBG during growth, a growth assay was carried out with the recapitulated IPMK over-expressing cell line. In this experiment, over-expression of IPMK in *D. discoideum* was found to confer a three-fold increase in resistance during growth to CBG at the 50 % inhibition

concentration. Given the many cellular roles of IPMK already described, the mechanism by which CBG inhibited growth through IPMK could not be determined. Thus, the next aim was to determine if CBG modified downstream effectors of IPMK, such as mTORC1 activity and higher order inositol phosphate production.

Chapter 5: Exploration of IPMK as a target for CBG in *D. discoideum*

5.1 Introduction

In the previous chapter, IPMK activity was suggested to be involved in the molecular mechanism of CBG. Initially, an insertional mutant library was screened for mutant cells resistant to CBG during growth. From this approach, six mutagenic insert locations were found in CBG-resistant mutants, and these provided six potential target proteins, one of which was the IPMK protein. The *D. discoideum* IPMK has an orthologue in *H. sapiens* involved in mTORC1 regulation (Kim et al., 2002; Kim et al., 2011), inositol phosphate production (Saiardi et al., 1999; Resnick et al., 2005), histone de-acetylase regulation (Watson et al., 2012), and AMPK and LBK1 regulation (Bang et al., 2012; Dailey and Kim, 2012; Bang et al., 2014). In the mutant screen, the mutagenic insert location 880 bp downstream of the *D. discoideum* IPMK gene was identified independently four times and found to elevate IPMK expression. To confirm this, an IPMK over-expressing cell line was created and found to be resistant to CBG during growth. To discover the mechanism of IPMK targeting by CBG, downstream signalling pathways were examined.

The *H. sapiens* IPMK protein has many cellular roles and functions, making it an interesting potential therapeutic target. One of the functions of IPMK is to act as a PI3-kinase, this regulates phosphatidylinositol (3,4,5)-trisphosphate (PIP_3) production and may regulate transcription in the nucleus in yeast (Resnick et al., 2005). The PI3-kinase function of IPMK activates protein kinase B (PKB) which goes on to activate mTORC1 activity (Maag et al., 2011). Furthermore, through non-catalytic binding with mTOR and Raptor, IPMK regulates mTORC1 signalling independently of this catalytic activity (Kim et al., 2011). Therefore, through many functions, IPMK regulates mTORC1 activity (Figure 1.4). The function of mTORC1 is to regulate cell growth and protein synthesis through the eukaryotic translation initiation factor 4E (eIF4E)-binding protein (4EBP) and cell size through ribosomal protein S6 kinase (S6K) (Yang et al., 2014). The regulation of mTORC1 activity could be therapeutically relevant as preclinical studies have suggested that cannabinoids up-regulate mTORC1 in the treatment of both multiple sclerosis (Arévalo-Martín et al., 2003; Serpell et al., 2013; Giacoppo et al., 2017) and psychosis (Renard et al., 2016; Renard et al., 2017(a)) and down-regulate mTORC1 in the treatment of epilepsy (Serra et al., 2019) and cancer (Franz et al., 2013; Sultan et al., 2018). Therefore, the ability of CBG to regulate mTORC1 activity through IPMK was analysed in this chapter.

5.2 Results

5.2.1 CBG and CBD, but not CBDA or CBDV, elevate mTORC1 activity in *D. discoideum*

To validate IPMK as a potential target for CBG, the effect of CBG treatment on an IPMK-regulated cellular process was analysed. The ability of IPMK to non-catalytically bind mTOR and to catalytically regulate mTOR activity through PIP_3 production provided a mechanism by which to measure the effect of CBG on IPMK activity (Kim et al., 2011; Blind et al., 2012). To carry this out, 4EBP1 phosphorylation (a downstream effector of mTORC1 Figure 5.1 A) was measured by western blot analysis, using an antibody which binds to phosphorylated threonine 46 in the *H. sapiens* 4EBP1 protein. An amino acid alignment (using Clustal W) indicated that this threonine is shared by both the *H. sapiens* and *D. discoideum* 4EBP1 proteins (Figure 5.1 B) and phylogenetic analysis (using MEGA 7 to produce a neighbour-joining tree with 500 Bootstrap replications) indicated that both proteins share an evolutionary origin (Figure 5.1 C).

Therefore, to measure mTORC1 signalling, wild type cells were kept in control conditions (in the presence of solvent only and in the absence of CBG) or in the presence of 0.25 µM CBG for 1 hour. Treatment with CBG in this experiment led to a 1.5-fold increase in mTORC1 activity, as evidenced by an increase in the phosphorylation of 4EBP1 compared to control conditions ($P<0.01$, One-Way ANOVA with Dunnett's Post-Hoc) (Figure 5.2). To determine if cannabinoids with a similar structure to CBG also increased mTORC1 activity, the same experiment was carried out with the treatment of *D. discoideum* cells with 0.25 µM CBD, cannabidiolic acid (CBDA) or cannabidivarin (CBDV) for one hour. From this, CBD was also found to increase mTORC1 activity 1.3-fold, as evidenced by an increase in the phosphorylation of 4EBP1 compared to control conditions ($P<0.05$, One-Way ANOVA with Dunnett's Post-Hoc) (Figure 5.2). However, CBDA and CBDV did not increase 4EBP1 phosphorylation compared to control conditions. Together, these data showed that CBG and CBD, and not CBDA or CBDV, regulated mTORC1 activity in *D. discoideum*.

5.2.2 The effects of CBG and CBD are IPMK-, PKB- and PI3K-dependent

To determine whether CBG- and CBD-dependent regulation of mTORC1 in *D. discoideum* was dependent on IPMK, mTORC1 activity in cells over-expressing dIPMK was measured. To carry this out, wild type cells and $dIPMK^+$ cells were maintained in control conditions (in the presence of solvent only) for one hour and $dIPMK^+$ cells were treated with 0.25 µM CBG or CBD for one hour, then levels of phosphorylated 4EBP1 were measured by western blot. In control conditions, cells over-expressing dIPMK had a 1.9-fold elevated level of mTORC1 activity

compared to wild type cells as evidenced by an elevated level of phosphorylated 4EBP1 (P<0.01, one-way ANOVA with Bonferroni's Multiple Comparison Test) (Figure 5.3). Treatment of dIPMK^{+} cells with CBG or CBD, both resulted in a 45 % reduction of mTORC1 activity, as evidenced by a decrease in the level of phosphorylated 4EBP1 compared to control conditions (P<0.05, one-way ANOVA with Bonferroni's Multiple Comparison Test) (Figure 5.3). Therefore, these data further suggested that CBG- and CBD-dependent regulation of mTORC1 occurred through IPMK.

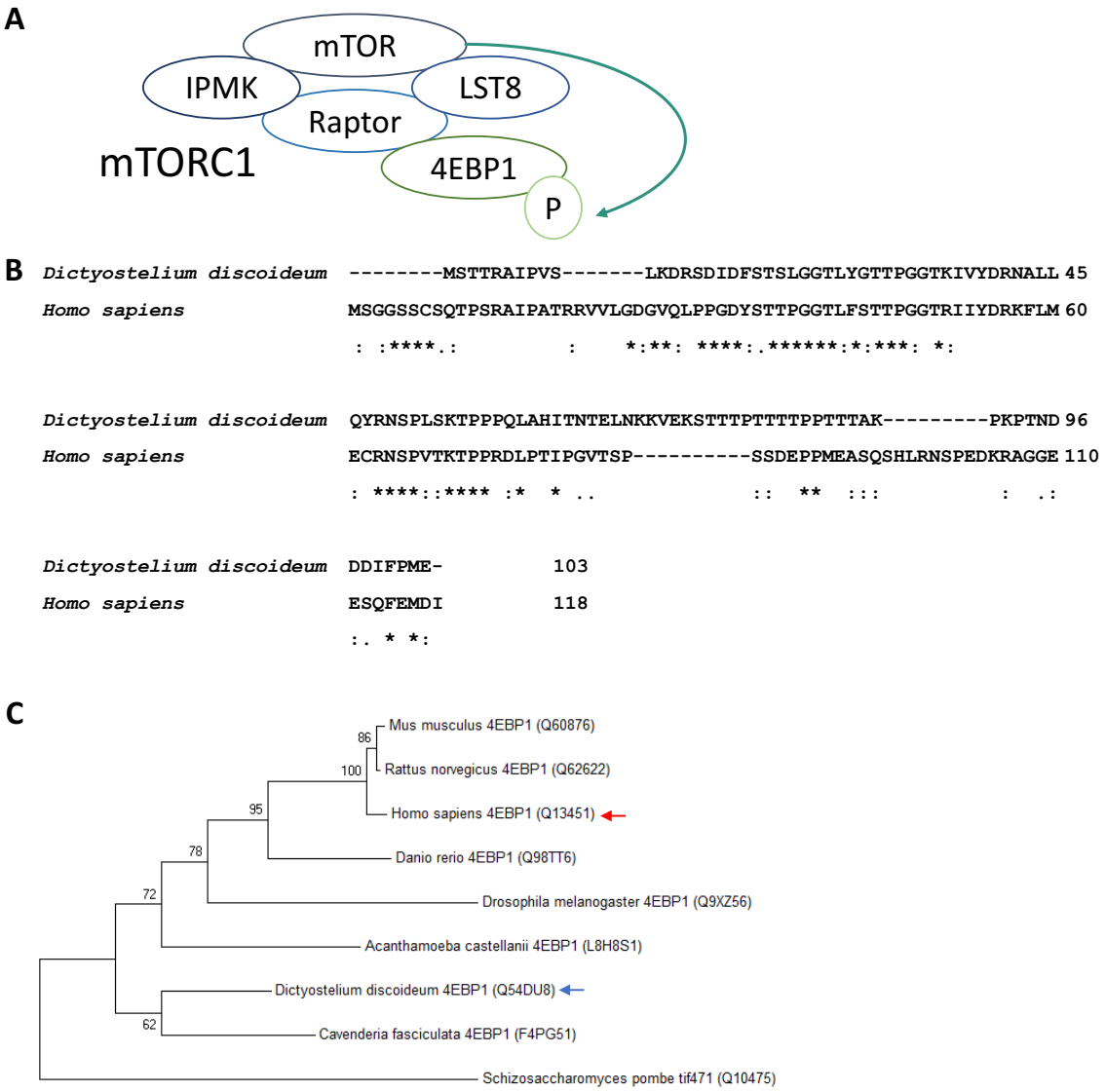

Figure 5.1: Similarity between *D. discoideum* and *H. sapiens* 4EBP1 proteins. **A:** Since binding of IPMK directly to mTOR in complex 1 (mTORC1) with Raptor and Lst8 enables the phosphorylation of the eukaryotic translation initiation factor 4E-binding protein 1 (4EBP1), this provided an indirect means to monitor IPMK activity, which was analysed to determine the effects of CBG, CBD, CBDA and CBDV on this cellular signalling pathway. **B:** *D. discoideum* (Q54DU8) and *H. sapiens* (Q60876) 4EBP1 sequence alignment was carried out on Clustal Omega. The two proteins shared an amino acid identity of 38.7%. Asterisks identical, colons are highly similar and full stops are similar. Both proteins share the threonine (46 in *Homo sapiens)* recognised by the anti-p4EBP1 antibody used in this study (green box). **C:** Phylogenetic analysis of 4EBP1 proteins suggests that the *D. discoideum* protein (blue arrow) is located within the same clade as the Human protein (red arrow), suggesting a common evolutionary origin.

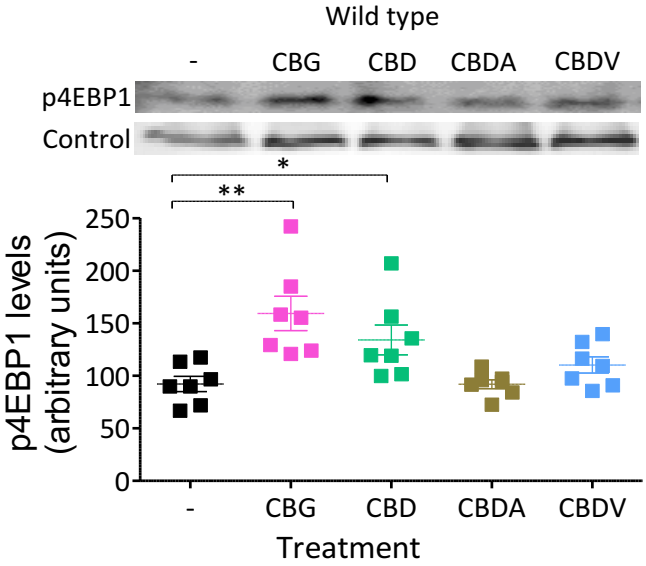

Figure 5.2: CBG and CBD upregulate mTORC1 activity in *D. discoideum*. Wild type (WT) cells were maintained in control conditions (in the absence of CBG, CBD, CBDV or CBDA (-)) or treated with 0.25 µM CBG, CBD, CBDA or CBDV for 1 hour. Samples were analysed for phosphorylation of 4EBP1 by western blot, n=7. CBG and CBD significantly increased mTORC1 activity, as evidenced by an increase in phosphorylated 4EBP1, however, CBDA and CBDV did not have this effect. Data shown represents mean±standard error of the mean. Data were normally distributed with Shapiro-Wilks and significance provided by One-Way ANOVA with Dunnett's Post-Hoc, * - p<0.05, ** - p<0.01. Streptavidin was used as a control protein to show that protein levels were consistent between samples.

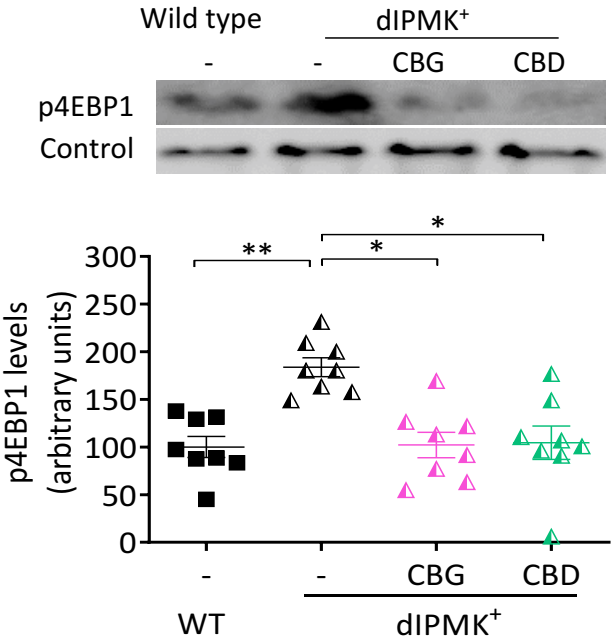

Figure 5.3: Elevation of IPMK abrogates the effects of CBG and CBD on mTORC1 activity in *D. discoideum*. dIPMK$^+$ cells were kept in control conditions or treated with 0.25 µM CBG or CBD for 1 hour and then samples were analysed for phosphorylation of 4EBP1 by western blot, n=8. In control conditions, dIPMK$^+$ cells had elevated mTORC1 activity compared to untreated wild type cells, as evidenced by an elevated level of phosphorylated 4EBP1. In dIPMK$^+$ cells both cannabinoids significantly reduced mTORC1 activity, as evidenced by a reduction in the level of phosphorylated 4EBP1. Streptavidin was used as a control protein to show that protein levels were consistent between samples. Data shown represents mean±standard error of the mean. Data were normally distributed with Shapiro-Wilks. A one-way ANOVA with Bonferroni's Multiple Comparison Test was carried out to test significance, * - p<0.05, ** - p<0.01.

5.2.3 The mechanism of action of CBG is PKB- and PI3K-dependent

As PKB is a key regulator of the mTORC1 pathway and orthologous PKB proteins exist in both *D. discoideum* and *H. sapiens*, PKB was examined for a role in regulating the molecular mechanism of CBG. From the two PKB proteins in *D. discoideum*, amino acid alignment (using Clustal W) indicated that PKBA shared 45 % amino acid identity (Figure 5.4 A) and all three main domains (pleckstrin homology domain, protein kinase domain and AGC-kinase domain) with the *H. sapiens* protein (Figure 5.4 B). Phylogenetic analysis (using MEGA 7 to produce a neighbour-joining tree with 500 Bootstrap replications) indicated that PKBA was more similar to the *H. sapiens* protein than PKGB (Figure 5.4 C).

Therefore, CBG growth assays were carried out using a *D. discoideum* cell line lacking PKBA ($PKBA^-$) in addition to a cell line lacking PKBA and over-expressing dIPMK ($PKBA^-dIPMK^+$), to examine if a reduction in PKB affected *D. discoideum* sensitivity to CBG during growth. In these experiments, $PKBA^-$ and $PKBA^-dIPMK^+$ cells were grown in the presence of increasing concentrations of CBG over 168 hours. Under control conditions (in the presence of solvent only), $PKBA^-$ and $PKBA^-dIPMK^+$ *D. discoideum* cell growth showed a lag phase until 96 hours, an exponential phase to 144 hours and a stationary phase starting at 168 hours (Figure 5.5 A and B). Similarly to wild type cells, CBG concentrations above 4 µM significantly inhibited $PKBA^-$ cell growth at 168 hours ($P<0.05$ for $PKBA^-$, Mann-Whitney test), however, CBG concentrations below 4 µM did not significantly inhibit $PKBA^-$ cell growth. Furthermore, in $PKBA^-dIPMK^+$ cells concentrations higher than 2 µM CBG significantly inhibited growth at 168 hours ($P<0.01$, Mann-Whitney test), however, concentrations below 2 µM had no significant effect on growth. Data arising from this analysis (rate of growth and Log of concentration) were used to calculate an IC_{50} for $PKBA^-$ cells of 2.16 µM and for $PKBA^-dIPMK^+$ cells of 1.74 µM, both of which were significantly higher than the wild type IC_{50} of 0.22 µM ($P<0.01$, one-way ANOVA with Bonferroni's Multiple Comparison Test) (Figure 5.5 C). In these experiments, over-expression of IPMK in PKBA-ablated cells did not significantly alter the IC_{50} of *D. discoideum* treated with CBG during growth (one-way ANOVA with Bonferroni's Multiple Comparison Test). These data showed PKBA ablation created a reduction in sensitivity to CBG in *D. discoideum* and that over-expression of dIPMK did not alter this reduction in sensitivity, which suggested that both PKBA and IPMK regulated *D. discoideum* response to CBG through a shared mechanism.

As PKBA and IPMK regulated the *D. discoideum* response to CBG during growth, the role of PKB was examined for an effect in mediating CBG regulation of mTORC1 signalling. Here, PKB regulates mTORC1 through TSC1/2/Rheb or sequestration into mTORC2 (Gunn and Hailes, 2008) (Figure 5.6 A). To examine the role of PKB in CBG- and CBD-dependent mTORC1 regulation, wild

type cells and PKBA$^-$ cells and cells lacking both PKBA and PKGB (PKBA$^-$PKGB$^-$) were maintained in control conditions (in the presence of solvent only) for one hour and PKBA$^-$ and PKBA$^-$PKGB$^-$ cells were treated with 0.25 µM CBG or CBD for one hour, then levels of phosphorylated 4EBP1 were measured by western blot. In control conditions, cells lacking PKBA had 1.9-fold elevated mTORC1 activity compared to wild type cells, as evidenced by an increase in 4EBP1 phosphorylation ($P<0.01$, one-way ANOVA with Bonferroni's Multiple Comparison Test) (Figure 5.6 B). In control conditions, cells lacking both PKBA and PKGB did not have a significantly different level of mTORC1 activity, as evidenced by a similar level of 4EBP1 phosphorylation to wild type cells (Figure 5.6 C). Following CBG or CBD treatment of PKBA$^-$ cells, mTORC1 activity increased a further 1.3- and 1.6-fold respectively, as evidenced by an increase in 4EBP1 phosphorylation ($P<0.05$ for CBG, $P<0.01$ for CBD, one-way ANOVA with Bonferroni's Multiple Comparison Test). However, treatment with either CBG or CBD did not alter mTORC1 activity in cells lacking both PKBA and PKGB, as evidenced by no change in the level of 4EBP1 phosphorylation (one-way ANOVA with Bonferroni's Multiple Comparison Test). In combination, these data suggested that PKB was necessary for CBG- and CBD-dependent regulation of mTORC1 activity in *D. discoideum*.

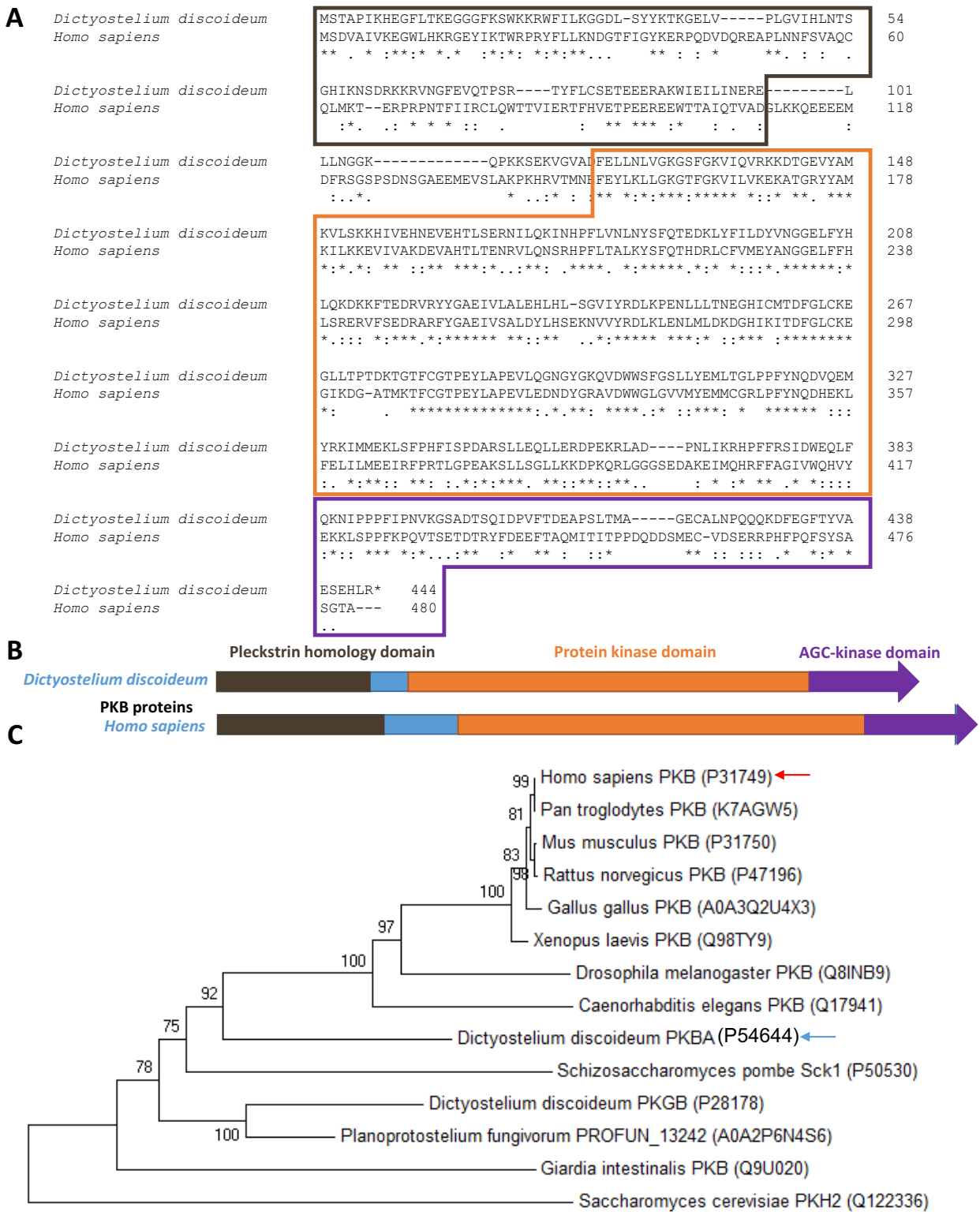

Figure 5.4: Similarity between *D. discoideum* and *H. sapiens* PKB proteins. A: *D. discoideum* (P54644) and *H. sapiens* (P13749) PKB sequence alignment was carried out on Clustal Omega. The two proteins share a sequence identity of 44.5 %. Asterisks identical, colons highly similar, full stops similar. **B:** Comparison of *H. sapiens* PKB and *D. discoideum* PKBA proteins. Both proteins share pleckstrin homology domains (black), protein kinase domains (orange) and AGC-kinase domains (purple). **C:** Phylogenetic analysis of PKB proteins suggest that the *D. discoideum* protein (blue arrow) is located within the same clade as the *H. sapiens* protein (red arrow), suggesting a common evolutionary origin. The *D. discoideum* PKBA protein appears to be more closely related to *H. sapiens* PKB protein than the *D. discoideum* PKGB protein.

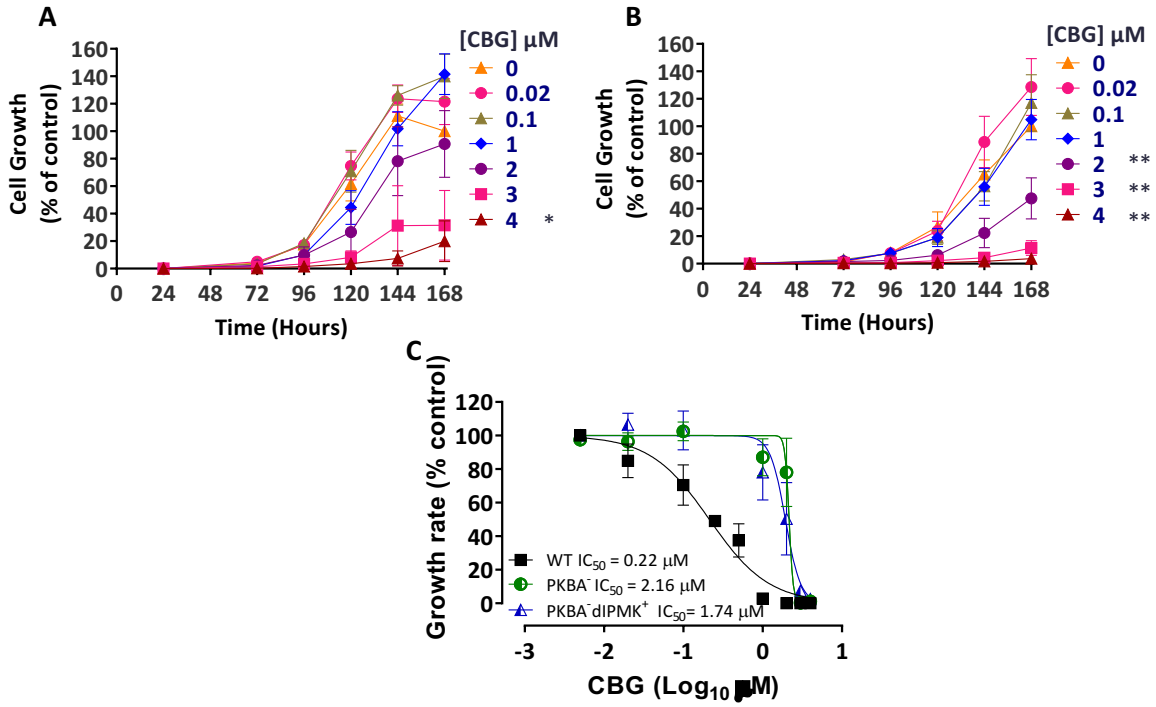

Figure 5.5: PKB ablation leads to resistance to CBG in growth in *D. discoideum*. A and B: Growth assays were carried out using PKBA$^-$ (n=7) and PKBA$^-$dIPMK$^+$ (n=5) cells. Growth was calculated as a % of each cell line in control conditions (in the absence of CBG). CBG inhibited growth in a concentration-dependent manner. Data arising from comparing the growth rate at differing concentrations of CBG was used to create a secondary plot. Data were not normally distributed (Shapiro-Wilks), therefore a Mann Whitney test was carried out to test for significance of inhibition by each concentration of CBG compared to control at 168 hours, * - p<0.05, ** - p<0.01. Graphs show mean ± SEM. **C:** Secondary plot analysis was used to determine the IC_{50}, PKBA$^-$ IC_{50} of 2.16 µM (n=7), and PKBA$^-$dIPMK$^+$ IC_{50} of 1.74 µM are significantly higher than wild type (WT) IC_{50} of 0.22 µM (n=10). No significant difference was found between PKBA$^-$ and PKBA$^-$dIPMK$^+$ cells. Data were normally distributed with Shapiro-Wilks therefore one-way ANOVA with Bonferroni's Multiple Comparison Test was carried out to determine significance.

As PKB had been implicated in the CBG- and CBD-dependent regulation of mTORC1 and PI3K signalling regulates PKB, the role of PI3K signalling on cannabinoid regulation of mTORC1 was examined. In this experiment, wild type cells were treated with a PI3K inhibitor (60 µM LY294002 (Van Haastert et al., 2007)) in control conditions (in the presence of solvent only) for one hour and treated with 0.25 µM CBG or CBD for one hour, then levels of phosphorylated 4EBP1 were measured by western blot. This analysis found no change in mTORC1 activity in cells with pharmacologically inhibited PI3K activity when treated with CBG or CBD, as evidenced by no

change in the level of 4EBP1 phosphorylation (Kruskal-Wallis test) (Figure 5.6 D). This indicated that PI3K activity was necessary for CBG- and CBD-dependent regulation of mTORC1 signalling.

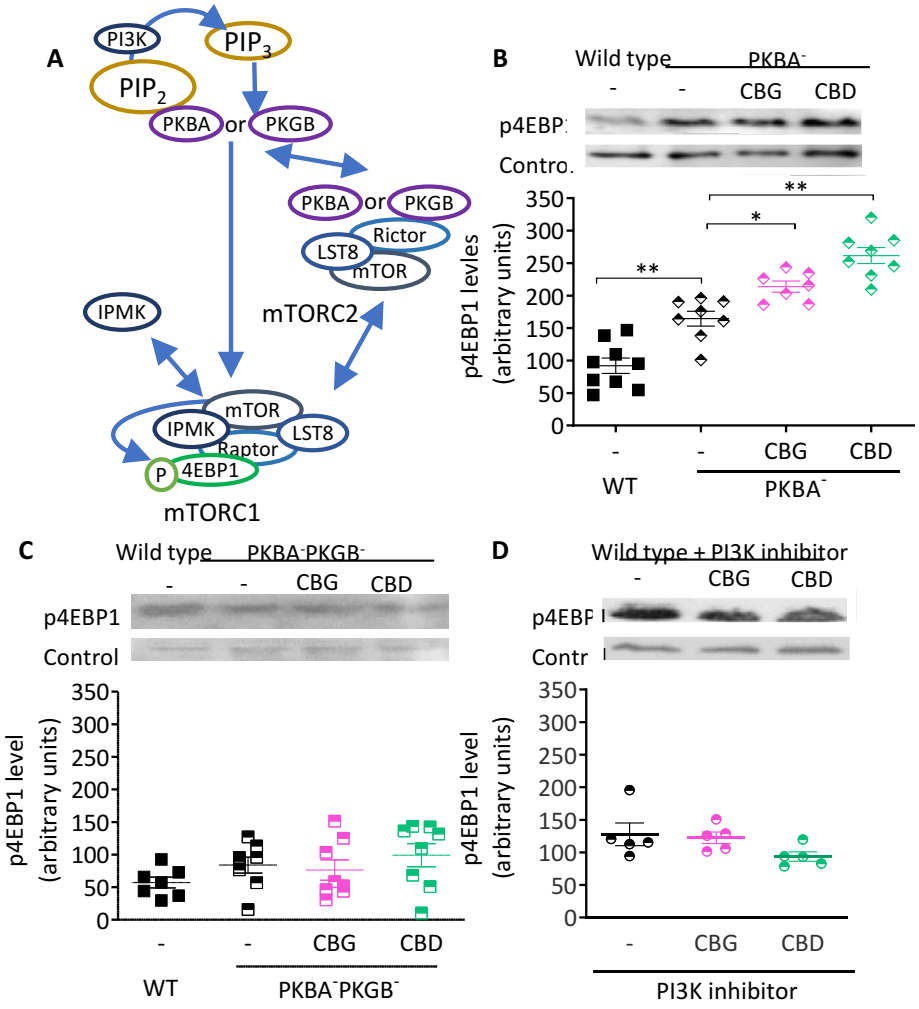

Figure 5.6: Cannabinoid-dependent effects on mTORC1 activation are regulated by PKB and PI3K activity in *D. discoideum*. A: Regulation of mTORC1 activity occurs through a complex pathway, initiated by PI3K, and proceeding through PKB (in *D. discoideum* PKBA (P54644) and PKGB (P28178)), and mTORC1 and mTORC2, where multiple components are shared between the two complexes. **B and C:** Wild type *D. discoideum* and cells lacking either PKBA or both PKBA and PKGB were maintained in control conditions (in the presence of solvent only and in the absence of CBG or CBD (-)) or treated with 0.25 µM CBG or CBD for 1 hour and then analysed for levels of phosphorylated 4EBP1 by western blot, n=8 and n=10. Streptavidin was used as a control protein to show that protein levels were consistent between samples. Data shown represents mean± standard error of the mean. Data were normally distributed with Shapiro-Wilks and significance provided by One-Way ANOVA with Bonferroni's Multiple Comparison Test, where * is $p<0.05$ and ** is $p<0.01$. **B:** PKBA$^-$ cells in control conditions had significantly elevated mTORC1 activity compared to wild type cells, as evidenced by an elevated level of 4EBP1 phosphorylation. In these cells CBG and CBD treatment significantly reduced mTORC1 activity. **C:** PKBA$^-$PKGB$^-$ cells in control conditions had a similar level of mTORC1 activity to wild type cells, as evidenced by a similar level of 4EBP1 phosphorylation. In these cells CBG and CBD treatment did not significantly alter mTORC1 activity. **D:** Wild type cells were treated with a pharmacological inhibitor of PI3K activity (LY294002: 60µM), and either maintained in control conditions (in the absence of CBG or CBD (-)) or treated with 0.25 µM CBG or CBD for 1 hour and then analysed for levels of phosphorylated 4EBP1 by western blot, n=5. Streptavidin was used as a control protein to show that protein levels were consistent between samples. Data shown represents mean±standard error of the mean. Normality of data was determined by the Shapiro-Wilk test and found to be not normally distributed. Significance was tested by Kruskal-Wallis test and no significance was found.

5.2.4 CBG regulates the IPMK-dependent activity of higher order inositol phosphate production in *D. discoideum*

To distinguish between a CBG- and CBD-dependent effect on IPMK or PI3K/PKB signalling, the effect of CBG or CBD treatment on production of higher order inositol phosphates in *D. discoideum* was examined. IPMK is essential for the synthesis of higher order inositol phosphates such as IP_{4-6} (Figure 5.7 A) (Saiardi et al., 1999; Maag et al., 2011; Kim et al., 2011). Therefore, wild type cells and cells over-expressing dIPMK were maintained in control conditions (in the presence of solvent only and the absence of CBG or CBD) or treated with CBG or CBD (0.25 µM for 1 and 24 hours) (Figure 5.7 B) and inositol phosphates were extracted and separated using polyacrylamide gel electrophoresis (Losito et al., 2009), and IP_6 levels were quantified. Here, CBD significantly elevated IP_6 levels following acute (1 hour) exposure (15 %) ($p<0.05$, Kruskal-Wallis test with Dunn's Multiple Comparison Post-test), and both CBG and CBD significantly elevated IP_6 levels following chronic (24 hours) exposure (15 %) (Figure 5.7 B) ($p<0.05$, Kruskal-Wallis test with Dunn's Multiple Comparison Post-test). Repeating this analysis in cells over-expressing dIPMK found that the CBG- and CBD-dependent elevated of IP_6 levels are lost (Figure 5.7 C).

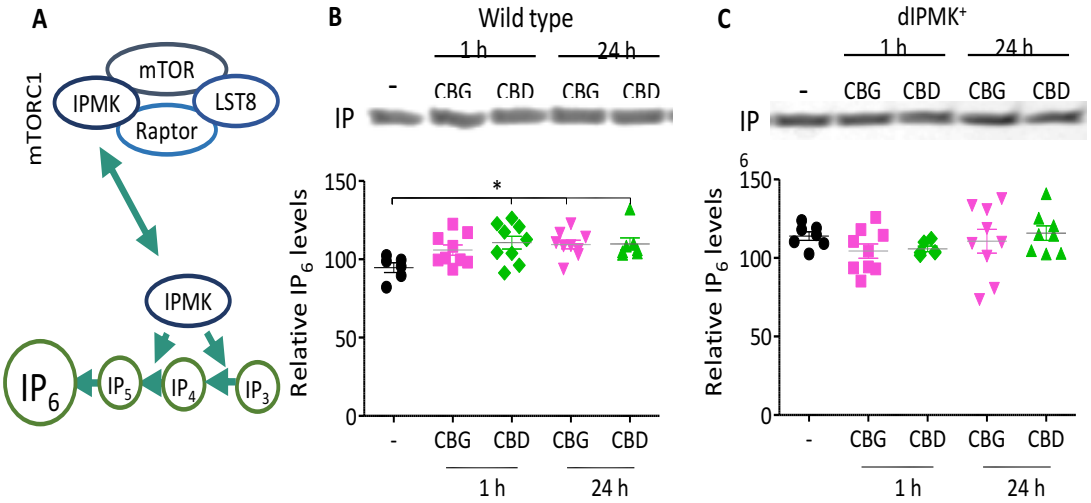

Figure 5.7: Cannabinoids upregulate catalytic activity of IPMK in *D. discoideum*. A: IPMK has a catalytic role in the creation of higher order inositol phosphates, the protein can catalyse IP_4 and IP_5 creation, which are essential for the creation of IP_6. **B:** Wild type *D. discoideum* cells were maintained in control conditions or treated with 0.25 µM CBG or CBD for 1 or 24 hours. The one-hour treatment of wild type with CBD ($p<0.05$) and 24-hour treatment with either CBG or CBD significantly increased IP_6 levels ($p<0.05$) compared to wild type untreated, n=6. Data were not normally distributed (Shapiro-Wilks), therefore a Kruskal-Wallis test with Dunn's Multiple Comparison Post-test was used to evaluate significance. **C:** *IPMK*$^+$ *D. discoideum* cells were exposed to 0.25 µM CBG or CBD or vehicle (-) control for 1 or 24 hours, n=6. No significant effects were found of cannabinoid treatment on IP_6 levels in *IPMK*$^+$ cells. Data were not normally distributed (Shapiro-Wilks), therefore a Kruskal-Wallis test with Dunn's Multiple Comparison Post-test was used to evaluate significance.

Together, these data indicate a role for CBG and CBD in activating IPMK to elevate the production of higher order inositol phosphates.

5.3 Discussion

In this chapter, the effects of CBG on the mTORC1 pathway in *D. discoideum* were characterised and the roles of IPMK, PKB and PI3K in these effects were examined. As IPMK is involved in mTORC1 signalling, the effects of CBG and other cannabinoids on mTORC1 activity were measured through phosphorylation of 4EBP1. Using this approach, CBG and CBD were found to elevate mTORC1 activity in wild type *D. discoideum* cells, an effect not shared by CBDA or CBDV. Following this, dIPMK-overexpression was found to result in an elevated level of mTORC1 activity, however, CBG and CBD reduced mTORC1 activity in dIPMK over-expressing cells. In addition, PKBA ablation resulted in an increased mTORC1 activation, while CBG and CBD treatment in PKBA ablated cells further increased mTORC1 activity. Furthermore, ablation of both PKB proteins or chemical inhibition of PI3K activity in *D. discoideum* blocked any increase in mTORC1 activity by CBG or CBD. Therefore, a potential mechanism of action for CBG and CBD of mTORC1 regulation through IPMK, PI3K and PKB in *D. discoideum* was discovered.

To measure mTORC1 activity in *D. discoideum*, 4EBP1 phosphorylation was analysed by western blot. Phosphorylation of 4EBP1 is routinely used as a readout for mTORC1 activation in many organisms (Qin et al., 2016; Woodcock et al., 2019; Chang et al., 2020). The protein 4EBP1 is a major translational repressor, which inhibits cap-dependent translation and therefore reduces protein production and cell growth (Woodcock et al., 2019). Once phosphorylated by an active mTORC1, 4EBP1 no longer inhibits cellular protein production. Phosphorylation of 4EBP1 has previously been measured in *D. discoideum* to determine mTORC1 activity (Rosel et al., 2012; Cardenal-Muñoz et al., 2017; Chang et al., 2020). However, in *D. discoideum* an antibody to detect total levels of the 4EBP1 protein is not available (Chang et al., 2020). Therefore, it is not possible to determine whether a proportion of phosphorylated 4EBP1 is changed or if the proportion of phosphorylated protein remains the same but the total amount of protein changes. However, during this study, the aim was to translate any findings into mammalian systems where the phosphorylation of 4EBP1 and total 4EBP1 protein can be measured (So et al., 2016). Therefore, in this study, the phosphorylation of 4EBP1 in *D. discoideum* was used to measure mTORC1 activity, with the aim to validate the results in mammalian models.

Investigation of the molecular mechanisms of CBG was the main aim of this study, however, other cannabinoids were also examined to determine any shared molecular targets in *D.*

discoideum. Interestingly, CBG and CBD both increased mTORC1 activity in wild type *D. discoideum* cells, however, two closely related cannabinoids, CBDV and CBDA did not have this effect. The differential response of *D. discoideum* mTORC1 activity to different cannabinoids may arise from the structural differences between the molecules. The active cannabinoids both have five-carbon chains on the third carbon of the benzyl ring and no carboxylic acid group (Citti et al., 2018). The combination of an absence of an acidic group and the presence of a five-carbon chain on these cannabinoids could be responsible for the ability to activate mTORC1, through steric or charge-related hindrance effects in target binding or in reaching the molecular target within a cell. In a previous study, both CBG and CBD in intraperitoneal administration were found at higher concentrations in the blood and brain of mice than CBDV (Deiana et al., 2012), consistent with a difference in transport across the plasma membrane. There is a possibility that higher concentrations of CBDV and CBDA would be capable of regulating mTORC1 activation, which could be explored in future studies in disease models. However, this study finds that CBG and CBD share a role in mTORC1 activation in *D. discoideum.*

In addition to CBG activation of mTORC1 activity, dIPMK over-expression in *D. discoideum* increased mTORC1 activity, mimicking the treatment of wild type cells with CBG or CBD. In this model, treatment of the dIPMK over-expressing cells with CBG or CBD decreased mTORC1 activity. Conversely, while ablation of PKBA also led to an increase in mTORC1 activity, treatment of PKBA ablated cells with CBG or CBD further increased mTORC1 activity. These data suggest that in *D. discoideum*, CBG and CBD treatment may enhance the direct role of IPMK in mTORC1 function. In wild type cells, this would increase mTORC1 activity and suggest that IPMK is a rate-limiting factor for mTORC1 activation. In dIPMK over-expressing cells, to maintain homeostasis, there could be an increased reliance on PIP_3 production by IPMK (Blind et al., 2012), thereby leaving cells with a reduced PI3K/PKB signalling pathway necessary for the activation of mTORC1. In this case, CBG or CBD treatment would increase IPMK direct involvement in mTORC1 function, and a reduction in PIP_3 production in the cell, therefore reducing mTORC1 activation overall. While this model suggests CBG- and CBD-dependent activation of IPMK is PI3K/PKB-independent, functional PI3K/PKB signalling remains necessary for the activation of mTORC1, supported by pharmacological inhibition of PI3K activity and ablation of PKB activity (in $PKBA^{-}PKGB^{-}$ cells) leading to a block of mTORC1 activation. In addition to previous reports of cannabinoids functioning through PI3K/PKB signalling (Giacoppo et al., 2017, Zuardi et al., 2009), these data suggest a novel mechanistic insight into CBG- and CBD-dependent regulation of mTORC1 through enhanced IPMK activity in the presence of a functionally active PI3K/PKB signalling pathway.

In the previous chapter, over-expression of dIPMK was found to increase the resistance of *D. discoideum* to CBG during growth, and in this chapter ablation of PKBA also resulted in resistance to this effect. However, PKBA ablated cells were found to be ten-fold more resistant to CBG than wild type cells and three-fold more resistant than dIPMK over-expressing cells. This could be because PKB is a regulator of mTORC1 activity (Gunn and Hailes, 2008), a downstream effector of mTORC2 signalling (Oh and Jacinto, 2011), and regulates between cell division, apoptosis or survival (Hövelmann et al., 2004). Given the complexity of PKB involvement in cell signalling pathways, it is difficult to discern the specific mechanism by which ablation of PKBA results in an increase in resistance to CBG during growth in *D. discoideum.* However, in *H. sapiens*, PKB over-expression can result in tumour formation, due to a reduced ability of cells to halt division, demonstrating the necessity of normal PKB function for correct cell growth (Hövelmann et al., 2004). In *D. discoideum* on the other hand, the two PKB proteins may work redundantly (Meili et al., 2000; Suess et al., 2017), such that loss of one protein results in a change in expression or activity of the other protein. If CBG acts on an activity specific to PKBA, while PKGB acts to regulate cellular processes independently of CBG, this would result in an increased ability of $PKBA^-$ cells to grow in the presence of CBG. Although further studies are necessary to examine the complex roles of PKB in growth regulation, in this study PKB was found to be a key regulator of *D. discoideum* response to CBG during growth.

To further determine the effect of CBG on IPMK and PKB activities, higher order inositol phosphate levels were measured. IPMK catalyses the production of IP_4 and IP_5 and is therefore necessary for both IP_6 and IP_7 production (Chakraborty et al., 2010). Both CBG and CBD were found to significantly increase IP_6 levels after 24-hour treatment in wild type *D. discoideum*, while over-expression of dIPMK blocked this effect. Furthermore, one-hour treatment with CBD significantly increased IP_6 levels. This increase is likely to be highly relevant to cell function since a previously reported 18% increase in IP_6 levels indicated that this change in IP_6 levels may alter calcium influx over the plasma membrane signal (Larsson et al., 1997). Therefore, these data suggest that CBG and CBD target IPMK activity and that CBG and CBD regulate mTORC1 through IPMK activity independently of PI3K/PKB (Kim et al., 2011, Saiardi et al., 1999, Maag et al., 2011b, Chakraborty et al., 2010). Inositol phosphate regulation is a key cellular process necessary for the regulation of histone modification (Watson et al., 2012), calcium signalling (Frederick et al., 2005), and PKB regulation (Maag et al., 2011). The key roles of IPMK in these cellular processes could explain the reduction in CBG sensitivity during growth in PKB ablated cells as IP_7 inhibits PKB activity (Mackenzie and Elliott, 2014). In this chapter, CBG is shown to increase IP_6 levels in *D. discoideum* after 24 hours, if these levels remain elevated then PKB would be inhibited and unable to signal for continued growth (Litman et al., 2007). However, IP_7 inhibits PKB by binding

to the pleckstrin homology domain which blocks the ability of PIP_3 to bind this domain (Calleja et al., 2007; Chakraborty et al., 2010). The PKGB protein does not contain this domain, therefore, if PKGB replaces some of the activity of PKBA after ablation of the latter, then IP_7 levels would no longer inhibit PKB activity and the cell would be more capable of growing in the presence of CBG. The observed change in IP_6 levels in this chapter suggests that CBG and CBD alter the production of inositol phosphates and therefore may affect IP_7 levels. Therefore, a potential mechanism of action of CBG through regulation of mTORC1 through IPMK in *D. discoideum* is identified, however, a mammalian model was necessary to validate this mechanism and determine potential therapeutic relevance.

Chapter 6: Translation of the mechanisms of action of CBG from *D. discoideum* into mammalian models

6.1 Introduction

In the previous chapter, a molecular mechanism of action of CBG and CBD was suggested to be regulation of mTORC1 activity through IPMK in *D. discoideum*. Here, in wild type cells when IPMK expression was at a normal level, CBG and CBD elevated mTORC1 activity. However, when IPMK expression was elevated, CBG and CBD inhibited mTORC1 activity, which suggested that CBG and CBD regulated mTORC1 in a homeostatic manner through IPMK. Furthermore, the CBG- and CBD-regulated elevation of mTORC1 activity in wild type cells was found to be dependent upon PI3K activity. While these mechanisms of action for CBG and CBD were demonstrated in *D. discoideum*, further analysis with mammalian proteins and in mammalian cells were needed to confirm the conservation of the effect.

To determine if CBG and CBD regulation of mTORC1 activity was conserved in mammals, three models were used, expression of the *H. sapiens* IPMK in *D. discoideum*, examination of mouse embryonic fibroblasts (MEFs) and primary peripheral blood mononuclear cells (PBMCs) from healthy volunteers and patients with multiple sclerosis (MS). MEFs were highly useful since a cell line lacking IPMK in MEFs was available for comparative analysis (Kim et al., 2011), allowing the assessment of MEF cells lacking IPMK or with pharmacologically inhibited PI3K activity to determine the dependence of CBG- and CBD-dependent mTORC1 regulation on these signalling components. Primary peripheral blood mononuclear cells (PBMCs) from healthy volunteers and patients with multiple sclerosis (MS) were used to determine whether regulation of mTORC1 in a disease model occurred following treatment with CBG, CBD, or a combination of THC and CBD (THC:CBD) at concentrations similar to the plasma concentrations achieved in patients with MS who take Sativex® (Leussink et al., 2012). PBMCs are the primary producers of pro-inflammatory cytokines which increase the progression of MS (Simpson et al., 2015). These cells include T lymphocytes, B cells and monocytes (Yu et al., 2007) that become activated in individuals with MS, crossing the blood-brain barrier and leading to axonal degradation and myelin damage in the central nervous system (CNS) (Bar-Or et al., 2003). In these cells, there is often an overactivation of mTORC1 activity and overproduction of pro-inflammatory cytokines (Carbone et al., 2014). Therefore, many MS therapies are immunomodulatory and target peripheral immune cells. In this study, the aim was to investigate if CBG, CBD, or a combination of THC and

CBD, treatment of PBMCs could similarly regulate mTORC1 activation as observed in *D. discoideum* and determine potential therapeutic relevance.

6.2 Results

6.2.1 The effect of CBG and CBD on human IPMK-expressing *D. discoideum*

To examine if the CBG molecular mechanism involving IPMK was conserved between *D. discoideum* and *H. sapiens*, the human IPMK protein was expressed in *D. discoideum.* This cell line was created using a C-terminal RFP over-expression plasmid which contained a human IPMK (hIPMK) insert, synthesized using a *D. discoideum* codon bias (Genscript) and then cloned into the RFP-containing plasmid (Figure 6.1 A) (pDM324 (Veltman et al., 2009)). To ensure the plasmid was constructed correctly, digestion with restriction enzymes that cleaved at the 5' and 3' ends of the hIPMK insert confirmed that an insert of the correct size (1260 bp) for hIPMK existed in this plasmid in the correct location (Figure 6.1 B). The whole gene was sequenced to ensure no mutations had occurred. Thereafter, the plasmid was transfected into *D. discoideum* and presence of the hIPMK-RFP protein was examined by western blot using an anti-RFP antibody. This analysis revealed that hIPMK-expressing cells (hIPMK$^+$) showed a specific 75 kDa RFP-containing protein, absent in wild type cells and consistent with the expression of full-length hIPMK-RFP (Figure 6.1 C). Furthermore, wild type and hIPMK$^+$ contained a similar level of protein, as evidenced by the control protein (streptavidin). This experiment confirmed that a heterologous *H. sapiens* IPMK-RFP protein was present in *D. discoideum* cells.

To determine the localisation of the hIPMK-RFP protein in *D. discoideum*, fluorescent microscopy was carried out. Growing cells expressing RFP-only, and hIPMK-RFP were imaged using a wide-field fluorescence microscope under agar to flatten cells, enabling clear cellular localisation. This analysis indicated that RFP-only localised mainly to the cytoplasm (Figure 6.1 D), while hIPMK-RFP was primarily localised in the nucleus, with some cytoplasmic localisation (Figure 6.1 E) as occurs in human cells (Nalaskowski et al., 2002). This contrasts with the previously examined dIPMK-RFP protein (Figure 4.7) which localised evenly to both the cytoplasm and nucleus. Therefore, *D. discoideum* cells were confirmed to express a correctly localised hIPMK-RFP protein. This was, therefore, an IPMK over-expressor cell line, but with the human IPMK.

To determine whether hIPMK expression in *D. discoideum* regulated sensitivity to CBG during growth, the hIPMK$^+$ cell line was examined for resistance to CBG treatment during growth. In these experiments, hIPMK$^+$ cells were grown in the presence of increasing concentrations of CBG over 168 hours. Under control conditions (in the presence of solvent only), hIPMK$^+$ *D. discoideum*

cell growth showed a lag phase until 96 hours, an exponential phase to 144 hours and a stationary phase starting at 168 hours (Figure 6.2 A). Similarly to wild type cells (Figure 3.1), CBG concentrations above 1 µM significantly inhibited hIPMK^{+} cell growth at 168 hours ($P<0.05$, Mann-Whitney test and $P<0.01$ for 2, 3 and 4 µM). Data arising from comparing the growth rate at differing concentrations of CBG was used to calculate a hIPMK^{+} IC_{50} for CBG of 1.03 µM (Figure 6.2 B), which was significantly higher than the wild type IC_{50} of 0.22 µM ($P<0.01$, one-way ANOVA with Bonferroni's Multiple Comparison Test (Figure 3.1) and dIPMK^{+} IC_{50} of 0.64 µM ($P<0.01$, one-way ANOVA with Bonferroni's Multiple Comparison Test (Figure 4.8)). These data showed expression of the human IPMK reduced sensitivity to CBG in *D. discoideum* during growth and potentially indicated that CBG could target both IPMK proteins.

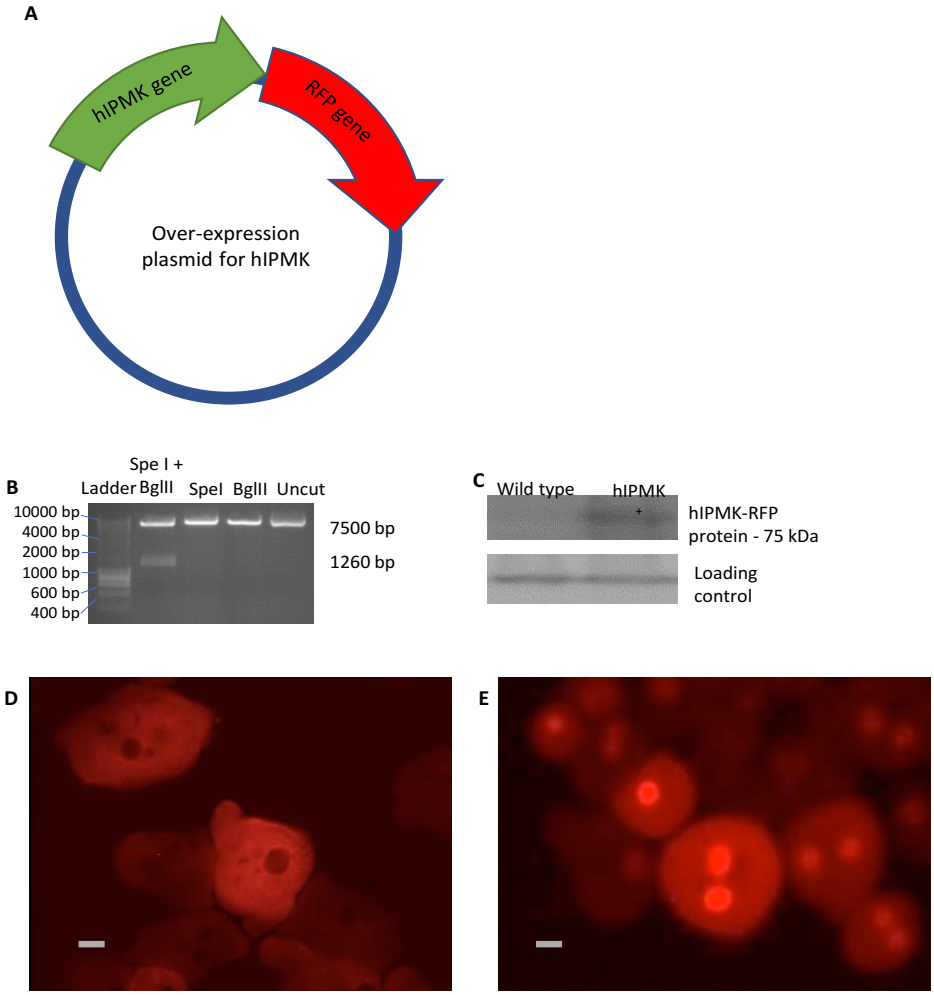

Figure 6.1: Production of a human IPMK-RFP expressing *D. discoideum* cell line. A: *H. sapiens* IPMK (hIPMK)-RFP plasmid was created in pDM324 (7564 bp) with an RFP tag at the C-terminal of the protein. **B:** *SpeI* and *BglII* restriction enzyme digestion sites at the 5' and 3' ends of the hIPMK gene insert (1260 bp), respectively were used to digest the plasmid and confirm the presence of the hIPMK insert. The plasmid was then transfected into wild type *D. discoideum.* **C:** Western blot analysis using an anti-RFP antibody was used to confirm that the hIPMK-RFP protein was expressed. Streptavidin was used as a control protein to show that protein levels were consistent between samples. **D:** Fluorescent images of RFP-only expressing cells, showing a mainly cytosolic localisation. **E:** Fluorescent images of hIPMK^{+} cells. The hIPMK protein localised to the nucleus, unlike the *D. discoideum* IPMK protein which localised to the cytoplasm (Figure 4.7). Scale bar 10 µm**.**

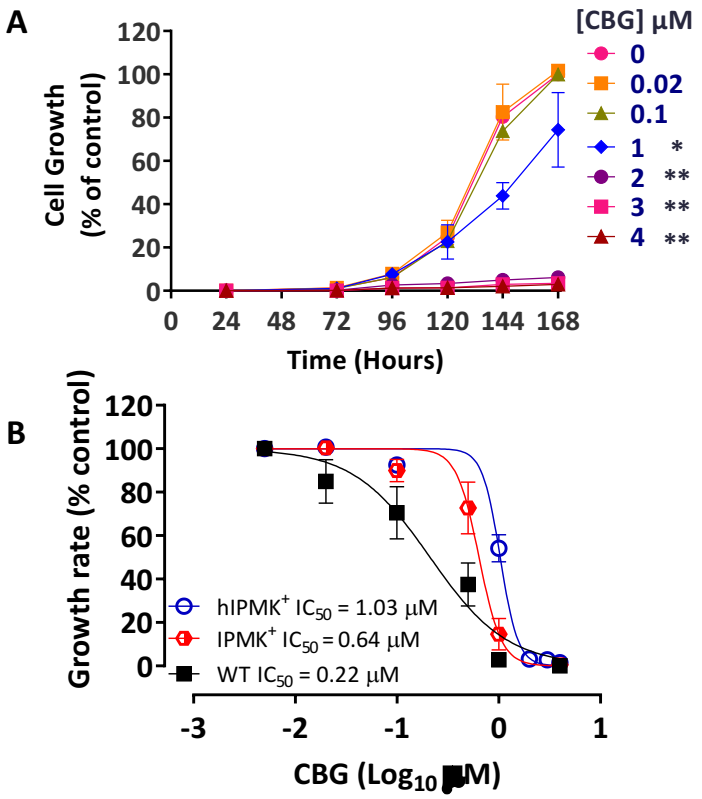

Figure 6.2: Expression of *H. sapiens* IPMK in *D. discoideum* leads to resistance to CBG in growth. A: hIPMK$^+$ cells were grown in the presence of increasing concentrations of CBG in shaking culture for one week. Growth was calculated as a % of each cell line in control conditions (in the absence of CBG), n=7. CBG inhibited growth in a concentration-dependent manner. Data arising from comparing the growth rate at differing concentrations of CBG was used to create a secondary plot. Data were not normally distributed (Shapiro-Wilks), therefore a Mann Whitney test was carried out to test for significance of inhibition by each concentration of CBG compared to control at 168 hours, * - $p<0.05$, ** - $p<0.01$. Graphs show mean ± SEM. **B:** Secondary plot analysis was used to determine the IC_{50}, hIPMK$^+$ IC_{50} = 1.03 µM (n=7). The wild type (WT) IC_{50} (0.22 µM) is significantly lower than hIPMK$^+$ IC_{50} ($p<0.01$) and dIPMK$^+$ IC_{50} (0.64 µM) ($p<0.01$). In addition, the dIPMK$^+$ IC_{50} is significantly lower than hIPMK$^+$ IC_{50} ($p<0.01$). Data were normally distributed according to Shapiro-Wilks. A one-way ANOVA with Bonferroni's Multiple Comparison Test was carried out to test significance.

To determine if hIPMK expression altered mTORC1 activity in *D. discoideum* cells following CBG and CBD treatment, 4EBP1 phosphorylation was measured in wild type and hIPMK$^+$ cells. To evaluate a potential change in the basal level of mTORC1 activity, wild type and hIPMK$^+$ cells were maintained in control conditions (in the presence of solvent only) for one hour, then levels of phosphorylated 4EBP1 were measured by western blot. Here, cells expressing hIPMK showed a 2.2-fold increase in mTORC1 activity, as evidenced by an elevated level of 4EBP1 phosphorylation compared to wild type cells (Figure 6.3) ($P<0.01$, one-way ANOVA with Bonferroni's Multiple Comparison Test). This showed that expression of hIPMK in wild type *D. discoideum* had a similar effect to over-expression of the endogenous protein (Figure 5.2). To evaluate the response to CBG and CBD, hIPMK$^+$ cells were treated with 0.25 µM CBG or CBD for

one hour, then levels of phosphorylated 4EBP1 were measured by western blot. Treatment of hIPMK^{+} cells with CBG or CBD resulted in a significant 35 % and 50 % reduction in mTORC1 activity, respectively, as evidenced by a decrease in the level of 4EBP1 phosphorylation (Figure 6.3) (P<0.01, one-way ANOVA with Bonferroni's Multiple Comparison Test). This result showed that elevated IPMK levels (using the human protein) increased basal mTORC1 activity and CBG or CBD treatment reduced this mTORC1 activity to wild type levels.

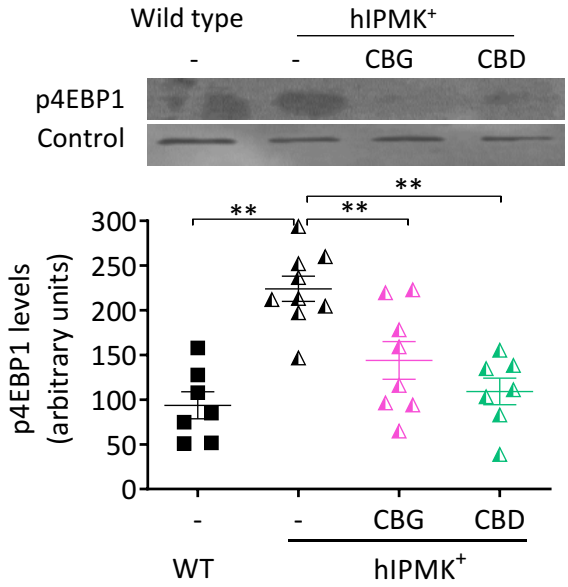

Figure 6.3: Expression of hIPMK reverses the CBG- and CBD-dependent elevation of mTORC1 activity in *D. discoideum*. *D. discoideum* cells expressing the human IPMK protein (hIPMK^{+}) were maintained in control conditions (in the absence of CBG or CBD (-)) or treated with 0.25 µM CBG or CBD for 1 hour and then analysed for levels of phosphorylated 4EBP1 by western blot, n=7. hIPMK^{+} cells in control conditions had significantly higher mTORC1 activity than untreated wild type cells. In hIPMK^{+} cells, CBG and CBD treatment significantly reduced mTORC1 activity. Streptavidin was used as a control protein to show that protein levels were consistent between samples. Data shown represents mean± standard error of the mean. Data were normally distributed with Shapiro-Wilks. A one-way ANOVA with Bonferroni's Multiple Comparison Test was carried out to test significance, ** - p<0.01.

6.2.2 The effect of CBG and CBD on mTORC1 activity in mouse embryonic fibroblasts

To examine if the CBG- and CBD-dependent regulation of mTORC1 activity was shared in a mammalian model, mouse embryonic fibroblasts (MEFs) were examined. Here, wild type MEF cells were maintained in control conditions (in the presence of solvent only) or treated with 4 µM CBG or CBD for 24 hours, then the levels of phosphorylated and total 4EBP1 were quantified by western blot. In these cells, mTORC1 activity was significantly elevated 1.5-fold by CBG or CBD treatment, as evidenced by an increase in the proportion of phosphorylated 4EBP1 to total 4EBP1 (Figure 6.4 A) (P<0.01, one-way ANOVA with Dunnett's Multiple Comparison

Test). This increase in the proportion of phosphorylated 4EBP1 was caused by a significant 1.3-fold increase in the phosphorylation of 4EBP1 (Figure 6.4 B) (P<0.01 and P<0.05 respectively, one-way ANOVA with Dunnett's Multiple Comparison Test) and an unchanged level of total 4EBP1 (Figure 6.4 C) (one-way ANOVA with Dunnett's Multiple Comparison Test). In combination, these data showed CBG- and CBD-dependent elevation of mTORC1 activity occurred in wild type MEFs.

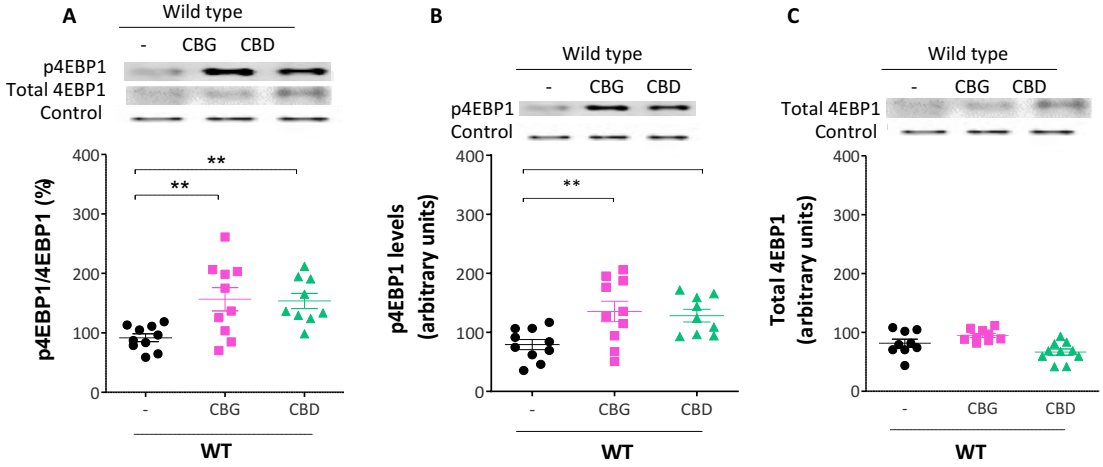

Figure 6.4: CBG and CBD upregulate mTORC1 activity in mouse embryonic fibroblasts. A-C: Wild type MEF cells were maintained in control conditions (in the absence of CBG or CBD (-)) or treated with 4 µM CBG or CBD for 24 hours and then were analysed for phosphorylated and total 4EBP1 levels. Actin was used as a control protein to show that protein levels were consistent between samples. Data shown represents mean± standard error of the mean. Data were normally distributed with Shapiro-Wilks and significance was tested using a One -Way ANOVA with Dunnett's Multiple Comparison Test, significance, * - p<0.05, ** - p<0.01, n=9. **A:** mTORC1 activity significantly increased in cells treated with CBG or CBD, as evidenced by an increase in the proportion of phosphorylated to total 4EBP1. **B:** Phosphorylation of 4EBP1 significantly increased in cells treated with CBG or CBD. **C:** Total 4EBP1 did not significantly change in cells treated with CBG or CBD.

To assess whether IPMK signalling was necessary for CBG- and CBD-dependent regulation of mTORC1 activity, MEF cells lacking the IPMK protein were examined for response to CBG and CBD. Here, MEF cells lacking the IPMK protein (Kim et al., 2011) were maintained in control conditions (in the presence of solvent only) or treated with 4 µM CBG or CBD for 24 hours, then the levels of phosphorylated and total 4EBP1 were quantified by western blot. In these cells, no significant change was observed in mTORC1 activity after treatment with CBG or CBD, as evidenced by no change in the proportion of phosphorylated 4EBP1 to total 4EBP1 (Figure 6.5 A) (one-way ANOVA with Dunnett's Multiple Comparison Test). Treatment with CBG or CBD did not significantly alter the phosphorylation of 4EBP1 (Figure 6.5 B) (one-way ANOVA with Dunnett's Multiple Comparison Test) or total 4EBP1 levels (Figure 6.5 C) (one-way ANOVA with Dunnett's Multiple Comparison Test). In combination, these data showed CBG- and CBD-dependent regulation of mTORC1 was dependent on the existence of the IPMK protein.

To determine if PI3K signalling was necessary for CBG regulation of mTORC1 activity in mammalian cells, as observed in *D. discoideum*, MEF cells were examined. Here, wild type MEF cells were treated with a PI3K inhibitor (10 µM Pictilisib (Yu et al., 2015; Beale et al., 2016)), and either maintained in control conditions (in the presence of solvent only) or treated with 4 µM CBG or CBD for 24 hours, then the levels of phosphorylated and total 4EBP1 were quantified by western blot. These experiments showed that no significant change in mTORC1 activity was observed in MEF cells lacking PI3K activity when treated with CBG or CBD, as evidenced by no

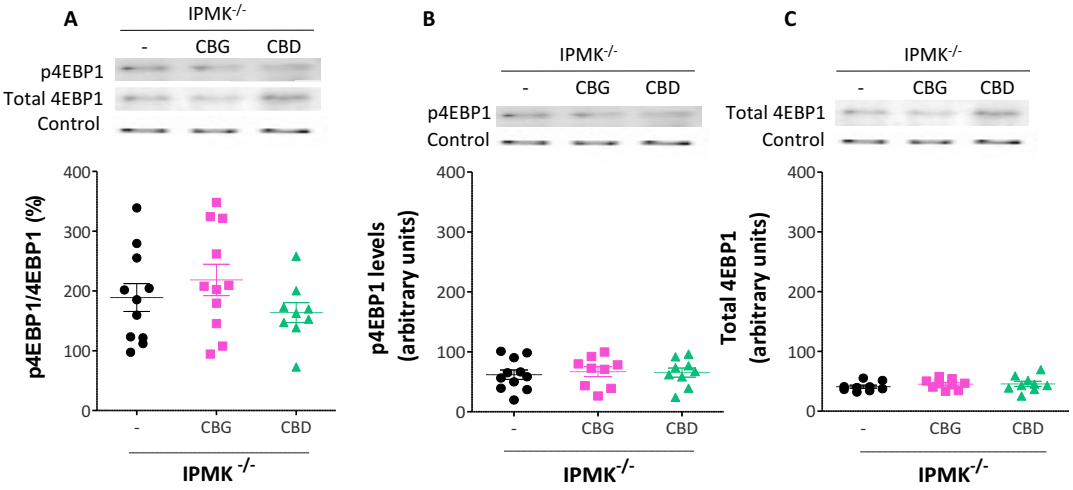

Figure 6.5: CBG and CBD do not upregulate mTORC1 in the absence of IPMK in mouse embryonic fibroblasts. A-C: MEF cells lacking the IPMK protein were maintained in control conditions (in the absence of CBG or CBD (-)) or treated with 4 µM CBG or CBD for 24 hours were analysed for phosphorylated and total 4EBP1 levels. Actin was used as a control protein to show that protein levels were consistent between samples. Data shown represents mean± standard error of the mean. Data were normally distributed with Shapiro-Wilks and significance was tested using a One -Way ANOVA with Dunnett's Multiple Comparison Test, n=9. **A:** mTORC1 activity did not significantly change in cells lacking IPMK when treated with CBG or CBD, as evidenced by no change in the proportion of phosphorylated to total 4EBP1. **B:** Phosphorylation of 4EBP1 did not significantly change in cells lacking IPMK when treated with CBG or CBD. **C:** Total 4EBP1 did not significantly change in cells lacking IPMK when treated with CBG or CBD.

change in the proportion of phosphorylated 4EBP1 to total 4EBP1 (Figure 6.6 A) (one-way ANOVA with Dunnett's Multiple Comparison Test). In PI3K inhibitor-treated MEF cells, CBG or CBD treatment did not alter the phosphorylation of 4EBP1 (Figure 6.6 B) (one-way ANOVA with Dunnett's Multiple Comparison Test) or total 4EBP1 levels (Figure 6.6 C) (one-way ANOVA with Dunnett's Multiple Comparison Test). In combination, these data showed PI3K signalling was necessary for CBG- and CBD-dependent regulation of mTORC1.

6.2.3 The effect of CBG, CBD and a THC:CBD mixture on mTORC1 activity in primary peripheral mononuclear cells derived from humans

Since CBG- and CBD-dependent regulation of mTORC1 activity was shown to be shared between *D. discoideum* and *M. musculus* MEF cells, primary *H. sapiens* PBMCs were examined to

determine if this effect was conserved in human cells in a clinical context. Here, primary PBMCs were extracted from healthy volunteers (demographics in Table 6.1 A) and maintained in control conditions (in the presence of solvent only) or treated with CBG or CBD (0.1 μM), or plant-derived highly purified THC:CBD combinations (0.02 μM:0.017 μM) for 24 hours (carried out by Trinity College Dublin). Following this, mTORC1 activity was analysed in primary PBMCs from healthy volunteers by quantification of phosphorylated and total 4EBP1 levels by western blot. In this analysis, mTORC1 activity was significantly elevated 1.3-fold following CBG treatment, 1.2-fold following CBD treatment and 1.6-fold following THC:CBD treatment, as evidenced by an increase in the proportion of phosphorylated 4EBP1 to total 4EBP1 (Figure 6.7 A, B, C) ($P<0.05$, Mann-Whitney Test). Surprisingly, this change in ratio was not driven by a significant change in the level of phosphorylated (Figure 6.7 D, E, F) or total 4EBP1 (Figure 6.7 G, H, I). In fact, the level of 4EBP1 phosphorylation appeared to not change following CBG treatment ($P=0.48$), however, a nonsignificant trend towards an increase in phosphorylated 4EBP1 was observed following CBD treatment ($P=0.18$) and following THC:CBD ($P=0.10$) (Mann-Whitney Test). In addition, the observed change in mTORC1 activity did not result from a significant change in the level of total 4EBP1 (Figure 6.7 G, I). In fact, the level of total 4EBP1 appeared to not change following CBD treatment ($P=0.59$), however, a nonsignificant trend towards a decrease in total 4EBP1 was observed following CBG treatment ($P=0.13$) and following THC:CBD treatment ($P=0.13$) (Mann-Whitney Test). In combination, these data showed a CBG-, CBD- and THC:CBD-dependent elevation of mTORC1 activity occurred in peripheral blood mononuclear cells from healthy volunteers.

To determine the potential therapeutic relevance of mTORC1 regulation in primary PBMCs, cells from healthy volunteers and patients with multiple sclerosis were compared. In this study, the volunteers and patients were age- and gender-matched and information on the disease duration and treatment was attained for the patients with MS (Table 6.1 A and B). In control conditions (in the presence of solvent only), cells from patients with multiple sclerosis were found to have a significant 1.7-fold higher level of mTORC1 activity compared to cells from healthy volunteers, as evidenced by the proportion of phosphorylated 4EBP1 compared to total 4EBP1 ($P<0.05$, Mann-Whitney Test) (Figure 6.8 A). Furthermore, cells derived from patients with multiple sclerosis showed a significant 3.5-fold higher level of phosphorylated 4EBP1 than cells from healthy volunteers ($P<0.01$, Mann-Whitney Test) (Figure 6.8 B). In addition, a nonsignificant trend towards an elevated level of total 4EBP1 was observed between cells from healthy volunteers and patients with multiple sclerosis ($P=0.13$) (Figure 6.8 C). In combination, these data showed that mTORC1 activity was at a constitutively elevated level in PBMCs from patients with MS.

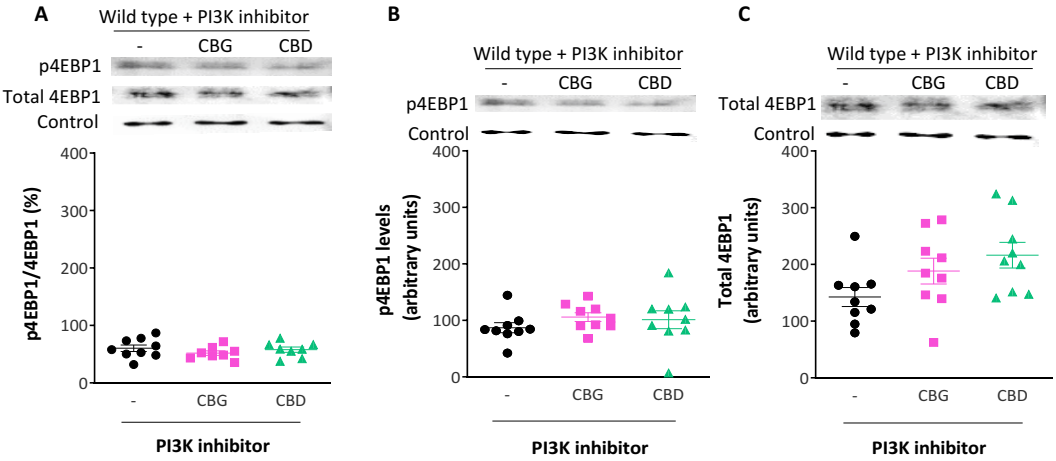

Figure 6.6: PI3K signalling is necessary for CBG and CBD activation of mTORC1 in mouse embryonic fibroblasts. A-C: Wild type MEF cells treated with a PI3K inhibitor (Pictilisib) and maintained in control conditions (in the absence of CBG or CBD (-)) or treated with 4 µM CBG or CBD for 24 hours were analysed for phosphorylated and total 4EBP1 levels by western blot. Actin was used as a control protein to show that protein levels were consistent between samples. Data shown represents mean± standard error of the mean. Data were normally distributed with Shapiro-Wilks and significance was tested using a One -Way ANOVA with Dunnett's Multiple Comparison Test, n=9. **A:** mTORC1 activity did not significantly change in cells treated with PI3K inhibitor compared with both the PI3K inhibitor and CBG or CBD treatment, as evidenced by no change in the proportion of phosphorylated to total 4EBP1. **B:** Phosphorylation of 4EBP1 did not significantly change in cells treated with PI3K inhibitor compared with the inhibitor and CBG or CBD treatment. **C:** Total 4EBP1 did not significantly change in cells treated with PI3K inhibitor compared with the inhibitor and CBG or CBD treatment.

Since PBMCs from patients with MS were found to have elevated mTORC1 activity compared to cells from healthy volunteers, cells from patients with MS were tested for CBG-, CBD- and THC:CBD-dependent regulation of mTORC1 activity. Here, primary PBMCs were extracted from patients with multiple sclerosis and maintained in control conditions (in the presence of solvent only) or treated with CBG or CBD (0.1 µM), or plant-derived highly purified THC:CBD combinations (0.02 µM:0.017 µM) for 24 hours (carried out by Trinity College Dublin). In this analysis, mTORC1 activity was significantly reduced 1.4-fold following CBG treatment, 2.2-fold following CBD treatment and 2.0-fold following THC:CBD treatment, as evidenced by a decrease in the proportion of phosphorylated 4EBP1 to total 4EBP1 (Figure 6.9 A, B, C) ($P<0.05$ for CBG treatment, $P<0.01$ for CBD or THC:CBD treatment, Mann-Whitney Test). This reduction was due to a reduction in phosphorylation of 4EBP1, which significantly reduced 2.2-fold following CBG treatment, 2.4-fold following CBD treatment and 2.8-fold following THC:CBD treatment (Figure 6.9 D, E, F) ($P<0.01$, Mann-Whitney Test). In addition, no significant change in total 4EBP1 levels was observed following CBG, CBD or THC:CBD treatment (Figure 6.9 G, H, I). More specifically, no trend in total 4EBP1 change was observed following CBD treatment ($P=0.59$), however, a nonsignificant trend towards an increase in total 4EBP1 following CBG treatment ($P=0.09$) and

following THC:CBD treatment (P=0.24) treatment was observed. In combination, these data showed a CBG-, CBD- and THC:CBD-dependent decrease of mTORC1 activity occurred in peripheral blood mononuclear cells from patients with multiple sclerosis.

To determine if levels of IPMK were responsible for the difference in mTORC1 activity seen in PBMCs from healthy volunteers and patients with multiple sclerosis, samples from both groups were analysed for total IPMK levels by Western blot analysis. From this analysis, the 47 kDa IPMK protein was not visualised (Figure 6.10), and no additional sample from this experiment was available to test for IPMK levels using other methodologies. The antibody used in this experiment has been used in previous studies to confirm the presence of the IPMK protein in human-derived cells (KB-3-1) and absence of the protein in IPMK-ablated cells (Pan et al., 2019). Thus, with the methodology and materials available, it was not possible to monitor differences in total IPMK levels between PBMCs from healthy volunteers and patients with multiple sclerosis.

A Healthy Volunteers

Age	Sex
41	F
53	F
34	M
40	M
45	F
39	F

B Patients with MS

Age	Sex	Treatment	Disease duration (months)
37	Male	Previously on Gilenya- stopped recently	120
21	Female	None	48
55	Male	Tecfidera	20+years
41	Female	Plegridy	13
25	Female	None	6
Not reported	Female	not reported	not reported

Table 6.1: Demographic breakdown for PBMC donation origin of healthy volunteers and patients with MS. A: The age and gender of each of the healthy volunteers. **B:** The age, gender, current treatment, and disease duration for the MS patients. Gilenya is a fingolimod and has an uncharacterised mechanism of action, suggested to have both immunological and nervous system activities (Chun and Brinkmann, 2011). Tecfidera is suggested to reduce oxidative stress and regulates antioxidant production (Robinson, 2014). Plegridy is an interferon beta-1a conjugated to a methoxy polyethylene glycol molecule and has an uncharacterised immunomodulatory effect (Hoy, 2015).

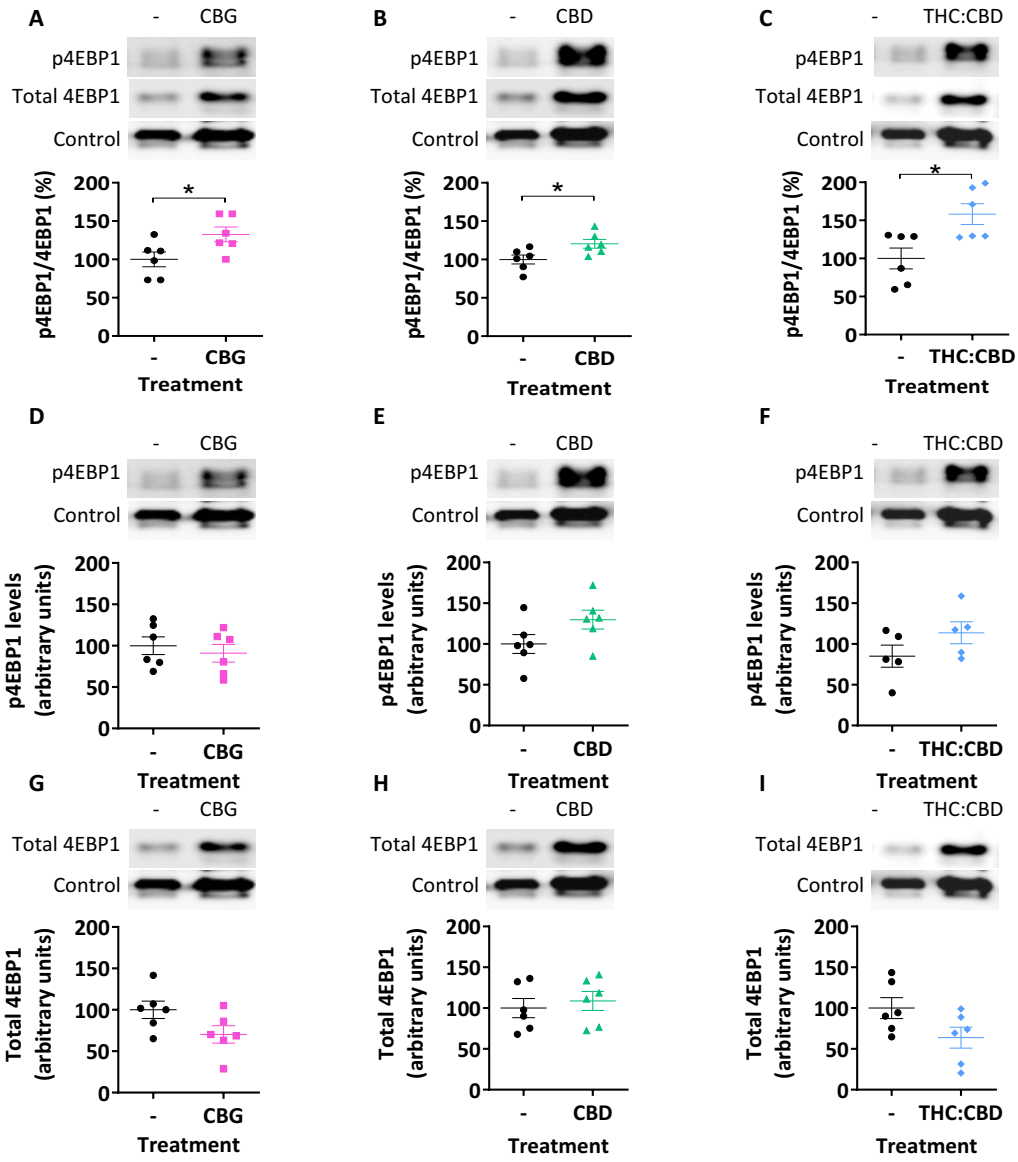

Figure 6.7: CBG-, CBD- and THC:CBD-dependent elevation of mTORC1 activity occurs in primary PBMCs from healthy volunteers. A-I: Primary PBMCs from healthy volunteers were maintained in control conditions (in the absence of CBG, CBD or THC (-)) or treated with 0.1 µM CBG or CBD or 0.02:0.017 µM THC:CBD for 24 hours and analysed for phosphorylated and total 4EBP1 levels. Actin was used as a control protein to show that protein levels were consistent between samples. Data shown represents mean± standard error of the mean. Data were not distributed normally according to Shapiro-Wilks, therefore a Mann Whitney test was carried out to test for significance, * - $p<0.05$. **A, B, C:** mTORC1 activity significantly increased with CBG, CBD or THC:CBD treatment of PBMC cells originating from healthy volunteers, as evidenced by an elevated proportion of phosphorylated 4EBP1 to total 4EBP1 (n=6). **D, E, F:** CBG, CBD or THC:CBD treatment of PBMC cells originating from healthy volunteers did not significantly alter phosphorylated 4EBP1 levels (n=6). **G, H, I:** CBG, CBD or THC:CBD treatment of PBMC cells originating from healthy volunteers did not significantly alter total 4EBP1 levels (n=6).

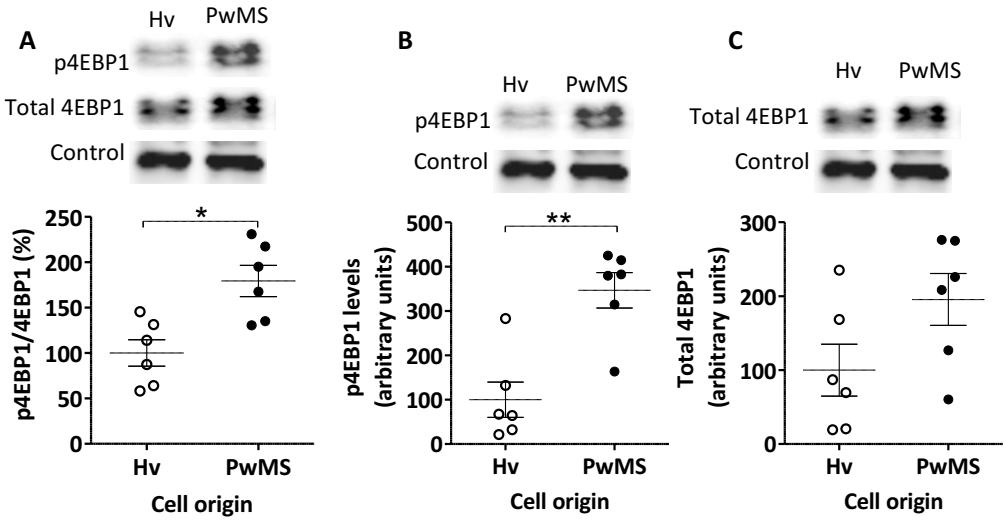

Figure 6.8: PBMCs from healthy volunteers and patients with multiple sclerosis have different constitutive mTORC1 activity. A-C: To examine the therapeutic relevance of mTORC1 activity in multiple sclerosis, mTORC1 activity was measured in PBMCs derived from healthy volunteers (Hv) and patients with multiple sclerosis (PwMS). Data shown represents mean± standard error of the mean. Data were not distributed according to Shapiro-Wilks, therefore a Mann Whitney test was carried out to test for significance, * - $p<0.05$, ** - $p<0.01$. Actin was used as a control protein to show that protein levels were consistent between samples. **A:** PBMCs originating in patients with multiple sclerosis were found to have a significantly higher level of mTORC1 activity, as evidenced by an elevated proportion of phosphorylated 4EBP1 to total 4EBP1 than cells from healthy volunteers. **B:** PBMCs originating in patients with multiple sclerosis were found to have a significantly higher level of phosphorylated 4EBP1 than from cells from healthy volunteers. **C:** PBMCs originating in patients with multiple sclerosis were not found to have a significantly different total 4EBP1 compared to cells from healthy volunteers.

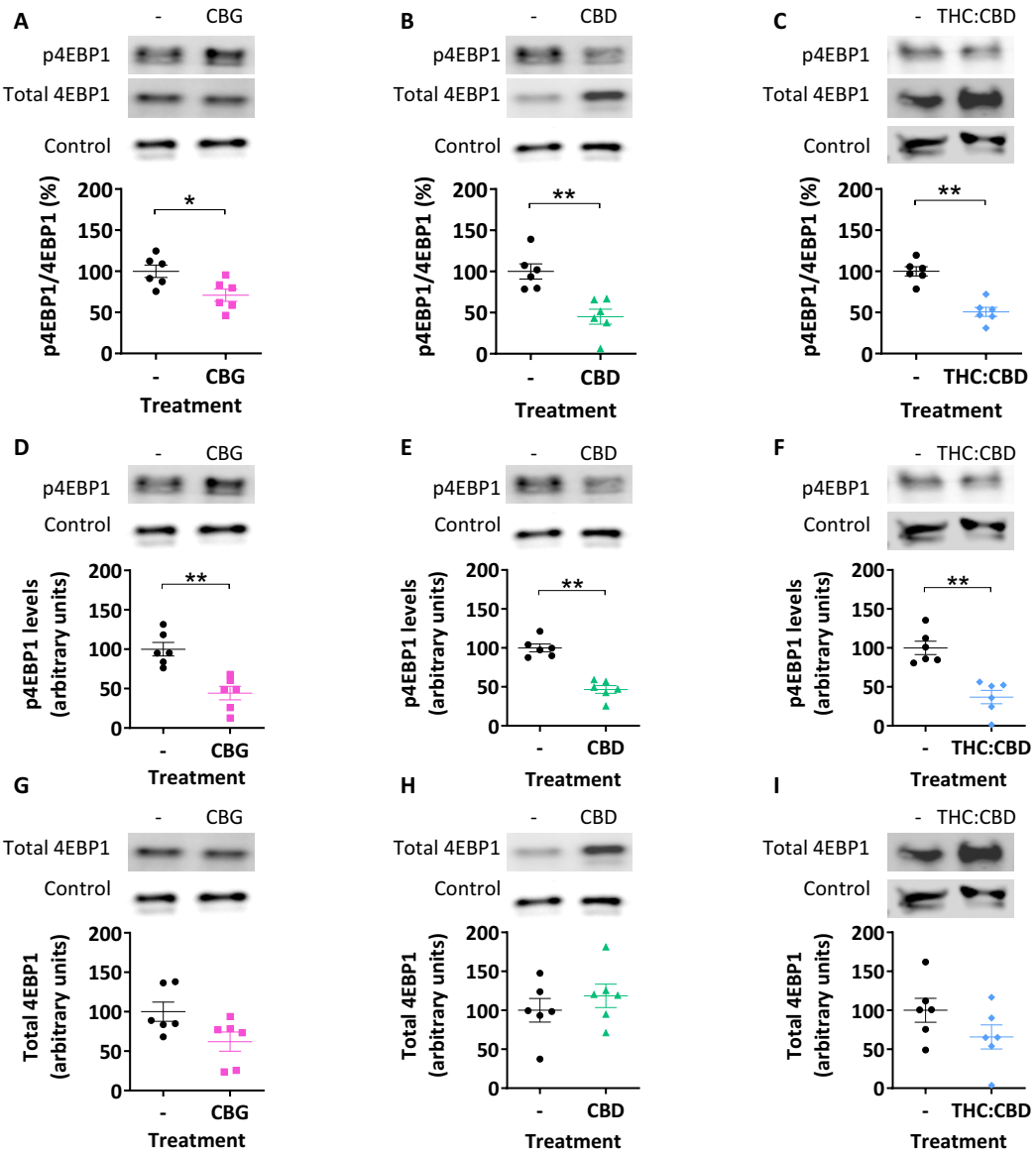

Figure 6.9: CBG-, CBD- and THC:CBD-dependent decrease of mTORC1 activity occurs in primary PBMCs from patients with MS. A-I: Primary PBMCs from patients with multiple sclerosis were maintained in control conditions (in the absence of CBG, CBD or THC (-)) or treated with 0.1 µM CBG or CBD or 0.02:0.017 µM THC:CBD for 24 hours and analysed for phosphorylated and total 4EBP1 levels. Actin was used as a control protein to show that protein levels were consistent between samples. Data shown represents mean± standard error of the mean. Data were not distributed according to Shapiro-Wilks, therefore a Mann Whitney test was carried out to test for significance, * - $p<0.05$, ** - $p<0.01$. **A, B, C:** mTORC1 activity significantly reduced with CBG, CBD or THC:CBD treatment of PBMC cells originating from patients with multiple sclerosis, as evidenced by a reduced proportion of phosphorylated 4EBP1 to total 4EBP1 (n=6). **D, E, F:** CBG, CBD or THC:CBD treatment of PBMCs from patients with multiple sclerosis significantly reduced phosphorylated 4EBP1 levels (n=6). **G, H, I:** CBG, CBD or THC:CBD treatment of PBMC cells originating from patients with multiple sclerosis did not significantly alter total 4EBP1 levels (n=6).

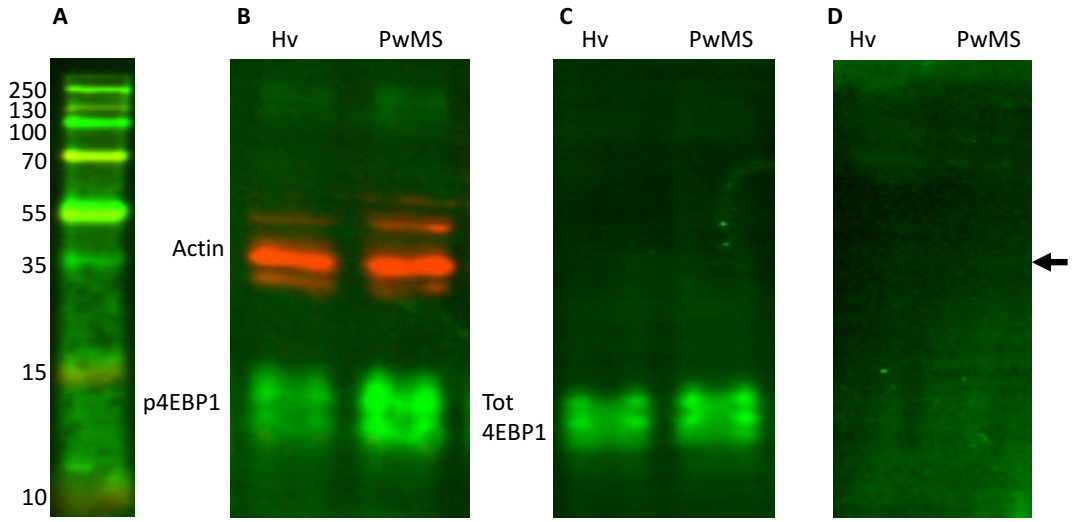

Figure 6.10: Attempt to measure IPMK levels in PBMCs from healthy volunteers (Hv) and patients with multiple sclerosis (PwMS). A: Protein ladder (Pageruler Plus Prestained ladder), indicating the size of proteins in the western blot. **B:** Western blot showing the presence of phosphorylation 4EBP1 and actin in PBMCs. **C:** Western blot showing the presence of total 4EBP1 in PBMCs. **D:** Western blot attempt to detect total IPMK protein in PBMCs using anti-IPMK antibody (ab96753), no band is detected at 47 kDa.

6.3 Discussion

In this chapter, the effects of CBG and CBD on the mTORC1 pathway were examined in *D. discoideum*, *M. musculus* and *H. sapiens* cells. In *D. discoideum*, expression of the human IPMK protein (over-expressing IPMK overall) was found to have elevated mTORC1 activity compared to wild type cells. In addition, treatment of hIPMK-expressing *D. discoideum* cells with CBG or CBD resulted in a decrease in mTORC1 activity, in contrast to an increase in mTORC1 activity following CBG or CBD treatment of wild type cells (Figure 5.2). The effect of CBG and CBD on mTORC1 activity was then examined in wild type mouse embryonic fibroblasts. In wild type MEFs, CBG and CBD elevated mTORC1 activity, while in cells lacking IPMK or with pharmacologically inhibited PI3K activity, CBG and CBD did not alter mTORC1 activity. Primary human peripheral blood mononuclear cells from healthy volunteers and patients with MS were then examined to determine if CBG- and CBD-dependent mTORC1 regulation was conserved in human cells. In cells from healthy volunteers CBG, CBD and a mixture of THC and CBD were found to elevate mTORC1 activity. However, in cells from patients with MS which showed a constitutively elevated level of mTORC1 activity, CBG, CBD and THC:CBD were found to reduce mTORC1 activity.

In this chapter expression of the human IPMK protein in *D. discoideum* was examined for its role in regulating response to CBG and CBD. In the previous chapter over-expression of the endogenous *D. discoideum*, IPMK protein in *D. discoideum* led to resistance to CBG during growth and reversed the effects of CBG and CBD treatment on mTORC1 activity. In contrast to the conservation of these phenotypes of dIPMK over-expression and hIPMK expression in *D. discoideum*, several differences were observed. These differences include cellular localisation of IPMK (hIPMK primarily in the nucleus, dIPMK in cytoplasm and nucleus), the degree of resistance to CBG during growth (hIPMK$^+$ 1.6-fold higher than dIPMK$^+$) and the degree of mTORC1 activity increase (2.2-fold for hIPMK$^+$ and 1.9-fold for dIPMK$^+$). Although a rationale for these differences has not been experimentally confirmed, they could arise from a difference of CBG or CBD binding to IPMK, differential binding of IPMK to other proteins, or cellular localisation of each protein. One approach to investigate this could be to examine the possible binding of CBG, CBD and THC to IPMK and subsequently investigate whether the IPMK proteins have different cannabinoid-binding affinities, which could be examined by biochemical binding affinity assays (Carrier et al., 2006). Another potential cause of the differences between dIPMK$^+$ and hIPMK$^+$ cells could be a differential binding affinity of each IPMK to protein binding partners such as mTOR. Previous studies have found that the human IPMK may have a higher binding affinity for mTOR than the *D. discoideum* IPMK (Kim et al., 2011), this could result in the elevated mTORC1 activity observed

in hIPMK^{+} cells. Alternatively, the difference could be a result of the increased nuclear-localisation of the human protein (Nalaskowski et al., 2002), as observed by fluorescence microscopy. In the nucleus, IPMK may act through PI3K activities to mediate transcriptional control or export of nuclear mRNA (Blind et al., 2012). Furthermore, IPMK may act to alter chromatin structure and global transcription through inositol phosphate production, which increases histone deacetylation (Watson et al., 2012; Millard et al., 2013). Finally, IPMK directly binds transcription factors, such as serum response factor (SRF) (Kim et al., 2013), cAMP-response element-binding protein (CREB) binding protein (CBP) (Xu et al., 2013(a)), and p53 (Xu et al., 2013(b)) and could, therefore, lead to the transcriptional control of a specific set of genes. The role of IPMK in transcriptional regulation was beyond the scope of this study, however, future experiments could examine the links between cannabinoid treatment and transcriptional differences in IPMK-regulated gene expression. Regardless, this chapter shows a conserved mechanism of action of CBG and CBD in regulating mTORC1, and resistance to CBG during growth, through both the *D. discoideum* and *H. sapiens* IPMK proteins.

In this chapter, CBG and CBD were found to elevate mTORC1 activity in wild type mouse cells and human cells from healthy volunteers. In MEFs, a concentration of 4 µM of CBG or CBD was chosen since this concentration was used in a variety of previous *in vitro* experiments (Rajesh et al., 2007; Qin et al., 2008; O'Sullivan et al., 2009; Kozela et al., 2011). The concentration of 4 µM CBG and CBD was found to increase mTORC1 activation in wild type MEF cells. However, this study did not examine lower concentrations of the cannabinoids, therefore, it is unclear if lower concentrations of CBG and CBD would activate mTORC1 in MEF cells. The concentration of CBG and CBD at 0.1 µM used to treat primary PBMCs in this chapter was based upon *in vivo* plasma levels of cannabinoids in treated patients from previous studies (Consroe et al., 1991; Haney et al., 2016). In one study, CBD administered orally at 10 mg/kg was present at 0.03 µM in the plasma of healthy human volunteers (Consroe et al., 1991). In another study, 800 mg of CBD administered orally, resulted in peak plasma concentrations of CBD (at one to two hours post-treatment) ranging between 0.006 and 0.866 µM (with an average of 0.245 µM) (Haney et al., 2016). These previous studies imply that 0.1 µM is a concentration that occurs in the plasma of humans when cannabinoids are orally administered, and therefore was chosen for these experiments. Interestingly, a much lower concentration of 0.02 µM:0.017 µM of a combination of THC and CBD showed the same effect. Previous studies investigating the anti-emetic properties of CBD and THC in *Suncus murinus* have suggested a synergistic effect of this kind on a different mechanism (Rock and Parker, 2015), which could be a future focus in the research of cannabinoids as therapeutics. Nevertheless, the CBG-, CBD- and THC:CBD-dependent regulation

of mTORC1 found in this chapter occurs at therapeutically relevant concentrations of cannabinoid, providing a basis for future clinical trials.

MEFs were used in this study to examine a role for IPMK and PI3K signalling in CBG- and CBD-dependent regulation of mTORC1 activity in a mammalian cell line. MEFs were previously used to explore IPMK-regulation of mTORC1 activity, and a null mutant was available to specify a role for this protein in CBG and CBD function (Kim et al., 2011). In this chapter, mTORC1 activity was found to be present in MEF cells lacking IPMK, however, this was not altered following CBG or CBD treatment. This indicated that IPMK activity was necessary for the elevation of mTORC1 activity found in wild type cells. In addition, treatment with a pharmacological PI3K inhibitor also resulted in a block of CBG- and CBD-dependent elevation of mTORC1 activity, suggesting that PI3K signalling is necessary for these effects. Previous research has indicated that the PI3K activity of IPMK may be responsible for 50 % of the production of PIP_3 in MEF cells (Maag et al., 2011). Therefore, the block in CBG- and CBD-dependent elevation of mTORC1 activity in cells lacking IPMK or PI3K activity could be directly related. This would imply that CBG and CBD regulate the PI3K activity of IPMK and that this is responsible for the increase in mTORC1 activity observed in wild type MEFs. Alternatively, CBG and CBD may alter another aspect of IPMK activity, such as mTORC1 binding (Kim et al., 2011) or IP_6 production (Kim et al., 2017), and this activity in addition to a functional PI3K signalling pathway is necessary for CBG- and CBD-dependent elevation of mTORC1 activity. Further experiments could use High-Performance Liquid Chromatography to measure PIP_3 levels in wild type MEFs and MEFs lacking IPMK treated with CBG and CBD to determine the role of IPMK-related PI3K activity in cannabinoid-regulation of mTORC1 activity (Maag et al., 2011). This chapter has indicated that both IPMK and functional PI3K signalling are necessary for CBG- and CBD-dependent elevation of mTORC1 activity and that the two could be linked.

Findings in this study indicate that PBMCs from MS patients contain constitutively elevated mTORC1 activity compared to cells from healthy volunteers and that treatment with CBG, CBD or THC:CBD reduced mTORC1 activity in cells from patients with MS. Previous research found that activation of immune cells, such as those present in PBMCs, occurs through elevated mTORC1 signalling (Gao et al., 2015; Herrero-Sánchez et al., 2016). The activation of cells present in PBMCs leads to the autoimmune inflammation that causes demyelination of neurons (Hasheminia et al., 2014). Previous studies found that CBD can decrease the activation of these cells (Kozela et al., 2011), consistent with the results found in this study. Furthermore, the activation of cells subtypes found in PBMCs is associated with bipolar disorder (Drexhage et al., 2011), potentially indicating therapeutic uses for CBG, CBD and THC beyond multiple sclerosis.

Previously discovered CBD deactivation of immune cells is therefore consistent with the CBG-, CBD- and THC:CBD-dependent downregulation of mTORC1 activity in PBMCs from patients with MS found in this chapter and indicates therapeutic targets for cannabinoids in MS treatment.

In immune cells constituent in PBMCs, mTOR activation results in NF-κB (nuclear factor) activation and nuclear translocation (Gao et al., 2015). NF-κB is a pro-inflammatory transcription factor, binding specific DNA sequences and promoting the transcription of inflammatory actors, such as TNF-α (tumour necrosis factor) and IL-6 (interleukin) (Wu et al., 2011; Hayden and Ghosh, 2012). Blocking mTOR activity in bone marrow, the progenitor tissue of immune cells, results in an inhibition of cell proliferation (Costa et al., 2006). mTOR inhibition has also been found to supress NF-κB and as a result reduce IL-6 expression (Müller-Krebs et al., 2013). In immune cells, the mTOR pathway controls proliferation, cell cycle progression, differentiation, survival, migration and metabolism (Herrero-Sánchez et al., 2016). In fact, PI3K inhibitors or mTOR inhibition are capable of blocking T cell proliferation and activation (Herrero-Sánchez et al., 2016). mTOR inhibition in T cells also reduces the total 4EBP1 (Herrero-Sánchez et al., 2016), consistent with the similar finding for CBG or THC:CBD treatment of PBMCs in this chapter. mTOR inhibitors, as well as reducing T cell activation, exert beneficial effects on models of MS (Russo et al., 2016). Indicating the potential therefore of cannabinoids as a treatment of MS, if the effect of mTOR inhibition is found *in vivo* as well.

In addition to MS, cannabinoids have been found to modulate mTOR signalling in other disease models. In these models, mTOR dysregulation has often been implicated as a potential causative or aggravative factor and therefore modulation of mTOR is seen as a potential therapeutic pathway. In some studies, cannabinoids have been found to reduce mTOR activity, as is consistent with the finding in this chapter that CBG, CBD and THC:CBD reduce mTOR activity in PBMCs from patients with MS. In a zebrafish model of tuberosclerosis complex disease, the disease model was found to have constitutively elevated mTOR signalling and CBD reduced this mTOR pathway activation (as assessed by abundance of phosphorylated S6 kinase) (Serra et al., 2019). In addition, in breast cancer cell lines in which constitutively elevated mTOR signalling occurs, CBD reduced mTOR pathway activation (assessed by analysis of the proportion of phosphorylated 4EBP1) (Shrivastava et al., 2011; Sultan et al., 2018). In other disease models, mTORC1 activity is activated during treatment with cannabinoids, consistent with the CBG-, CBD-dependent activation of mTORC1 activity observed in wild type mouse cells and primary PBMCs from healthy volunteers found in this thesis. In neurons of a mouse experimental autoimmune encephalomyelitis model of MS, mTOR activity was found to be constitutively reduced, and CBD elevated mTOR activity to normal levels (assessed by analysis of the

proportion of phosphorylated S6 kinase, mTOR and PKB) (Giacoppo et al., 2017). CBD also treated symptoms of an amphetamine-induced rat model of schizophrenia, and elevated mTORC1 activity (assessed by analysis of the proportion of phosphorylated S6 kinase and mTOR) (Renard et al., 2016). The mechanisms behind these apparently contradictory effects of CBD treatment are unknown, however, this thesis finds the two opposite effects of CBD-dependent mTOR regulation occur in both *D. discoideum* and primary PBMCs from humans. In this study, the opposite effects of cannabinoid treatment on mTORC1 activity appear to be dependent upon the basal state of the cells examined, and in *D. discoideum* the level of IPMK protein. Therefore, a potentially therapeutically relevant pro-homeostatic role of CBG, CBD and THC in combination with CBD in mTOR regulation is indicated.

Since previous chapters have evidenced a role for IPMK in CBG- and CBD-dependent mTORC1 regulation, levels of IPMK were investigated in PBMCs from healthy volunteers and patients with MS. Unfortunately, IPMK was not detected in either group using western blot analysis. As the antibody against IPMK had previously been used to detect the IPMK protein in human (KB-3-1) cells (Pan et al., 2019), there is a possibility that IPMK levels in the PBMCs tested were too low to be measured by western blot. Therefore, further analysis of IPMK levels in these cells could be analysed using techniques such as immunoprecipitation or quantitative analysis of protein by ELISA to analyse protein levels (Lin et al., 2013) or qPCR to analyse mRNA expression levels (Rocha et al., 2016). In addition, future studies may examine the levels of IPMK in patients with MS and examine whether mutations in IPMK or at promoter sites surrounding IPMK correlate with the incidence of MS. In fact, IPMK has been demonstrated to have a noncatalytic role in enhancing toll-like receptor (TLR) signalling in macrophages, by stabilising tumour necrosis factor (TNF) receptor-associated factor 6 (TRAF6) (Kim et al., 2017). IPMK depletion in macrophages reduces TNF-signalling and reduces pro-inflammatory cytokine production, which would be consistent with MS patients showing higher IPMK activity giving rise to increased mTORC1 activity compared to healthy controls (evidenced in our analysis). Due to these central roles, IPMK could play in regulating disease progression of multiple sclerosis, IPMK expression should be examined in immune cells in multiple sclerosis and IPMK should be further explored as a potential therapeutic target.

7 Discussion

7.1 Summary

This research aimed to identify and characterise molecular mechanisms of the cannabinoid CBG, with potential translation to therapeutically relevant models. CBG is of importance since it is a component of *C. sativa* extracts currently prescribed as treatments for multiple sclerosis (MS) (Etges et al., 2016) and epilepsy (Abu-Sawwa and Stehling, 2020). To find potential molecular mechanisms of CBG, the simple model organism *Dictyostelium discoideum* was employed. This model organism had previously been used to identify molecular mechanisms for CBD (Perry et al., 2020), curcumin and its derivatives (Cocorocchio et al., 2018), valproic acid (Chang et al., 2015), naringenin (Waheed et al., 2014), and bitter tastants (Robery et al., 2013). These various studies have confirmed that *D. discoideum* can be used to identify molecular mechanisms of bioactive and pharmacologically active molecules.

The first approach to identify molecular mechanisms for CBG in *D. discoideum* was to investigate if CBG shared molecular mechanisms with CBD. Commonly investigated targets of cannabinoids, TRPs (Otto et al., 2016) and cannabinoid receptors (McPartland et al., 2006(a); McPartland et al., 2006(b); Dey et al., 2010), are not present in *D. discoideum* and thus could not be examined. However, adenosine transport has also been suggested to be a potential target of CBD, where CBD inhibits adenosine transport through the equilibrative nucleoside transporter 1 (ENT1) protein in rat cells (Liou et al., 2008). Bioinformatic analysis suggested than the *D. discoideum* ENT1 protein was an orthologue of the rat and human protein and was therefore examined for a role as part of a molecular mechanism of CBG. The *D. discoideum* ENT1 protein was ablated, and the ENT1$^-$ cell line was found to result in a reduction in sensitivity to CBG during growth. Furthermore, CBG treatment of microglial cells was found to increase extracellular adenosine, while leaving intracellular adenosine unchanged, implying that CBG may block adenosine transport into microglia cells. As adenosine transport regulates DNA methylation (Williams-Karnesky et al., 2013), a cell line lacking a DNA methyltransferase protein (DNMA) in *D. discoideum* was explored for sensitivity to CBG during growth. DNMA$^-$ cells also showed reduced sensitivity to CBG during growth, consistent with that shown following loss of ENT1. Following this, DNA methylation was analysed in *D. discoideum* in response to CBG treatment. Here, CBG, pharmacological inhibition of ENT1, and ablation of ENT1 were all found to elevate DNA methylation in *D. discoideum*, while ENT1 ablation blocked the effects of CBG on DNA methylation. These results indicate that CBG functions in a similar mechanism to CBD through the inhibition of ENT1 activity in both *D. discoideum* and mouse astroglial cells to regulate adenosine transport.

The second approach to identify molecular mechanisms for CBG in *D. discoideum* was an unbiased approach. Here, a mutant library was screened to identify proteins responsible for CBG sensitivity during growth in *D. discoideum*. This method identified two potential proteins involved in the molecular mechanisms of CBG which had *H. sapiens* orthologues, thus allowing for translational experiments. The two proteins identified were the regulator of chromosome condensation 1 (RCC1) domain-containing (RC) protein and the inositol polyphosphate multikinase (IPMK) protein. IPMK contained an orthologue of the protein in *H. sapiens*, while RC only shared domains with a *H. sapiens* protein. The mutant identified relating to IPMK was found to have a mutagenic insert downstream from the stop codon, and with RT-PCR this was found to elevate IPMK gene expression. To confirm the role of IPMK in controlling sensitivity to CBG during growth, a *D. discoideum* cell line over-expressing the *D. discoideum* IPMK (dIPMK-RFP) was created. Over-expression of IPMK (dIPMK$^+$ or hIPMK$^+$) resulted in reduced sensitivity to CBG during growth. As IPMK is a key component in the mTORC1 signalling pathway, mTORC1 activity was measured by western blot analysis of 4EBP1 phosphorylation. In addition, both CBG and CBD were found to elevate mTORC1 activity in wild type *D. discoideum*. Interestingly, IPMK over-expressing cell lines (dIPMK or hIPMK) were found to have elevated mTORC1 activity compared to wild type cells, and CBG and CBD treatment reduced mTORC1 activity in these cells. These experiments suggest that CBG and CBD may have a homeostatic effect on mTORC1 activity dependent upon IPMK levels. In *D. discoideum*, further experiments showed that the CBG- and CBD-dependent elevation of mTORC1 activity was dependent upon the presence of PKB and PI3K activity. From these experiments, it is likely that CBG and CBD function through modulation of IPMK activity in *D. discoideum* in a PKB- and PI3K-dependent manner to regulate mTORC1 activity.

To confirm the therapeutic relevance of the IPMK dependent mechanism proposed in *D. discoideum*, two models were employed to determine whether a mechanism involved IPMK resulting in the regulation of mTORC1 activity by CBG and CBD was conserved in mammalian cells. In wild type mouse embryonic fibroblast cells (MEFs), CBG and CBD were found to elevate mTORC1 activity, consistent with findings from wild type *D. discoideum*. However, in MEF cells lacking IPMK, or with pharmacologically inhibited PI3K activity, CBG and CBD did not affect mTORC1 activity. This indicated that both CBG and CBD elevate mTORC1 activity in *D. discoideum* and mammalian cells and that this is dependent upon IPMK and PI3K in mammalian cells. To investigate the therapeutic relevance of these findings, primary peripheral blood mononuclear cells (PBMCs) from healthy volunteers and patients with MS were examined, since these cells are the primary producers of pro-inflammatory cytokines which increase the progression of MS (Simpson et al., 2015). PBMCs from patients with MS were found to have an

elevated basal level of mTORC1 compared to PBMCs from healthy volunteers. Treatment of PBMCs from healthy volunteers with CBG, CBD or a mixture of THC and CBD (THC:CBD) resulted in the elevation of mTORC1 activity, consistent with that observed in wild type *D. discoideum* and MEF cells. Treatment with CBG, CBD or THC:CBD resulted in a reduction of mTORC1 activity in PBMCs from patients with MS with elevated basal mTORC1 activity. Thus, the effect of cannabinoid treatment of PBMCs from patients with MS was similar to that found in IPMK-over-expressing *D. discoideum*. This result provided significant clinical relevance, since in MS mTORC1 signalling results in activation of immune cells within PBMCs and this causes myelin damage and axonal degradation (Bar-Or et al., 2003; Yu et al., 2007; Carbone et al., 2014; Simpson et al., 2015), and thus this could be alleviated using CBG or CBD

7.2 The potential of synergistic cannabinoid treatment

Research has indicated that cannabinoids may have synergistic therapeutic effects when used together (Mammana et al., 2019). This is consistent with our findings in PBMCs that a mixture of THC and CBD modified mTORC1 activity at 0.02 µM:0.017 µM, while CBG and CBD were found to modify mTORC1 activity at 0.1 µM. While experiments at lower concentrations of CBG and CBD were not carried out, this could indicate that cannabinoids have synergistic effects on molecular mechanisms. Similarly, a combination of CBG and CBD was more effective than either alone as an anti-inflammatory, anti-oxidant and anti-apoptotic agent in a cellular model of the neurodegenerative disease amyotrophic lateral sclerosis (Mammana et al., 2019). Another study found that THCA and CBGA had synergistic cytotoxic effects against colon cancer cells (Nallathambi et al., 2018). Further experiments found that a mixture of THC, CBG and CBD showed a stronger cytotoxic effect on leukaemia cells than CBD alone (Mazuz et al., 2020). In addition, whole extracts of *C. sativa* containing multiple cannabinoids were more effective at elevating intracellular calcium levels in hippocampal neurons and glia than individual treatment with THC or CBD alone (Ryan et al., 2006). Thus, further studies on different combinations of cannabinoids need to be carried out to establish the optimal combination for each specific potential therapeutic mechanism.

7.4 Links to previously suggested molecular mechanisms of cannabinoids

Previous studies have indicated that the molecular mechanisms of phytocannabinoids could include cannabinoid receptors (Arévalo-Martín et al., 2003), adenosine (Carrier et al., 2006), TRPV1 (Borrelli et al., 2014), GPR55 (Devinsky et al., 2014), glycine and the one-carbon cycle (Perry et al., 2020), as well as PI3K/PKB/mTOR activity (Giacoppo et al., 2017). This thesis adds to the current understanding of cannabinoid regulation of adenosine transport and mTOR activity by implicating CBG as well as CBD in this activity, as well as proposing IPMK as a potential

modulator of CBG and CBD activity on mTORC1 signalling. Furthermore, the mechanisms proposed in this thesis may relate to or overlap with several of the existing mechanisms suggested for cannabinoids. The potential CBD molecular mechanism of glycine and one-carbon cycle regulation may be related to adenosine transport and DNA methylation, as both are involved in the same pathway (Perry et al., 2020). Furthermore, TRPV1 has been implicated as an upstream regulator of mTORC1, potentially through AMPK (Maiese, 2017; Bort et al., 2019), however since this cannabinoid receptor is not found in *D. discoideum* (McPartland et al., 2006(a); McPartland et al., 2006(b); Dey et al., 2010), this indicates that CBG- and CBD-dependent mTORC1 regulation in *D. discoideum* is independent of TRPV1. Thus, this thesis adds to prior knowledge on the mechanism of action of cannabinoids and indicates a potential novel target for this class of compounds, IPMK.

7.5 Adenosine transport regulation as a molecular mechanism for CBG

The data in this thesis indicate that CBG regulates a signalling pathway related to adenosine transport through ENT1 in both *D. discoideum* and microglia. This is consistent with previous research indicating that CBD, similar in structure to CBG, inhibited adenosine uptake through ENT1 (Liou et al., 2008). Here, CBD was found to block diabetes-induced retinal damage in a rat model through adenosine transport inhibition. In addition, CBD enhanced the adenosine-dependent suppression of TNF-α in the diabetes model (Liou et al., 2008). The suppression of TNF-α reduced inflammation in the retina and therefore provided a potential treatment of diabetes-induced neurodegeneration through adenosine modulation by CBD (Liou et al., 2008). This thesis, therefore, suggests that CBG may share a molecular mechanism involved adenosine transport regulation with CBD and may therefore also be a potential treatment for this type of neurodegeneration.

Adenosine is an endogenous anticonvulsant and seizure terminator working through adenosine A1 receptor activation (During and Spencer, 1992; Lado and Moshé, 2008; Weltha et al., 2019). This anticonvulsant effect occurs through upregulation of presynaptic inhibition of neurons, which prevents runaway excitation in feed-forward synaptic circuits (Huber et al., 2001; Boison, 2012) and stabilises the postsynaptic membrane potential (Figure 7.1 A) (Baldwin et al., 2004). Both of these mechanisms act to stop the spread of a seizure and as a result, elevated extracellular adenosine levels can reduce seizure frequency (Li et al., 2008; Fukuda et al., 2010). In epilepsy, a reduction in extracellular adenosine levels could be caused by over-expression of adenosine kinase (ADK), which phosphorylates adenosine to create adenosine monophosphate (AMP) (Li et al., 2008). This results in the storage of adenosine in astrocytes as AMP, ADP and ATP, leading to this cell type becoming an adenosine sink (Figure 7.1 B) (Lovatt et al., 2012). This reduction in extracellular free adenosine, therefore, increases seizure frequency. CBD inhibition

of adenosine uptake through equilibrative nucleoside transporters into astrocytes would elevate free adenosine, which in turn could act to reduce seizure frequency and severity (Figure 7.1 C) (Pandolfo et al., 2011; Mijangos-Moreno et al., 2014). The discovery in this thesis that CBG may also inhibit adenosine uptake through ENT1, mimicking the ENT inhibitor NBTI, implies a potential shared mechanism with CBD and future therapeutic possibilities for the treatment of epilepsy. To examine this, *D. discoideum* intra- and extracellular adenosine levels could be measured during treatment with CBG and compared to CBD treatment.

Our research indicates that in *D. discoideum* CBG modulates DNA methylation, a downstream and intracellular component of adenosine signalling. This CBG-dependent elevation of DNA methylation is occurring through an adenosine transport-dependent mechanism. Some studies have examined the effects of cannabinoid treatment on DNA methylation. For example, in a rat model of neurodegeneration, iron treatment reduced mitochondrial DNA methylation, while co-treatment with CBD mitigated this reduction (da Silva et al., 2018). In human keratinocytes, CBD and CBG both increased DNA methylation at the keratin 10 gene, while only CBD increased global DNA methylation levels (Pucci et al., 2013). The CBG-dependent increase in DNA methylation in *D. discoideum* implies that CBG blocks the uptake of adenosine into *D. discoideum*, leading to a greater extracellular concentration of adenosine and lower intracellular concentration, consistent with the findings in microglia cells. This is because the relationship between adenosine and DNA methylation is inverse, as DNA methylation relies on methyl group donation (Kredich and Martin, 1977; Boison et al., 2002). Donation of a methyl group from s-adenosylmethionine results in the production of s-adenosylhomocysteine, which is converted into adenosine and homocysteine and occurs at equilibrium and is inhibited if adenosine and homocysteine are not continually removed. Therefore, elevated intracellular adenosine levels block the pathway and result in decreased DNA methylation, and decreased adenosine enables the pathway to continue and results in increased DNA methylation (Kredich and Martin, 1977; Boison et al., 2002). The data from this thesis implies that adenosine transport into the cell is blocked by CBG, resulting in a lower intracellular concentration of adenosine and elevated DNA methylation in *D. discoideum*. This is consistent with the finding that CBG increased extracellular adenosine in microglia, potentially by blocking adenosine transport into the cells.

Regulation of DNA methylation in the context of adenosine levels may be an important mechanism for the progression of epilepsy and therefore treatment of the disease. DNA methylation dysregulation is implicated in epileptogenesis (Williams-Karnesky et al., 2013). In a rat epilepsy model, adenosine was found to inhibit DNA methylation, leading to an inhibition of epileptogenesis. Over-expression of adenosine kinase (ADK) reduced the level of adenosine in rat cells, resulting in DNA hypermethylation and progression of epilepsy (Williams-Karnesky et

al., 2013). In the weeks following a brain injury or seizure, inflammatory processes are activated and lead to astroglia activation which results in increased ADK expression (Li et al., 2008; Li et al., 2012). Over-expression of ADK, therefore, results in an adenosine deficiency and a subsequent increase in DNA methylation. Therapeutic adenosine augmentation has been found to restore normal DNA methylation levels and prevent the progression of epilepsy in the long term (Williams-Karnesky et al., 2013). A block in adenosine transport through ENT1 by CBD or CBG indicated that these cannabinoids may block the effects of astroglia as an adenosine sink, and counter the over-expression of ADK (Liou et al., 2008). However, this could also block adenosine transport into other cell types, which would be deficient in adenosine in this scenario. Therefore, future research must focus on the *in vivo* effects of cannabinoid treatment for epilepsy, specifically on adenosine transport into different cell types in the central nervous system and how DNA methylation changes in each cell type.

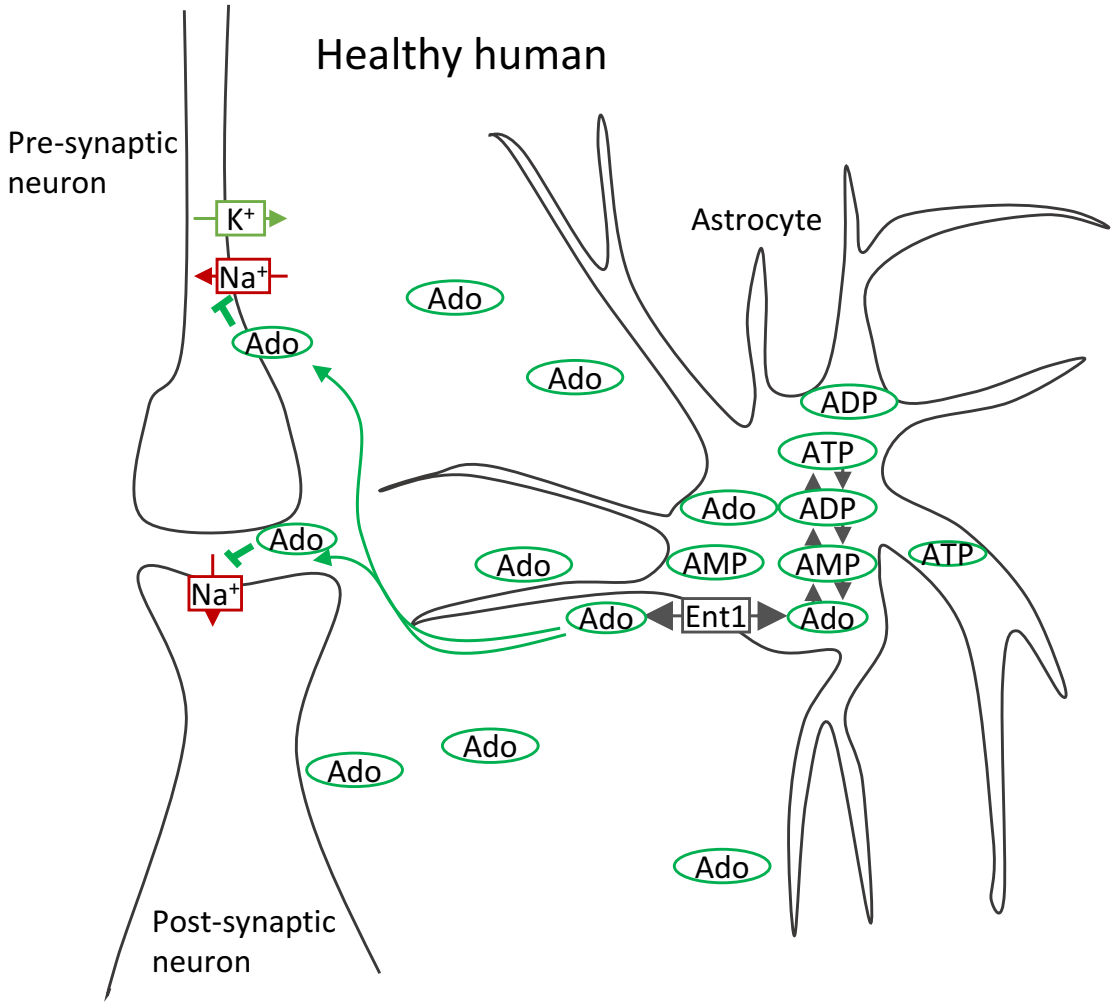

Figure 7.1: Adenosine and epilepsy. A: Astrocytes act as adenosine storage. Adenosine is released to inhibit synaptic signalling and then taken up, back into astrocytes.

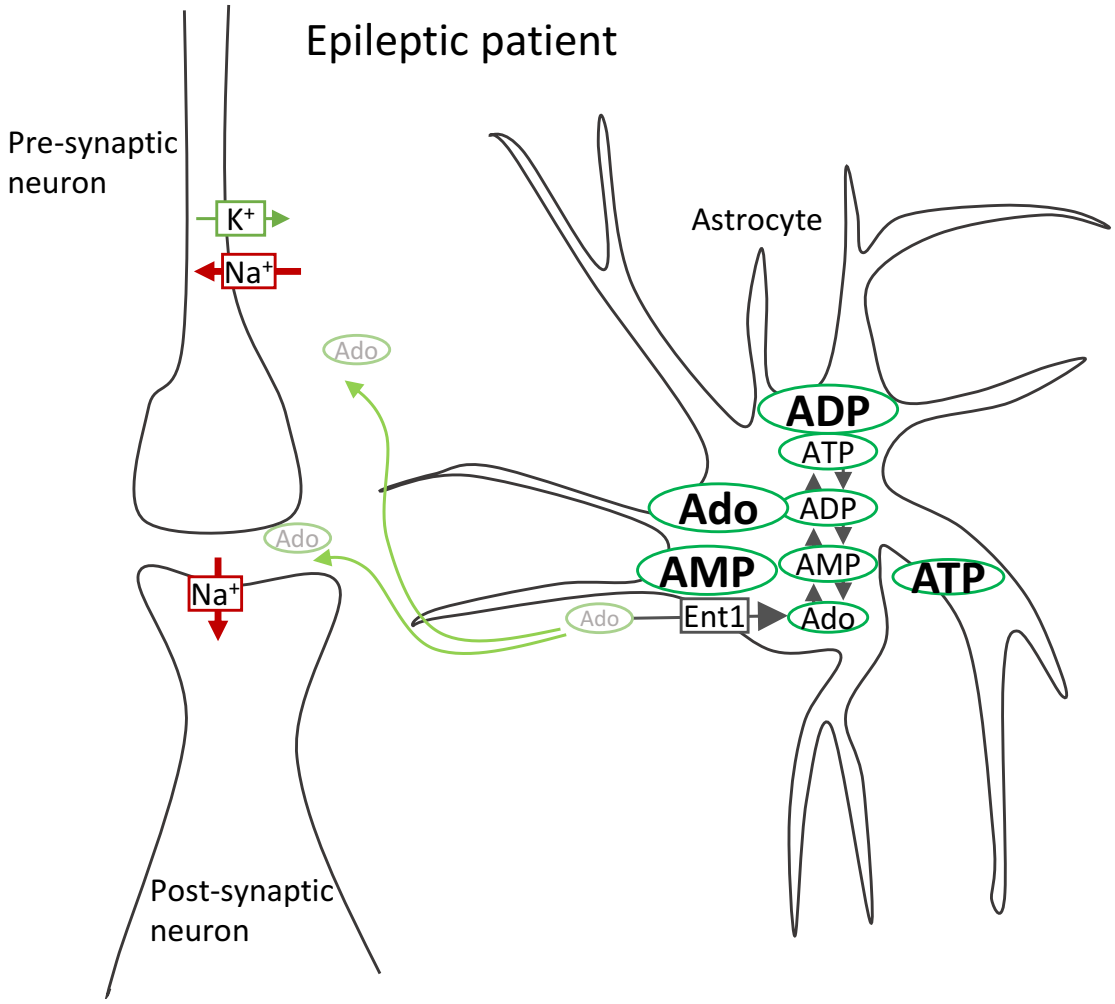

Figure 7.1: Adenosine and epilepsy. B: In an epileptic patient with a mutated ENT1 protein or over-expressed ADK, adenosine is only taken up into astrocytes and not released.

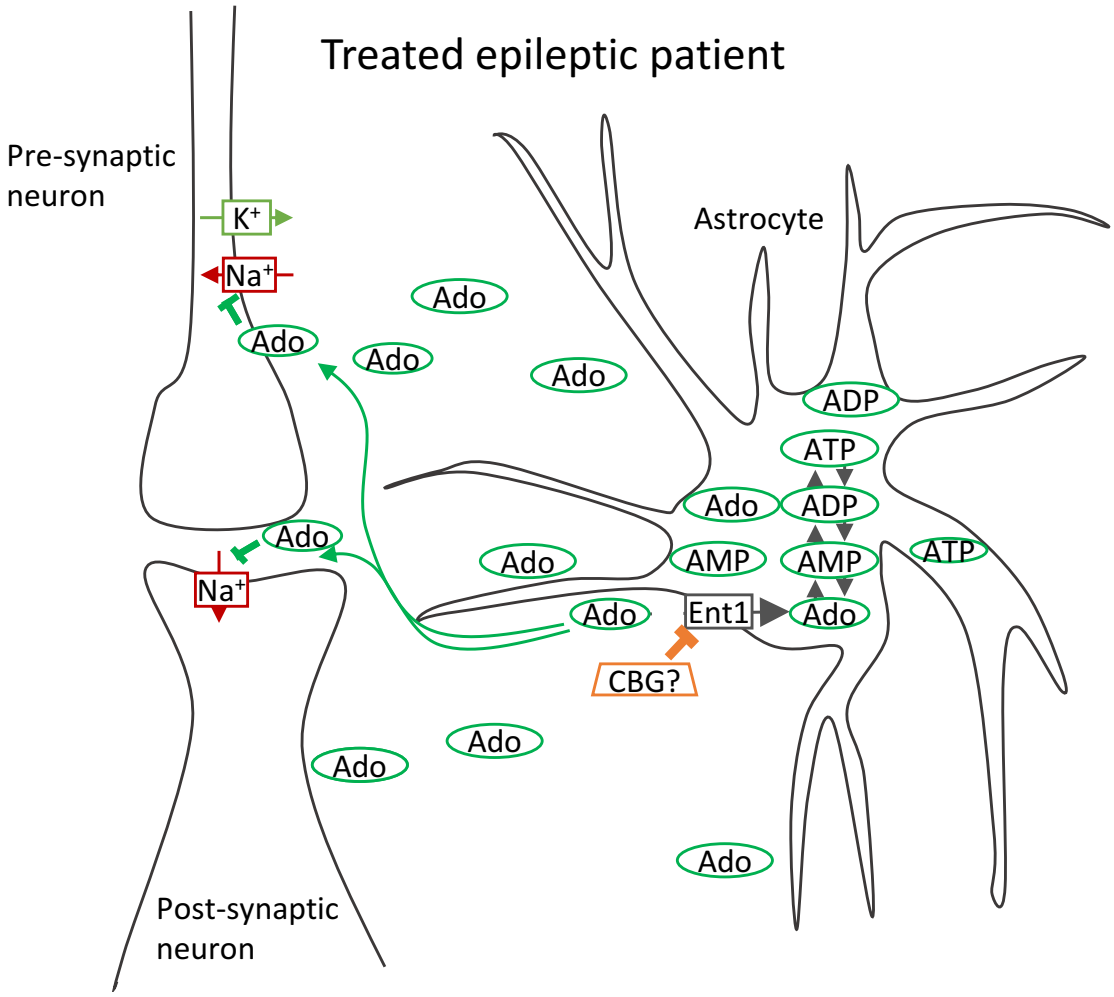

Figure 7.1: Adenosine and epilepsy.. **C:** CBG or CBD inhibition of adenosine uptake through ENT1 could result in elevated free adenosine, therefore inhibiting synaptic activity.

7.6 The IPMK- and mTORC1-related molecular mechanism of CBG

Previous studies of the mechanisms of action of cannabinoids have implicated regulation of the PI3K/PKB/mTOR pathway as a target of these compounds. In this thesis, a CBG- and CBD-dependent mechanism of mTORC1 regulation is identified in *D. discoideum*, *M. musculus* and *H. sapiens* cells. This is consistent with previous studies indicating that cannabinoids regulate the mTOR pathway (Shrivastava et al., 2011; Renard et al., 2016; Giacoppo et al., 2017; Sultan et al., 2018; Serra et al., 2019). The mechanism described in both *D. discoideum* and *M. musculus* for CBG and CBD is through an IPMK-dependent regulation of mTORC1 and is also dependent on the presence of PI3K activity. This adds to the previous understanding of the role of cannabinoids in mTOR regulation and provides a possible target of cannabinoids in the signalling pathway.

IPMK has key cellular roles related to mTORC1 activity which could be modulated by CBG. These are the production of higher order inositol phosphates (Kim et al., 2017(a)), production of PIP_3 (Blind et al., 2012), and non-catalytic binding of IPMK to mTORC1 (Kim et al., 2011) and AMPK (Bang et al., 2012). Although the data found in this thesis do not identify how CBG regulates IPMK activity, a model can be proposed. The model would indicate that IPMK binding to mTORC1 in wild type cells is a limiting factor for mTORC1 activation (Figure 7.2 A i). Here, CBG and CBD would increase the likelihood of IPMK binding to mTORC1, resulting in elevated mTORC1 activity following CBG or CBD treatment in wild type *D. discoideum*, MEFs and PBMCs from healthy controls (Figure 7.2 A ii). In IPMK over-expressing *D. discoideum* cells ($dIPMK^+$ and $hIPMK^+$), elevated IPMK expressions leads to IPMK becoming a major source of PIP_3 production elevating mTORC1 activity through PKB signalling (Figure 7.2 B i). In this case, when CBG and CBD treatment increase binding to mTORC1, PIP_3 production would decrease. Since PI3K activity represents a rate limiting factor for mTORC1 activation, with the cell unable to produce as much PIP_3, mTORC1 activity would decrease to similar levels as in wild type (Figure 7.2 B ii). The effect observed in IPMK over-expressing cells appears similar to that observed in both *D. discoideum* and MEF cells following pharmacological PI3K inhibition. In the absence of PI3K activity, the mTORC1 pathway is inactive, thus not responsive to enhanced binding of IPMK to mTORC1 through cannabinoid treatment (Figure 7.2 C i). Instead the lack of PI3K signalling results in no change in mTORC1 activity (Figure 7.2 C ii). In cells lacking IPMK (Figure 7.2 D i), CBG treatment cannot elevate mTORC1 activity (Figure 7.2 D ii).

Furthermore, the results found here indicate that of the two PKB proteins in *D. discoideum*, PKBA may be more likely to form mTORC2 and PKGB more likely to signal mTORC1. Therefore, lack of PKBA could result in an elevated amount of mTOR and LST8 proteins available for mTORC1 signalling, thus elevating mTORC1 activity (Figure 7.2 E i). CBG and CBD treatment of PKBA-ablated cells would result in an increase of mTORC1 activity due to the same mechanism as occurs in wild type cells, with free IPMK likely to bind and activate mTORC1 (Figure 7.2 E ii). In *D. discoideum* cells lacking both PKBA and PKGB (both PKB proteins), PKB-signalling could no longer act on mTORC1 signalling (Figure 7.2 F i), thus CBG or CBD treatment of these cells would not result in elevation of mTORC1 activity (as in PI3K inhibitor-treated cells) (Figure 7.2 F ii). These proposed mechanisms require further exploration to verify. Furthermore, experiments in mammalian cells are necessary to confirm the whole mechanism is conserved. However, the outcomes of these proposed mechanisms are consistent with CBG and CBD modulating the activity of IPMK and could explain the effects seen in human PBMCs.

Another aspect of the molecular mechanisms of CBG and CBD acting via IPMK, is that treatment with both cannabinoids elevated IP_6 levels in wild type *D. discoideum*. While treatment with CBG

and CBD did not affect IP_6 levels in dIPMK-over expressing cells. This could indicate that CBG and CBD may increase IPMK binding to mTORC1, decrease the production of PIP_3 through IPMK and increase the catalytic activity of IPMK to produce IP_6. However, in cells over-expressing IPMK, there is likely a large proportion of the IPMK protein already able to produce IP_6, and therefore the limiting factor is likely to be a substrate for this production. As IP_7 can inhibit PKBA activity (Chakraborty et al., 2010), this also explains the elevated mTORC1 activity seen in PKBA-ablated cells. In these cells, IP_7 would no longer be able to inhibit mTORC1 activity through PKBA, and therefore an elevated mTORC1 activity would be found. Furthermore, treatment with CBG or CBD would allow a further increase in mTORC1 activity through non-catalytic binding of IPMK to mTOR.

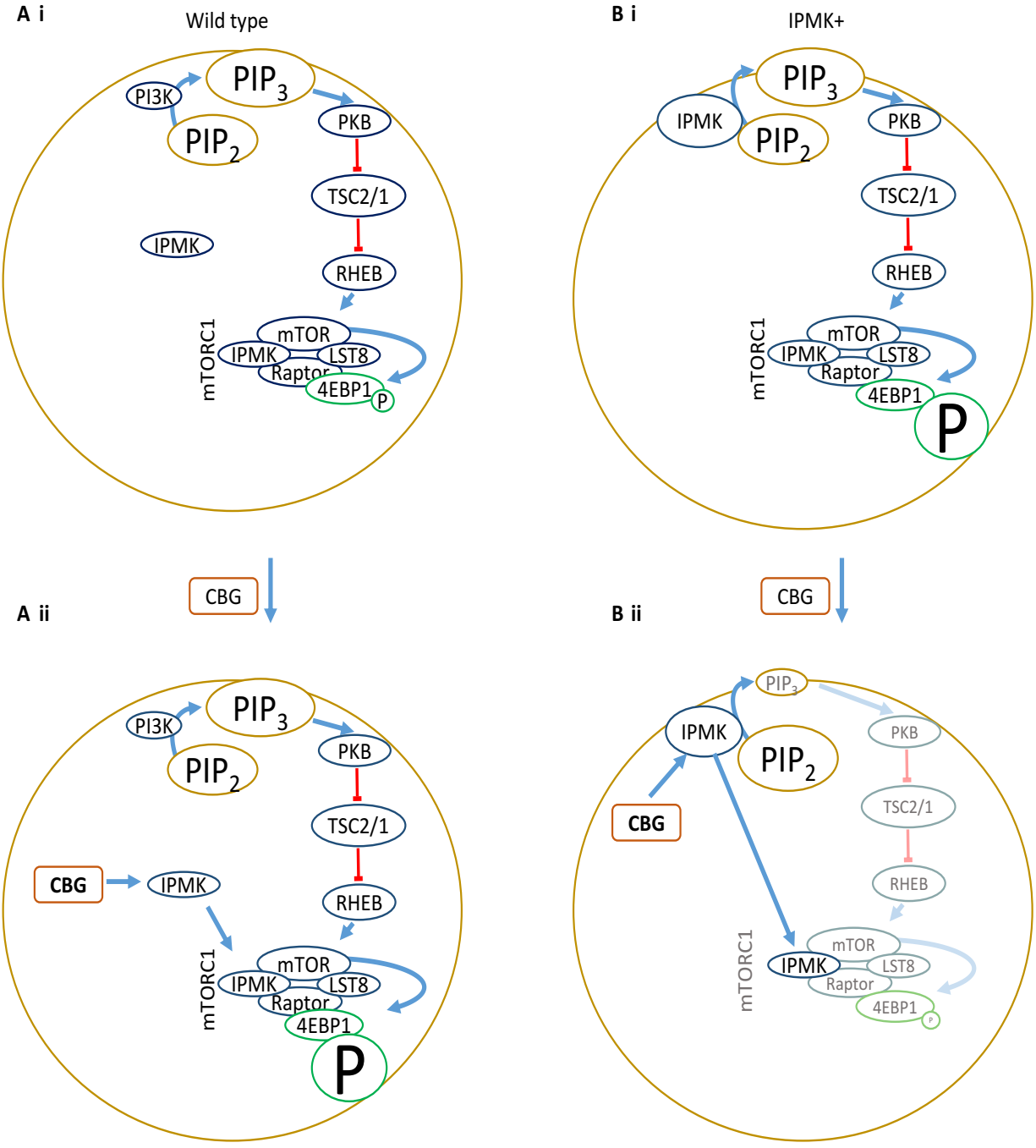

Figure 7.2: CBG and mTOR. A i: Wild type cells have a basal level of mTORC1 signalling. **Ii:** CBG treatment of wild type cells elevated mTORC1 signalling. **B i:** IPMK over-expressing cells have elevated basal mTORC1 signalling. **Ii:** CBG treatment of IPMK over-expressing cells reduces mTORC1 signalling.

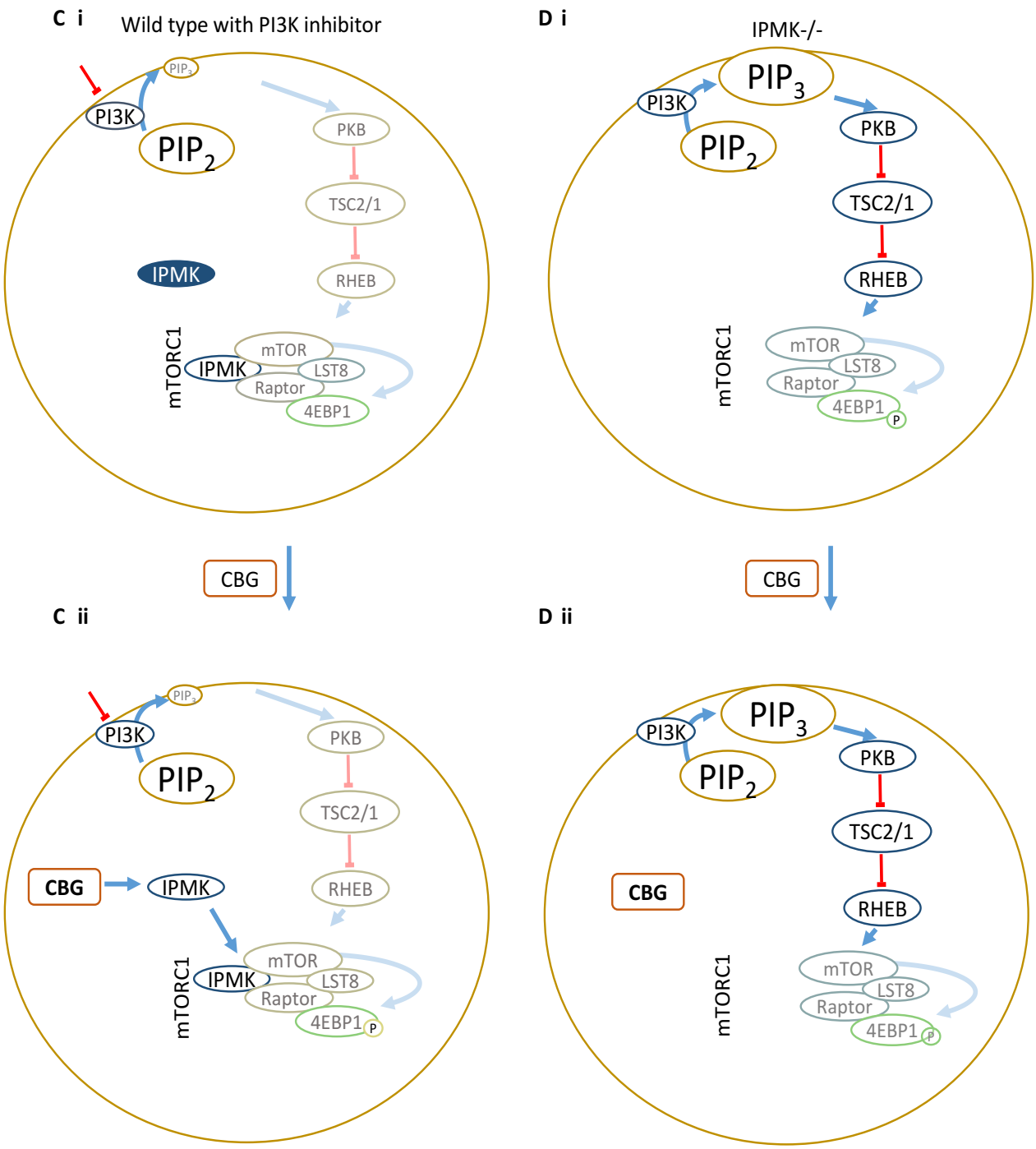

Figure 7.2: CBG and mTOR. C i: PI3K treatment reduces mTORC1 signalling. **Ii:** CBG does not alter mTORC1 activity in PI3K inhibitor-treated cells. **D i:** Cells lacking IPMK have lower basal mTORC1 signalling. **Ii:** CBG treatment of cells lacking IPMK does not alter mTORC1 activity.

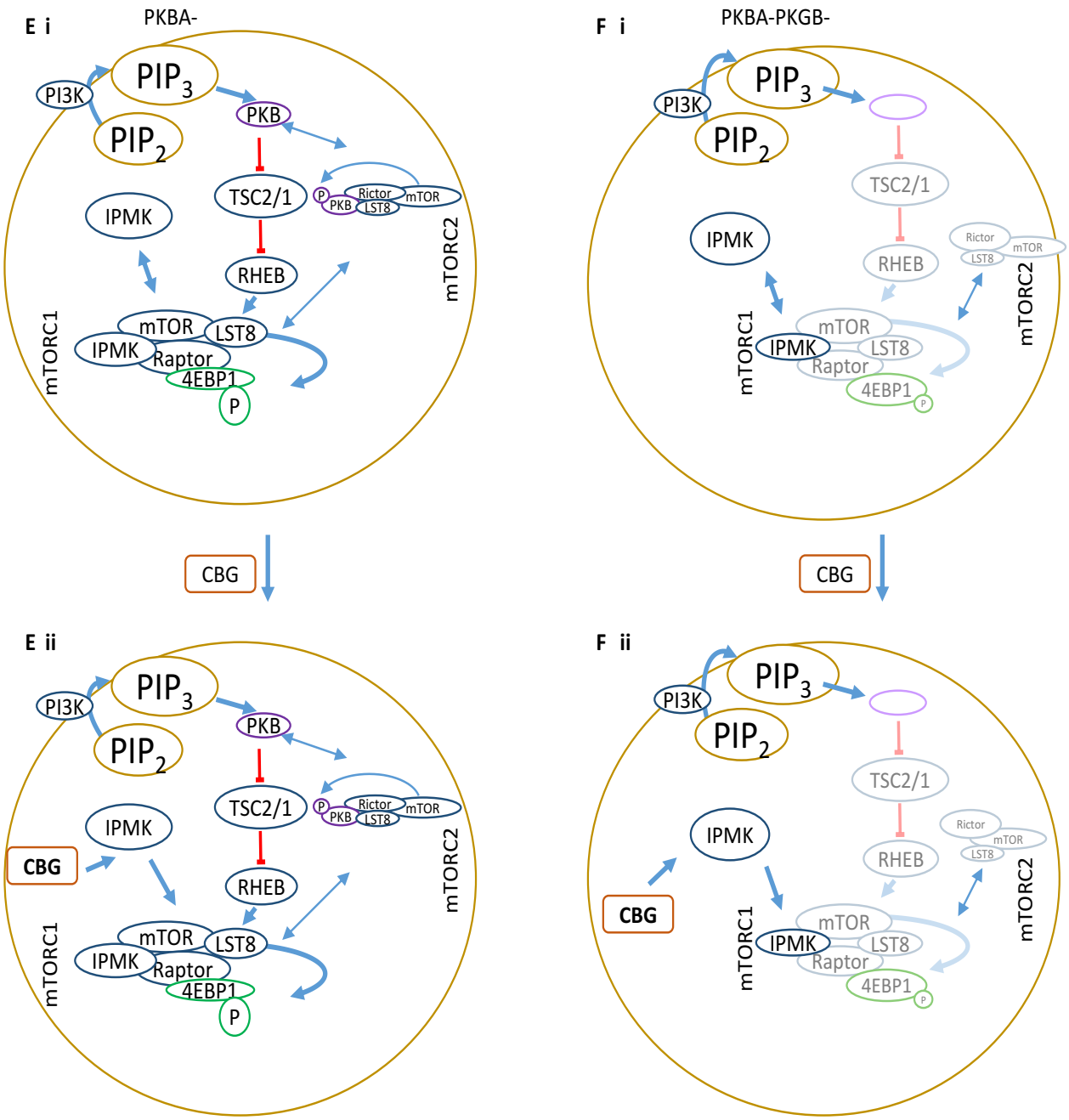

Figure 7.2: CBG and mTOR. E i: Cells lacking PKBA have elevated mTORC1 activity. **Ii:** CBG treatment of cells lacking PKBA elevates mTORC1 activity. **F i:** Cells lacking PKBA and PKGB have unaltered mTORC1 activity to wild type cells, but likely lower PKB-related signalling. **Ii:** CBG treatment of cells lacking PKBA and PKGB does not elevate mTORC1 activity.

7.7 CBG as a therapeutic for MS treatment

The results of this study could propose a molecular mechanism for cannabinoids in the treatment of MS. In healthy central nervous systems, immune cells do not attack neurons and myelin sheaths are present on the neurons (Figure 7.3 A). At the onset of MS, immune cells are activated by elevated mTOR signalling (Rajesh et al., 2007; Simpson et al., 2015; Gao et al., 2015) and begin to target myelin sheaths (Figure 7.3 B). This process leads to myelin degradation, and improper and interrupted neuronal signalling (Linker et al., 2011; Wingerchuk and Carter, 2014), and reduced mTORC1 signalling in neurons due to pro-inflammatory cytokines released by immune cells (Giacoppo et al., 2017). This thesis shows that cannabinoid treatment of MS reduces mTORC1 signalling in immune cells, which could reduce the activation of these cells *in vivo* and thus reduce the degradation of myelin (Figure 7.3 C). The removal of pro-inflammatory cytokines from the neurons allows the myelin repair to begin as a result of restored mTORC1 signalling (Giacoppo et al., 2017). Thus, this thesis suggests a mechanism of cannabinoids that could support myelin repair in MS due to the proposed stabilisation of IPMK/mTORC1 in activated cells.

To determine the ability of cannabinoids to treat MS, experimental procedures examining a reduction in disease-related symptoms are necessary. One such example would be to examine if myelin degradation on neurons is altered by cannabinoid treatment (Goebbels et al., 2017). In model mice, ablation of PTEN which catalyses the production of PIP_2 from PIP_3 resulted in elevated myelination due to increased axonal size (Goebbels et al., 2017). This implicated elevated mTORC1 signalling in remyelination and indicated a method by which the therapeutic ability of cannabinoids to treat MS could be measured. In MS, activated immune cells degrade myelin sheaths on neurons, resulting in misfiring of neurons which causes symptoms such as spasticity associated with MS (Arévalo-Martín et al., 2003). Remyelination, or blocking of immune cell degradation of myelin, is a key aspect of any MS treatment. Other studies have found that cannabinoids can elevate mTOR activity in neurons (Giacoppo et al., 2017). Conversely, this thesis indicates that in immune cells from patients with MS, cannabinoids can reduce mTORC1 activity, which could result in a lower quantity of activated immune cells (Gao et al., 2015). The differential modulation of mTOR activity in different cell types could be key to any therapeutic use of cannabinoids to treat MS, and further experiments such as myelination assays *in vivo* could be employed to examine this.

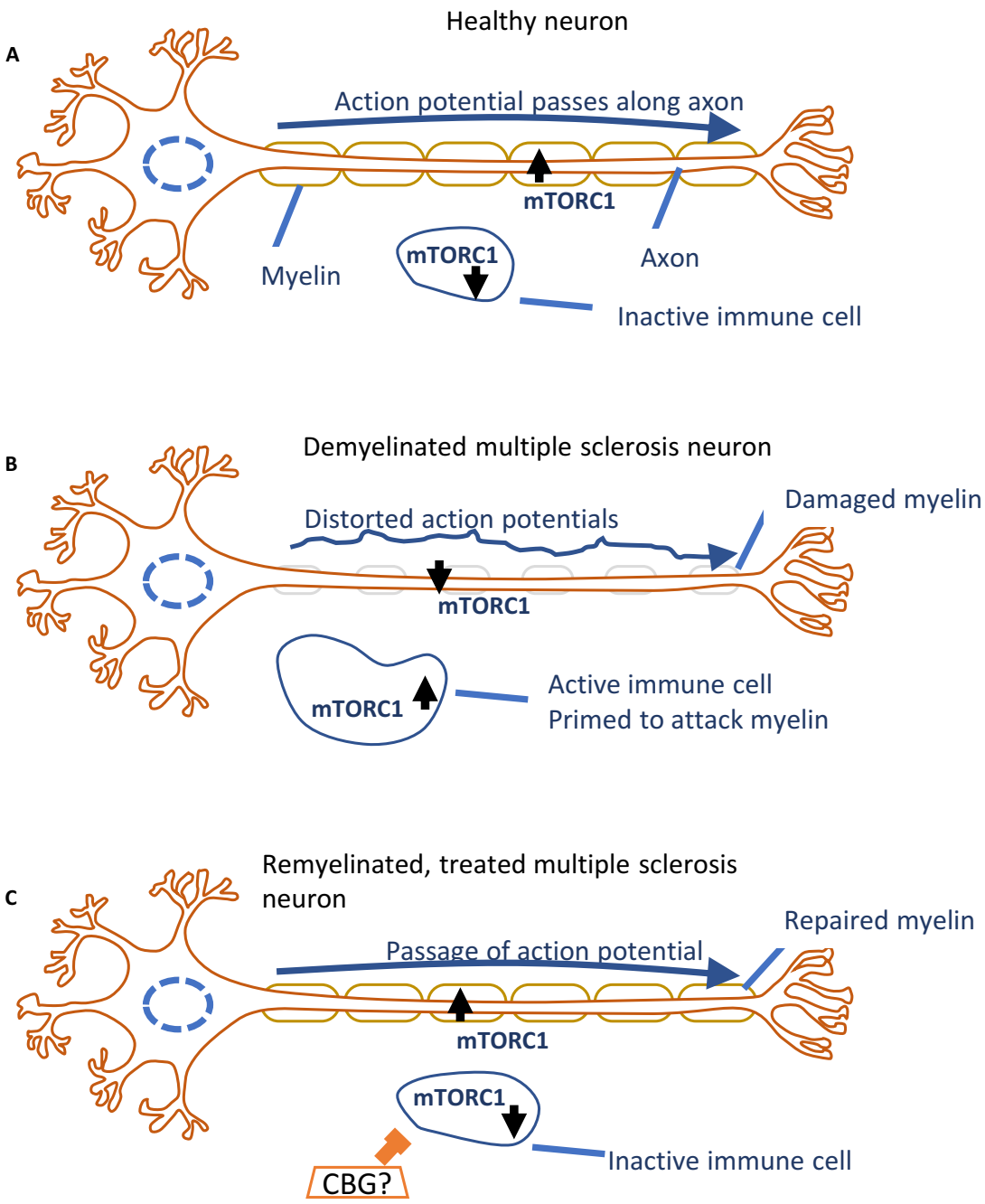

Figure 7.3: CBG as a potential therapeutic for MS. A: Neurons in healthy individuals have myelin sheaths and immune cells do not attack myelin. **B:** In MS immune cells are activated with elevated mTORC1 signalling, the immune cells attack myelin, and this results in myelin degradation and lower repair signalling through mTORC1. **C:** CBG treatment may reduce mTORC1 signalling in immune cells during MS, this reduces the attacking of myelin, allowing myelin to repair through elevated mTORC1 signalling.

This study, along with previous studies, provides evidence of the necessity of personalised medicine. The PBMCs from patients with MS displayed elevated mTORC1 activity, which was reduced by cannabinoid treatment, whereas cannabinoid treatment of PBMCs from healthy controls elevated mTORC1 activity. This indicates both a potential treatment of MS and a potential negative side effect of treatment in healthy individuals (or individuals with MS without

an elevated mTORC1 activity in immune cells). Other studies have indicated a therapeutic modulation of mTOR activity to treat MS is cell type-specific (Giacoppo et al., 2017). To be certain that cannabinoids can result in the treatment of MS in all cases analysis of mTORC1 activity for each patient before receiving treatment needs to be carried out. Alternatively, mTORC1 activity *in vivo* could be analysed for different cell types in a mouse model of MS (Giacoppo et al., 2017). Furthermore, if IPMK over-expression is a causative factor of MS and the elevated level of mTORC1 activity in PBMCs from patients with MS observed in this thesis, then an examination of IPMK expression levels could provide a means to determine whether cannabinoid treatment could be effective.

The causes of MS are still unknown, although there are probably multiple causes and are likely to be highly complex (Tselis, 2012). Therefore, there is a need for personalised medicine for MS treatment (Gafson et al., 2017). Clinical trials have revealed that Sativex® treatment works for around half of patients (Zettl et al., 2016). In PBMCs from healthy volunteers CBG, CBD and THC:CBD elevate mTORC1 activity, which enhances immune cell activation and could exacerbate MS-related symptoms (Carbone et al., 2014). Further *in vivo* experiments are therefore necessary to clarify the roles of cannabinoids in modifying mTORC1 activity, and to determine the specific therapeutic effects these might have on a patient by patient basis.

7.8 Future Work

7.8.1 Characterising the mTOR pathway in *D. discoideum*

This thesis indicates that IPMK is a key component of mTORC1 activity in *D. discoideum*, with what appears to be an ability to up- and downregulate activity depending on conditions. Very little, if anything, had been examined of IPMK in *D. discoideum* prior to this. Therefore, future work could focus on a full examination of how IPMK can have alternating regulatory roles of mTORC1 in *D. discoideum*. This could be carried out by blocking the ability of IPMK to carry out each of its three main actions: higher inositol phosphate production (Kim, Ahn, et al., 2017), PIP_3 production (Blind et al., 2012) and non-catalytic mTORC1 binding (Kim, Ahn, et al., 2017). This could be carried out by point mutation or removal of sections of the IPMK protein to determine how each plays a role. For example, if the PIP_3 production region is removed, but the other two left intact, and this is not lethal to the cell, then it could be examined what over-expression of IPMK has in this cell line and how it reacts to CBG.

The amount of PIP_3 produced by IPMK should also be analysed in *D. discoideum* using mass spectrometry (Kielkowska et al., 2014). This could be carried in wild type cells compared to IPMK overexpressor cells, determining the proportion of PIP_3 made in the overexpressor. PIP_3 production in relation to CBG treatment in both cell lines could also be determined, thus further

clarifying the role of CBG in mTORC1 regulation. The role of CBG in mTORC1 regulation could also be analysed by examining the reaction of other mTOR signalling pathway components undergoing CBG treatment, for example LST8 (Rosel et al., 2012), TSC1 and TSC2 (Serfontein et al., 2011), AMPK, RHEB, Raptor, Rictor and S6 kinase (Jaiswal et al., 2019)i.

Furthermore, given that it appears lethal to ablate IPMK, to discover why this is lethal, removal of the different key components of IPMK one at a time until no longer possible could help determine this. This would then help to understand the essential role IPMK plays in most eukaryotes (Saiardi et al., 2018). It is possible that the combination of components in IPMK is what makes it essential, potentially carrying out multiple actions at a time and specifically localising them. This would be indicated if ablation of any component of IPMK was found to be lethal.

Another interesting experiment would be to add the nuclear localisation signal (Nalaskowski et al., 2002) to the *D. discoideum* protein and determine if this has any impact on mTORC1 signalling, or resistance to CBG, for example. Then also add the section of the *H. sapiens* IPMK protein that ensures a tighter binding of IPMK to mTOR (Kim et al., 2011) to the *D. discoideum* protein and determine how this affects mTORC1 signalling. It may be that the *D. discoideum* protein, though lacking the full mTOR binding domain, still binds as efficiently to the *D. discoideum* mTOR. To determine this, pulldown experiments could be carried out with different combinations of truncated or extended IPMK, and examine which has a higher binding affinity to mTOR.

Although it was not possible to create an IPMK knockout mutant in this thesis, newer techniques that are often quicker and more efficient could be attempted, for example using CRISPR (Sekine et al., 2018). In addition, if it is the production of higher order inositol phosphates or PIP_3 that makes IPMK an essential protein, these could be artificially added when knocking out the gene. Furthermore, knockdowns of IPMK could be created using techniques such as RNA interference (Xu, Sen, et al., 2013), inducible CRISPR (Zhang et al., 2019), transcription activator-like effector nucleases (Kowalko et al., 2016), small interfering RNAs (Kuhlmann et al., 2005) or short hairpin RNAs (Pan et al., 2019). Creating a knockdown could allow examination of IP levels, PIP_3 levels and mTORC1 activity in the absence of the vast majority of IPMK protein. This could potentially indicate to what extent IPMK carries out each of the three activities, showing which it has a greater or lesser impact on.

7.8.2 Characterising the role of CBG in adenosine regulation in *D. discoideum*

This thesis indicates that CBG regulates adenosine transport through ENT1 in *D. discoideum*. To investigate whether or not CBG blocks adenosine uptake into *D. discoideum* cells, as the data

indicates, cells could be treated with CBG in the presence of tritium-labelled adenosine ([3H]adenosine) (Carrier et al., 2006). Previous studies have found that in blocking adenosine transport through ENT1, CBD blocks the uptake of tritium-labelled adenosine. However, when CBD blocks adenosine uptake, the intracellular content of adenosine does not change, and instead the accumulated tritium-labelled adenosine increases, potentially because the cell makes up for the lack of taken up adenosine by synthesising more (Carrier et al., 2006). Similar experiments in the *D. discoideum* model set up would reveal both if CBG has the same effect as CBD on ENT1 and if this mechanism is consistent between mammals and the amoeba. Further to this, tritium-labelled adenosine could be used to determine whether ablation of ENT1 actually halts adenosine uptake into cells. Another method to define any direct interaction between adenosine and CBG at ENT1 would be to carry out a competitive inhibition assay (Woodcock et al., 2019). These assays would be used to determine if CBG inhibits adenosine transport through ENT1 and if it does this by blocking the active site of ENT1 and being transported instead. If it does fully or mostly, then the phenotypes found in this thesis are explained, however, if it does not, the other ENT proteins in *D. discoideum* could be ablated and the phenotype and adenosine uptake in those cells examined.

7.8.3 Confirming the mechanisms of action of CBG in mammals *in vivo*

mTOR

This thesis indicates that CBG regulates mTOR activity through IPMK. To examine if this is the case in mammals, first a cell line overexpressing IPMK could be treated similarly to *D. discoideum* in this thesis with CBG and examine whether IPMK overexpressing cells have elevated mTORC1 compared to wild type, whether CBG activates mTORC1 in wild type, and whether CBG downregulates mTORC1 in IPMK overexpressing cells. If this is the case in cell lines, then experiments can be carried forward to *in vivo*. Remyelination assays in a complex cell culture could also be a useful experiment to determine if CBG has the capacity to actually enhance myelination rather than just slow down degradation of the myelin.

In an MS mouse model (EAE), IPMK expression could be examined both in the CNS (neurons, oligodendrocytes, myelin sheaths, etc.) and in the immune system (monocytes, PBMCs, etc.). This would perhaps given an early indication to the relevance of IPMK to MS disease and possible treatment. Regardless, as cannabinoids appear to successfully treat this model of MS, mTORC1 activity in both the CNS and immune cells could be measured in wild type mice and MS mice. To examine fully the effect of mTORC1 on disease progression and treatment, multiple timepoints should be analysed, prior to inducing of the disease model, immediately after inducing, prior to treatment, immediately after treatment and after long term treatment. Although this thesis finds specific effects of CBG treatment on mTORC1 activity, this is just after one treatment with

the compound, and long term treatment or multiple treatments may well have different effects. Disease progression should also be measured in the model and health of the wild type mouse should be measured. If in the wild type mice immune cells have elevated mTORC1 activity after CBG treatment, as occurs in wild type *D. discoideum*, then this could indicate the potential danger of mis-prescribing CBG to patients without elevated mTORC1 in immune cells. Inflammation markers, such as TNF-α and IL-6 should be measured in both the wild type and disease model, in treated and untreated to examine the effect of both the disease and treatment on inflammation (Gugliandolo et al., 2018). Again, if CBG were to increase these markers, then this would represent a potential risk in prescribing to certain patients or misuse of the compound.

If CBG treatment of the mouse model of MS appears to be both safe and effective, then trials in humans can begin. Again, with healthy volunteers and MS patients. As the causes of MS are relatively unknown and various, the efficacy of CBG in treating MS in humans may well be reduced compared to a mouse in control conditions. This should be examined and the specific differences of the disease in those in which CBG is effective noted. Measuring IPMK in PBMCs may be one way to determine how effective CBG will be in treating MS, if this is found in mice previously. If IPMK appears to be a key regulator of MS progression or treatment, and no mutation is found within the gene itself, the surrounding area of the gene could be examined for mutations in promoter regions. If no mutation is present, then other aspects of the mTOR signalling pathway could be examined for mutations in patients with MS.

As hyperactivation of mTOR has been associated with drug-resistant epilepsy (Samueli et al., 2016) and cancer (Alayev and Holz, 2013), it would be essential to determine whether CBG treatment can increase the risk of this in healthy individuals and whether CBG treatment of patients with MS could result in any similar effects. CBG elevates mTORC1 in wild type *D. discoideum* and so ensuring this does not happen in humans would be a key finding before using it as a treatment.

Adenosine

In this thesis CBG is found to regulate adenosine transport across the plasma membrane. This could be beneficial for the treatment of epilepsy, as astrocytes store a large amount of adenosine as AMP, ADP and ATP (Diógenes et al., 2014). If CBG prevented the accumulation of adenosine in astrocytes then, this could be beneficial. However, if CBG prevents the uptake of adenosine into all cell types, which it may well do, this could eventually result in adenosine depletion after long term treatment and could also reduce the ability of cells to proliferate or repair DNA, as adenosine is a nucleotide. Although, adenosine can be synthesised by cells, so this may not be the case, it should still be examined. If intracellular adenosine in all cell types is

decreased by CBG treatment due to a reduction in uptake, this could increase DNA methylation would actually exacerbates epileptogenesis (Weltha et al., 2019). Direct adenosine treatment in the brain of mice reduces epilepsy and DNA methylation, CBG may have the opposite effect and therefore a key experiment would be how long term CBG treatment affects DNA methylation in the brain of epilepsy mouse models and wild type mice. If CBG treatment increases DNA methylation in both mice types, it may be worth evaluating the risk of long term CBG treatment. In this thesis it is found that CBG treatment does indeed enhance DNA methylation and that ENT1 inhibition or ablation has the same effect, it would therefore seem likely that this would occur in all cell types, if CBG inhibits adenosine uptake.

7.8.4 CBG in the treatment of other diseases

Schizophrenia and psychosis

The efficacy of cannabinoids in treating schizophrenia and psychosis has also been examined by previous studies. These severe mental disorders are characterised by hallucinations, delusions, increased anxiety and cognitive deficits, occurring in around 1% of individuals globally (around 24 million people) (Adams et al., 2005; Purcell et al., 2009). Most schizophrenia treatments involve the use of dopaminergic receptor inhibition, which reduces the likelihood and threshold of action potentials in neurons, and therefore reduces the misfiring and spread of action potentials that occurs during schizophrenia (Renard et al., 2016). In amphetamine-induced schizophrenic rats, CBD injected directly into the nucleus accumbens shell (a common target region of anti-psychotic drugs) resulted in a reduction in schizophrenic symptoms as well as reduced dopaminergic neuronal activation in the ventral tegmental area (Renard et al., 2016).

An initial study on a rat model of psychosis found that CBD was an effective anti-psychotic with few side-effects (Zuardi et al., 1991). In a mouse model of schizophrenia and psychosis lacking the neuregulin 1 protein, long-term treatment with CBD enhanced social interaction and in wild type mice decreased anxiety-related behaviour (Long et al., 2012). In a rat model of emotional processing impairment in schizophrenia, CBD decreased freezing response, which is a symptom of schizophrenia (Levin et al., 2012). Another study found that CBD was an effective treatment of schizophrenia in amphetamine-induced model rats, as CBD treatment reduced schizophrenia-related psychopathology (Renard et al., 2016). The same research group discovered the need to determine effects of specific cannabinoids on the disease, as adolescent rat exposure of THC was found to result in schizophrenia-like symptoms in adult rats (Renard et al., 2017(a)). Further study in the area found that CBD treatment may mitigate the anxiety-causing effects of THC in a dose-dependent manner (Szkudlarek et al., 2019). For schizophrenia and psychosis, there appear to be specific effects related to different cannabinoids as treatments. CBD appears to

ameliorate schizophrenia- and psychosis-related symptoms, while THC may cause these symptoms.

Interestingly, the amphetamine-induced mouse model of schizophrenia had reduced mTOR signalling compared to healthy mice in the nucleus accumbens shell, while CBD treatment alleviated symptoms and elevated mTOR signalling even more than in healthy mice (Renard et al., 2016). THC exposure in adolescent rats that cause schizophrenia-like symptoms, also caused hyperactivity in the mesocorticolimbic dopamine pathway and dysregulation and alteration in prefrontal cortical molecular pathways involved in dopaminergic regulation (Renard et al., 2017(a)). THC exposure here reduced mTOR signalling, perhaps indicating that mTOR reduction is either causative or correlative with schizophrenia, and elevation of mTOR could again be a potential treatment of schizophrenia, or a side effect of treatment. As CBG and CBD were able to elevate mTOR signalling in this thesis in wild type *D. discoideum*, mouse cells and human PBMCs, this suggests a potential shared mechanism and a potential therapeutic use for CBG along with CBD in treating schizophrenia.

There is also a theory that schizophrenia develops or worsens in a similar way to epilepsy. That is, over-expression of ADK (specifically in astrocytes and similar adenosine sinks) can cause schizophrenia and that augmentation of adenosine can treat the disease or improve symptoms (Shen et al., 2012). If this is the case, then CBG may have a similar effect as it would on epilepsy treatment, by blocking adenosine uptake into adenosine sinks, it would leave more in the extracellular space for signalling via adenosine receptors. CBG could therefore be explored as a schizophrenia treatment through two different mechanisms explored in this thesis.

Cancer

The therapeutic potential of cannabinoids for cancer treatment has also been explored in multiple models of cancer pathologies. In a mouse model of breast cancer, CBD was found to have a low-toxicity profile and inhibited the proliferative and invasive phenotype of breast cancer cells (McAllister et al., 2007). Using a mouse mammary tumour cell line implanted into mice, CBD reduced the metastasis of cancer cells and cell proliferation, potentially through an anti-oxidant mechanism (McAllister et al., 2011). CBD also enhanced apoptosis in multiple human breast cancer cell lines at a higher rate than non-cancer cells (Shrivastava et al., 2011; Sultan et al., 2018). In addition, CBD was found to exert chemo-preventive effects, to protect DNA from oxidative damage and to reduce cell proliferation in an azoxymethane-induced mouse model of colonic cancer (Aviello et al., 2012). Furthermore, CBG was found to selectively inhibit the growth of colonic cancer cells in a mouse model (Borrelli et al., 2014). CBG could therefore be further explored as a potential treatment of cancer, given the effects of CBG on cell

proliferation in *D. discoideum* and the potential to reduce mTOR signalling in cells with hyperactivated mTOR.

8 References

Abrams, D.I. 2018. The therapeutic effects of Cannabis and cannabinoids: An update from the National Academies of Sciences, Engineering and Medicine report. *European Journal of Internal Medicine*. **49**, pp.7–11.

Abu-Sawwa, R. and Stehling, C. 2020. Epidiolex (Cannabidiol) primer: Frequently asked questions for patients and caregivers. *Journal of Pediatric Pharmacology and Therapeutics*. **25**(1), pp.75–77.

Adams, C.E., Rathbone, J., Thornley, B., Clarke, M., Borrill, J., Wahlbeck, K. and Awad, A.G. 2005. Chlorpromazine for schizophrenia: A cochrane systematic review of 50 years of randomised controlled trials. *BMC Medicine*. **3**(1), p.15.

Alayev, A. and Holz, M.K. 2013. mTOR signaling for biological control and cancer. *Journal of Cellular Physiology*. **228**(8), pp.1658–1664.

Albrecht, P., Bouchachia, I., Goebels, N., Henke, N., Hofstetter, H.H., Issberner, A., Kovacs, Z., Lewerenz, J., Lisak, D., Maher, P., Mausberg, A.K., Quasthoff, K., Zimmermann, C., Hartung, H.P. and Methner, A. 2012. Effects of dimethyl fumarate on neuroprotection and immunomodulation. *Journal of Neuroinflammation*. **9**, p.163.

Ambrósio, A.F., Soares-da-Silva, P., Carvalho, C.M. and Carvalho, A.P. 2002. Mechanisms of action of carbamazepine and its derivatives, oxcarbazepine, BIA 2-093, and BIA 2-024. *Neurochemical Research*. **27**(1–2), pp.121–130.

Antonini, J.M., Kodali, V., Meighan, T.G., Roach, K.A., Roberts, J.R., Salmen, R., Boyce, G.R., Zeidler-Erdely, P.C., Kashon, M., Erdely, A. and Shoeb, M. 2019. Effect of Age, High-Fat Diet, and Rat Strain on Serum Biomarkers and Telomere Length and Global DNA Methylation in Peripheral Blood Mononuclear Cells. *Scientific Reports*. **9**(1), p.1996.

Arévalo-Martín, Á., Vela, J.M., Molina-Holgado, E., Borrell, J. and Guaza, C. 2003. Therapeutic action of cannabinoids in a murine model of multiple sclerosis. *Journal of Neuroscience*. **23**(7), pp.2511–2516.

Augustin, K., Khabbush, A., Williams, S., Eaton, S., Orford, M., Cross, J.H., Heales, S.J.R., Walker, M.C. and Williams, R.S.B. 2018. Mechanisms of action for the medium-chain triglyceride ketogenic diet in neurological and metabolic disorders. *The Lancet Neurology*. **17**(1), pp.84–93.

Aviello, G., Romano, B., Borrelli, F., Capasso, R., Gallo, L., Piscitelli, F., Di Marzo, V. and Izzo, A.A. 2012. Chemopreventive effect of the non-psychotropic phytocannabinoid cannabidiol on experimental colon cancer. *Journal of Molecular Medicine*. **90**(8), pp.925–934.

Baker, D., Pryce, G., Ludovic Croxford, J., Brown, P., Pertwee, R.G., Huffman, J.W. and Layward, L. 2000. Cannabinoids control spasticity and tremor in a multiple sclerosis model. *Nature*. **404**(6773), pp.84–87.

Baldwin, S.A., Beal, P.R., Yao, S.Y.M., King, A.E., Cass, C.E. and Young, J.D. 2004. The equilibrative nucleoside transporter family, SLC29. *Pflugers Archiv European Journal of Physiology*. **447**(5), pp.735–743.

Bang, S., Chen, Y., Ahima, R.S. and Kim, S.F. 2014. Convergence of IPMK and LKB1-AMPK signaling pathways on metformin action. *Molecular Endocrinology*. **28**(7), pp.1186–1193.

Bang, S., Kim, S., Dailey, M.J., Chen, Y., Moran, T.H., Snyder, S.H. and Kim, S.F. 2012. AMP-activated protein kinase is physiologically regulated by inositol polyphosphate multikinase. *Proceedings of the National Academy of Sciences of the United States of America*. **109**(2), pp.616–620.

Bapteste, E., Brinkmann, H., Lee, J.A., Moore, D. V., Sensen, C.W., Gordon, P., Duruflé, L., Gaasterland, T., Lopez, P., Müller, M. and Philippe, H. 2002. The analysis of 100 genes supports the grouping of three highly divergent amoebae: *Dictyostelium*, *Entamoeba*, and *Mastigamoeba*. *Proceedings of the National Academy of Sciences of the United States of America*. **99**(3), pp.1414–1419.

Bar-Or, A., Nuttall, R.K., Duddy, M., Alter, A., Kim, H.J., Ifergan, I., Pennington, C.J., Bourgoin, P., Edwards, D.R. and Yong, V.W. 2003. Analyses of all matrix metalloproteinase members in leukocytes emphasize monocytes as major inflammatory mediators in multiple sclerosis. *Brain*. **126**(12), pp.2738–2749.

Beale, G., Haagensen, E.J., Thomas, H.D., Wang, L.Z., Revill, C.H., Payne, S.L., Golding, B.T., Hardcastle, I.R., Newell, D.R., Griffin, R.J. and Cano, C. 2016. Combined PI3K and CDK2 inhibition induces cell death and enhances in vivo antitumour activity in colorectal cancer. *British Journal of Cancer*. **115**(6), pp.682–690.

Berkovich, R. and Weiner, L.P. 2015. Effects of dimethyl fumarate on lymphocyte subsets. *Multiple Sclerosis and Related Disorders*. **4**(4), pp.339–341.

Bermudez-Silva, F.J., Romero-Zerbo, S.Y., Haissaguerre, M., Ruz-Maldonado, I., Lhamyani, S., El Bekay, R., Tabarin, A., Marsicano, G. and Cota, D. 2016. The cannabinoid CB1 receptor and mTORC1 signalling pathways interact to modulate glucose homeostasis in mice. *DMM Disease Models and Mechanisms*. **9**(1), pp.51–61.

Bisogno, T., Hanuš, L., De Petrocellis, L., Tchilibon, S., Ponde, D.E., Brandi, I., Moriello, A.S., Davis, J.B., Mechoulam, R. and Di Marzo, V. 2001. Molecular targets for cannabidiol and its

synthetic analogues: Effect on vanilloid VR1 receptors and on the cellular uptake and enzymatic hydrolysis of anandamide. *British Journal of Pharmacology*. **134**(4), pp.845–852.

Blind, R.D., Suzawa, M. and Ingraham, H.A. 2012. Direct modification and activation of a nuclear receptor - PIP2 complex by the inositol lipid kinase IPMK. *Science Signaling*. **5**(229), p.ra44.

Blümcke, I., Thom, M. and Wiestler, O.D. 2002. Ammon's horn sclerosis: a maldevelopmental disorder associated with temporal lobe epilepsy. *Brain pathology (Zurich, Switzerland)*. **12**(2), pp.199–211.

Boer, K., Crino, P.B., Gorter, J.A., Nellist, M., Jansen, F.E., Spliet, W.G.M., van Rijen, P.C., Wittink, F.R.A., Breit, T.M., Troost, D., Wadman, W.J. and Aronica, E. 2010. Gene expression analysis of tuberous sclerosis complex cortical tubers reveals increased expression of adhesion and inflammatory factors. *Brain pathology (Zurich, Switzerland)*. **20**(4), pp.704–19.

Boison, D. 2013. Adenosine and seizure termination: Endogenous mechanisms. *Epilepsy Currents*. **13**(1), pp.35–37.

Boison, D. 2012. Adenosine dysfunction in epilepsy. *Glia*. **60**(8), pp.1234–1243.

Boison, D. and Aronica, E. 2015. Comorbidities in Neurology: Is adenosine the common link? *Neuropharmacology*. **97**, pp.18–34.

Boison, D., Scheurer, L., Zumsteg, V., Rülicke, T., Litynski, P., Fowler, B., Brandner, S. and Mohler, H. 2002. Neonatal hepatic steatosis by disruption of the adenosine kinase gene. *Proceedings of the National Academy of Sciences of the United States of America*. **99**(10), pp.6985–6990.

Boison, D. and Steinhäuser, C. 2018. Epilepsy and astrocyte energy metabolism. *Glia*. **66**(6), pp.1235–1243.

Borrelli, F., Fasolino, I., Romano, B., Capasso, R., Maiello, F., Coppola, D., Orlando, P., Battista, G., Pagano, E., Di Marzo, V. and Izzo, A.A. 2013. Beneficial effect of the non-psychotropic plant cannabinoid cannabigerol on experimental inflammatory bowel disease. *Biochemical Pharmacology*. **85**(9), pp.1306–1316.

Borrelli, F., Pagano, E., Romano, B., Panzera, S., Maiello, F., Coppola, D., De Petrocellis, L., Buono, L., Orlando, P. and Izzo, A.A. 2014. Colon carcinogenesis is inhibited by the TRPM8 antagonist cannabigerol, a Cannabis-derived non-psychotropic cannabinoid. *Carcinogenesis*. **35**(12), pp.2787–2797.

Borriss, R., Zemek, J., Augustín, J., Páčová, Z. and Kuniak, L. 1980. β-1,3-1,4-Glucanase in sporenbildenden Mikroorganismen. *Zentralblatt für Bakteriologie, Parasitenkunde,*

Infektionskrankheiten und Hygiene. Zweite Naturwissenschaftliche Abteilung: Mikrobiologie der Landwirtschaft, der Technologie und des Umweltschutzes. **135**(5), pp.435–442.

Bort, A., Sánchez, B.G., Mateos-Gómez, P.A., Díaz-Laviada, I. and Rodríguez-Henche, N. 2019. Capsaicin targets lipogenesis in hepG2 cells through AMPK activation, AKT inhibition and ppars regulation. *International Journal of Molecular Sciences*. **20**(7), p.1660.

Boswell-Casteel, R.C. and Hays, F.A. 2017. Equilibrative nucleoside transporters—A review. *Nucleosides, Nucleotides and Nucleic Acids*. **36**(1), pp.7–30.

Breen, G., Harwood, A.J., Gregory, K., Sinclair, M., Collier, D., St Clair, D. and Williams, R.S.B. 2004. Two peptidase activities decrease in treated bipolar disorder not schizophrenic patients. *Bipolar disorders*. **6**(2), pp.156–61.

Brenner, M. and Thoms, S.D. 1984. Caffeine blocks activation of cyclic AMP synthesis in Dictyostelium discoideum. *Developmental Biology*. **101**(1), pp.136–146.

Brierley, D.I., Harman, J.R., Giallourou, N., Leishman, E., Roashan, A.E., Mellows, B.A.D., Bradshaw, H.B., Swann, J.R., Patel, K., Whalley, B.J. and Williams, C.M. 2019. Chemotherapy-induced cachexia dysregulates hypothalamic and systemic lipoamines and is attenuated by cannabigerol. *Journal of Cachexia, Sarcopenia and Muscle*. **10**(4), pp.844–859.

Brierley, D.I., Samuels, J., Duncan, M., Whalley, B.J. and Williams, C.M. 2016. Cannabigerol is a novel, well-tolerated appetite stimulant in pre-satiated rats. *Psychopharmacology*. **233**(19–20), pp.3603–3613.

Busquets-Garcia, A., Bains, J. and Marsicano, G. 2018. CB1 Receptor Signaling in the Brain: Extracting Specificity from Ubiquity. *Neuropsychopharmacology : official publication of the American College of Neuropsychopharmacology*. **43**(1), pp.4–20.

Butler, K.M., Moody, O.A., Schuler, E., Coryell, J., Alexander, J.J., Jenkins, A. and Escayg, A. 2018. De novo variants in GABRA2 and GABRA5 alter receptor function and contribute to early-onset epilepsy. *Brain*. **141**(8), pp.2392–2405.

Butrica, J.L. 2002. The medical use of cannabis among the Greeks and Romans. *Journal of Cannabis Therapeutics*. **2**(2), pp.51–70.

Calhoun, S.R., Galloway, G.P. and Smith, D.E. 1998. Abuse Potential of Dronabinol (Marinol®). *Journal of Psychoactive Drugs*. **30**(2), pp.187–196.

Calleja, V., Alcor, D., Laguerre, M., Park, J., Vojnovic, B., Hemmings, B.A., Downward, J., Parker,

P.J. and Larijani, B. 2007. Intramolecular and intermolecular interactions of protein kinase B define its activation in vivo. *PLoS Biology*. **5**(4), pp.780–791.

Calvo-Garrido, J., King, J.S., Muñoz-Braceras, S. and Escalante, R. 2014. Vmp1 Regulates PtdIns3P Signaling During Autophagosome Formation in Dictyostelium discoideum. *Traffic*. **15**(11), pp.1235–1246.

Cang, C., Zhou, Y., Navarro, B., Seo, Y.J., Aranda, K., Shi, L., Battaglia-Hsu, S., Nissim, I., Clapham, D.E. and Ren, D. 2013. MTOR regulates lysosomal ATP-sensitive two-pore Na+ channels to adapt to metabolic state. *Cell*. **152**(4), pp.778–790.

Carbone, F., De Rosa, V., Carrieri, P.B., Montella, S., Bruzzese, D., Porcellini, A., Procaccini, C., La Cava, A. and Matarese, G. 2014. Regulatory T cell proliferative potential is impaired in human autoimmune disease. *Nature Medicine*. **20**(1), pp.69–74.

Cardenal-Muñoz, E., Arafah, S., López-Jiménez, A.T., Kicka, S., Falaise, A., Bach, F., Schaad, O., King, J.S., Hagedorn, M. and Soldati, T. 2017. *Mycobacterium marinum* antagonistically induces an autophagic response while repressing the autophagic flux in a TORC1- and ESX-1-dependent manner. *PLoS Pathogens*. **13**(4), p.e1006344.

Carrier, E.J., Auchampach, J.A. and Hillard, C.J. 2006. Inhibition of an equilibrative nucleoside transporter by cannabidiol: A mechanism of cannabinoid immunosuppression. *Proceedings of the National Academy of Sciences of the United States of America*. **103**(20), pp.7895–7900.

Castillo, A., Tolón, M.R., Fernández-Ruiz, J., Romero, J. and Martinez-Orgado, J. 2010. The neuroprotective effect of cannabidiol in an in vitro model of newborn hypoxic-ischemic brain damage in mice is mediated by CB2 and adenosine receptors. *Neurobiology of Disease*. **37**(2), pp.434–440.

Cendes, F. 2005. Mesial temporal lobe epilepsy syndrome: an updated overview. *Journal of Epilepsy and Clinical Neurophysiology*. **11**(3), pp.141–144.

Cestari, I., Anupama, A. and Stuart, K. 2018. Inositol polyphosphate multikinase regulation of *Trypanosoma brucei* life stage development. *Molecular Biology of the Cell*. **29**(9), pp.1137–1152.

Chakraborty, A., Koldobskiy, M.A., Bello, N.T., Maxwell, M., Potter, J.J., Juluri, K.R., Maag, D., Kim, S., Huang, A.S., Dailey, M.J., Saleh, M., Snowman, A.M., Moran, T.H., Mezey, E. and Snyder, S.H. 2010. Inositol pyrophosphates inhibit akt signaling, thereby regulating insulin sensitivity and weight gain. *Cell*. **143**(6), pp.897–910.

Chang, F.S., Wang, Y., Dmitriev, P., Gross, J., Galione, A. and Pears, C. 2020. A two-pore channel

protein required for regulating mTORC1 activity on starvation. *BMC Biology*. **18**(1), p.8.

Chang, P., Orabi, B., Deranieh, R.M., Dham, M., Hoeller, O., Shimshoni, J.A., Yagen, B., Bialer, M., Greenberg, M.L., Walker, M.C. and Williams, R.S.B. 2012. The antiepileptic drug valproic acid and other medium-chain fatty acids acutely reduce phosphoinositide levels independently of inositol in *Dictyostelium*. *DMM Disease Models and Mechanisms*. **5**(1), pp.115–124.

Chang, P., Terbach, N., Plant, N., Chen, P.E., Walker, M.C. and Williams, R.S.B. 2013. Seizure control by ketogenic diet-associated medium chain fatty acids. *Neuropharmacology*. **69**, pp.105–114.

Chang, P., Walker, M.C. and Williams, R.S.B. 2014. Seizure-induced reduction in PIP3 levels contributes to seizure-activity and is rescued by valproic acid. *Neurobiology of Disease*. **62**, pp.296–306.

Chang, P., Zuckermann, A.M.E., Williams, S., Close, A.J., Cano-Jaimez, M., McEvoy, J.P., Spencer, J., Walker, M.C. and Williams, R.S.B. 2015. Seizure control by derivatives of medium chain fatty acids associated with the ketogenic diet show novel branching-point structure for enhanced potency. *Journal of Pharmacology and Experimental Therapeutics*. **352**(1), pp.43–52.

Chen, D., Gao, M., Gao, F., Su, Q. and Wu, J. 2017. Brain cannabinoid receptor 2: expression, function and modulation. *Acta Pharmacologica Sinica*. **38**(3), pp.312–316.

Chisholm, R.L. and Firtel, R.A. 2004. Insights into morphogenesis from a simple developmental system. *Nature Reviews Molecular Cell Biology*. **5**(7), pp.531–541.

Chiu, P., Olsen, D.M., Borys, H.K., Karler, R. and Turkanis, S.A. 1979. The Influence of Cannabidiol and Δ9-Tetrahydrocannabinol on Cobalt Epilepsy in Rats. *Epilepsia*. **20**(4), pp.365–375.

Chiurchiù, V., van der Stelt, M., Centonze, D. and Maccarrone, M. 2018. The endocannabinoid system and its therapeutic exploitation in multiple sclerosis: Clues for other neuroinflammatory diseases. *Progress in Neurobiology*. **160**, pp.82–100.

Choi, S.R., Howell, O.W., Carassiti, D., Magliozzi, R., Gveric, D., Muraro, P.A., Nicholas, R., Roncaroli, F. and Reynolds, R. 2012. Meningeal inflammation plays a role in the pathology of primary progressive multiple sclerosis. *Brain : a journal of neurology*. **135**(Pt 10), pp.2925–37.

Chun, J. and Brinkmann, V. 2011. A mechanistically novel, first oral therapy for multiple sclerosis: the development of fingolimod (FTY720, Gilenya). *Discovery medicine*. **12**(64), pp.213–228.

Citraro, R., Russo, E., Scicchitano, F., van Rijn, C.M., Cosco, D., Avagliano, C., Russo, R., D'Agostino, G., Petrosino, S., Guida, F., Gatta, L., van Luijtelaar, G., Maione, S., Di Marzo, V., Calignano, A. and De Sarro, G. 2013. Antiepileptic action of N-palmitoylethanolamine through CB1 and PPAR-α receptor activation in a genetic model of absence epilepsy. *Neuropharmacology*. **69**, pp.115–126.

Citti, C., Braghiroli, D., Vandelli, M.A. and Cannazza, G. 2018. Pharmaceutical and biomedical analysis of cannabinoids: A critical review. *Journal of Pharmaceutical and Biomedical Analysis*. **147**, pp.565–579.

Cocorocchio, M., Baldwin, A.J., Stewart, B., Kim, L., Harwood, A.J., Thompson, C.R.L., Andrews, P.L.R. and Williams, R.S.B. 2018. Curcumin and derivatives function through protein phosphatase 2A and presenilin orthologues in *Dictyostelium discoideum*. *DMM Disease Models and Mechanisms*. **11**(1), p.dmm032375.

Cohen, J.A., Barkhof, F., Comi, G., Hartung, H.P., Khatri, B.O., Montalban, X., Pelletier, J., Capra, R., Gallo, P., Izquierdo, G., Tiel-Wilck, K., De Vera, A., Jin, J., Stites, T., Wu, S., Aradhye, S. and Kappos, L. 2010. Oral fingolimod or intramuscular interferon for relapsing multiple sclerosis. *New England Journal of Medicine*. **362**(5), pp.402–415.

Colasanti, B.K. 1990. A Comparison of the Ocular and Central Effects of Δ9-Tetrahydrocannabinol and Cannabigerol. *Journal of Ocular Pharmacology*. **6**(4), pp.259–269.

Coles, A.J., Twyman, C.L., Arnold, D.L., Cohen, J.A., Confavreux, C., Fox, E.J., Hartung, H.P., Havrdova, E., Selmaj, K.W., Weiner, H.L., Miller, T., Fisher, E., Sandbrink, R., Lake, S.L., Margolin, D.H., Oyuela, P., Panzara, M.A. and Compston, D.A.S. 2012. Alemtuzumab for patients with relapsing multiple sclerosis after disease-modifying therapy: A randomised controlled phase 3 trial. *The Lancet*. **380**(9856), pp.1829–1839.

Consroe, P., Benedito, M.A.C., Leite, J.R., Carlini, E.A. and Mechoulam, R. 1982. Effects of cannabidiol on behavioral seizures caused by convulsant drugs or current in mice. *European Journal of Pharmacology*. **83**(3–4), pp.293–298.

Consroe, P., Laguna, J., Allender, J., Snider, S., Stern, L., Sandyk, R., Kennedy, K. and Schram, K. 1991. Controlled clinical trial of cannabidiol in Huntington's disease. *Pharmacology, Biochemistry and Behavior*. **40**(3), pp.701–708.

Consultancy.eu 2019. Europe blooms to world's largest legal cannabis market. , p.1. Available from: https://www.consultancy.eu/news/2307/europe-to-become-the-worlds-largest-legal-cannabis-market.

Cook, M.J., O'Brien, T.J., Berkovic, S.F., Murphy, M., Morokoff, A., Fabinyi, G., D'Souza, W., Yerra,

R., Archer, J., Litewka, L., Hosking, S., Lightfoot, P., Ruedebusch, V., Sheffield, W.D., Snyder, D., Leyde, K. and Himes, D. 2013. Prediction of seizure likelihood with a long-term, implanted seizure advisory system in patients with drug-resistant epilepsy: A first-in-man study. *The Lancet Neurology*. **12**(6), pp.563–571.

Cossburn, M., Pace, A.A., Jones, J., Ali, R., Ingram, G., Baker, K., Hirst, C., Zajicek, J., Scolding, N., Boggild, M., Pickersgill, T., Ben-Shlomo, Y., Coles, A. and Robertson, N.P. 2011. Autoimmune disease after alemtuzumab treatment for multiple sclerosis in a multicenter cohort. *Neurology*. **77**(6), pp.573–579.

Cosson, P., Zulianello, L., Join-Lambert, O., Faurisson, F., Gebbie, L., Benghezal, M., Van Delden, C., Kocjancic Curty, L. and Köhler, T. 2002. *Pseudomonas aeruginosa* virulence analyzed in a Dictyostelium discoideum host system. *Journal of Bacteriology*. **184**(11), pp.3027–3033.

Costa, L.F., Balcells, M., Edelman, E.R., Nadler, L.M. and Cardoso, A.A. 2006. Proangiogenic stimulation of bone marrow endothelium engages mTOR and is inhibited by simultaneous blockade of mTOR and NF-kappaB. *Blood*. **107**(1), pp.285–92.

Crino, P.B. 2015. mTOR signaling in epilepsy: insights from malformations of cortical development. *Cold Spring Harbor perspectives in medicine*. **5**(4).

Cubillos-Rojas, M., Amair-Pinedo, F., Peiró-Jordán, R., Bartrons, R., Ventura, F. and Rosa, J.L. 2014. The E3 ubiquitin protein ligase HERC2 modulates the activity of tumor protein p53 by regulating its oligomerization. *Journal of Biological Chemistry*. **289**(21), pp.14782–14795.

Cubillos-Rojas, M., Schneider, T., Hadjebi, O., Pedrazza, L., de Oliveira, J.R., Langa, F., Guénet, J.L., Duran, J., de Anta, J.M., Alcántara, S., Ruiz, R., Pérez-Villegas, E.M., Aguilar-Montilla, F.J., Carrión, Á.M., Armengol, J.A., Baple, E., Crosby, A.H., Bartrons, R., Ventura, F. and Rosa, J.L. 2016. The HERC2 ubiquitin ligase is essential for embryonic development and regulates motor coordination. *Oncotarget*. **7**(35), pp.56083–56106.

Cunha, J.M., Carlini, E.A., Pereira, A.E., Ramos, O.L., Pimentel, C., Gagliardi, R., Sanvito, W.L., Lander, N. and Mechoulam, R. 1980. Chronic administration of cannabidiol to healthy volunteers and epileptic patients. *Pharmacology*. **21**(3), pp.175–185.

Dailey, M.J. and Kim, S. 2012. Inositol polyphosphate multikinase: An emerging player for the central action of AMP-activated protein kinase. *Biochemical and Biophysical Research Communications*. **421**(1), pp.1–3.

Davidson, A.J., King, J.S. and Insall, R.H. 2013. The use of streptavidin conjugates as immunoblot loading controls and mitochondrial markers for use with *Dictyostelium discoideum*.

BioTechniques. **55**(1), pp.39–41.

Davies, J.A. 1995. Mechanisms of action of antiepileptic drugs. *Seizure: European Journal of Epilepsy*. **4**(4), pp.267–271.

Degenhardt, F., Stehle, F. and Kayser, O. 2017. *Chapter 2 - The Biosynthesis of Cannabinoids* [Online]. Elsevier Inc. Available from: http://dx.doi.org/10.1016/B978-0-12-800756-3/00002-8.

Deiana, S., Watanabe, A., Yamasaki, Y., Amada, N., Arthur, M., Fleming, S., Woodcock, H., Dorward, P., Pigliacampo, B., Close, S., Platt, B. and Riedel, G. 2012. Plasma and brain pharmacokinetic profile of cannabidiol (CBD), cannabidivarine (CBDV), Δ 9-tetrahydrocannabivarin (THCV) and cannabigerol (CBG) in rats and mice following oral and intraperitoneal administration and CBD action on obsessive-compulsive behav. *Psychopharmacology*. **219**(3), pp.859–873.

Devinsky, O., Cilio, M.R., Cross, H., Fernandez-Ruiz, J., French, J., Hill, C., Katz, R., Di Marzo, V., Jutras-Aswad, D., Notcutt, W.G., Martinez-Orgado, J., Robson, P.J., Rohrback, B.G., Thiele, E., Whalley, B. and Friedman, D. 2014. Cannabidiol: Pharmacology and potential therapeutic role in epilepsy and other neuropsychiatric disorders. *Epilepsia*. **55**(6), pp.791–802.

Devinsky, O., Nabbout, R., Miller, I., Laux, L., Zolnowska, M., Wright, S. and Roberts, C. 2019. Long-term cannabidiol treatment in patients with Dravet syndrome: An open-label extension trial. *Epilepsia*. **60**(2), pp.294–302.

Devinsky, O., Patel, A.D., Cross, J.H., Villanueva, V., Wirrell, E.C., Privitera, M., Greenwood, S.M., Roberts, C., Checketts, D., VanLandingham, K.E. and Zuberi, S.M. 2018. Effect of cannabidiol on drop seizures in the lennox–gastaut syndrome. *New England Journal of Medicine*. **378**(20), pp.1888–1897.

Devinsky, O., Verducci, C., Thiele, E.A., Laux, L.C., Patel, A.D., Filloux, F., Szaflarski, J.P., Wilfong, A., Clark, G.D., Park, Y.D., Seltzer, L.E., Bebin, E.M., Flamini, R., Wechsler, R.T. and Friedman, D. 2018. Open-label use of highly purified CBD (Epidiolex®) in patients with CDKL5 deficiency disorder and Aicardi, Dup15q, and Doose syndromes. *Epilepsy and Behavior*. **86**, pp.131–137.

Dey, R., Pernin, P. and Bodennec, J. 2010. Endocannabinoids inhibit the growth of free-living amoebae. *Antimicrobial Agents and Chemotherapy*. **54**(7), pp.3065–3067.

Dhib-Jalbut, S. 2002. Mechanisms of action of interferons and glatiramer acetate in multiple sclerosis. *Neurology*. **58**(8 SUPPL. 5), pp.S3-9.

Dinauer, M., Steck, T. and Devreotes, P. 1980. Cyclic 3', 5'-AMP relay *Dictyostelium discoideum.* V. Adaptation of the cAMP signaling response during cAMP stimulation. *The Journal of Cell Biology*. **86**(2), pp.554–561.

Diógenes, M.J., Neves-Tomé, R., Fucile, S., Martinello, K., Scianni, M., Theofilas, P., Lopatář, J., Ribeiro, J.A., Maggi, L., Frenguelli, B.G., Limatola, C., Boison, D. and Sebastião, A.M. 2014. Homeostatic control of synaptic activity by endogenous adenosine is mediated by adenosine kinase. *Cerebral Cortex*. **24**(1), pp.67–80.

Drexhage, R.C., Hoogenboezem, T.H., Versnel, M.A., Berghout, A., Nolen, W.A. and Drexhage, H.A. 2011. The activation of monocyte and T cell networks in patients with bipolar disorder. *Brain, Behavior, and Immunity*. **25**(6), pp.1206–1213.

Duffy, S. and MacVicar, B.A. 1999. Modulation of neuronal excitability by astrocytes. *Advances in neurology*. **79**, pp.573–81.

During, M.J. and Spencer, D.D. 1992. Adenosine: A potential mediator of seizure arrest and postictal refractoriness. *Annals of Neurology*. **32**(5), pp.618–624.

Dzhala, V.I., Talos, D.M., Sdrulla, D.A., Brumback, A.C., Mathews, G.C., Benke, T.A., Delpire, E., Jensen, F.E. and Staley, K.J. 2005. NKCC1 transporter facilitates seizures in the developing brain. *Nature medicine*. **11**(11), pp.1205–13.

Eichinger, I., Pachebat, J.A., Glöckner, G., Rajandream, M.A., Sucgang, R., Berriman, M., Song, J., Olsen, R., Szafranski, K., Xu, Q., Tunggal, B., Kummerfeld, S., Madera, M., Konfortov, B.A., Rivero, F., Bankier, A.T., Lehmann, R., Hamlin, N., Davies, R., Gaudet, P., Fey, P., Pilcher, K., Chen, G., Saunders, D., Sodergren, E., Davis, P., Kerhornou, A., Nie, X., Hall, N., Anjard, C., Hemphill, L., Bason, N., Farbrother, P., Desany, B., Just, E., Morio, T., Rost, R., Churcher, C., Cooper, J., Haydock, S., Van Driessche, N., Cronin, A., Goodhead, I., Muzny, D., Mourier, T., Pain, A., Lu, M., Harper, D., Lindsay, R., Hauser, H., James, K., Quiles, M., Madan Babu, M., Saito, T., Buchrieser, C., Wardroper, A., Felder, M., Thangavelu, M., Johnson, D., Knights, A., Loulseged, H., Mungall, K., Oliver, K., Price, C., Quail, M.A., Urushihara, H., Hernandez, J., Rabbinowitsch, E., Steffen, D., Sanders, M., Ma, J., Kohara, Y., Sharp, S., Simmonds, M., Spiegler, S., Tivey, A., Sugano, S., White, B., Walker, D., Woodward, J., Winckler, T., Tanaka, Y., Shaulsky, G., Schleicher, M., Weinstock, G., Rosenthal, A., Cox, E.C., Chisholm, R.L., Gibbs, R., Loomis, W.F., Platzer, M., Kay, R.R., Williams, J., Dear, P.H., Noegel, A.A., Barrell, B. and Kuspa, A. 2005. The genome of the social amoeba *Dictyostelium discoideum*. *Nature*. **435**(7038), pp.43–57.

Elliott, D.M., Singh, N., Nagarkatti, M. and Nagarkatti, P.S. 2018. Cannabidiol attenuates experimental autoimmune encephalomyelitis model of multiple sclerosis through

induction of myeloid-derived suppressor cells. *Frontiers in Immunology*. **9**(AUG).

Etges, T., Karolia, K., Grint, T., Taylor, A., Lauder, H., Daka, B. and Wright, S. 2016. An observational postmarketing safety registry of patients in the UK, Germany, and Switzerland who have been prescribed Sativex® (THC: CBD, nabiximols) oromucosal spray. *Therapeutics and Clinical Risk Management*. **12**, pp.1667–1675.

Faix, J., Kreppel, L., Shaulsky, G., Schleicher, M. and Kimmel, A.R. 2004. A rapid and efficient method to generate multiple gene disruptions in *Dictyostelium discoideum* using a single selectable marker and the Cre-loxP system. *Nucleic acids research*. **32**(19), p.e143.

Farinholt, T., Dinh, C. and Kuspa, A. 2019. Microbiome management in the social amoeba *Dictyostelium discoideum* compared to humans. *International Journal of Developmental Biology*. **63**(9–10), pp.447–450.

Fawley, J.A., Hofmann, M.E. and Andresen, M.C. 2014. Cannabinoid 1 and Transient Receptor Potential Vanilloid 1 Receptors Discretely Modulate Evoked Glutamate Separately from Spontaneous Glutamate Transmission. *Journal of Neuroscience*. **34**(24), pp.8324–8332.

Fedele, D.E., Li, T., Lan, J.Q., Fredholm, B.B. and Boison, D. 2006. Adenosine A1 receptors are crucial in keeping an epileptic focus localized. *Experimental Neurology*. **200**(1), pp.184–190.

Ferrè, L., Nuara, A., Pavan, G., Radaelli, M., Moiola, L., Rodegher, M., Colombo, B., Keller Sarmiento, I.J., Martinelli, V., Leocani, L., Martinelli Boneschi, F., Comi, G. and Esposito, F. 2016. Efficacy and safety of nabiximols (Sativex®) on multiple sclerosis spasticity in a real-life Italian monocentric study. *Neurological Sciences*. **37**(2), pp.235–242.

Fišar, Z. 2009. Phytocannabinoids and endocannabinoids. *Current Drug Abuse Reviews*. **2**(1), pp.51–75.

Fisher, R.S., Acevedo, C., Arzimanoglou, A., Bogacz, A., Cross, J.H., Elger, C.E., Engel, J., Forsgren, L., French, J.A., Glynn, M., Hesdorffer, D.C., Lee, B.I., Mathern, G.W., Moshé, S.L., Perucca, E., Scheffer, I.E., Tomson, T., Watanabe, M. and Wiebe, S. 2014. ILAE Official Report: A practical clinical definition of epilepsy. *Epilepsia*. **55**(4), pp.475–482.

Flachenecker, P., Henze, T. and Zettl, U.K. 2014. Nabiximols (THC/CBD Oromucosal Spray, Sativex®) in clinical practice - results of a multicenter, non-interventional study (MOVE 2) in patients with multiple sclerosis spasticity. *European Neurology*. **71**(5–6), pp.271–279.

Fox, E.J., Vasquez, A., Grainger, W., Ma, T.S., Von Hehn, C., Walsh, J., Li, J. and Zambrano, J. 2016. Gastrointestinal tolerability of delayed-release dimethyl fumarate in a multicenter, open-label study of patients with relapsing forms of multiple sclerosis (MANAGE). *International*

Journal of MS Care. **18**(1), pp.9–18.

Franz, D.N., Agricola, K.D., Tudor, C.A. and Krueger, D.A. 2013. Everolimus for tumor recurrence after surgical resection for subependymal giant cell astrocytoma associated with tuberous sclerosis complex. *Journal of child neurology*. **28**(5), pp.602–607.

Frederick, J.P., Mattiske, D., Wofford, J.A., Megosh, L.C., Drake, L.Y., Chiou, S.T., Hogan, B.L.M. and York, J.D. 2005. An essential role for an inositol polyphosphate multikinase, Ipk2, in mouse embryogenesis and second messenger production. *Proceedings of the National Academy of Sciences of the United States of America*. **102**(24), pp.8454–8459.

Freeman, T.P., Hindocha, C., Green, S.F. and Bloomfield, M.A.P. 2019. Medicinal use of cannabis based products and cannabinoids. *BMJ (Online)*. **365**, p.l1141.

Fukuda, M., Suzuki, Y., Hino, H., Kuzume, K., Morimoto, T. and Ishii, E. 2010. Adenosine A1 receptor blockage mediates theophylline-associated seizures. *Epilepsia*. **51**(3), pp.483–487.

Fukuzawa, M., Zhukovskaya, N. V., Yamada, Y., Araki, T. and Williams, J.G. 2006. Regulation of *Dictyostelium* prestalk-specific gene expression by a SHAQKY family MYB transcription factor. *Development*. **133**(9), pp.1715–1724.

Gafson, A., Craner, M.J. and Matthews, P.M. 2017. Personalised medicine for multiple sclerosis care. *Multiple Sclerosis*. **23**(3), pp.362–369.

Galiazzo, G., Giancola, F., Stanzani, A., Fracassi, F., Bernardini, C., Forni, M., Pietra, M. and Chiocchetti, R. 2018. Localization of cannabinoid receptors CB1, CB2, GPR55, and PPARα in the canine gastrointestinal tract. *Histochemistry and Cell Biology*. **150**(2), pp.187–205.

GAMES and Transatlantic Multiple Sclerosis Genetics Cooperative 2003. A meta-analysis of whole genome linkage screens in multiple sclerosis. *Journal of neuroimmunology*. **143**(1–2), pp.39–46.

Gao, S., Liu, W., Zhuo, X., Wang, L., Wang, G., Sun, T., Zhao, Z., Liu, J., Tian, Y., Zhou, J., Yuan, Z. and Wu, Y. 2015. The activation of mTOR is required for monocyte pro-inflammatory response in patients with coronary artery disease. *Clinical Science*. **128**(8), pp.517–526.

Giacoppo, S., Galuppo, M., Pollastro, F., Grassi, G., Bramanti, P. and Mazzon, E. 2015. A new formulation of cannabidiol in cream shows therapeutic effects in a mouse model of experimental autoimmune encephalomyelitis. *DARU, Journal of Pharmaceutical Sciences*. **23**(1), p.48.

Giacoppo, S., Pollastro, F., Grassi, G., Bramanti, P. and Mazzon, E. 2017. Target regulation of

PI3K/Akt/mTOR pathway by cannabidiol in treatment of experimental multiple sclerosis. *Fitoterapia*. **116**, pp.77–84.

Goebbels, S., Wieser, G.L., Pieper, A., Spitzer, S., Weege, B., Yan, K., Edgar, J.M., Yagensky, O., Wichert, S.P., Agarwal, A., Karram, K., Renier, N., Tessier-Lavigne, M., Rossner, M.J., Káradóttir, R.T. and Nave, K.A. 2017. A neuronal PI(3,4,5)P 3 -dependent program of oligodendrocyte precursor recruitment and myelination. *Nature Neuroscience*. **20**(1), pp.10–15.

Gordon, E. and Devinsky, O. 2001. Alcohol and marijuana: Effects on epilepsy and use by patients with epilepsy. *Epilepsia*. **42**(10), pp.1266–1272.

Grassi, G., Giacoppo, S., Rajan, T., Galuppo, M., Pollastro, F., Grassi, G., Bramanti, P. and Mazzon, E. 2016. Purified Cannabidiol, the main non-psychotropic component of Cannabis sativa, alone, counteracts neuronal apoptosis in experimental multiple sclerosis. *European review for medical and pharmacological sciences*. **19**, pp.4906–4919.

Gray, R.A., Stott, C.G., Jones, N.A., Di Marzo, V. and Whalley, B.J. 2019. Anticonvulsive Properties of Cannabidiol in a Model of Generalized Seizure Are Transient Receptor Potential Vanilloid 1 Dependent. *Cannabis and Cannabinoid Research*., can.2019.0028.

Greene, S., Watanabe, K., Braatz-Trulson, J. and Lou, L. 1995. Inhibition of dihydroorotate dehydrogenase by the immunosuppressive agent leflunomide. *Biochemical Pharmacology*. **50**(6), pp.861–867.

Grenz, A., Bauerle, J.D., Dalton, J.H., Ridyard, D., Badulak, A., Tak, E., McNamee, E.N., Clambey, E., Moldovan, R., Reyes, G., Klawitter, J., Ambler, K., Magee, K., Christians, U., Brodsky, K.S., Ravid, K., Choi, D.S., Wen, J., Lukashev, D., Blackburn, M.R., Osswald, H., Coe, I.R., Nürnberg, B., Haase, V.H., Xia, Y., Sitkovsky, M. and Eltzschig, H.K. 2012. Equilibrative nucleoside transporter 1 (ENT1) regulates postischemic blood flow during acute kidney injury in mice. *Journal of Clinical Investigation*. **122**(2), pp.693–710.

Gruenheit, N., Baldwin, A., Stewart, B., Jaques, S., Keller, T., Parkinson, K., Chisholm, R., Harwood, A. and Thompson, C.R.L. 2019. REMI-seq: Development of methods and resources for functional genomics in *Dictyostelium*. *bioRxiv*., p.582072.

Gu, B., Zhu, M., Glass, M.R., Rougié, M., Nikolova, V.D., Moy, S.S., Carney, P.R. and Philpot, B.D. 2019. Cannabidiol attenuates seizures and EEG abnormalities in Angelman syndrome model mice. *Journal of Clinical Investigation*. **129**(12), pp.5462–5467.

Gugliandolo, A., Pollastro, F., Grassi, G., Bramanti, P. and Mazzon, E. 2018. In vitro model of neuroinflammation: Efficacy of cannabigerol, a non-psychoactive cannabinoid.

International Journal of Molecular Sciences. **19**(7), p.1992.

Gunn, R.M. and Hailes, H.C. 2008. Insights into the PI3-K-PKB-mTOR signalling pathway from small molecules. *Journal of Chemical Biology*. **1**(1–4), pp.49–62.

GVR 2020. Legal Marijuana Market Size Worth $73.6 Billion By 2027. Available from: https://www.grandviewresearch.com/press-release/global-legal-marijuana-market.

Haarmann, A., Nowak, E., Deiß, A., van der Pol, S., Monoranu, C.M., Kooij, G., Müller, N., van der Valk, P., Stoll, G., de Vries, H.E., Berberich-Siebelt, F. and Buttmann, M. 2015. Soluble VCAM-1 impairs human brain endothelial barrier integrity via integrin α-4-transduced outside-in signalling. *Acta Neuropathologica*. **129**(5), pp.639–652.

Van Haastert, P.J.M., Keizer-Gunnink, I. and Kortholt, A. 2007. Essential role of PI3-kinase and phospholipase A2 in *Dictyostelium discoideum* chemotaxis. *Journal of Cell Biology*. **177**(5), pp.809–816.

Halford, J., Marsh, E., Mazurkiewicz-Beldzinska, M., Gunning, B., Checketts, D., Roberts, C. and Thiele, E. 2018. Long-term Safety and Efficacy of Cannabidiol (CBD) in Patients with Lennox-Gastaut Syndrome (LGS): Results from Open-label Extension Trial (GWPCARE5) (P1.264). *Neurology*. **90**(15 Supplement), P1.264.

Hamasaki, T., Otsubo, H., Uchikawa, H., Yamada, K. and Kuratsu, J. 2014. Olfactory auras caused by a very focal isolated epileptic network in the amygdala. *Epilepsy & Behavior Case Reports*. **2**, pp.142–144.

Haney, M., Malcolm, R.J., Babalonis, S., Nuzzo, P.A., Cooper, Z.D., Bedi, G., Gray, K.M., McRae-Clark, A., Lofwall, M.R., Sparenborg, S. and Walsh, S.L. 2016. Oral Cannabidiol does not Alter the Subjective, Reinforcing or Cardiovascular Effects of Smoked Cannabis. *Neuropsychopharmacology*. **41**(8), pp.1974–1982.

Harlalka, G. V., Baple, E.L., Cross, H., Kühnle, S., Cubillos-Rojas, M., Matentzoglu, K., Patton, M.A., Wagner, K., Coblentz, R., Ford, D.L., Mackay, D.J.G., Chioza, B.A., Scheffner, M., Rosa, J.L. and Crosby, A.H. 2013. Mutation of HERC2 causes developmental delay with angelman-like features. *Journal of Medical Genetics*. **50**(2), pp.65–73.

Hartung, H.P., Gonsette, R., König, N., Kwiecinski, H., Guseo, A., Morrissey, S.P., Krapf, H., Zwingers, T., Albrecht, H., Basedow-Rajwich, B., Hofmeister, R., Pöllmann, W., Starck, M., Beer, K., Hopf, H.C., Köhler, J., Lensch, E., Besinger, U., Vom Dahl, M., Hendrich, A., Löser, M., Braun, M., Greiling, H.W., Greve, H., Kohl, D., Merkel, M., Conrad, B., Konstanzer, A., Kornhuber, M., Dierkes, W., Munz, T., Zenker, O., Flachenecker, P.M., Weilbach, F.X., Haas, J., Hauser, U., Kömpf, D., Moser, A., Scholz, J., Weigle, L.J., Branas, C., Sadzot, B., Cras, P.,

Dams, L., Vande Gaer, L., Demonty, L., Lissoir, F., Guillaume, D., Seeldrayers, P., Peeters, B., Hosszu, Z., Jofejü, E., Janiec, K., Lubos, L., Waigt, A., Kaminska, A.M. and Zakrzewska-Pniewska, B. 2002. Mitoxantrone in progressive multiple sclerosis: A placebo-controlled, double-blind, randomised, multicentre trial. *Lancet*. **360**(9350), pp.2018–2025.

Hasheminia, S.J., Zarkesh-Esfahani, S.H., Tolouei, S., Shaygannejad, V., Shirzad, H. and Chaleshtory, M.H. 2014. Toll like receptor 2 and 4 expression in peripheral blood mononuclear cells of multiple sclerosis patients. *Iranian Journal of Immunology*. **11**(2), pp.74–83.

Hauser, S.L. and Oksenberg, J.R. 2006. The Neurobiology of Multiple Sclerosis: Genes, Inflammation, and Neurodegeneration. *Neuron*. **52**(1), pp.61–76.

Hayden, M.S. and Ghosh, S. 2012. NF- B, the first quarter-century: remarkable progress and outstanding questions. *Genes & Development*. **26**(3), pp.203–234.

Hejazi, N., Zhou, C., Oz, M., Sun, H., Jiang, H.Y. and Zhang, L. 2006. Δ9-Tetrahydrocannabinol and endogenous cannabinoid anandamide directly potentiate the function of glycine receptors. *Molecular Pharmacology*. **69**(3), pp.991–997.

Helen E. Scharfman, P.D. 2007. The Neurobiology of Epilepsy. *Current Neurology and Neuroscience Reports*., pp.348–354.

Herkenham, M., Lynn, A.B., Johnson, M.R., Melvin, L.S., De Costa, B.R. and Rice, K.C. 1991. Characterization and localization of cannabinoid receptors in rat brain: A quantitative in vitro autoradiographic study. *Journal of Neuroscience*. **11**(2), pp.563–583.

Hermes, M., Osswald, H. and Kloor, D. 2007. Role of S-adenosylhomocysteine hydrolase in adenosine-induced apoptosis in HepG2 cells. *Experimental Cell Research*. **313**(2), pp.264–283.

Herrero-Sánchez, M.C., Rodríguez-Serrano, C., Almeida, J., San Segundo, L., Inogés, S., Santos-Briz, Á., García-Briñón, J., Corchete, L.A., San Miguel, J.F., Del Cañizo, C. and Blanco, B. 2016. Targeting of PI3K/AKT/mTOR pathway to inhibit T cell activation and prevent graft-versus-host disease development. *Journal of Hematology and Oncology*. **9**(1), p.113.

Hill, A.J., Jones, N.A., Smith, I., Hill, C.L., Williams, C.M., Stephens, G.J. and Whalley, B.J. 2014. Voltage-gated sodium (NaV) channel blockade by plant cannabinoids does not confer anticonvulsant effects per se. *Neuroscience Letters*. **566**, pp.269–274.

Hilliard, A., Stott, C., Wright, S., Guy, G., Pryce, G., Al-Izki, S., Bolton, C. and Giovannoni, G. 2012. Evaluation of the Effects of Sativex® (THC BDS: CBD BDS) on Inhibition of Spasticity in a Chronic Relapsing Experimental Allergic Autoimmune Encephalomyelitis: A Model of

Multiple Sclerosis. *ISRN Neurology*. **2012**, pp.1–7.

Holland, C.M., Charil, A., Csapo, I., Liptak, Z., Ichise, M., Khoury, S.J., Bakshi, R., Weiner, H.L. and Guttmann, C.R.G. 2012. The relationship between normal cerebral perfusion patterns and white matter lesion distribution in 1,249 patients with multiple sclerosis. *Journal of neuroimaging : official journal of the American Society of Neuroimaging*. **22**(2), pp.129–36.

Holm, L.E., Lundell, G. and Walinder, G. 1980. Incidence of malignant thyroid tumors in humans after exposure to diagnostic doses of iodine-131. I. Retrospective cohort study. *Journal of the National Cancer Institute*. **64**(5), pp.1055–9.

Hövelmann, S., Beckers, T.L. and Schmidt, M. 2004. Molecular alterations in apoptotic pathways after PKB/Akt-mediated chemoresistance in NCI H460 cells. *British Journal of Cancer*. **90**(12), pp.2370–2377.

Howell, O.W., Reeves, C.A., Nicholas, R., Carassiti, D., Radotra, B., Gentleman, S.M., Serafini, B., Aloisi, F., Roncaroli, F., Magliozzi, R. and Reynolds, R. 2011. Meningeal inflammation is widespread and linked to cortical pathology in multiple sclerosis. *Brain : a journal of neurology*. **134**(Pt 9), pp.2755–71.

Howlett, A.C., Barth, F., Bonner, T.I., Cabral, G., Casellas, P., Devane, W.A., Felder, C.C., Herkenham, M., Mackie, K., Martin, B.R., Mechoulam, R. and Pertwee, R.G. 2002. International Union of Pharmacology. XXVII. Classification of cannabinoid receptors. *Pharmacological Reviews*. **54**(2), pp.161–202.

Hoy, S.M. 2015. Peginterferon beta-1a: A review of its use in patients with relapsing-remitting multiple sclerosis. *CNS Drugs*. **29**(2), pp.171–179.

Huang, J. and Manning, B.D. 2009. A complex interplay between Akt, TSC2 and the two mTOR complexes. *Biochemical Society Transactions*. **37**(1), pp.217–222.

Huber, A., Padrun, V., Déglon, N., Aebischer, P., Möhler, H. and Boison, D. 2001. Grafts of adenosine-releasing cells suppress seizures in kindling epilepsy. *Proceedings of the National Academy of Sciences of the United States of America*. **98**(13), pp.7611–7616.

Ikeda, K.M. and Mirsattari, S.M. 2017. Evolution of epilepsy in hemimegalencephaly from infancy to adulthood: Case report and review of the literature. *Epilepsy & Behavior Case Reports*. **7**, pp.45–48.

Insall, R.H. 2005. The Dictyostelium genome: The private life of a social model revealed? *Genome Biology*. **6**(6), p.222.

Ishimaru, Y. and Matsunami, H. 2009. Transient receptor potential (TRP) channels and taste

sensation. *Journal of Dental Research*. **88**(3), pp.212–218.

Izuchi, S., Terachi, T., Sakamoto, M., Mikami, T. and Sugita, M. 1990. Structure and expression of tomato mitochondrial genes coding for tRNACys (GCA), tRNAAsn (GUU) and tRNATyr (GUA): A native tRNACys gene is present in dicot plants but absent in monocot plants. *Current Genetics*. **18**(3), pp.239–243.

Jackson, S.G., Zhang, Y., Haslam, R.J. and Junop, M.S. 2007. Structural analysis of the carboxy terminal PH domain of pleckstrin bound to D-myo-inositol 1,2,3,5,6-pentakisphosphate. *BMC Structural Biology*. **7**(1), p.80.

Jaenisch, R. and Bird, A. 2003. Epigenetic regulation of gene expression: How the genome integrates intrinsic and environmental signals. *Nature Genetics*. **33**(3S), pp.245–254.

Jaiswal, P., Majithia, A.R., Rosel, D., Liao, X.-H., Khurana, T. and Kimmel, A.R. 2019. Integrated actions of mTOR complexes 1 and 2 for growth and development of *Dictyostelium*. *The International Journal of Developmental Biology*. **63**(8-9–10), pp.521–527.

Jimmerson, L.C., Bushman, L.R., Ray, M.L., Anderson, P.L. and Kiser, J.J. 2017. A LC-MS/MS Method for Quantifying Adenosine, Guanosine and Inosine Nucleotides in Human Cells. *Pharmaceutical Research*. **34**(1), pp.73–83.

Johnston, D. and Brown, T.H. 1984. The synaptic nature of the paroxysmal depolarizing shift in hippocampal neurons. *Annals of Neurology*. **16**(S1), pp.S65–S71.

Jones, N.A., Hill, A.J., Smith, I., Bevan, S.A., Williams, C.M., Whalley, B.J. and Stephens, G.J. 2010. Cannabidiol displays antiepileptiform and antiseizure properties in vitro and in vivo. *Journal of Pharmacology and Experimental Therapeutics*. **332**(2), pp.569–577.

Kälviäinen, R., Salmenperä, T., Partanen, K., Vainio, P., Riekkinen, P. and Pitkänen, A. 1998. Recurrent seizures may cause hippocampal damage in temporal lobe epilepsy. *Neurology*. **50**(5), pp.1377–82.

Kao, Y.H., Lin, M.S., Chen, C.M., Wu, Y.R., Chen, H.M., Lai, H.L., Chern, Y. and Lin, C.J. 2017. Targeting ENT1 and adenosine tone for the treatment of Huntington's disease. *Human Molecular Genetics*. **26**(3), pp.467–478.

Kaplan, J.S., Stella, N., Catterall, W.A. and Westenbroek, R.E. 2017. Cannabidiol attenuates seizures and social deficits in a mouse model of Dravet syndrome. *Proceedings of the National Academy of Sciences of the United States of America*. **114**(42), pp.11229–11234.

Katoh, M., Curk, T., Xu, Q., Zupan, B., Kuspa, A. and Shaulsky, G. 2006. Developmentally regulated DNA methylation in *Dictyostelium discoideum*. *Eukaryotic Cell*. **5**(1), pp.18–25.

Kazyken, D., Magnuson, B., Bodur, C., Acosta-Jaquez, H.A., Zhang, D., Tong, X., Barnes, T.M., Steinl, G.K., Patterson, N.E., Altheim, C.H., Sharma, N., Inoki, K., Cartee, G.D., Bridges, D., Yin, L., Riddle, S.M. and Fingar, D.C. 2019. AMPK directly activates mTORC2 to promote cell survival during acute energetic stress. *Science Signaling*. **12**(585), p.eaav3249.

Keating, G.M. 2017. Delta-9-Tetrahydrocannabinol/Cannabidiol Oromucosal Spray (Sativex®): A Review in Multiple Sclerosis-Related Spasticity. *Drugs*. **77**(5), pp.563–574.

Keim, M., Williams, R.S.B. and Harwood, A.J. 2004. An inverse PCR technique to rapidly isolate the flanking DNA of *Dictyostelium* insertion mutants. *Applied Biochemistry and Biotechnology - Part B Molecular Biotechnology*. **26**(3), pp.221–224.

Kelly, E., Sharma, D., Wilkinson, C.J. and Williams, R.S.B. 2018. Diacylglycerol kinase (DGKA) regulates the effect of the epilepsy and bipolar disorder treatment valproic acid in *Dictyostelium discoideum*. *DMM Disease Models and Mechanisms*. **11**(9), p.dmm035600.

Kielkowska, A., Niewczas, I., Anderson, K.E., Durrant, T.N., Clark, J., Stephens, L.R. and Hawkins, P.T. 2014. A new approach to measuring phosphoinositides in cells by mass spectrometry. *Advances in Biological Regulation*. **54**, pp.131–141.

Kim, D.H., Sarbassov, D.D., Ali, S.M., King, J.E., Latek, R.R., Erdjument-Bromage, H., Tempst, P. and Sabatini, D.M. 2002. mTOR interacts with raptor to form a nutrient-sensitive complex that signals to the cell growth machinery. *Cell*. **110**(2), pp.163–175.

Kim, E., Ahn, H., Kim, M.G., Lee, H. and Kim, S. 2017. The expanding significance of inositol polyphosphate multikinase as a signaling hub. *Molecules and Cells*. **40**(5), pp.315–321.

Kim, E., Beon, J., Lee, S., Park, J. and Kim, S. 2016. IPMK: A versatile regulator of nuclear signaling events. *Advances in Biological Regulation*. **61**, pp.25–32.

Kim, E., Beon, J., Lee, S., Park, S.J., Ahn, H., Kim, M.G., Park, J.E., Kim, W., Yuk, J.M., Kang, S.J., Lee, S.H., Jo, E.K., Seong, R.H. and Kim, S. 2017. Inositol polyphosphate multikinase promotes Toll-like receptor–induced inflammation by stabilizing TRAF6. *Science Advances*. **3**(4), p.e1602296.

Kim, E., Tyagi, R., Lee, J.Y., Park, J., Kim, Y.R., Beon, J., Chen, P.Y., Cha, J.Y., Snyder, S.H. and Kim, S. 2013. Inositol polyphosphate multikinase is a coactivator for serum response factor-dependent induction of immediate early genes. *Proceedings of the National Academy of Sciences of the United States of America*. **110**(49), pp.19938–19943.

Kim, S., Kim, S.F., Maag, D., Maxwell, M.J., Resnick, A.C., Juluri, K.R., Chakraborty, A., Koldobskiy, M.A., Cha, S.H., Barrow, R., Snowman, A.M. and Snyder, S.H. 2011. Amino acid signaling to mTOR mediated by inositol polyphosphate multikinase. *Cell Metabolism*. **13**(2), pp.215–

221.

King, J.S., Teo, R., Ryves, J., Reddy, J. V., Peters, O., Orabi, B., Hoeller, O., Williams, R.S.B. and Harwood, A.J. 2009. The mood stabiliser lithium suppresses PIP3 signalling in *Dictyostelium* and human cells. *DMM Disease Models and Mechanisms*. **2**(5–6), pp.306–312.

Klein, B.D., Jacobson, C.A., Metcalf, C.S., Smith, M.D., Wilcox, K.S., Hampson, A.J. and Kehne, J.H. 2017. Evaluation of Cannabidiol in Animal Seizure Models by the Epilepsy Therapy Screening Program (ETSP). *Neurochemical Research*. **42**(7), pp.1939–1948.

Kleinschmidt-DeMasters, B.K. and Tyler, K.L. 2005. Progressive multifocal leukoencephalopathy complicating treatment with natalizumab and interferon beta-1a for multiple sclerosis. *New England Journal of Medicine*. **353**(4), pp.369–374.

Koehler, J., Feneberg, W., Meier, M. and Pöllmann, W. 2014. Clinical experience with THC:CBD oromucosal spray in patients with multiple sclerosis-related spasticity. *International Journal of Neuroscience*. **124**(9), pp.652–656.

Kong, W., Li, H., Tuma, R.F. and Ganea, D. 2014. Selective CB2 receptor activation ameliorates EAE by reducing Th17 differentiation and immune cell accumulation in the CNS. *Cellular Immunology*. **287**(1), pp.1–17.

Korematsu, S., Miyahara, H., Nagakura, T., Suenobu, S. and Izumi, T. 2008. Theophylline-associated seizures and their clinical characterizations. *Pediatrics international : official journal of the Japan Pediatric Society*. **50**(1), pp.95–8.

Kornek, B. 2000. Multiple Sclerosis and Chronic Autoimmune Encephalomyelitis. *The American Journal of Pathology*. **157**(1), pp.267–276.

Kornek, B., Storch, M.K., Weissert, R., Wallstroem, E., Stefferl, A., Olsson, T., Linington, C., Schmidbauer, M. and Lassmann, H. 2000. Multiple sclerosis and chronic autoimmune encephalomyelitis: A comparative quantitative study of axonal injury in active, inactive, and remyelinated lesions. *American Journal of Pathology*. **157**(1), pp.267–276.

Kourtis, N. and Tavernarakis, N. 2009. Autophagy and cell death in model organisms. *Cell Death and Differentiation*. **16**(1), pp.21–30.

Kowalko, J.E., Ma, L. and Jeffery, W.R. 2016. Genome Editing in *Astyanax mexicanus* Using Transcription Activator-like Effector Nucleases (TALENs). *Journal of Visualized Experiments*. (112).

Kozela, E., Lev, N., Kaushansky, N., Eilam, R., Rimmerman, N., Levy, R., Ben-Nun, A., Juknat, A. and Vogel, Z. 2011. Cannabidiol inhibits pathogenic T cells, decreases spinal microglial

activation and ameliorates multiple sclerosis-like disease in C57BL/6 mice. *British Journal of Pharmacology*. **163**(7), pp.1507–1519.

Kredich, N.M. and Martin, D.W. 1977. Role of S-adenosylhomocysteine in adenosine-mediated toxicity in cultured mouse T lymphoma cells. *Cell*. **12**(4), pp.931–938.

Kuhlmann, M., Borisova, B.E., Kaller, M., Larsson, P., Stach, D., Na, J., Eichinger, L., Lyko, F., Ambros, V., Söderbom, F., Hammann, C. and Nellen, W. 2005. Silencing of retrotransposons in *Dictyostelium* by DNA methylation and RNAi. *Nucleic Acids Research*. **33**(19), pp.6405–6417.

Kullmann, D.M. and Semyanov, A. 2002. Glutamatergic Modulation of GABAergic Signaling Among Hippocampal Interneurons: Novel Mechanisms Regulating Hippocampal Excitability. *Epilepsia*. **43**, pp.174–178.

Kuspa, A. and Loomis, W.F. 1992. Tagging developmental genes in *Dictyostelium* by restriction enzyme- mediated integration of plasmid DNA. *Proceedings of the National Academy of Sciences of the United States of America*. **89**(18), pp.8803–8807.

Kutzelnigg, A., Lucchinetti, C.F., Stadelmann, C., Brück, W., Rauschka, H., Bergmann, M., Schmidbauer, M., Parisi, J.E. and Lassmann, H. 2005. Cortical demyelination and diffuse white matter injury in multiple sclerosis. *Brain : a journal of neurology*. **128**(Pt 11), pp.2705–12.

Lado, F.A. and Moshé, S.L. 2008. How do seizures stop? *Epilepsia*. **49**(10), pp.1651–1664.

Laplante, M. and Sabatini, D.M. 2009. mTOR signaling at a glance. *Journal of Cell Science*. **122**(20), pp.3589–3594.

Laprairie, R.B., Bagher, A.M., Kelly, M.E.M. and Denovan-Wright, E.M. 2015. Cannabidiol is a negative allosteric modulator of the cannabinoid CB1 receptor. *British Journal of Pharmacology*. **172**(20), pp.4790–4805.

Larsson, O., Barker, C.J., Sjöholm, Å., Carlqvist, H., Michell, R.H., Bertorello, A., Nilsson, T., Honkanen, R.E., Mayr, G.W., Zwiller, J. and Berggren, P.O. 1997. Inhibition of phosphatases and increased Ca2+ channel activity by inositol hexakisphosphate. *Science*. **278**(5337), pp.471–474.

LaSarge, C.L. and Danzer, S.C. 2014. Mechanisms regulating neuronal excitability and seizure development following mTOR pathway hyperactivation. *Frontiers in Molecular Neuroscience*. **7**.

Lauckner, J.E., Jensen, J.B., Chen, H.Y., Lu, H.C., Hille, B. and Mackie, K. 2008. GPR55 is a

cannabinoid receptor that increases intracellular calcium and inhibits M current. *Proceedings of the National Academy of Sciences of the United States of America*. **105**(7), pp.2699–2704.

Lee, C.C., Chang, C.P., Lin, C.J., Lai, H.L., Kao, Y.H., Cheng, S.J., Chen, H.M., Liao, Y.P., Faivre, E., Buée, L., Blum, D., Fang, J.M. and Chern, Y. 2018. Adenosine Augmentation Evoked by an ENT1 Inhibitor Improves Memory Impairment and Neuronal Plasticity in the APP/PS1 Mouse Model of Alzheimer's Disease. *Molecular Neurobiology*. **55**(12), pp.8936–8952.

Leppik, I.E. 2004. Zonisamide: Chemistry, mechanism of action, and pharmacokinetics. *Seizure*. **13**(SUPPL. 1), pp.S5–S9.

Leussink, V.I., Husseini, L., Warnke, C., Hartung, H.P., Broussalis, E. and Kieseier, B.C. 2012. Symptomatic therapy in multiple sclerosis: The role of cannabinoids in treating spasticity. *Therapeutic Advances in Neurological Disorders*. **5**(5), pp.255–266.

Levenson, J.M., Roth, T.L., Lubin, F.D., Miller, C.A., Huang, I.-C., Desai, P., Malone, L.M. and Sweatt, J.D. 2006. Evidence That DNA (Cytosine-5) Methyltransferase Regulates Synaptic Plasticity in the Hippocampus. *Journal of Biological Chemistry*. **281**(23), pp.15763–15773.

Levin, R., Almeida, V., Fiel Peres, F., Bendlin Calzavara, M., Derci da Silva, N., Akimi Suiama, M., Tamie Niigaki, S., Waldo Zuardi, A., Eduardo Cecilio Hallak, J., Alexandre Crippa, J. and Costhek Abilio, V. 2012. Antipsychotic Profile of Cannabidiol and Rimonabant in an Animal Model of Emotional Context Processing in Schizophrenia. *Current Pharmaceutical Design*. **18**(32), pp.4960–4965.

Levine, H. and Reynolds, W. 1991. Streaming instability of aggregating slime mold amoebae. *Physical Review Letters*. **66**(18), pp.2400–2403.

Leweke, F.M., Piomelli, D., Pahlisch, F., Muhl, D., Gerth, C.W., Hoyer, C., Klosterkötter, J., Hellmich, M. and Koethe, D. 2012. Cannabidiol enhances anandamide signaling and alleviates psychotic symptoms of schizophrenia. *Translational Psychiatry*. **2**(3), p.e94.

Li, H.L. 1973. An archaeological and historical account of cannabis in China. *Economic Botany*. **28**(4), pp.437–448.

Li, T., Lytle, N., Lan, J.Q., Sandau, U.S. and Boison, D. 2012. Local disruption of glial adenosine homeostasis in mice associates with focal electrographic seizures: A first step in epileptogenesis? *Glia*. **60**(1), pp.83–95.

Li, T., Ren, G., Lusardi, T., Wilz, A., Lan, J.Q., Iwasato, T., Itohara, S., Simon, R.P. and Boison, D. 2008. Adenosine kinase is a target for the prediction and prevention of epileptogenesis in mice. *Journal of Clinical Investigation*. **118**(2), pp.571–582.

Lim, J.S., Kim, W., Kang, H.-C., Kim, S.H., Park, A.H., Park, E.K., Cho, Y.-W., Kim, S., Kim, H.M., Kim, J.A., Kim, J., Rhee, H., Kang, S.-G., Kim, H.D., Kim, D., Kim, D.-S. and Lee, J.H. 2015. Brain somatic mutations in MTOR cause focal cortical dysplasia type II leading to intractable epilepsy. *Nature medicine*. **21**(4), pp.395–400.

Lin, D., Alborn, W.E., Slebos, R.J.C. and Liebler, D.C. 2013. Comparison of protein immunoprecipitation-multiple reaction monitoring with ELISA for assay of biomarker candidates in plasma. *Journal of Proteome Research*. **12**(12), pp.5996–6003.

Linker, R.A., Lee, D.H., Ryan, S., Van Dam, A.M., Conrad, R., Bista, P., Zeng, W., Hronowsky, X., Buko, A., Chollate, S., Ellrichmann, G., Brück, W., Dawson, K., Goelz, S., Wiese, S., Scannevin, R.H., Lukashev, M. and Gold, R. 2011. Fumaric acid esters exert neuroprotective effects in neuroinflammation via activation of the Nrf2 antioxidant pathway. *Brain*. **134**(3), pp.678–692.

Liou, G.I., Auchampach, J.A., Hillard, C.J., Zhu, G., Yousufzai, B., Mian, S., Khan, S. and Khalifa, Y. 2008. Mediation of cannabidiol anti-inflammation in the retina by equilibrative nucleoside transporter and A2A adenosine receptor. *Investigative Ophthalmology and Visual Science*. **49**(12), pp.5526–5531.

Litman, P., Ohne, O., Ben-Yaakov, S., Shemesh-Darvish, L., Yechezkel, T., Salitra, Y., Rubnov, S., Cohen, I., Senderowitz, H., Kidron, D., Livnah, O., Levitzki, A. and Livnah, N. 2007. A novel substrate mimetic inhibitor of PKB/Akt inhibits prostate cancer tumor growth in mice by blocking the PKB pathway. *Biochemistry*. **46**(16), pp.4716–4724.

Liu, Q.R., Pan, C.H., Hishimoto, A., Li, C.Y., Xi, Z.X., Llorente-Berzal, A., Viveros, M.P., Ishiguro, H., Arinami, T., Onaivi, E.S. and Uhl, G.R. 2009. Species differences in cannabinoid receptor 2 (CNR2 gene): Identification of novel human and rodent CB2 isoforms, differential tissue expression and regulation by cannabinoid receptor ligands. *Genes, Brain and Behavior*. **8**(5), pp.519–530.

Long, L.E., Chesworth, R., Huang, X.F., Wong, A., Spiro, A., McGregor, I.S., Arnold, J.C. and Karl, T. 2012. Distinct neurobehavioural effects of cannabidiol in transmembrane domain neuregulin 1 mutant mice K. Hashimoto, ed. *PLoS ONE*. **7**(4), p.e34129.

Losito, O., Szijgyarto, Z., Resnick, A.C. and Saiardi, A. 2009. Inositol pyrophosphates and their unique metabolic complexity: Analysis by gel electrophoresis. *PLoS ONE*. **4**(5), p.e5580.

Lovatt, D., Xu, Q., Liu, W., Takano, T., Smith, N.A., Schnermann, J., Tieu, K. and Nedergaard, M. 2012. Neuronal adenosine release, and not astrocytic ATP release, mediates feedback inhibition of excitatory activity. *Proceedings of the National Academy of Sciences of the*

United States of America. **109**(16), pp.6265–6270.

Lozano, I. 2001. The therapeutic use of *Cannabis sativa* (L.) in Arabic medicine. *Journal of Cannabis Therapeutics*. **1**(1), pp.63–70.

Ludányi, A., Eross, L., Czirják, S., Vajda, J., Halász, P., Watanabe, M., Palkovits, M., Maglóczky, Z., Freund, T.F. and Katona, I. 2008. Downregulation of the CB1 cannabinoid receptor and related molecular elements of the endocannabinoid system in epileptic human hippocampus. *The Journal of neuroscience : the official journal of the Society for Neuroscience*. **28**(12), pp.2976–90.

Maag, D., Maxwell, M.J., Hardesty, D.A., Boucher, K.L., Choudhari, N., Hanno, A.G., Ma, J.F., Snowman, A.S., Pietropaoli, J.W., Xu, R., Storm, P.B., Saiardi, A., Snyder, S.H. and Resnick, A.C. 2011. Inositol polyphosphate multikinase is a physiologic PI3-kinase that activates Akt/PKB. *Proceedings of the National Academy of Sciences of the United States of America*. **108**(4), pp.1391–1396.

Mackenzie, R.W.A. and Elliott, B.T. 2014. Akt/PKB activation and insulin signaling: A novel insulin signaling pathway in the treatment of type 2 diabetes. *Diabetes, Metabolic Syndrome and Obesity: Targets and Therapy*. **7**, pp.55–64.

Maiese, K. 2017. Warming Up to New Possibilities with the Capsaicin Receptor TRPV1: mTOR, AMPK, and Erythropoietin. *Current Neurovascular Research*. **14**(2).

Malabanan, M.M. and Blind, R.D. 2016. Inositol polyphosphate multikinase (IPMK) in transcriptional regulation and nuclear inositide metabolism. *Biochemical Society Transactions*. **44**(1), pp.279–285.

Malfitano, A.M., Laezza, C., D'Alessandro, A., Procaccini, C., Saccomanni, G., Tuccinardi, T., Manera, C., Macchia, M., Matarese, G., Gazzerro, P. and Bifulco, M. 2013. Effects on Immune Cells of a New 1,8-Naphthyridin-2-One Derivative and Its Analogues as Selective CB2 Agonists: Implications in Multiple Sclerosis P. Villoslada, ed. *PLoS ONE*. **8**(5), p.e62511.

Mammana, S., Cavalli, E., Gugliandolo, A., Silvestro, S., Pollastro, F., Bramanti, P. and Mazzon, E. 2019. Could the combination of two non-psychotropic cannabinoids counteract neuroinflammation? Effectiveness of cannabidiol associated with cannabigerol. *Medicina (Lithuania)*. **55**(11), p.747.

Mansouri, H., Asrar, Z. and Szopa, J. 2009. Effects of ABA on primary terpenoids and Δ9-tetrahydrocannabinol in Cannabis sativa L. at flowering stage. *Plant Growth Regulation*. **58**(3), pp.269–277.

Marée, A.F. and Hogeweg, P. 2002. Modelling Dictyostelium discoideum morphogenesis: The

culmination. *Bulletin of Mathematical Biology*. **64**(2), pp.327–353.

Maresz, K., Pryce, G., Ponomarev, E.D., Marsicano, G., Croxford, J.L., Shriver, L.P., Ledent, C., Cheng, X., Carrier, E.J., Mann, M.K., Giovannoni, G., Pertwee, R.G., Yamamura, T., Buckley, N.E., Hillard, C.J., Lutz, B., Baker, D. and Dittel, B.N. 2007. Direct suppression of CNS autoimmune inflammation via the cannabinoid receptor CB1 on neurons and CB2 on autoreactive T cells. *Nature Medicine*. **13**(4), pp.492–497.

Marriott, J.J., Miyasaki, J.M., Gronseth, G., O'Connor, P.W. and Therapeutics and Technology Assessment Subcommittee of the American Academy of Neurology 2010. Evidence Report: The efficacy and safety of mitoxantrone (Novantrone) in the treatment of multiple sclerosis: Report of the Therapeutics and Technology Assessment Subcommittee of the American Academy of Neurology. *Neurology*. **74**(18), pp.1463–70.

Mazuz, M., Tiroler, A., Moyal, L., Hodak, E., Nadarajan, S., Vinayaka, A.C., Gorovitz-Haris, B., Lubin, I., Drori, A., Drori, G., Cauwenberghe, O. Van, Faigenboim, A., Namdar, D., Amitay-Laish, I. and Koltai, H. 2020. Synergistic cytotoxic activity of cannabinoids from cannabis sativa against cutaneous T-cell lymphoma (CTCL) in-vitro and ex-vivo . *Oncotarget*. **11**(13).

McAllister, S.D., Christian, R.T., Horowitz, M.P., Garcia, A. and Desprez, P.Y. 2007. Cannabidiol as a novel inhibitor of Id-1 gene expression in aggressive breast cancer cells. *Molecular Cancer Therapeutics*. **6**(11), pp.2921–2927.

McAllister, S.D., Murase, R., Christian, R.T., Lau, D., Zielinski, A.J., Allison, J., Almanza, C., Pakdel, A., Lee, J., Limbad, C., Liu, Y., Debs, R.J., Moore, D.H. and Desprez, P.Y. 2011. Pathways mediating the effects of cannabidiol on the reduction of breast cancer cell proliferation, invasion, and metastasis. *Breast Cancer Research and Treatment*. **129**(1), pp.37–47.

McCoy, B., Wang, L., Zak, M., Al-Mehmadi, S., Kabir, N., Alhadid, K., McDonald, K., Zhang, G., Sharma, R., Whitney, R., Sinopoli, K. and Snead, O.C. 2018. A prospective open-label trial of a CBD/THC cannabis oil in dravet syndrome. *Annals of Clinical and Translational Neurology*. **5**(9), pp.1077–1088.

McPartland, J. M., Agraval, J., Gleeson, D., Heasman, K. and Glass, M. 2006. Cannabinoid receptors in invertebrates. *Journal of Evolutionary Biology*. **19**(2), pp.366–373.

McPartland, J M., Matias, I., Di Marzo, V. and Glass, M. 2006. Evolutionary origins of the endocannabinoid system. *Gene*. **370**(1–2), pp.64–74.

Mechoulam, R., Hanuš, L.O., Pertwee, R. and Howlett, A.C. 2014. Early phytocannabinoid chemistry to endocannabinoids and beyond. *Nature Reviews Neuroscience*. **15**(11), pp.757–764.

Meier, F. and Rosenthal, F. 1976. *The Herb, Hashish versus Medieval Muslim Society* [Online]. Brill Archives. Available from: https://books.google.it/books/about/The_herb_hashish_versus_medieval_Muslim.html?id=1inFAAAAIAAJ&redir_esc=y.

De Meijer, E.P.M. and Hammond, K.M. 2005. The inheritance of chemical phenotype in Cannabis sativa L. (II): Cannabigerol predominant plants. *Euphytica*. **145**(1–2), pp.189–198.

Meili, R., Ellsworth, C. and Firtel, R.A. 2000. A novel Akt/PKB-related kinase is essential for morphogenesis in Dictyostelium. *Current Biology*. **10**(12), pp.708–717.

Meisler, M.H., Kearney, J., Ottman, R. and Escayg, A. 2001. Identification of epilepsy genes in human and mouse. *Annual review of genetics*. **35**, pp.567–88.

Mievis, S., Blum, D. and Ledent, C. 2011. Worsening of Huntington disease phenotype in CB1 receptor knockout mice. *Neurobiology of Disease*. **42**(3), pp.524–529.

Mijangos-Moreno, S., Poot-Aké, A., Arankowsky-Sandoval, G. and Murillo-Rodríguez, E. 2014. Intrahypothalamic injection of cannabidiol increases the extracellular levels of adenosine in nucleus accumbens in rats. *Neuroscience Research*. **84**, pp.60–63.

Millard, C.J., Watson, P.J., Celardo, I., Gordiyenko, Y., Cowley, S.M., Robinson, C. V., Fairall, L. and Schwabe, J.W.R. 2013. Class I HDACs share a common mechanism of regulation by inositol phosphates. *Molecular Cell*. **51**(1), pp.57–67.

Misty, R., Martinez, R., Ali, H. and Steimle, P.A. 2006. Naringenin is a novel inhibitor of *Dictyostelium* cell proliferation and cell migration. *Biochemical and Biophysical Research Communications*. **345**(1), pp.516–522.

Miyamoto, S., Murota, K., Kuwataz, G., Imai, M., Nagao, A. and Terao, J. 2002. Antioxidant Activity of Phytic Acid Hydrolysis Products on Iron Ion-Induced Oxidative Damage in Biological System *In*: *ACS Symposium Series* [Online]., pp.241–250. Available from: https://pubs.acs.org/doi/abs/10.1021/bk-2002-0807.ch018.

Modin, H., Olsson, W., Hillert, J. and Masterman, T. 2004. Modes of action of HLA-DR susceptibility specificities in multiple sclerosis. *American journal of human genetics*. **74**(6), pp.1321–2.

Montalban, X., Hauser, S.L., Kappos, L., Arnold, D.L., Bar-Or, A., Comi, G., De Seze, J., Giovannoni, G., Hartung, H.-P. and Hemmer, B. 2017. Ocrelizumab versus placebo in primary progressive multiple sclerosis. *New England Journal of Medicine*. **376**(3), pp.209–220.

Moore, L.D., Le, T. and Fan, G. 2013. DNA methylation and its basic function.

Neuropsychopharmacology. **38**(1), pp.23–38.

Moreno-Martet, M., Feliú, A., Espejo-Porras, F., Mecha, M., Carrillo-Salinas, F.J., Fernández-Ruiz, J., Guaza, C. and de Lago, E. 2015. The disease-modifying effects of a Sativex®-like combination of phytocannabinoids in mice with experimental autoimmune encephalomyelitis are preferentially due to Δ9-tetrahydrocannabinol acting through CB1 receptors. *Multiple Sclerosis and Related Disorders*. **4**(6), pp.505–511.

Mühlebner, A., van Scheppingen, J., Hulshof, H.M., Scholl, T., Iyer, A.M., Anink, J.J., van den Ouweland, A.M.W., Nellist, M.D., Jansen, F.E., Spliet, W.G.M., Krsek, P., Benova, B., Zamecnik, J., Crino, P.B., Prayer, D., Czech, T., Wöhrer, A., Rahimi, J., Höftberger, R., Hainfellner, J.A., Feucht, M. and Aronica, E. 2016. Novel Histopathological Patterns in Cortical Tubers of Epilepsy Surgery Patients with Tuberous Sclerosis Complex. *PloS one*. **11**(6), p.e0157396.

Müller-Krebs, S., Weber, L., Tsobaneli, J., Kihm, L.P., Reiser, J., Zeier, M. and Schwenger, V. 2013. Cellular Effects of Everolimus and Sirolimus on Podocytes M. P. Rastaldi, ed. *PLoS ONE*. **8**(11), p.e80340.

Muller, C., Morales, P. and Reggio, P.H. 2019. Cannabinoid ligands targeting TRP channels. *Frontiers in Molecular Neuroscience*. **11**.

Müller, S., Windhof, I.M., Maximov, V., Jurkowski, T., Jeltsch, A., Förstner, K.U., Sharma, C.M., Gräf, R. and Nellen, W. 2013. Target recognition, RNA methylation activity and transcriptional regulation of the *Dictyostelium discoideum* Dnmt2-homologue (DnmA). *Nucleic Acids Research*. **41**(18), pp.8615–8627.

Nalaskowski, M.M., Deschermeier, C., Fanick, W. and Mayr, G.W. 2002. The human homologue of yeast ArgRIII protein is an inositol phosphate multikinase with predominantly nuclear localization. *Biochemical Journal*. **366**(2), pp.549–556.

Nallathambi, R., Mazuz, M., Namdar, D., Shik, M., Namintzer, D., Vinayaka, A.C., Ion, A., Faigenboim, A., Nasser, A., Laish, I., Konikoff, F.M. and Koltai, H. 2018. Identification of synergistic interaction between cannabis-derived compounds for cytotoxic activity in colorectal cancer cell lines and colon polyps that induces apoptosis-related cell death and distinct gene expression. *Cannabis and Cannabinoid Research*. **3**(1), pp.120–135.

Nam, H.W., Lee, M.R., Zhu, Y., Wu, J., Hinton, D.J., Choi, S., Kim, T., Hammack, N., Yin, J.C.P. and Choi, D.S. 2011. Type 1 equilibrative nucleoside transporter regulates ethanol drinking through accumbal N-methyl-D-aspartate receptor signaling. *Biological Psychiatry*. **69**(11), pp.1043–1051.

Nazıroğlu, M., Dikici, D.M. and Dursun, Ş. 2012. Role of Oxidative Stress and Ca2+ Signaling on Molecular Pathways of Neuropathic Pain in Diabetes: Focus on TRP Channels. *Neurochemical Research*. **37**(10), pp.2065–2075.

NHS 2018. Overview - Multiple sclerosis. Available from: nhs.uk/conditions/multiple-sclerosis.

O'Connor, P., Wolinsky, J.S., Confavreux, C., Comi, G., Kappos, L., Olsson, T.P., Benzerdjeb, H., Truffinet, P., Wang, L., Miller, A. and Freedman, M.S. 2011. Randomized trial of oral teriflunomide for relapsing multiple sclerosis. *New England Journal of Medicine*. **365**(14), pp.1293–1303.

O'Sullivan, S.E., Sun, Y., Bennett, A.J., Randall, M.D. and Kendall, D.A. 2009. Time-dependent vascular actions of cannabidiol in the rat aorta. *European Journal of Pharmacology*. **612**(1–3), pp.61–68.

Ogunbayo, O.A., Duan, J., Xiong, J., Wang, Q., Feng, X., Ma, J., Zhu, M.X. and Evans, A.M. 2018. MTORC1 controls lysosomal Ca2+ release through the two-pore channel TPC2. *Science Signaling*. **11**(525), p.eaao5775.

Oh, W.J. and Jacinto, E. 2011. mTOR complex 2 signaling and functions. *Cell Cycle*. **10**(14), pp.2305–2316.

Oksenberg, J.R. and Barcellos, L.F. 2005. Multiple sclerosis genetics: leaving no stone unturned. *Genes & Immunity*. **6**(5), pp.375–387.

Osbaldeston, T.A. 2000. *De Materia Medica - Indexes* [Online]. Available from: http://panaceavera.com/dematerialast.html.

Otto, G.P., Cocorocchio, M., Munoz, L., Tyson, R.A., Bretschneider, T. and Williams, R.S.B. 2016. Employing Dictyostelium as an advantageous 3Rs model for pharmacogenetic research *In*: *Methods in Molecular Biology* [Online]., pp.123–130. Available from: http://link.springer.com/10.1007/978-1-4939-3480-5_9.

Pal, P.B., Sonowal, H., Shukla, K., Srivastava, S.K. and Ramana, K. V. 2019. Aldose reductase regulates hyperglycemia-induced huvec death via SIRT1/AMPK-α1/mTOR pathway. *Journal of Molecular Endocrinology*. **63**(1), pp.11–25.

Pan, C., Jin, L., Wang, X., Li, Y., Chun, J., Boese, A.C., Li, D., Kang, H.B., Zhang, G., Zhou, L., Chen, G.Z., Saba, N.F., Shin, D.M., Magliocca, K.R., Owonikoko, T.K., Mao, H., Lonial, S. and Kang, S. 2019. Inositol-triphosphate 3-kinase B confers cisplatin resistance by regulating NOX4-dependent redox balance. *Journal of Clinical Investigation*. **129**(6), pp.2431–2445.

Pandolfo, P., Silveirinha, V., Santos-Rodrigues, A. Dos, Venance, L., Ledent, C., Takahashi, R.N.,

Cunha, R.A. and Köfalvi, A. 2011. Cannabinoids inhibit the synaptic uptake of adenosine and dopamine in the rat and mouse striatum. *European Journal of Pharmacology*. **655**(1–3), pp.38–45.

Paradisi, A., Pasquariello, N., Barcaroli, D. and Maccarrone, M. 2008. Anandamide regulates keratinocyte differentiation by inducing DNA methylation in a CB1 receptor-dependent manner. *Journal of Biological Chemistry*. **283**(10), pp.6005–6012.

Parent, C.A. and Devreotes, P.N. 1996. Molecular Genetics of Signal Transduction in Dictyostelium. *Annual Review of Biochemistry*. **65**(1), pp.411–440.

Pastor-Anglada, M. and Pérez-Torras, S. 2018. Who is who in Adenosine transport. *Frontiers in Pharmacology*. **9**(JUN), p.627.

Pekny, M. and Nilsson, M. 2005. Astrocyte activation and reactive gliosis. *Glia*. **50**(4), pp.427–34.

Perrotin-Brunel, H., Buijs, W., Spronsen, J. Van, Roosmalen, M.J.E.V., Peters, C.J., Verpoorte, R. and Witkamp, G.J. 2011. Decarboxylation of Δ9-tetrahydrocannabinol: Kinetics and molecular modeling. *Journal of Molecular Structure*. **987**(1–3), pp.67–73.

Perry, C. 2019. *Identifying the molecular mechanisms of the anticonvulsant drugs cannabidiol , cannabidivarin and cannabidiolic acid using the model organism Dictyostelium discoideum*. Thesis: *Royal Holloway, University of London*.

Perry, C.J., Finch, P., Müller-Taubenberger, A., Leung, K.Y., Warren, E.C., Damstra-Oddy, J., Sharma, D., Patra, P.H., Glyn, S., Boberska, J., Stewart, B., Baldwin, A., Piscitelli, F., Harvey, R.J., Harwood, A., Thompson, C., Claus, S.P., Greene, N.D.E., McNeish, A.J., Williams, C.M., Whalley, B.J. and Williams, R.S.B. 2020. A new mechanism for cannabidiol in regulating the one-carbon cycle and methionine levels in *Dictyostelium* and in mammalian epilepsy models. *British Journal of Pharmacology*. **177**(4), pp.912–928.

Perucca, E. 2017. Cannabinoids in the Treatment of Epilepsy: Hard Evidence at Last? *Journal of Epilepsy Research*. **7**(2), pp.61–76.

De Petrocellis, L., Ligresti, A., Moriello, A.S., Allarà, M., Bisogno, T., Petrosino, S., Stott, C.G. and Di Marzo, V. 2011. Effects of cannabinoids and cannabinoid-enriched Cannabis extracts on TRP channels and endocannabinoid metabolic enzymes. *British Journal of Pharmacology*. **163**(7), pp.1479–1494.

De Petrocellis, L., Starowicz, K., Moriello, A.S., Vivese, M., Orlando, P. and Di Marzo, V. 2007. Regulation of transient receptor potential channels of melastatin type 8 (TRPM8): Effect of cAMP, cannabinoid CB1 receptors and endovanilloids. *Experimental Cell Research*. **313**(9),

pp.1911–1920.

Pisani, F., Livermore, T., Rose, G., Chubb, J.R., Gaspari, M. and Saiardi, A. 2014. Analysis of *Dictyostelium discoideum* inositol pyrophosphate metabolism by gel electrophoresis T. Soldati, ed. *PLoS ONE*. **9**(1), p.e85533.

Plamont, M.A., Billon-Denis, E., Maurin, S., Gauron, C., Pimenta, F.M., Specht, C.G., Shi, J., Quérard, J., Pan, B., Rossignol, J., Morellet, N., Volovitch, M., Lescop, E., Chen, Y., Triller, A., Vriz, S., Le Saux, T., Jullien, L. and Gautier, A. 2016. Small fluorescence-activating and absorption-shifting tag for tunable protein imaging in vivo. *Proceedings of the National Academy of Sciences of the United States of America*. **113**(3), pp.497–502.

Potter, D.J., Clark, P. and Brown, M.B. 2008. Potency of Δ9-THC and other cannabinoids in cannabis in England in 2005: Implications for psychoactivity and pharmacology. *Journal of Forensic Sciences*. **53**(1), pp.90–94.

Pryce, G., Ahmed, Z., Hankey, D.J.R., Jackson, S.J., Croxford, J.L., Pocock, J.M., Ledent, C., Petzold, A., Thompson, A.J., Giovannoni, G., Cuzner, M.L. and Baker, D. 2003. Cannabinoids inhibit neurodegeneration in models of multiple sclerosis. *Brain*. **126**(10), pp.2191–2202.

Pryce, G., Riddall, D.R., Selwood, D.L., Giovannoni, G. and Baker, D. 2015. Neuroprotection in Experimental Autoimmune Encephalomyelitis and Progressive Multiple Sclerosis by Cannabis-Based Cannabinoids. *Journal of Neuroimmune Pharmacology*. **10**(2), pp.281–292.

PubMed 2020. PubMed. [Accessed 7 May 2020]. Available from: https://www.ncbi.nlm.nih.gov/pubmed/.

Pucci, M., Rapino, C., Di Francesco, A., Dainese, E., D'Addario, C. and Maccarrone, M. 2013. Epigenetic control of skin differentiation genes by phytocannabinoids. *British Journal of Pharmacology*. **170**(3), pp.581–591.

Purcell, S.M., Wray, N.R., Stone, J.L., Visscher, P.M., O'Donovan, M.C., Sullivan, P.F., Ruderfer, D.M., McQuillin, A., Morris, D.W., Oĝdushlaine, C.T., Corvin, A., Holmans, P.A., Oĝdonovan, M.C., MacGregor, S., Gurling, H., Blackwood, D.H.R., Craddock, N.J., Gill, M., Hultman, C.M., Kirov, G.K., Lichtenstein, P., Muir, W.J., Owen, M.J., Pato, C.N., Scolnick, E.M., St Clair, D., Williams, N.M., Georgieva, L., Nikolov, I., Norton, N., Williams, H., Toncheva, D., Milanova, V., Thelander, E.F., O'Dushlaine, C.T., Kenny, E., Quinn, E.M., Choudhury, K., Datta, S., Pimm, J., Thirumalai, S., Puri, V., Krasucki, R., Lawrence, J., Quested, D., Bass, N., Crombie, C., Fraser, G., Leh Kuan, S., Walker, N., McGhee, K.A., Pickard, B., Malloy, P., MacLean, A.W., Van Beck, M., Pato, M.T., Medeiros, H., Middleton, F., Carvalho, C., Morley, C.,

Fanous, A., Conti, D., Knowles, J.A., Paz Ferreira, C., MacEdo, A., Helena Azevedo, M., Kirby, A.N., Ferreira, M.A.R., Daly, M.J., Chambert, K., Kuruvilla, F., Gabriel, S.B., Ardlie, K., Moran, J.L. and Sklar, P. 2009. Common polygenic variation contributes to risk of schizophrenia and bipolar disorder. *Nature*. **460**(7256), pp.748–752.

Qin, N., Neeper, M.P., Liu, Y., Hutchinson, T.L., Lubin, M. Lou and Flores, C.M. 2008. TRPV2 is activated by cannabidiol and mediates CGRP release in cultured rat dorsal root ganglion neurons. *Journal of Neuroscience*. **28**(24), pp.6231–6238.

Qin, X., Jiang, B. and Zhang, Y. 2016. 4E-BP1, a multifactor regulated multifunctional protein. *Cell Cycle*. **15**(6), pp.781–786.

Rahimi, A., Faizi, M., Talebi, F., Noorbakhsh, F., Kahrizi, F. and Naderi, N. 2015. Interaction between the protective effects of cannabidiol and palmitoylethanolamide in experimental model of multiple sclerosis in C57BL/6 mice. *Neuroscience*. **290**, pp.279–287.

Rajesh, M., Mukhopadhyay, P., Bátkai, S., Haskó, G., Liaudet, L., Drel, V.R., Obrosova, I.G. and Pacher, P. 2007. Cannabidiol attenuates high glucose-induced endothelial cell inflammatory response and barrier disruption. *American Journal of Physiology - Heart and Circulatory Physiology*. **293**(1), pp.H610–H619.

Raper, K.B. 1941. *Dictyostelium Minutum*, a Second New Species of Slime Mold from Decaying Forest Leaves. *Mycologia*. **33**(6), p.633.

Ratchford, J.N., Costello, K., Reich, D.S. and Calabresi, P.A. 2012. Varicella-zoster virus encephalitis and vasculopathy in a patient treated with fingolimod. *Neurology*. **79**(19), pp.2002–2004.

Renard, J., Loureiro, M., Rosen, L.G., Zunder, J., De Oliveira, C., Schmid, S., Rushlow, W.J. and Laviolette, S.R. 2016. Cannabidiol counteracts amphetamine-induced neuronal and behavioral sensitization of the mesolimbic dopamine pathway through a novel mTOR/p70S6 kinase signaling pathway. *Journal of Neuroscience*. **36**(18), pp.5160–5169.

Renard, J., Norris, C., Rushlow, W. and Laviolette, S.R. 2017 (b). Neuronal and molecular effects of cannabidiol on the mesolimbic dopamine system: Implications for novel schizophrenia treatments. *Neuroscience and Biobehavioral Reviews*. **75**, pp.157–165.

Renard, J., Rosen, L.G., Loureiro, M., De Oliveira, C., Schmid, S., Rushlow, W.J. and Laviolette, S.R. 2017 (a). Adolescent Cannabinoid Exposure Induces a Persistent Sub-Cortical Hyper-Dopaminergic State and Associated Molecular Adaptations in the Prefrontal Cortex. *Cerebral cortex (New York, N.Y. : 1991)*. **27**(2), pp.1297–1310.

Resnick, A.C., Snowman, A.M., Kang, B.M., Hurt, K.J., Snyder, S.H. and Saiardi, A. 2005. Inositol

polyphosphate multikinase is a nuclear PI3-kinase with transcriptional regulatory activity. *Proceedings of the National Academy of Sciences of the United States of America*. **102**(36), pp.12783–12788.

Riccio, P. and Rossano, R. 2015. Nutrition facts in multiple sclerosis. *ASN Neuro*. **7**(1), pp.1–20.

Robery, S., Mukanowa, J., Percie du Sert, N., Andrews, P.L.R. and Williams, R.S.B. 2011. Investigating the effect of emetic compounds on chemotaxis in *Dictyostelium* identifies a non-sentient model for bitter and hot tastant research A. J. Harwood, ed. *PLoS ONE*. **6**(9), p.e24439.

Robery, S., Tyson, R., Dinh, C., Kuspa, A., Noegel, A.A., Bretschneider, T., Andrews, P.L.R. and Williams, R.S.B. 2013. A novel human receptor involved in bitter tastant detection identified using *Dictyostelium discoideum*. *Journal of Cell Science*. **126**(23), pp.5465–5476.

Robinson, A. 2014. Dimethyl fumarate (Tecfidera) for multiple sclerosis. *The Nurse practitioner*. **39**(7), pp.10–11.

Robinson, A.P., Harp, C.T., Noronha, A. and Miller, S.D. 2014. The experimental autoimmune encephalomyelitis (EAE) model of MS. utility for understanding disease pathophysiology and treatment. *In*: *Handbook of Clinical Neurology* [Online]., pp.173–189. Available from: https://linkinghub.elsevier.com/retrieve/pii/B978044452001200008X.

Rocha, A.J., Miranda, R. de S., Sousa, A.J.S. and da Silva, A.L.C. 2016. Guidelines for Successful Quantitative Gene Expression in Real- Time qPCR Assays *In*: *Polymerase Chain Reaction for Biomedical Applications* [Online]. InTech. Available from: http://www.intechopen.com/books/polymerase-chain-reaction-for-biomedical-applications/guidelines-for-successful-quantitative-gene-expression-in-real-time-qpcr-assays.

Rock, E.M. and Parker, L.A. 2015. Synergy Between Cannabidiol, Cannabidiolic Acid, and Δ9-Tetrahydrocannabinol in the Regulation of Emesis in the *Suncus Murinus* (House Musk Shrew). *Behavioral Neuroscience*. **129**(3), pp.368–370.

Rog, D.J., Nurmikko, T.J., Friede, T. and Young, C.A. 2005. Randomized, controlled trial of cannabis-based medicine in central pain in multiple sclerosis. *Neurology*. **65**(6), pp.812–819.

Rog, D.J., Nurmikko, T.J. and Young, C.A. 2007. Oromucosal Δ9-tetrahydrocannabinol/cannabidiol for neuropathic pain associated with multiple sclerosis: An uncontrolled, open-label, 2-year extension trial. *Clinical Therapeutics*. **29**(9), pp.2068–2079.

Romigi, A., Bari, M., Placidi, F., Marciani, M.G., Malaponti, M., Torelli, F., Izzi, F., Prosperetti, C., Zannino, S., Corte, F., Chiaramonte, C. and Maccarrone, M. 2010. Cerebrospinal fluid levels of the endocannabinoid anandamide are reduced in patients with untreated newly diagnosed temporal lobe epilepsy. *Epilepsia*. **51**(5), pp.768–72.

Rosel, D., Khurana, T., Majithia, A., Huang, X., Bhandari, R. and Kimmel, A.R. 2012. TOR complex 2 (TORC2) in *Dictyostelium* suppresses phagocytic nutrient capture independently of TORC1-mediated nutrient sensing. *Development*. **139**(5), pp.37–48.

Rosse, G. 2017. Indolinone Inhibitors of ENT1 for the Treatment of Schizophrenia. *ACS Medicinal Chemistry Letters*. **8**(10), pp.995–996.

Rot, G., Parikh, A., Curk, T., Kuspa, A., Shaulsky, G. and Zupan, B. 2009. dictyExpress: A Dictyostelium discoideum gene expression database with an explorative data analysis web-based interface. *BMC Bioinformatics*. **10**(1), p.265.

Rountree, M.R., Bachman, K.E. and Baylin, S.B. 2000. DNMT1 binds HDAC2 and a new co-repressor, DMAP1, to form a complex at replication foci. *Nature Genetics*. **25**(3), pp.269–277.

Rowley, S., Sun, X., Lima, I. V, Tavenier, A., de Oliveira, A.C.P., Dey, S.K. and Danzer, S.C. 2017. Cannabinoid receptor 1/2 double-knockout mice develop epilepsy. *Epilepsia*. **58**(12), pp.e162–e166.

Rudick, R.A., Lee, J.-C., Simon, J. and Fisher, E. 2006. Significance of T2 lesions in multiple sclerosis: A 13-year longitudinal study. *Annals of Neurology*. **60**(2), pp.236–242.

Russo, C. Dello, Navarra, P. and Lisi, L. 2016. mTOR in Multiple Sclerosis *In*: *Molecules to Medicine with mTOR* [Online]. Elsevier, pp.331–343. Available from: https://linkinghub.elsevier.com/retrieve/pii/B9780128027332000049.

Russo, E. 2005. Cannabinoids as Therapeutics. *Cannabinoids as Therapeutics*. (March 2006).

Russo, E., Citraro, R., Donato, G., Camastra, C., Iuliano, R., Cuzzocrea, S., Constanti, A. and De Sarro, G. 2013. MTOR inhibition modulates epileptogenesis, seizures and depressive behavior in a genetic rat model of absence epilepsy. *Neuropharmacology*. **69**, pp.25–36.

Russo, E.B. 2007. History of cannabis and its preparations in saga, science, and sobriquet. *Chemistry and Biodiversity*. **4**(8), pp.1614–1648.

Ryan, D., Drysdale, A.J., Pertwee, R.G. and Platt, B. 2006. Differential effects of cannabis extracts and pure plant cannabinoids on hippocampal neurones and glia. *Neuroscience Letters*. **408**(3), pp.236–241.

Ryberg, E., Larsson, N., Sjögren, S., Hjorth, S., Hermansson, N.O., Leonova, J., Elebring, T., Nilsson, K., Drmota, T. and Greasley, P.J. 2007. The orphan receptor GPR55 is a novel cannabinoid receptor. *British Journal of Pharmacology*. **152**(7), pp.1092–1101.

Ryley Parrish, R., Albertson, A.J., Buckingham, S.C., Hablitz, J.J., Mascia, K.L., Davis Haselden, W. and Lubin, F.D. 2013. Status epilepticus triggers early and late alterations in brain-derived neurotrophic factor and NMDA glutamate receptor Grin2b DNA methylation levels in the hippocampus. *Neuroscience*. **248**, pp.602–619.

Rzezak, P., Fuentes, D., Guimarães, C.A., Thome-Souza, S., Kuczynski, E., Li, L.M., Franzon, R.C., Leite, C.C., Guerreiro, M. and Valente, K.D. 2007. Frontal Lobe Dysfunction in Children With Temporal Lobe Epilepsy. *Pediatric Neurology*. **37**(3), pp.176–185.

Saiardi, A., Azevedo, C., Desfougères, Y., Portela-Torres, P. and Wilson, M.S.C. 2018. Microbial inositol polyphosphate metabolic pathway as drug development target. *Advances in Biological Regulation*. **67**, pp.74–83.

Saiardi, A., Erdjument-Bromage, H., Snowman, A.M., Tempst, P. and Snyder, S.H. 1999. Synthesis of diphosphoinositol pentakisphosphate by a newly identified family of higher inositol polyphosphate kinases. *Current Biology*. **9**(22), pp.1323–1326.

Saiki, S., Sasazawa, Y., Imamichi, Y., Kawajiri, S., Fujimaki, T., Tanida, I., Kobayashi, H., Sato, F., Sato, S., Ishikawa, K.I., Imoto, M. and Hattori, N. 2011. Caffeine induces apoptosis by enhancement of autophagy via PI3K/Akt/mTOR/p70S6K inhibition. *Autophagy*. **7**(2), pp.176–187.

Samueli, S., Abraham, K., Dressler, A., Gröppel, G., Mühlebner-Fahrngruber, A., Scholl, T., Kasprian, G., Laccone, F. and Feucht, M. 2016. Efficacy and safety of Everolimus in children with TSC - associated epilepsy - Pilot data from an open single-center prospective study. *Orphanet Journal of Rare Diseases*. **11**(1), pp.1–8.

Saxton, R.A. and Sabatini, D.M. 2017. mTOR Signaling in Growth, Metabolism, and Disease. *Cell*. **168**(6), pp.960–976.

Schaf, J., Damstra-Oddy, J. and Williams, R.S.B. 2019. Dictyostelium discoideum as a pharmacological model system to study the mechanisms of medicinal drugs and natural products. *International Journal of Developmental Biology*. **63**(9–10), pp.541–550.

Schilde, C. and Schaap, P. 2013. The Amoebozoa *In*:, pp.1–15. Available from: http://link.springer.com/10.1007/978-1-62703-302-2_1.

Schmutz, M., Brugger, F., Gentsch, C., McLean, M.J. and Olpe, H.R. 1994. Oxcarbazepine: Preclinical Anticonvulsant Profile and Putative Mechanisms of Action. *Epilepsia*. **35**,

pp.S47–S50.

Sekine, R., Kawata, T. and Muramoto, T. 2018. CRISPR/Cas9 mediated targeting of multiple genes in *Dictyostelium*. *Scientific Reports*. **8**(1), p.8471.

Serfontein, J., Nisbet, R.E.R., Howe, C.J. and de Vries, P.J. 2011. Conservation of Structural and Functional Elements of TSC1 and TSC2: A Bioinformatic Comparison Across Animal Models. *Behavior Genetics*. **41**(3), pp.349–356.

Serpell, M.G., Notcutt, W. and Collin, C. 2013. Sativex® long-term use: An open-label trial in patients with spasticity due to multiple sclerosis. *Journal of Neurology*. **260**(1), pp.285–295.

Serra, I., Scheldeman, C., Bazelot, M., Whalley, B.J., Dallas, M.L., de Witte, P.A.M. and Williams, C.M. 2019. Cannabidiol modulates phosphorylated rpS6 signalling in a zebrafish model of Tuberous Sclerosis Complex. *Behavioural Brain Research*. **363**, pp.135–144.

Shaltiel, G., Shamir, A., Shapiro, J., Ding, D., Dalton, E., Bialer, M., Harwood, A.J., Belmaker, R.H., Greenberg, M.L. and Agam, G. 2004. Valproate decreases inositol biosynthesis. *Biological Psychiatry*. **56**(11), pp.868–874.

Sharma, D., Otto, G., Warren, E.C., Beesley, P., King, J.S. and Williams, R.S.B. 2019. Gamma secretase orthologs are required for lysosomal activity and autophagic degradation in *Dictyostelium discoideum*, independent of PSEN (presenilin) proteolytic function. *Autophagy*. **15**(8), pp.1407–1418.

Shaw, R.J. and Cantley, L.C. 2006. Ras, PI(3)K and mTOR signalling controls tumour cell growth. *Nature*. **441**(7092), pp.424–430.

Shen, H.Y., Singer, P., Lytle, N., Wei, C.J., Lan, J.Q., Williams-Karnesky, R.L., Chen, J.F., Yee, B.K. and Boison, D. 2012. Adenosine augmentation ameliorates psychotic and cognitive endophenotypes of schizophrenia. *Journal of Clinical Investigation*. **122**(7), pp.2567–2577.

Shoudai, K., Peters, J.H., McDougall, S.J., Fawley, J.A. and Andresen, M.C. 2010. Thermally Active TRPV1 Tonically Drives Central Spontaneous Glutamate Release. *Journal of Neuroscience*. **30**(43), pp.14470–14475.

Shrivastava, A., Kuzontkoski, P.M., Groopman, J.E. and Prasad, A. 2011. Cannabidiol induces programmed cell death in breast cancer cells by coordinating the cross-talk between apoptosis and autophagy. *Molecular Cancer Therapeutics*. **10**(7), pp.1161–1172.

da Silva, V.K., de Freitas, B.S., Dornelles, V.C., Kist, L.W., Bogo, M.R., Silva, M.C., Streck, E.L., Hallak, J.E., Zuardi, A.W., Crippa, J.A.S. and Schröder, N. 2018. Novel insights into mitochondrial molecular targets of iron-induced neurodegeneration: Reversal by

cannabidiol. *Brain Research Bulletin*. **139**, pp.1–8.

Simpson, S., Stewart, N., Van Der Mei, I., Otahal, P., Charlesworth, J., Ponsonby, A.L., Blizzard, L., Dwyer, T., Pittas, F., Gies, P. and Taylor, B. 2015. Stimulated PBMC-produced IFN-γ and TNF-α are associated with altered relapse risk in multiple sclerosis: Results from a prospective cohort study. *Journal of Neurology, Neurosurgery and Psychiatry*. **86**(2), pp.200–207.

Singer, G., Araki, T. and Weijer, C.J. 2019. Oscillatory cAMP cell-cell signalling persists during multicellular Dictyostelium development. *Communications Biology*. **2**(1), p.139.

So, L., Lee, J., Palafox, M., Mallya, S., Woxland, C.G., Arguello, M., Truitt, M.L., Sonenberg, N., Ruggero, D. and Fruman, D.A. 2016. The 4E-BP-eIF4E axis promotes rapamycinsensitive growth and proliferation in lymphocytes. *Science Signaling*. **9**(430), p.ra57.

Spencer, S.S. and Spencer, D.D. 1994. Entorhinal-Hippocampal Interactions in Medial Temporal Lobe Epilepsy. *Epilepsia*. **35**(4), pp.721–727.

Sperk, G., Furtinger, S., Schwarzer, C. and Pirker, S. 2004. GABA and its receptors in epilepsy. *Advances in Experimental Medicine and Biology*. **548**, pp.92–103.

Steinert, M. and Heuner, K. 2005. Dictyostelium as host model for pathogenesis. *Cellular Microbiology*. **7**(3), pp.307–314.

Steinhäuser, C. and Boison, D. 2012. Epilepsy: crucial role for astrocytes. *Glia*. **60**(8), p.1191.

Studer, F.E., Fedele, D.E., Marowsky, A., Schwerdel, C., Wernli, K., Vogt, K., Fritschy, J.M. and Boison, D. 2006. Shift of adenosine kinase expression from neurons to astrocytes during postnatal development suggests dual functionality of the enzyme. *Neuroscience*. **142**(1), pp.125–37.

Suess, P.M., Watson, J., Chen, W. and Gomer, R.H. 2017. Extracellular polyphosphate signals through Ras and Akt to prime Dictyostelium discoideum cells for development. *Journal of Cell Science*. **130**(14), pp.2394–2404.

Sultan, A.S., Marie, M.A. and Sheweita, S.A. 2018. Novel mechanism of cannabidiol-induced apoptosis in breast cancer cell lines. *Breast*. **41**, pp.34–41.

Sun, F.-J., Guo, W., Zheng, D.-H., Zhang, C.-Q., Li, S., Liu, S.-Y., Yin, Q., Yang, H. and Shu, H.-F. 2013. Increased Expression of TRPV1 in the Cortex and Hippocampus from Patients with Mesial Temporal Lobe Epilepsy. *Journal of Molecular Neuroscience*. **49**(1), pp.182–193.

Sun, Y., Olson, R., Horning, M., Armstrong, N., Mayer, M. and Gouaux, E. 2002. Mechanism of glutamate receptor desensitization. *Nature*. **417**(6886), pp.245–253.

Swift, W., Wong, A., Li, K.M., Arnold, J.C. and McGregor, I.S. 2013. Analysis of Cannabis Seizures in NSW, Australia: Cannabis Potency and Cannabinoid Profile M. Taffe, ed. *PLoS ONE*. **8**(7), p.e70052.

Sypert, G.W. and Ward, A.A. 1974. Changes in extracellular potassium activity during neocortical propagated seizures. *Experimental Neurology*. **45**(1), pp.19–41.

Szaflarski, J.P. and Martina Bebin, E. 2014. Cannabis, cannabidiol, and epilepsy - From receptors to clinical response. *Epilepsy and Behavior*. **41**, pp.277–282.

Szkudlarek, H.J., Desai, S.J., Renard, J., Pereira, B., Norris, C., Jobson, C.E.L., Rajakumar, N., Allman, B.L. and Laviolette, S.R. 2019. Δ-9-Tetrahydrocannabinol and Cannabidiol produce dissociable effects on prefrontal cortical executive function and regulation of affective behaviors. *Neuropsychopharmacology*. **44**(4), pp.817–825.

Tallantyre, E.C., Brookes, M.J., Dixon, J.E., Morgan, P.S., Evangelou, N. and Morris, P.G. 2008. DEMONSTRATING THE PERIVASCULAR DISTRIBUTION OF MS LESIONS IN VIVO WITH 7-TESLA MRI. *Neurology*. **70**(22), pp.2076–2078.

Tariqul Islam, A.F.M., Scavello, M., Lotfi, P., Daniel, D., Haldeman, P. and Charest, P.G. 2019. Caffeine inhibits PI3K and mTORC2 in *Dictyostelium* and differentially affects multiple other cAMP chemoattractant signaling effectors. *Molecular and Cellular Biochemistry*., pp.1–12.

Taura, F., Sirikantaramas, S., Shoyama, Yoshinari, Shoyama, Yukihiro and Morimoto, S. 2007. Phytocannabiniods in Cannabis sativa: Recent studies on biosynthetic enzymes. *Chemistry and Biodiversity*. **4**(8), pp.1649–1663.

Tillner, J., Nau, H., Winckler, T. and Dingermann, T. 1998. Evaluation of the teratogenic potential of valproic acid analogues in transgenic *Dictyostelium discoideum* strains. *Toxicology in Vitro*. **12**(4), pp.463–469.

Traub, R.D., Michelson-Law, H., Bibbig, A.E.J., Buhl, E.H. and Whittington, M.A. 2004. Gap Junctions, Fast Oscillations and the Initiation of Seizures *In*:, pp.110–122. Available from: http://link.springer.com/10.1007/978-1-4757-6376-8_9.

Tselis, A. 2012. Epstein-Barr virus cause of multiple sclerosis. *Current Opinion in Rheumatology*. **24**(4), pp.424–428.

Uchinomiya, K. and Iwasa, Y. 2013. Evolution of stalk/spore ratio in a social amoeba: Cell-to-cell interaction via a signaling chemical shaped by cheating risk. *Journal of Theoretical Biology*. **336**, pp.110–118.

Umathe, S.N., Manna, S.S.S. and Jain, N.S. 2012. Endocannabinoid analogues exacerbate marble-

burying behavior in mice via TRPV1 receptor. *Neuropharmacology*. **62**(5–6), pp.2024–2033.

Vaillend, C., Mason, S.E., Cuttle, M.F. and Alger, B.E. 2002. Mechanisms of neuronal hyperexcitability caused by partial inhibition of Na+-K+-ATPases in the rat CA1 hippocampal region. *Journal of neurophysiology*. **88**(6), pp.2963–78.

Valdeolivas, S., Navarrete, C., Cantarero, I., Bellido, M.L., Muñoz, E. and Sagredo, O. 2015. Neuroprotective Properties of Cannabigerol in Huntington's Disease: Studies in R6/2 Mice and 3-Nitropropionate-lesioned Mice. *Neurotherapeutics*. **12**(1), pp.185–199.

Valdeolivas, S., Satta, V., Pertwee, R.G., Fernández-Ruiz, J. and Sagredo, O. 2012. Sativex®-like combination of phytocannabinoids is neuroprotective in malonate-lesioned rats, an inflammatory model of Huntington's disease: Role of CB1 and CB2 receptors. *ACS Chemical Neuroscience*. **3**(5), pp.400–406.

Vandrey, R., Raber, J.C., Raber, M.E., Douglass, B., Miller, C. and Bonn-Miller, M.O. 2015. Cannabinoid dose and label accuracy in edible medical cannabis products. *JAMA - Journal of the American Medical Association*. **313**(24), pp.2491–2493.

Veltman, D.M., Akar, G., Bosgraaf, L. and Van Haastert, P.J.M. 2009. A new set of small, extrachromosomal expression vectors for *Dictyostelium discoideum*. *Plasmid*. **61**(2), pp.110–118.

Vilela, L.R., Lima, I. V., Kunsch, É.B., Pinto, H.P.P., de Miranda, A.S., Vieira, É.L.M., de Oliveira, A.C.P., Moraes, M.F.D., Teixeira, A.L. and Moreira, F.A. 2017. Anticonvulsant effect of cannabidiol in the pentylenetetrazole model: Pharmacological mechanisms, electroencephalographic profile, and brain cytokine levels. *Epilepsy and Behavior*. **75**, pp.29–35.

Vinet, L. and Zhedanov, A. 2011. *A 'missing' family of classical orthogonal polynomials*.

Waheed, A., Ludtmann, M.H.R., Pakes, N., Robery, S., Kuspa, A., Dinh, C., Baines, D., Williams, R.S.B. and Carew, M.A. 2014. Naringenin inhibits the growth of *Dictyostelium* and MDCK-derived cysts in a TRPP2 (polycystin-2)-dependent manner. *British Journal of Pharmacology*. **171**(10), pp.2659–2670.

Wahl, S.E., McLane, L.E., Bercury, K.K., Macklin, W.B. and Wood, T.L. 2014. Mammalian target of rapamycin promotes oligodendrocyte differentiation, initiation and extent of CNS myelination. *Journal of Neuroscience*. **34**(13), pp.4453–4465.

Wallace, M.J., Martin, B.R. and DeLorenzo, R.J. 2002. Evidence for a physiological role of endocannabinoids in the modulation of seizure threshold and severity. *European Journal*

of Pharmacology. **452**(3), pp.295–301.

Watson, C.T., Szutorisz, H., Garg, P., Martin, Q., Landry, J.A., Sharp, A.J. and Hurd, Y.L. 2015. Genome-Wide DNA Methylation Profiling Reveals Epigenetic Changes in the Rat Nucleus Accumbens Associated with Cross-Generational Effects of Adolescent THC Exposure. *Neuropsychopharmacology*. **40**(13), pp.2993–3005.

Watson, P.J., Fairall, L., Santos, G.M. and Schwabe, J.W.R. 2012. Structure of HDAC3 bound to co-repressor and inositol tetraphosphate. *Nature*. **481**(7381), pp.335–340.

Weiner, H.L., Carlson, C., Ridgway, E.B., Zaroff, C.M., Miles, D., LaJoie, J. and Devinsky, O. 2006. Epilepsy surgery in young children with tuberous sclerosis: results of a novel approach. *Pediatrics*. **117**(5), pp.1494–502.

Weltha, L., Reemmer, J. and Boison, D. 2019. The role of adenosine in epilepsy. *Brain Research Bulletin*. **151**, pp.46–54.

Wessels, D., Shutt, D., Voss, E. and Soll, D.R. 1996. Chemotactic decisions by *Dictyostelium* amoebae in spatial gradients and natural waves of cAMP are made by pseudopods formed primarily off the substratum. *In*: *Molecular Biology of the Cell*. AMER SOC CELL BIOLOGY 8120 WOODMONT AVE, STE 750, BETHESDA, MD 20814-2755 USA, p.1349.

Wiedenmann, J., Oswald, F. and Nienhaus, G.U. 2009. Fluorescent proteins for live cell imaging: Opportunities, limitations, and challenges. *IUBMB Life*. **61**(11), pp.1029–1042.

Wilkinson, J.D. and Williamson, E.M. 2007. Cannabinoids inhibit human keratinocyte proliferation through a non-CB1/CB2 mechanism and have a potential therapeutic value in the treatment of psoriasis. *Journal of Dermatological Science*. **45**(2), pp.87–92.

Williams-Karnesky, R.L., Sandau, U.S., Lusardi, T.A., Lytle, N.K., Farrell, J.M., Pritchard, E.M., Kaplan, D.L. and Boison, D. 2013. Epigenetic changes induced by adenosine augmentation therapy prevent epileptogenesis. *Journal of Clinical Investigation*. **123**(8), pp.3552–3563.

Williams, C.A., Beaudet, A.L., Clayton-Smith, J., Knoll, J.H., Kyllerman, M., Laan, L.A., Magenis, R.E., Moncla, A., Schinzel, A.A., Summers, J.A. and Wagstaff, J. 2006. Angelman syndrome 2005: Updated consensus for diagnostic criteria. *American Journal of Medical Genetics*. **140 A**(5), pp.413–418.

Williams, J.G. 2010. *Dictyostelium* finds new roles to model. *Genetics*. **185**(3), pp.717–726.

Williams, R.S.B. 2005. Pharmacogenetics in model systems: Defining a common mechanism of action for mood stabilisers. *Progress in Neuro-Psychopharmacology and Biological Psychiatry*. **29**(6), pp.1029–1037.

Williams, R.S.B., Boeckeler, K., Gräf, R., Müller-Taubenberger, A., Li, Z., Isberg, R.R., Wessels, D., Soll, D.R., Alexander, H. and Alexander, S. 2006. Towards a molecular understanding of human diseases using *Dictyostelium discoideum*. *Trends in Molecular Medicine*. **12**(9), pp.415–424.

Williams, R.S.B., Cheng, L., Mudge, A.W. and Harwood, A.J. 2002. A common mechanism of action for three mood-stabilizing drugs. *Nature*. **417**(6886), pp.292–295.

Wingerchuk, D.M. and Carter, J.L. 2014. Multiple sclerosis: Current and emerging disease-modifying therapies and treatment strategies. *Mayo Clinic Proceedings*. **89**(2), pp.225–240.

Woodcock, H. V., Eley, J.D., Guillotin, D., Platé, M., Nanthakumar, C.B., Martufi, M., Peace, S., Joberty, G., Poeckel, D., Good, R.B., Taylor, A.R., Zinn, N., Redding, M., Forty, E.J., Hynds, R.E., Swanton, C., Karsdal, M., Maher, T.M., Bergamini, G., Marshall, R.P., Blanchard, A.D., Mercer, P.F. and Chambers, R.C. 2019. The mTORC1/4E-BP1 axis represents a critical signaling node during fibrogenesis. *Nature Communications*. **10**(1), p.6.

World Health Organization 2016. WHO | Epilepsy. *WHO*. [Online]. [Accessed 1 April 2017]. Available from: http://who.int/mediacentre/factsheets/fs999/en/.

Wray, S., Havrdova, E., Snydman, D.R., Arnold, D.L., Cohen, J.A., Coles, A.J., Hartung, H.P., Selmaj, K.W., Weiner, H.L., Daizadeh, N., Margolin, D.H., Chirieac, M.C. and Compston, D.A.S. 2018. Infection risk with alemtuzumab decreases over time: pooled analysis of 6-year data from the CAMMS223, CARE-MS I, and CARE-MS II studies and the CAMMS03409 extension study. *Multiple Sclerosis Journal*. **I**, pp.1–13.

Wu, Y., Zhang, W., Liu, W., Zhuo, X., Zhao, Z. and Yuan, Z. 2011. The double-faced metabolic and inflammatory effects of standard drug therapy in patients after percutaneous treatment with drug-eluting stent. *Atherosclerosis*. **215**(1), pp.170–175.

Wu, Y., Zhang, Z., Liao, X., Qi, L., Liu, Y. and Wang, Z. 2016. Effect of high-fat diet-induced obesity on the Akt/FoxO/Smad signaling pathway and the follicular development of the mouse ovary. *Molecular Medicine Reports*. **14**(4), pp.3894–3900.

Xu, K., Dai, X.L., Huang, H.C. and Jiang, Z.F. 2011. Targeting HDACs: A promising therapy for Alzheimer's disease. *Oxidative Medicine and Cellular Longevity*. **2011**, pp.1–5.

Xu, R., Paul, B.D., Smith, D.R., Tyagi, R., Rao, F., Khan, A.B., Blech, D.J., Vandiver, M.S., Harraz, M.M., Guha, P., Ahmed, I., Sen, N., Gallagher, M. and Snyder, S.H. 2013. Inositol polyphosphate multikinase is a transcriptional coactivator required for immediate early gene induction. *Proceedings of the National Academy of Sciences of the United States of America*. **110**(40), pp.16181–16186.

Xu, R., Sen, N., Paul, B.D., Snowman, A.M., Rao, F., Vandiver, M.S., Xu, J. and Snyder, S.H. 2013. Inositol polyphosphate multikinase is a coactivator of p53-mediated transcription and cell death. *Science Signaling*. **6**(269), pp.ra22–ra22.

Yaari, Y., Selzer, M.E. and Pincus, J.H. 1986. Phenytoin: Mechanisms of its anticonvulsant action. *Annals of Neurology*. **20**(2), pp.171–184.

Yang, L., Miao, L., Liang, F., Huang, H., Teng, X., Li, S., Nuriddinov, J., Selzer, M.E. and Hu, Y. 2014. The mTORC1 effectors S6K1 and 4E-BP play different roles in CNS axon regeneration. *Nature Communications*. **5**, p.5416.

Yousaf, R., Gu, C., Ahmed, Z.M., Khan, S.N., Friedman, T.B., Riazuddin, Sheikh, Shears, S.B. and Riazuddin, Saima 2018. Mutations in Diphosphoinositol-Pentakisphosphate Kinase PPIP5K2 are associated with hearing loss in human and mouse K. B. Avraham, ed. *PLoS Genetics*. **14**(3), p.e1007297.

Yu, J.S.L., Ramasamy, T.S., Murphy, N., Holt, M.K., Czapiewski, R., Wei, S.K. and Cui, W. 2015. PI3K/mTORC2 regulates TGF-β/Activin signalling by modulating Smad2/3 activity via linker phosphorylation. *Nature Communications*. **6**(1), p.7212.

Yu, S., Vincent, A., Opriessnig, T., Carpenter, S., Kitikoon, P., Halbur, P.G. and Thacker, E. 2007. Quantification of PCV2 capsid transcript in peripheral blood mononuclear cells (PBMCs) in vitro. *Veterinary Microbiology*. **123**(1–3), pp.34–42.

Zettl, U.K., Rommer, P., Hipp, P. and Patejdl, R. 2016. Evidence for the efficacy and effectiveness of THC-CBD oromucosal spray in symptom management of patients with spasticity due to multiple sclerosis. *Therapeutic Advances in Neurological Disorders*. **9**(1), pp.9–30.

Zhang, Jingfang, Chen, L., Zhang, Ju and Wang, Y. 2019. Drug Inducible CRISPR/Cas Systems. *Computational and Structural Biotechnology Journal*. **17**, pp.1171–1177.

Zhang, Y.N., Dong, H.T., Yang, F.B., Wang, Z.Q., Ma, Z.H., Ma, S.Z., Ma, X.D. and Duan, L. 2018. Nrf2-ARE signaling pathway regulates the expressions of AIR and ENT1 in the brain of epileptic rats. *European Review for Medical and Pharmacological Sciences*. **22**(20), pp.6896–6904.

Zhao, X., Li, G. and Liang, S. 2013. Several affinity tags commonly used in chromatographic purification. *Journal of Analytical Methods in Chemistry*. **2013**, pp.1–8.

Zuardi, A.W., Antunes Rodrigues, J. and Cunha, J.M. 1991. Effects of cannabidiol in animal models predictive of antipsychotic activity. *Psychopharmacology*. **104**(2), pp.260–264.

Zygmunt, P.M., Petersson, J., Andersson, D.A., Chuang, H.H., Sørgård, M., Di Marzo, V., Julius, D.

and Högestätt, E.D. 1999. Vanilloid receptors on sensory nerves mediate the vasodilator action of anandamide. *Nature*. **400**(6743), pp.452–457.

9 Appendix

9.1 Materials

9.1.1 Reagents and products

0.2 µm PVDF membrane (Fisher, 88520), 1-mm width electroporation cuvette (Sigma-Aldrich, Z706078-50EA), 100% Ethanol (VWR, 20821.330DP), 2-mercaptoethanol (2-ME) (Sigma-Aldrich, M6250), 5x loading buffer (Bioline, BIO-37045), absorbent filter pads (Millipore, AP1004700), agarose (Bioline, B10-41026), Ampicillin (Sigma-Aldrich, A1593), blasticidin (Apollo Scientific, BIB4432), bromophenol blue (Sigma-Aldrich, B0126), DMSO (VWR, VWRV0231), Dulbecco's Modified Eagle Medium (DMEM) (Sigma-Aldrich, D0819), ethidium bromide (Bio-Rad, 1610433), Ethylenediaminetetraacetic acid (EDTA) (Sigma-Aldrich, E9884), fetal bovine serum (FBS) (ThermoFisher, 26140087), G418 (PAA laboratories, 11558616), glucose (Sigma-Aldrich, G8270), HCl (VWR, 20252), glycerol (Sigma-Aldrich, G5516), HEPES (Sigma-Aldrich, H3375), HL5 media (ForMedium, HLB0103), Horse serum (Sigma-Aldrich, H0146-5ML), K_2CO_3 (Sigma-Aldrich, P5833), K_2HPO_4 (Sigma-Aldrich, 1551128), KCl (Sigma-Aldrich, P9333), KH_2PO_4 (Sigma-Aldrich, NIST200B), LY294002 (Cambridge Bioscience, CAY70920),Lymphoprep™ (Axis-Shield, 1114545), $MgCl_2$ (Sigma-Aldrich, M8266), $MgSO_4$ (Sigma-Aldrich, M7506), NaCl (Sigma-Aldrich, S9888), NaH_2PO_4 (Sigma-Aldrich, S8282), $NaHCO_3$ (Sigma-Aldrich, S5761), nitrocellulose filter (Millipore, HABP04700), nuclease-free water (Sigma-Aldrich, W4502), nonyl phenoxypolyethoxylethanol 40 (NP40) substitute (Sigma-Aldrich, 74385), Odyssey chemifluorescent substrate kit chemifluorescent substrate (Li-Cor, 928-30005), OrangeG (Sigma-Aldrich, penicillin and streptomycin (Thermo Fisher Scientific, 15140122), perchloric acid (Sigma-Aldrich, 311421), Pictilisib (AbCam, ab141352), protease inhibitor (ThermoFisher, 87786), phosphatase Inhibitor Cocktail 2 (Sigma-Aldrich, P5726), phosphatase Inhibitor Cocktail 3 (Sigma-Aldrich, P0044), plates (Corning, 353801), proteinase K (Fermentas, EO0491), radioimmunoprecipitation assay (RIPA) buffer (ThermoFisher, 89900), SM agar (ForMedium, SMA0102), sodium acetate (Sigma-Aldrich, S2889), sodium dodecyl sulfate (SDS) solution (Sigma-Aldrich, L3771), tissue culture flasks (Corning® CellBIND® Surface cell culture flasks, Sigma-Aldrich, CLS3289) Tris acetate ethylenediaminetetraacetic acid (EDTA) (TAE) buffer (Severn Biotech Limited, 20-6001-50), Tris buffer saline (TBS) (Fisher, 10776834), Trizma (Tris)-HCl pH 8.3 (Sigma-Aldrich, T1503), Trypsin (Sigma-Aldrich, T4049), TWEEN Tween 20 (Sigma-Aldrich, P1379), and whatman filter paper (Sigma-Aldrich, WHA3030917), O3756).

9.1.2 Cannabinoids

Cannabigerol (CBG), cannabidiol (CBD), cannabidivarin (CBDV), cannabidiolic acid (CBDA) and THC:CBD combinations (20 nM:17 nM) were provided by GW pharmaceuticals, England. Stock concentrations of these were 100 mM. Cannabinoids were dissolved in DMSO (except for use on PBMCs, where ethanol was used). Use of cannabinoids in media resulted in media concentrations of 0.5 % (v/v) DMSO (or ethanol). In all experiments, a constant solvent level of 0.5 % (v/v) was used.

9.1.3 Molecular weight standards

Page ruler^{TM} prestained protein ladder (Thermo Scientific, 26616) for western blots and 1 kb DNA hyperladder (Bioline, BIO-33053) for gel electrophoresis.

9.1.4 Restriction enzymes

Enzymes used in this thesis: *SpeI* (ER1251), *PstI* (ER0611), *KpnI* (ER0521), *BamHI* (ER0052), *RsaI* (ER1122), *BglII* (ER0081), *NcoI* (ER0572). Buffer: Tango buffer (Thermo Scientific, BY5).

9.1.5 Other enzymes

GoTaq® G2 Flexi DNA Polymerase (Promega, M7801), Q5 high fidelity DNA polymerase (New England Biolabs, M0491), T4 DNA ligase (Fermentas, 15224041).

9.1.6 Antibodies

Anti-phospho-4EBP1 (rabbit, Cell Signalling Technology, 9459), anti-total 4EBP1 (rabbit, NEB, 4923), anti-actin (mouse, Sigma-Aldrich, A1978), anti-IPMK antibody (ab96753), anti-RFP (rat, Chromotek, 5F8), Streptavidin (Alexa Fluor™ 680 conjugate, Thermo Fisher, S21378), Anti-rabbit immunoglobulins (goat, Horseradish peroxidase (HRP), Agilent Technologies, P0448), Anti-mouse immunoglobulins (rabbit, DyLight™ 680 Conjugate, Cell Signalling Technology, 5470), Anti-rat immunoglobulins (goat, IRDye® 800CW, Li-Cor Biosciences, 926-32219).

9.1.7 Commercial kits

DNeasy® Blood and tissue kit (Qiagen, 69506), Wizard Genomic DNA Purification Kit (Promega, A1120), QIAquick® PCR purification kit (Qiagen, 28104), TOPO TA Cloning® kit (Invitrogen, K450002), Plasmid mini-prep kit (Qiagen, 27104), HiSpeed Plasmid Maxi Kit (Qiagen, 12643),

RNeasy mini-kit (Qiagen, 74104), First-strand cDNA synthesis kit (Thermo Scientific, K1612), DNA-free kit (Ambion, AM1906), Methylated DNA Quantification Kit (Colorimetric) (Abcam, ab117128).

9.1.8 Primers

No.	Name	Use	Sequence 5'-3' (restriction sites underlined)	Rest. enzyme
1	ENT1 KO 3' genomic reverse	Production of ENT1 knockout plasmid	CCAGTGGATCCAGTTACTAAATAAC	
2	ENT1 KO 3' vector reverse	Production of ENT1 knockout plasmid	ATAGGTACCCAAAATGAGTTGATACCCAAATAC	*KpnI*
3	ENT1 KO 3' genomic forward	Production of ENT1 knockout plasmid	ATACCATGGTTGGTGATTTCATTGGAAG	*NcoI*
4	ENT1 KO 5' vector forward	Production of ENT1 knockout plasmid	ATAACTAGTGATATAACAGAAACATCAAAAGCAC	*SpeI*
5	ENT1 KO 5' genomic reverse	Production of ENT1 knockout plasmid	ATACTGCAGCCTGTATATTCGCCTGGAAAC	*PstI*
6	ENT1 KO 5' genomic forward	Production of ENT1 knockout plasmid	GACAAACAGAGATGAATATTCACC	
7	ENT1 RT PCR 5' forward	RT-PCR analysis of ENT1 expression	GATGGTGATGCCAAACCA	
8	ENT1 RT PCR 3' reverse	RT-PCR analysis of ENT1 expression	CAAAATGAGTTGATACCCAAATAC	
9	ENT1 OE 5' forward	Production of ENT1 over-expressor plasmid	ATAAGATCTATGACAAACAGAGATGAATATTC	*BglII*
10	ENT1 OE 3' reverse	Production of ENT1 over-expressor plasmid	ATAACTAGTGAAATTAATACCAGTGGATCCAG	*SpeI*
11	Ig7F	RT-PCR for Ig7 control	GTACTGTGAAGGAAAGATGAAAAG	
12	Ig7R	RT-PCR for Ig7 control	CTATGGACCTTAGCGCTC	
13	p9	Inverse PCR of mutant library/screening Kos	TGTATGCTATACGAAGTTATCC	
14	p10	Inverse PCR of mutant library	GTAGAAGTAGCGACAGAGAAG	
15	p13	Screening KOs	TGAATGGTGAAGATAAATATATGC	
16	M13	Sequencing TOPO cloned PCR products	CAGGAAACAGCTATGACC	
17	T7	Sequencing TOPO cloned PCR products	TAATACGACTCACTATAGGG	
18	IPMK RT PCR 5' forward primer	Examining expression of dIPMK in CBG-resistant mutant	GGGTATTGAAGATTTAACATATGG	
19	IPMK RT and PCR 3' forward primer	Examining expression of dIPMK in CBG-resistant mutant	GTTGGTGGAGTTAATGGATCTAC	
20	IPMK qPCR 5' forward primer	Examining expression of dIPMK in CBG-resistant mutant	GGTTTAAATACATACCCTTCATC	
21	IPMK OE 5' forward	Production of dIPMK over-expressor plasmid	ATAAGATCTATGTCATCATCATCACTTA	*BglII*
22	IPMK OE 3' reverse	Production of dIPMK over-expressor plasmid	ATAACTAGTATTTTCAGATAATAATTG	*SpeI*
23	IPMK KO 3' genomic reverse	Production of dIPMK knockout plasmid	ATAGTTGGTGGAGTTAATGGATCTAC	
24	IPMK KO 3' vector reverse	Production of dIPMK knockout plasmid	ATAGGTACCCCAATATTTGAGTCATC	*KpnI*
25	IPMK KO 3' genomic forward	Production of dIPMK knockout plasmid	ATACCATGGGGTGCAAAACTT	*NcoI*
26	IPMK KO 5' genomic reverse	Production of dIPMK knockout plasmid	ATACTGCAGCCATATGTTAAATCTTCA	*PstI*
27	IPMK KO 5' vector forward	Production of dIPMK knockout plasmid	ATAACTAGTGGATGGAGGAAGTGAAAATAT	*SpeI*
28	IPMK KO 5' genomic forward	Production of dIPMK knockout plasmid	ATACCATTAGAAGATCAAATTGCAGG	
29	hPMK OE 5' forward	Production of hIPMK over-expressor plasmid	AGATCTATGGCAACAGAACC	*BglII*
30	hIPMK OE 3' reverse	Production of hIPMK over-expressor plasmid	ACTAGTATTATCTAAAATTGATC	*SpeI*

Table 9.1: Primer sequences, name, function and restriction enzyme cut sites. All primers used in this thesis are contained within this table.

All primers were obtained from Sigma Aldrich. The primers are at synthesis scale of expected yields of 0.025 µmole. They arrive desalted and dry. Primers are stored at -20 °C. Primers are dissolved in nuclease-free water to 100 µM, then aliquots are made at 10 µM for general use, the final concentration of each primer in a PCR is 0.5 µM.

9.1.9 Equipment

Dissection microscope (Leica) with a QICAM FAST 1394 camera (QImaging). LCMS-8050 triple quadrupole mass spectrometer (Shimadzu Corp., Japan). NanoDrop ND-1000 spectrophotometer (Thermo Scientific). Odyssey CLx (Li-Cor). PowerWave Colorimetric plate reader (Biotek). Olympus IX71 wide-field fluorescence microscope at 96 x magnification with a QICAM FAST 1394 camera. peqSTAR Thermocycler (VWR) PCR machine. Rotorgene Q qPCR machine (Qiagen) Shimadzu Nexera UHPLC system.

9.1.10 Cell lines and plasmids

All *D. discoideum* cell lines and plasmids were obtained from the *Dictyostelium* stock center (https://www.dictybase.org/StockCenter).

D. discoideum cells from stock center:

Wild type (AX3) - DBS0235543

Wild type (AX2) - DBS0235535

PKBA$^-$ - DBS0236784

DNMA$^-$ - DBS0235917

Plasmids from stock center:

pLPBLP - Plasmid-9

pDM324 - Plasmid-541

9.2 Data tables for growth curves

Data below is that which growth curves are derived from. It is presented as normalised to 0 µM CBG for each biological repeat (n). Where data is missing, it was not recorded for that repeat due to either contamination or not carrying out the experiment. For each concentration, the rows are each day that data was recorded.

WT (AX3)

0 µM CBG

											Mean	SD
0.1	0.1	0.1	0.1	0.1	0.1	0.1	0.1	0.1	0.1	0.1	0.09	0.02
1.6	1.6	2.7	1.7	5.1		10.0	3.9	2.9	0.9	1.5	3.18	2.56
6.9	8.3	9.3	8.9	37.2	10.4	47.1	18.3	9.6	2.0	12.0	15.44	13.27
28.5	27.9	40.5	43.6	74.5	56.7	89.4	114.5	32.5	8.5	24.8	49.21	30.30
66.1	78.2	111.0	96.4	80.7	92.2	104.2	127.5	90.4	51.5	70.2	88.05	20.72
100.0	100.0	100.0	100.0	100.0	100.0	100.0	100.0	100.0	100.0	100.0	100.00	0.00

0.02 µM CBG

		0.1	0.1	0.1	0.1	0.1	0.1	0.1	0.1	0.1	0.09	0.02
		2.4	1.3	6.3		8.5	4.3	1.9	0.6	1.5	3.33	2.60
		9.2	7.7	31.7	11.0	44.7	16.8	9.2	1.1	9.8	15.67	13.00
		32.3	32.1	74.3	54.2	82.4	121.7	27.7	2.1	23.8	50.08	34.82
		93.0	97.8	78.3	83.9	97.2	121.7	80.7	4.7	67.9	80.58	30.46
		86.0	120.1	87.9	98.8	94.1	108.7	103.6	25.3	95.2	91.08	25.30

0.1 µM CBG

0.1	0.1	0.1	0.1	0.1	0.1	0.1	0.1	0.1	0.1	0.1	0.09	0.02
0.9	1.2	1.7	1.7	3.8		5.4	2.2	0.9	0.2	1.5	1.94	1.47
3.8	3.3	6.7	6.4	18.0	10.2	23.0	11.9	3.2	0.2	4.4	8.28	6.63
20.7	14.9	19.3	28.5	54.1	35.6	87.1	34.8	9.4	0.6	22.9	29.80	22.69
16.5	34.7	91.0	97.8	77.8	64.1	81.2	113.0	37.3	1.1	51.2	60.51	33.82
67.2	69.2	92.0	118.7	67.7	81.1	82.4	121.7	79.5	3.9	95.2	79.89	29.91

0.5 µM CBG

0.1	0.1	0.1	0.1	0.1	0.1	0.1	0.1	0.1		0.1	0.10	0.01
0.4	0.3	0.4	0.7	0.6		0.8	1.4	0.6		0.3	0.61	0.33
0.9	1.1	1.8	2.4	3.4	2.4	5.0	4.3	2.7		2.2	2.63	1.25
2.3	2.3	2.8	11.8	13.5	9.2	16.9	14.5	4.6		2.1	7.98	5.54
7.5	9.3	15.5	39.9	36.4	43.7	63.5	46.4	16.9		9.0	28.81	18.61
24.1	20.7	47.8	99.2	61.6	70.0	82.4	72.5	55.4		32.8	56.63	24.34

1 µM CBG

0.1	0.1	0.1	0.1	0.1	0.1	0.1	0.1	0.1	0.1	0.1	0.09	0.02
0.3	0.1	0.2	0.1	0.2		0.4	0.3	0.3	0.0	0.3	0.21	0.11
0.3	0.4	0.4	0.1	0.1	0.2	0.5	1.1	1.0	0.1	0.7	0.43	0.34
1.0	0.8	0.6	0.2	0.6	0.3	1.1	0.9	2.9	0.1	0.6	0.82	0.73
2.3	1.9	2.8	0.7	1.1	1.2	3.0		12.0	0.3	1.7	2.70	3.22
6.9	5.7	6.5	1.5	1.8	5.1	10.6		30.4	0.6	1.7	7.07	8.31

4 µM CBG

0.1	0.1	0.1	0.1	0.1	0.1	0.1	0.1	0.1		0.1	0.10	0.01
0.0	0.0	0.0	0.0		0.0	0.0	0.1	0.2		0.1	0.05	0.06
0.0	0.0	0.0	0.0	0.0	0.0	0.0	0.1	0.0		0.1	0.03	0.04
0.0	0.0	0.1	0.1	0.0	0.0	0.0	0.0	0.0		0.1	0.03	0.04
0.0	0.0	0.0	0.0	0.0	0.0	0.0	0.0	0.0		0.2	0.04	0.07
0.0	0.0	0.1	0.1	0.0	0.0	0.0	0.0	0.0		0.3	0.06	0.09

ENT1-

0 µM CBG								Mean	SD
0.0	0.1	0.1	0.1	0.1	0.1	0.1	0.2	0.09	0.06
2.3	1.8	3.8	2.2	4.5		5.4	1.8	3.11	1.35
9.7	10.6	11.6	8.6	27.1	15.6	26.0	8.7	14.74	7.13
32.6	27.9	48.6	38.6	55.3	63.0	51.9	24.2	42.76	13.08
75.2	64.3	100.0	85.8	69.1	130.2	100.0	78.9	87.95	20.12
100.0	100.0	100.0	100.0	100.0	100.0	100.0	100.0	100.00	0.00

0.02 µM CBG									
		0.1	0.1	0.1	0.1	0.1	0.2	0.11	0.05
		4.9	2.0	4.7		6.5	2.1	4.05	1.75
		18.0	7.4	17.6	20.2	23.4	7.4	15.68	6.14
		72.2	22.1	53.4	71.7	54.5	23.7	49.61	20.27
		117.8	73.7	92.1	106.8	102.6	76.3	94.89	15.95
		88.9	104.3	131.6	100.0	103.9	113.2	106.96	13.14

0.1 µM CBG									
0.0	0.1	0.1	0.1	0.1	0.1	0.1	0.2	0.09	0.06
2.1	1.4	4.1	1.7	2.9		4.7	2.0	2.72	1.16
5.1	5.5	9.9	3.0	28.4	22.4	14.0	5.3	11.71	8.68
22.2	17.2	43.6	12.1	27.6	72.1	42.9	16.4	31.76	18.80
61.0	47.2	108.9	40.3	66.8	134.0	87.0	76.3	77.69	29.50
113.0	77.1	91.1	93.3	84.2	109.4	102.6	89.5	95.03	11.59

0.5 µM CBG									
0.0	0.1	0.1	0.1	0.1	0.1	0.1	0.2	0.09	0.06
0.6	0.6	1.9	1.0	1.0		2.9	1.6	1.38	0.76
4.7	1.7	5.5	1.3	2.3	7.5	14.0	5.3	5.29	3.86
13.2	6.3	11.4	4.9	4.6	22.2	35.1	15.8	14.19	9.69
39.6	27.6	41.1	12.8	15.9	77.3	71.4	47.4	41.63	22.06
75.3	49.5	104.4	47.6	36.8	133.1	106.5	73.7	78.38	31.62

1 µM CBG									
0.0	0.1	0.1	0.1	0.1	0.1	0.1	0.2	0.09	0.06
0.2	0.3	0.6	0.2	0.3		2.9	1.4	0.83	0.92
1.0	0.8	1.5	0.2	0.3	0.9	7.0	2.5	1.79	2.09
1.9	1.4	4.1	0.2	0.7	2.9	10.1	9.5	3.85	3.62
4.7	3.3	11.1	0.4	2.0	5.7	53.2	21.1	12.69	16.52
18.5	9.2	21.9	0.8	5.3	8.9	68.8	52.6	23.25	22.90

4 µM CBG									
0.0	0.1	0.1	0.1	0.1	0.1	0.1	0.2	0.09	0.06
0.1	0.0	0.0	0.1	0.0		0.3	0.2	0.10	0.11

0.0	0.0	0.2	0.1	0.0	0.0	0.8	0.3	0.18	0.27
0.1	0.0	0.2	0.1	0.0	0.0	1.0	0.4	0.23	0.33
0.0	0.1	0.0	0.0	0.1	0.0	1.4	1.3	0.35	0.56
0.1	0.1	0.1	0.1	0.2	0.0	1.8	1.3	0.44	0.63

WT (AX2)

0 µM CBG

							Mean	SD
0.6	1.0	0.0	0.0	0.0	0.0	0.1	0.24	0.37
7.6	9.7	11.2		2.8	2.0	1.5	5.80	3.85
15.8	23.2	22.9	11.9	5.4	6.4	12.0	13.93	6.64
24.7	34.8	37.6	22.2	8.0	30.8	24.8	26.13	9.08
57.0	74.9	54.1	54.8	54.5	69.0	70.2	62.07	8.27
100.0	100.0	100.0	100.0	100.0	100.0	100.0	100.00	0.00

0.02 µM CBG

0.6	1.0	0.0	0.0	0.0	0.0	0.1	0.24	0.37
8.2	7.7	8.2		3.7	1.8	1.5	5.20	2.95
12.7	15.5	21.8	10.4	4.8	4.2	9.8	11.30	5.65
20.9	30.0	40.0	18.5	5.7	23.5	23.8	23.20	9.71
39.9	69.1	84.1	74.1	40.8	56.3	67.9	61.73	15.54
57.6	81.2	148.8	139.3	79.5	60.5	95.2	94.59	33.54

0.1 µM CBG

0.6	1.0	0.0	0.0	0.0	0.0	0.1	0.24	0.37
7.0	8.7	6.5		2.6	1.7	1.5	4.67	2.81
10.8	16.4	22.4	9.6	4.4	3.9	4.4	10.26	6.49
19.6	23.2	45.9	26.7	5.3	18.1	22.9	23.08	11.26
28.5	53.6	63.5	68.1	19.4	56.3	51.2	48.67	16.71
43.0	89.9	107.6	135.6	52.2	54.5	95.2	82.57	31.45

0.5 µM CBG

0.6	1.0	0.0	0.0			0.1	0.34	0.39
4.4	6.3	5.3				0.3	4.07	2.28
10.1	13.0	11.2	9.6			2.2	9.23	3.71
10.8	22.2	37.1	7.4			2.1	15.91	12.46
18.4	46.4	54.7	36.3			9.0	32.96	17.02
56.3	71.0	77.1	63.0			32.8	60.03	15.34

1 µM CBG

0.6	1.0	0.0	0.0	0.0	0.0	0.1	0.24	0.37
1.9	4.3	4.7		1.3	1.2	0.3	2.29	1.65
2.5	5.3	13.5	2.2	2.1	2.0	0.7	4.06	4.07
1.3	10.1	14.1	2.2	2.9	10.8	0.6	6.00	5.09
2.5	13.5	23.5	7.4	9.4	14.4	1.7	10.35	7.04
7.0	19.8	45.3	17.8	22.6	25.3	1.7	19.93	13.01

4 µM CBG

0.6	1.0	0.0	0.0	0.0	0.0	0.1	0.24	0.37

0.0	0.0	4.1		0.4	0.0	0.1			0.76	1.51
0.0	0.5	11.8	0.0	0.4	0.2	0.1			1.85	4.05
0.6	0.0	3.5	0.0	0.4	0.3	0.1			0.71	1.17
0.0	1.0	6.5	1.5	2.6	0.4	0.2			1.73	2.09
1.9	1.0	28.8	5.2	5.3	0.5	0.3			6.14	9.46

DNMA-

0 µM CBG

									Mean	SD
0.0	0.0	0.0	0.0	0.1	0.0	0.3	0.1	0.3	0.09	0.12
		3.5		3.1		5.8	2.0	2.4	3.37	1.32
12.8	11.7	9.4	15.8	8.4	36.8	12.6	3.9	7.0	13.17	9.00
41.0	60.5	59.9	42.8	21.6	123.1	22.2	11.6	11.4	43.80	33.13
112.6	122.4	100.0	91.4	91.5	147.8	59.3	44.7	65.3	92.77	30.80
100.0	100.0	100.0	100.0	100.0	100.0	100.0	100.0	100.0	100.00	0.00

0.02 µM CBG

0.0	0.0	0.0	0.0	0.1	0.0	0.3	0.1	0.3	0.09	0.12
		2.4		3.3		7.0	1.4	2.4	3.31	1.92
13.4	16.5	7.5	12.9	13.5	14.4	8.7	3.5	6.7	10.79	4.07
50.5	61.8	33.2	29.8	25.0	47.6	18.5	12.1	9.8	32.05	17.00
92.6	110.5	75.0	110.4	91.5	160.1	55.6	51.3	61.2	89.79	32.48
124.2	119.8	133.4	100.0	119.2	100.0	103.7	102.6	97.9	111.19	12.28

0.1 µM CBG

0.0	0.0		0.0	0.1		0.3	0.1	0.3	0.12	0.13
						4.3	1.4	2.4	2.72	1.19
13.2	13.3		19.1	104.3		6.7	3.9	4.9	23.62	33.31
45.2	47.3		31.1	168.1		15.6	15.8	13.1	48.02	50.77
102.1	122.4		84.4	187.3		55.6	59.2	61.2	96.02	43.77
83.1	147.4		115.6	106.4		107.4	102.6	91.8	107.78	18.98

0.5 µM CBG

						0.3	0.1	0.3	0.24	0.10
						1.6	3.2	2.6	2.47	0.63
						6.1	4.7	5.9	5.56	0.59
						13.3	6.3	11.4	10.36	2.96
						32.6	34.2	40.8	35.86	3.54
						74.1	69.7	81.6	75.13	4.89

1 µM CBG

0.0	0.0	0.0	0.0	0.1	0.0	0.3	0.1	0.3	0.09	0.12
		2.1		3.3		2.5	2.1	2.0	2.38	0.51
12.3	10.2	5.1	10.0	6.8	12.2	3.6	4.2	2.4	7.43	3.61
33.6	35.5	16.9	25.9	18.2	19.9	11.1	10.8	9.0	20.10	9.18
100.0	77.6	36.6	61.0	76.6	84.6	13.3	30.3	28.5	56.50	28.44
80.0	136.9	83.3	79.2	122.4	123.1	30.4	77.6	61.2	88.23	31.83

2 µM CBG

		0.0	0.0	0.1	0.0	0.3	0.1	0.3	0.12	0.13
		1.7		2.3		1.6	1.8	2.4	1.98	0.33
		4.4	4.7	4.1	7.3	1.9	3.2	3.1	4.09	1.56
		10.9	16.8	8.0	12.8	7.4	4.3	5.7	9.41	4.04
		26.6	23.6	20.4	41.5	8.1	14.5	24.5	22.72	9.68
		106.7	61.7	42.5	76.9	9.6	30.3	28.5	50.88	30.71

3 µM CBG

		0.0	0.0	0.1	0.0	0.1			0.04	0.05
		2.4		1.6		0.9			1.64	0.62
		5.1	6.1	2.0	4.5	3.2			4.16	1.46
		11.5	20.7	3.2	11.0	3.5			9.97	6.44
		33.2	33.7	4.1	21.4	6.8			19.86	12.58
		78.3	68.8	11.4	36.8	17.6			42.60	26.80

4 µM CBG

0.0	0.0	0.0	0.0	0.1	0.0	0.3	0.1	0.3	0.09	0.12
0.5	0.2	0.9		0.0		0.3	0.5	1.5	0.56	0.47
0.0	0.0	1.4	8.2	1.6	1.7	0.3	2.1	1.8	1.91	2.36
0.0	0.0	2.6	22.0	7.2	6.0	6.4	2.3	2.0	5.38	6.39
0.0	0.0	13.6	48.0	3.9	16.8	7.6	7.9	6.5	11.58	13.90
0.1	0.2	18.6	68.8	7.6	30.7	7.9	23.2	8.3	18.37	20.30

IPMK+

0 µM CBG

						Mean	SD
0.1	0.1	0.1	0.1	0.0	0.0	0.06	0.05
1.8	4.6	4.8	7.1	2.5	4.2	4.17	1.72
6.7	25.0	14.8	20.0	29.2	33.6	21.55	8.99
21.9	65.0	86.9	51.3	66.6	78.3	61.67	20.99
57.2	77.0	111.6	117.2	90.0	96.7	91.60	20.33
100.0	100.0	100.0	100.0	100.0	100.0	100.00	0.00

0.02 µM CBG

0.1	0.1	0.1	0.1	0.0	0.0	0.06	0.05
1.3	3.2	6.0	2.4	2.2	4.1	3.19	1.52
2.9	24.2	22.4	11.9	29.6	33.9	20.81	10.52
19.1	44.0	65.2	35.9	70.0	81.6	52.63	21.52
57.2	78.0	105.8	104.7	91.7	101.7	89.83	17.44
96.9	80.0	100.0	134.4	101.7	103.3	102.71	16.13

0.1 µM CBG

0.1	0.1	0.1	0.1	0.0	0.0	0.06	0.05
1.9	3.9	3.8	4.1	2.3	2.7	3.11	0.87
3.4	23.2	14.3	22.5	29.2	33.6	21.05	9.88
15.3	58.0	86.9	38.1	73.3	78.3	58.33	24.84
45.0	61.0	116.0	112.5	92.0	86.6	85.51	25.63
106.3	70.0	89.8	109.4	100.0	87.3	93.80	13.29

0.5 µM CBG

0.1	0.1	0.1	0.1	0.0	0.0	0.06	0.05
0.9	2.2	1.3	1.4	2.3	3.8	2.00	0.95
2.8	6.8	2.3	4.9	29.6	31.9	13.04	12.62
11.8	18.0	10.7	11.9	73.3	58.3	30.66	25.33
35.3	62.0	40.5	43.8	90.0	86.6	59.71	21.85
79.7	120.0	66.6	104.7	100.0	86.6	92.95	17.45

1 µM CBG

0.1	0.1	0.1	0.1	0.0	0.0	0.06	0.05
0.9	0.3	0.9	0.3	0.5	0.3	0.55	0.28
2.2	1.4	1.2	1.9	1.1	3.1	1.84	0.69
7.7	2.4	3.7	4.1	1.9	5.3	4.19	1.91
27.5	5.3	10.7	14.4	2.3	6.6	11.13	8.27
86.8	13.8	23.4	35.9	5.5	12.2	29.61	27.31

4 µM CBG

0.1	0.1	0.1	0.1	0.0	0.0	0.06	0.05
0.1	0.0	0.0	0.0	0.0	0.0	0.01	0.02
0.2	0.1	0.0	0.1	0.0	0.1	0.08	0.07
0.0	0.1	0.0	0.1	0.1	0.6	0.14	0.21
0.1	0.0	0.0	0.1	1.1	0.9	0.37	0.47
0.1	0.1	0.0	0.3	1.5	1.1	0.51	0.58

			PKBA-					
			0 µM CBG				Mean	SD
0.1	0.0	0.1	0.0	0.0	0.0	0.0	0.03	0.05
4.1				3.8			3.99	0.15
20.0	20.6	24.3	6.7	22.3	23.0	5.6	17.50	7.31
93.0	64.1	70.0	18.0	80.0	92.6	14.5	61.73	30.42
128.1	149.1	114.0	81.8	96.0	115.4	93.3	111.10	21.27
100.0	100.0	100.0	100.0	100.0	100.0	100.0	100.00	0.00
			0.02 µM CBG					
0.1	0.0	0.1	0.0	0.0	0.0	0.0	0.03	0.05
5.6				4.4			5.01	0.60
25.3	14.2	23.9	15.6	17.9	16.8	6.7	17.19	5.77
93.0	79.2	74.5	90.9	78.0	92.3	15.7	74.79	25.13
124.6	151.0	138.0	242.7704*	94.0	110.8	249.1541*	123.68	20.01
110.5	118.9	100.0	215.4	80.0	100.0	125.8	121.52	40.74
			0.1 µM CBG					
0.1	0.0	0.1	0.0	0.0	0.0	0.0	0.03	0.05
3.6				3.1			3.35	0.23
17.9	11.9	24.7	35.0	13.9	18.4	7.0	18.40	8.51
47.7	51.9	68.0	145.6	74.0	90.8	18.1	70.84	37.18
140.4	107.6	114.0	218.469*	144.1	124.6	302.5824*	126.13	14.27
112.3	156.7	112.0	227.6	134.1	101.5	135.6	139.97	39.70
			1 µM CBG					
0.1	0.0	0.1	0.0	0.0	0.0	0.0	0.03	0.05
0.7				3.0			1.83	1.13
4.6	8.4	10.7	14.9	15.5	12.2	3.7	9.99	4.35
11.8	37.6	37.0	42.3	86.0	89.2	7.4	44.47	29.94
122.8	126.5	100.0	218.469*	106.0	112.3	43.0	101.77	27.80
138.6	134.0	138.0	218.5	154.1	92.3	115.6	141.58	36.35
			2 µM CBG					
			0.0	0.0	0.0	0.0	0.00	0.00
				2.3			2.32	0.00
			4.1	5.4	27.9	1.8	9.82	10.53
			18.6	9.9	75.4	2.7	26.62	28.70
			91.5	59.1	140.0	22.1	78.19	43.34
			154.7	63.9	100.0	44.3	90.74	41.97
			3 µM CBG					
			0.0	0.0	0.0	0.0	0.00	0.00
				1.4			1.44	0.00
			3.5	1.3	8.2	0.8	3.45	2.93
			8.9	1.8	21.1	0.9	8.16	8.10
			2.8	2.5	118.5	1.1	31.21	50.39
			8.9	3.8	107.7	5.6	31.51	44.03

4 µM CBG

0.1	0.0	0.1	0.0	0.0	0.0	0.0	0.03	0.05
0.1	0.0	0.0		1.0			0.26	0.41
0.0	0.0	0.1	5.0	0.7	4.2	0.7	1.53	1.97
0.1	0.2	0.1	14.9	0.6	8.2	0.8	3.55	5.39
0.1	1.3	0.1	9.5	0.8	39.6	0.8	7.45	13.49
0.1	4.1	0.2	20.4	5.8	107.7	1.2	19.92	36.43

PKBA-IPMK+

0 µM CBG

							Mean	SD
0.0		0.3	0.0	0.0	0.0	0.0	0.05	0.11
0.2						2.3	1.28	1.06
2.6		2.9	16.5	3.0	1.9	20.7	7.93	7.64
9.8		13.8	73.3	18.5	3.2	42.8	26.90	24.15
57.8		71.3	102.2	49.9	27.9	81.2	65.05	23.61
100.0		100.0	100.0	100.0	100.0	100.0	100.00	0.00

0.02 µM CBG

0.0		0.3	0.0	0.0	0.0	0.0	0.05	0.11
1.2						2.4	1.78	0.62
3.7		4.9	13.0	3.3	1.9	19.4	7.69	6.35
9.8		21.8	48.8	20.4	3.2	38.9	23.82	15.75
60.4		157.3	120.0	84.3	25.9	83.5	88.58	41.79
113.2		228.9	131.2	103.1	94.0	101.3	128.62	46.38

0.1 µM CBG

0.0		0.3	0.0	0.0	0.0	0.0	0.05	0.11
3.8						2.1	2.94	0.86
4.9		4.0	12.3	4.1	0.8	19.4	7.58	6.32
16.1		6.3	31.0	15.4	8.7	36.3	18.97	11.05
81.5		24.9	75.5	43.6	30.7	81.8	56.35	24.01
155.4		200.3	95.5	84.3	67.9	98.7	117.03	45.97

1 µM CBG

0.0		0.3	0.0	0.0	0.0	0.0	0.05	0.11
2.2						2.3	2.25	0.04
5.6		2.0	11.6	2.9	3.4	20.7	7.69	6.62
13.5		5.4	32.1	6.3	11.5	45.4	19.04	14.73
100.0		10.9	64.4	24.8	57.9	77.9	55.99	30.27
150.1	164.4699*		115.6	59.3	102.0	97.4	104.87	29.34

2 µM CBG

0.0		0.3	0.0	0.0	0.0	0.0	0.05	0.11
1.2						2.0	1.59	0.43
1.5		2.3	3.4	2.0	1.8	3.3	2.38	0.71
1.6		4.0	10.1	3.8	2.7	14.7	6.14	4.68
2.1		7.7	31.9	8.5	12.7	71.4	22.38	23.82
6.1		22.6	88.9	19.2	59.9	88.3	47.51	33.33

3 µM CBG

0.0		0.3	0.0	0.0	0.0	0.0	0.05	0.11
0.7						0.5	0.60	0.14
0.7		0.6	0.8	1.1	0.9	0.5	0.77	0.20
0.6		1.1	2.4	1.1	1.0	7.2	2.24	2.27
1.8		1.4	6.1	1.5	3.8	11.0	4.27	3.42

3.0		5.4	7.8	4.1	10.3	37.6	11.37	11.97
			4 µM CBG					
0.0		0.3	0.0	0.0	0.0	0.0	0.05	0.11
0.5						0.1	0.32	0.21
0.9		0.0	0.1	0.3	0.6	0.1	0.34	0.34
0.8		1.4	0.7	0.1	1.0	0.1	0.70	0.47
0.7		1.7	3.4	1.6	1.8	1.0	1.72	0.85
1.6		3.7	3.8	4.8	6.7	1.1	3.62	1.86
			hIPMK+					
			0 µM CBG				Mean	SD
0.0	0.0	0.0	0.0	0.0	0.0	0.0	0.00	0.00
				1.5	1.1	1.0	1.22	0.22
9.7	4.8	7.2	8.3	3.8	4.4	3.7	6.00	2.21
23.0	18.7	36.4	50.8	9.5	26.5	8.3	24.73	13.95
92.6	91.1	104.8	105.3	27.9	103.1	37.8	80.37	30.62
100.0	100.0	100.0	100.0	100.0	100.0	100.0	100.00	0.00
			0.02 µM CBG					
0.0	0.0	0.0	0.0	0.0	0.0	0.0	0.00	0.00
				2.3	1.1	0.8	1.39	0.67
15.0	4.7	8.3	13.2	5.4	4.6	3.8	7.87	4.20
36.3	17.6	38.0	49.1	12.3	26.5	8.6	26.90	13.82
113.3	88.6	103.2	105.3	29.5	100.0	38.1	82.56	31.66
109.1	89.9	103.2	105.3	104.0	101.6	98.3	101.61	5.70
			0.1 µM CBG					
0.0	0.0	0.0	0.0	0.0	0.0	0.0	0.00	0.00
				1.0	1.4	0.7	1.07	0.29
8.0	4.8	8.4	8.6	5.8	4.0	3.8	6.20	1.96
37.2	18.1	23.7	38.5	9.9	23.3	9.7	22.92	10.79
73.5	88.6	103.2	87.7	29.9	95.0	38.1	73.70	26.53
107.0	88.6	101.6	105.3	108.0	93.7	95.4	99.95	6.90
			1 µM CBG					
0.0	0.0	0.0	0.0	0.0	0.0	0.0	0.00	0.00
				1.4	0.8	1.1	1.08	0.22
21.2	4.1	6.2	12.5	3.4	3.0	2.8	7.61	6.40
64.6	11.3	17.4	35.0	4.2	17.1	8.3	22.56	19.44
64.6	49.3	51.6	57.8	19.9	33.0	30.8	43.86	15.01
175.2	70.9	58.7	63.1	63.9	46.8	42.0	74.38	42.21
			2 µM CBG					
0.0	0.0	0.0	0.0	0.0	0.0	0.0	0.00	0.00
				0.2	0.1	0.3	0.22	0.07
8.8	2.4	3.1	2.3	0.8	0.5	0.5	2.64	2.71
9.7	3.3	2.7	4.4	1.4	0.8	0.7	3.31	2.91
10.6	6.2	5.6	8.5	1.8	1.1	1.0	4.99	3.52
15.9	6.5	6.9	8.3	3.2	1.3	1.0	6.15	4.78
			3 µM CBG					
0.0	0.0	0.0	0.0	0.0			0.00	0.00
				0.1			0.08	0.00
1.8	0.9	2.0	1.3	0.1			1.20	0.69
2.7	1.0	1.5	1.5	0.3			1.38	0.77
5.3	1.9	2.9	3.2	1.4			2.95	1.34

7.1	2.1	3.8	2.9	1.5			3.46	1.96
			4 μM CBG					
0.0	0.0	0.0	0.0	0.0	0.0	0.0	0.00	0.00
				0.2	0.1	0.1	0.11	0.04
2.7	1.4	2.7	0.9	0.2	0.5	0.2	1.22	1.02
3.5	1.2	2.7	0.9	0.2	0.7	0.3	1.36	1.19
2.7	2.5	4.0	1.8	1.5	1.0	0.5	2.00	1.08
8.0	2.6	4.2	2.2	1.8	1.1	0.6	2.91	2.33